VAN HEERDEN, E

INTEGRATED SIMULATION OF BUILDING THERMAL PERFORMANCE, HVAC SYSTEM AND CONTROL

PhD UP 1997

Integrated simulation of building thermal performance, HVAC system and control

by

EUGÉNE VAN HEERDEN

Thesis presented in partial fulfilment
of the requirements for the degree of
PHILOSOPHIAE DOCTOR

in the

Faculty of Engineering
University of Pretoria
PRETORIA

JUNE 1997

I would like to thank Prof. E.H. Mathews for his enthusiasm, motivation and support during this project.

Special thanks to Transfer of Energy Momentum and Mass (Pty) Ltd. for their financial support during this study.

Thanks to C. Lombard for many hours of fruitful discussions.

Thanks also to the department of Mechanical and Aeronautical Engineering at the University of Pretoria for the time that I was permitted to spend on completing this study.

To my colleagues and students for their input, suggestions and criticism, thank you. Especially to D. Arndt and S. Weggelaar for helping with, and doing many simulations and measurements.

Thank you to J. Vorster and D. Burger for their contribution to the implementation of the proposed models.

To my parents for affording me many opportunities, thank you.

Anita, thank you for your understanding, love and support. I dedicate this study to you.

Integrated simulation of building thermal performance, HVAC system and control

EUGÉNE VAN HEERDEN

Supervisor: Prof. E.H. Mathews
Department: Mechanical and Aeronautical Engineering,
UNIVERSITY OF PRETORIA
Degree: Philosophiae Doctor
Search terms: Thermal simulation tool, HVAC simulation,
System simulation, Building modelling,
Energy management systems

Practicing engineers need an integrated building, HVAC and control simulation tool for optimum HVAC design and retrofit. Various tools are available to the researchers, but these are not appropriate for the consulting engineer. To provide the engineer with a tool which can be used for typical HVAC projects, new models for building, HVAC and control simulation are introduced and integrated in a user-friendly, quick-to-use tool.

The new thermal model for buildings is based on a transfer matrix description of the heat transfer through the building shell. It makes provision for the various heat flow paths that make up the overall heat flow through the building structure.

The model has been extensively verified with one hundred and three case studies. These case studies were conducted on a variety of buildings, ranging from a 4 m^2 bathroom, to a 7755 m^2 factory building. Eight of the case studies were conducted independently in the Negev Desert in Israel.

The thermal model is also used in a program that was custom-made for the AGREMENT Board (certification board for the thermal performance of new low-cost housing projects). Extensions to the standard tool were introduced to predict the potential for condensation on the various surfaces. Standard user patterns were incorporated in the program so that all the buildings are evaluated on the same basis.

In the second part of this study the implementation of integrated simulation is discussed. A solution algorithm, based on the Tarjan depth first-search algorithm, was implemented. This ensures that the minimum number of variables are identified. A quasi-Newton solution algorithm is used to solve the resultant simultaneous equations.

Various extensions to the HVAC and control models and simulation originally suggested by Rousseau [1] were implemented. Firstly, the steady-state models were extended by using a simplified time-constant approach to emulate the dynamic response of the equipment. Secondly, a CO_2 model for the building zone was implemented. Thirdly, the partload performance of particular equipment was implemented.

Further extensions to the simulation tool were implemented so that energy management strategies could be simulated. A detailed discussion of the implications of the energy management systems was given and the benefits of using these strategies were clearly illustrated, in this study.

Finally, the simulation tool was verified by three case studies. The buildings used for the verification ranged from a five-storeyed office and laboratory building, to a domestic dwelling. The energy consumption and the dynamics of the HVAC systems could be predicted sufficiently accurately to warrant the use of the tool for future building retrofit studies.

Integrated simulation of building thermal performance, HVAC system and control

EUGÉNE VAN HEERDEN

Promotor:	Prof. E.H. Mathews
Departement:	Meganiese en Lugvaartkundige Ingenieurswese, UNIVERSITEIT VAN PRETORIA
Graad:	Philosophiae Doctor
Sleutelterme:	Thermal simulation tool, HVAC simulation, System simulation, Building modelling, Energy management systems

Praktiseerende ingenieurs het 'n behoefte aan 'n geïntegreerde gebou, lugversorgingstelsel en beheer simulasie gereedskap vir ontwerp en opgradering fases. Verskeie sagteware pakkette wat op die navorsers gemik is bestaan, maar is nie geskik vir die praktiserende ingenieur nie. Om gereedskap wat vir tipiese lugversorgingsprojekte gebruik kan word vir die konsultant beskikbaar te stel word die nuwe gebou, lugversorgingstelsel en beheer modellering in 'n gebruikersvriendelike pakket geïntegreer.

Die nuwe termiese model vir geboue is gebaseer op 'n oordragmatriksbeskrywing van die warmte-oordrag deur die gebou. Die model maak voorsiening vir die belangrikste warmte-oordragspaaie deur die geboustruktuur.

Die geboumodel is geverifieer deur een-honderd-en-drie gevallestudies. 'n Groot verskeidenheid geboue is in die gevalle studies gebruik. Agt van die studies is onafhanklik in die Negev-woestyn in Israel gedoen. Die vloerareas van die geboue het gewissel van 'n 4 m^2 badkamer tot 'n 7755 m^2 fabriek.

Die termiese model word ook gebruik in 'n program wat spesifiek vir die AGREMENT Raad (die raad wat die termiese gedrag van nuwe lae koste geboue evalueer) ontwikkel is. Uitbreidings om kondensasie op die verskillende oppervlaktes te voorspel, is geïmplementeer in die standaard termiese gedrag gereedskap. Standaard gebruikerspatrone word in die program aangeneem sodat alle geboue op dieselfde gronde geëvalueer word.

Geïntegreerde simulasie word in die tweede deel van die studie bespreek. 'n Oplossingsalgoritme wat gebaseer is op die Tarjan-diepte eerste soektog-algoritme is geïmplementeer. Hierdie algoritme verseker dat die minimum aantal veranderlikes geïdentifiseer word. 'n Kwasi-Newton oplossingsalgoritme word dan gebruik om die gesamentlike vergelykings op te los.

Verskeie uitbreidings aan die lugversorgings en beheer modelle en simulasie wat deur Rousseau [1] voorgestel is, is geïmplementeer. Eerstens is die gestadigde komponent modelle uitgebrei deur 'n eenvoudige tyd-konstante benadering om die dinamiese gedrag van die komponente te emuleer. Tweedens is 'n CO_2-model vir die gebousone geïmplementeer. Derdens is die deellasgedrag van spesifieke komponente geïmplementeer.

Verdere uitbreidings is geïmplementeer om energiebestuurstrategieë te simuleer. 'n Gedetailleerde bespreking van die implikasies van energiebestuurstrategieë is gedoen en die voordele daarvan is uitgewys.

Laastens is die simulasiegereedskap geverifieer met behulp van drie gevallestudies. Die geboue wat gebruik is, het gestrek van 'n vyfverdieping kantoor- en laboratoriumgebou tot 'n woonhuis.

Die energieverbruik en dinamika van die lugversorgingstelsel kon met voldoende akkuraatheid gesimuleer word om die gebruik van die gereedskap vir toekomstige energiestudies te regverdig.

Contents

List of Figures

List of Tables

Bibliography

[1] P.G. Rousseau, *Integrated Building and HVAC Thermal Simulation*, PhD thesis, Mechanical Engineering, University of Pretoria, 1994.

[2] ASHRAE, *1993 Fundamentals Handbook (SI)*, American Society of Heating, Refrigerating and Air-Conditioning Engineers, Inc., 1993.

Chapter 1

INTRODUCTION

The background to this study is given in this chapter. After the importance of integrated simulation is established, an investigation into the state-of-the-art is made. Two major fields are investigated, namely building thermal modelling, and HVAC system component modelling and its integrated simulation.

The need, major contributions and outline of this study are also presented in this chapter.

1.1 PROBLEMS ENCOUNTERED BY THE HVAC CONSULTING ENGINEER

1.1.1 Introduction

At the early design stage of a building, the engineer is asked to advise the architect on enhancing the building envelope to reduce the HVAC system size and the energy consumption. This must be accomplished without compromising the indoor thermal environment. The engineer is also expected to provide a budget price for the best HVAC system option.

He must further compare life cycle costs for different HVAC options. Both the minimum system size and life cycle cost can only be achieved successfully if a fully integrated simulation of the building, its HVAC system, and its controls can be performed by the engineer.

The consulting engineer is also frequently asked to give advice to the building owner on how energy savings can be achieved in existing buildings. Similar problems to the ones encountered during design are also found here. Additional complications are however present. The building owner would only be interested in retrofits that have short payback periods. Again this can only be achieved successfully if a fully integrated simulation of the building its HVAC system and controls can be done.

All of the above must usually be accomplished in very limited time. The engineer can thus not use the tools available to researchers, who have ample time in hand. This means that at present, minimum system size simulation, life cycle costing, and very efficient retrofits are not done satisfactorily in practice.

With an integrated building, HVAC and control simulation tool developed with the consulting engineer's specifications in mind, the consulting engineer will be able to provide a better service by solving the abovementioned problems.

1.1.2 A practical problem with a new HVAC design

A practical example best illustrates the need for the proposed integrated tool. An HVAC project, in which the author was involved, is briefly mentioned here. The work began by meeting the architect. The architect enquired about the best HVAC options for the specific building.

The development consists of seven buildings on one site. Two of the buildings are three-storeyed while the rest are double-storeyed. The total floor area is 18 833 m^2. A parking basement is provided under the buildings.

The options that had to be considered were console and split air-conditioning units, versus a chilled water central plant with fan coil units in the ceiling voids of the building zones. Answers were expected within five working days.

For the author to provide a good service and the necessary information for the architect and the developer he needed to perform a full design and life-cycle costing analyses for the various options. This presupposed that a reasonable estimate of the energy consumption, maximum demands and indoor thermal comfort for each month could be made.

To realise the maximum benefit of a central system, the consultant must suggest the best control strategy. (It is not possible to use specific control strategies with console units.) For this an integrated simulation tool is needed.

To the knowledge of the author, no consultants do a full and accurate life-cycle costing analysis including detail control and comfort simulations at this early design stage - or at any stage of the design! This is an unfortunate state of affairs since good control strategies can reduce the system size and energy consumption by up to 50% without compromising indoor comfort.

With comprehensive and quality information, good decisions can be made. Especially at this early design stage decisions significantly influence the initial and operating cost of the HVAC system. It is also the easiest to alter the course of the project at this stage. During the more advanced stages of the design any alterations will have many more cost implications.

The need for an integrated simulation tool was clearly felt when the different options had to be compared for this project.

1.1.3 A practical problem with an HVAC retrofit

An integrated simulation tool is not only needed for new designs, but also for HVAC retrofits. The author was involved with a retrofit project where the client wanted to save energy without compromising the indoor comfort.

The building is a multi-storeyed combined laboratory and office building situated approximately 35 km west of Pretoria. The building was built in the seventies and fitted with a constant volume reheat HVAC system. Originally the system was designed as a constant volume system with the supply air temperature fixed for a given zone, irrespective of the load occurring inside the building or of the outside conditions.

Usually, the most cost-effective solution to such a problem is improved control. However, to find the best control strategy is a difficult problem. The best way to solve this is by integrated building, HVAC system, and its control simulations. With the proposed tool it would be possible to simulate all possible options and choose the best one that would still ensure indoor comfort.

1.1.4 Closure

Existing research tools were found to be too difficult to use in the time limits set by the client for both the design and retrofit options. To achieve what is needed in practice a user-friendly, quick to use tool must be developed for the practicing engineer to generate this information. Such a tool was therefore developed in chapters 2, 3, 5 and 6. The solutions results for the two examples mentioned in sections 1.1.2 and 1.1.3 can be seen in sections 7.4 and 7.5.

1.2 EXISTING TECHNIQUES

1.2.1 The need for an integrated tool

The need for a simulation tool that can be used to give quick and fairly accurate answers at the initial design stage, and for retrofit studies are established in the previous sections. It is now time to give the specifications of the consulting engineer for such a tool. These can then be used to evaluate existing tools. The specifications are the following:

1. The tool should be easy to use.
2. The tool should be robust, and the user should be able to use the tool without detailed knowledge of the simulation procedure.
3. Taking the limited time that the consulting engineer has to provide the answers into account, the simulation time should not be excessively long.
4. The tool should be flexible enough to simulate all commonly used systems without undue simplifications.
5. The answers should be sufficiently accurate to warrant the tool's use for sizing, energy and indoor comfort simulations.

In order to either choose or develop a tool, a literature survey to establish the state-of-the-art will be pursued next. It is not the intention to re-invent the wheel. Firstly the building model must be considered because it is the basis of an integrated simulation tool.

1.2.2 Building thermal models

There are a number of building thermal models already available. They are discussed in detail by Richards [1]. He recommends lumped parameter models of which the QUICK program [2] is a good example.

The philosophy used in the QUICK program [2] fits in with what the author is trying to achieve here. For this reason, the building model and philosophy used in QUICK are used as a basis for this study. Unfortunately the model was originally intended as a passive simulation tool, and has some shortcomings. The most important is that internal loads are not accurately dealt with by the building model. The solution to this problem will be discussed in more detail in chapter 2.

After the building model is established, the HVAC system, its controls and its integration must be considered. Here we are not so fortunate to have a method or computer package that fits in with our philosophy. A more detailed investigation is therefore warranted.

1.2.3 Simulation techniques

In this section we will consider integrated simulations. Most simulation and energy analysis tools were found not to be fully integrated.

In the editorial of HVAC&R of October 1995 entitled *HVAC and the Building: Siamese Twins (An Integrated Design Approach)* [3], H. Hens makes the point that 'we are left with a need to find an optimal marriage between building and HVAC design'. Both the title and the statement emphasize the need to consider the building and the HVAC system in an integrated way.

There are a myriad of energy analysis tools available. Some of these are (adapted from [4]): DOE-2 [5] developed by the Lawrence Berkeley Laboratory, E-CUBE [6] originally developed by the American Gas Association, AXCESS [7] developed by Edison Electric Institute, COMTECH [8] developed by the Electric Power Research Institute, HAP E-20 [9] developed by Carrier, BLAST [10] developed by the U.S. Army Construction Engineering Research Laboratory, TAS [11] originally developed by Amazon Energy in the UK and now supported by Environmental Design Solutions Limited, and TRACE [12] developed by the Trane Company. Of these, DOE-2 is probably the most popular and comprehensive, while TAS is the most user-friendly.

System simulation programs include (again adapted from [4]) APACHE [13], CABERETS [14], HVACSIM+ [15, 16], HVAC-DYNAMIC [17, 18] and TRNSYS [19].

The primary function of an energy analysis program is to calculate system energy consumption. Various HVAC systems can be compared to reveal the system with the lowest energy consumption.

System simulation programs endeavour to predict the dynamic response of the HVAC system and the building, i.e. indoor air conditions, system operation points and energy usage. In general, these tools are more flexible with fewer restrictions placed on the applicability.

Simulation techniques cannot be discussed totally divorced from the building and HVAC system models. Calculations are usually performed sequentially (see Athienitis [20]). Firstly, a load calculation is performed using a building model, and specifying the indoor temperature.

Secondly, the system calculations are performed, determining the thermodynamic response of the various components in the air-handling units. Thirdly, the plant equipment responsible for energy conversion, such as boilers and chillers, is calculated. For these simulations, various control sequences can be specified.

Some of the techniques implemented in the design tools will be discussed in detail, also referring to the way in which the building and system simulation is performed.

In DOE-2 [5], the load calculation is based on the combined response factor method and the weighing factor method. The system model is then applied to the load output of the building model, and the plant model is applied to the results of the system model. This decoupling of the various elements could result in errors. The real controller will invariably not keep the indoor temperature exactly at the right temperature resulting in the storing effects being incorrectly simulated.

This problem is addressed in the DOE-2 (see ASHRAE [21]) program by using air weighting factors, but even so substantial errors can be introduced if the indoor temperatures vary greatly. Varying indoor temperatures can be encountered due to a number of conditions, such as large internal loads in a well-insulated building, badly tuned controllers, and large diurnal outdoor temperature swings.

As described by Rousseau [22], the decoupling of the system and plant models also poses problems. It could happen that the system requires a larger capacity than the plant can deliver. In DOE-2 an overload is reported, but in real life this would imply that the indoor temperature cannot be maintained seeing that the load cannot be offset.

For a detailed discussion on the Custom Weighting Factor Method as implemented in DOE-2, reference [23] can be consulted.

A separate load calculation model based on the response factor method is used to determine the loads that are used in the building model of HVACSIM+. No load modelling is attempted with the system simulation. Thus the problem of varying indoor temperature will also be experienced here [22].

This is not entirely true. According to Cheol Park [24], the building model is not necessarily solved at each time step, since the building response is not as fast as the system's response. The building model can however be solved in an integrated fashion.

In the HVACSIM+ program it is assumed that the plant has infinite capacity. A realistic interaction between the plant and the system can thus not be simulated [22]. This method of simulating the plant can be used if, for example, the water inlet temperature to the secondary cooling equipment is specified as a boundary condition [24]. However, the program can simulate the plant operation in detail.

The execution time on an AT personal computer to obtain a simulation for a typical HVAC system (consisting of a heating coil, pumps, piping, a valve and a controller) for 24-hour operation could take up to 10 hours. This information is a little outdated. The only other substantiating remark found in the literature was the comment by Hanby [25]: HVACSIM+ and TRNSYS '... generally have long execution times, often of the order of real time, which inhibits their use in a design context.'

APACHE makes use of a detailed finite difference technique to simulate the building envelope. It is well known that these techniques require substantial numerical effort to solve. The building model should however be suitable for use as a comparison tool in order to compare simpler solution procedures. This is done by Tindale [26].

A number of validation studies have been recorded in the available literature. Not all of them will be mentioned here but some are of interest. Zmeureanu et al. [27] discussed inter-program and analytical validation of a program CBS-MASS. Unfortunately the program does not include HVAC system simulation, but the comparisons provide valuable information on the agreement of the cooling load calculations and the indoor temperature responses. The program is compared to BLAST and TARP [28]. The comparisons show differences of less than 7 per cent between the estimations of peak load and of daily total load provided by the CBS-MASS program and the predictions of the BLAST and TARP programs.

In 1988 Winkelmann [29] reviewed six building energy simulation programs, HVACSIM+, GEMS, ENET, TARP, BESA, and BEVA. HVACSIM+ uses a hierarchical description and a variable time stepping method. A component-based methodology is followed based on the TRNSYS program. The simulation procedure is:

1. A building is divided into components each of which is described by a FORTRAN subroutine from a component library.
2. The user assembles an arbitrary system by linking component inputs and outputs, and by assigning component performance parameters.
3. The program solves the resultant set of non-linear algebraic and differential equations to determine the system's response at each time step.

The user is expected to break the system into blocks and superblocks in order to increase computation efficiency.

GEMS [30] follows a state-space approach used in control theory. In GEMS, the system processes are cast into the state-space form by deriving lumped parameter equations at each node from Taylor series expansions or conservation equations. Sparse-matrix techniques and user-selected integration methods are then used to solve the resultant system of equations.

GEMS allows a wide range of simulation detail to be handled, from full thermal coupling between zones, to simplified, fast executing models for non-critical components. The state-space approach relies heavily on matrix manipulation, so in the 1980's it was ideally suited to computers with array processors.

An approach developed by the IBM Los Angeles Scientific Centre is called ENET. This program generates customised, optimised code that reduces the number of variables that have to be solved. At the time, the procedure only handled steady-state time-independent systems.

TARP [31] is an evolutionary development of BLAST. TARP does not have equipment simulation capabilities, but does contain detail of interzone heat transfer. Heat balances are calculated at each time step between the various surfaces and the room air, which is assumed constant throughout the room. Air flow through the rooms is calculated by taking the wind and thermal effects into account.

BESA (building energy system analysis) consists of twelve packages tailored to the needs of building design processes [32]. The packages were planned to be menu driven, and designed to run on a personal computer. One component of the packages is a small time step TRNSYS-like component-based simulation capable of modelling energy management control systems.

The last approach, discussed by Winkelmann, is BEVA macroscopic analysis. This tool uses measured data from the building to set up the transfer functions for the building performance. The tool can then be used to predict future trends.

Hensen [33] reported in 1993 that: 'early research focussed on the relation between building design and energy consumption. Only later was more attention directed to the plant side of the overall problem domain.' He also points out that with the former approach the HVAC system is more or less neglected, while in the latter approach the complex building energy flow dynamics were over-simplified. He comes to the conclusion that both the building and the HVAC system must be simulated in similar detail and completeness.

A historical description of the development of building energy calculations is provided by J.M. Ayres and E. Stamper [34]. In their opinion, the most widely used and continuously supported proprietary programs are TRACE, HAP, HCC(loads), and ESP(energy). The first two have been discussed previously and the last one was developed by Automated Procedures for Engineering Consultants Inc.(APEC).

The two major public domain software tools are BLAST and DOE-2 (again according to reference [34]). These tools evolved from two opposing load calculation methods. BLAST is based on an ASHRAE heat balance algorithm, and DOE-2 is based on transfer functions and weighting factors.

As stated earlier, their perspective is a historical one and few technical details of the programs and procedures are given. They do however end their discussion with the opinion that most of the

future effort will be used to improve the user interface.

Energy efficiency retrofit studies conducted in Sweden, and reported on in reference [35], are based on Carrier's HAP (Hourly Analysis Program).

Staib et al. [36] reason that the downturn in the economy (in the USA) and stricter environmental policy are prompting more building owners to undertake retrofit projects. One of the primary steps is to model the existing building, and to compare various suggestions for energy savings using energy analysis programs. Unfortunately they do not recommend any programs.

Athienitis [37] proposes a methodology for integrated building and HVAC system thermal analysis. This method uses LaPlace transfer functions of the building and the HVAC system and controls. Integrating the complete system is done by obtaining the transfer function for a system as a whole from standard block diagram control theory. The response of the system is obtained by an efficient numerical LaPlace transform inversion technique.

Markov models are investigated for simulation of long-term building and HVAC systems by Hanby and Dil [25]. They propose techniques for finding the optimal discretisation of the simulation models to reduce the error introduced by the discretisation.

They claim that this modelling technique can reduce the execution time of the simulations when compared to simulations performed on HVACSIM+ and TRNSYS (which they claim 'generally have long execution times, often of the order of real time, which inhibits their use in a design context.'). They do give accuracy and number of variables (bins) obtained, but do not compare the execution times with the two simulation codes mentioned.

Many integrated design tools are proposed. The ICAtest [38] system employs a common building model (CBM) that can provide building data to a range of design tools. These include a simple thermal design simulation tool SUNCODE, DOE-2, weather data files and the DXF exchange standard for CAD systems.

A second integration project is the EU COMBINE project [39, 40]. This project uses the STEP standard as the data standard between various building design programs. These include inter alia DOE-2, a lightning tool, VENT (a duct sizing program), and ESP (a building simulation program).

Robin et al. [41] report on the SETIS program. This program supports the thermal design of buildings and the HVAC system. SETIS also has decision-making abilities facilitating the adherence to design goals previously fixed by the user.

They also point out the shortcomings of software systems that are available. Firstly, these systems often dissociate the building envelope and the HVAC system. Secondly, the largest part of the software is devoted to qualitative studies. These approaches are restrictive in the whole design process. They propose a systems approach to solving this problem.

An interesting application of a building simulation tool is using it as an emulator for testing energy management and control system. The emulator uses building simulation programs to determine the response of the system to inputs that are generated by real controller hardware. Feedback from the building simulation program occurs via a digital to analogue interface.

In the specific application reported in reference [42], the simulation software used is HVACSIM+ and TRNSYS. This gives us an indication that these are the most comprehensive simulation tools. Applications for such an emulator are:

1. testing and comparison of EMC systems,
2. designing and testing control strategies,
3. pre-commissioning EMC systems, and others.

Simulation tools are not to be used blindly. To substantiate this statement, refer to Haberl et al. [43] and Norford et al. [44]. Haberl et al. [43] propose an algorithm to calibrate the simulation program DOE-2 (DOE-2.1D).

The hundreds of input variables are adjusted to obtain good agreement between measured and simulated results. They distinguish between weather dependent and non-weather dependent data. A procedure is proposed for the calibration of non-weather dependent data.

They report a discrepancy of 26% (under estimation) between the uncalibrated program and measured data for the same six-month period. After the calibration, the discrepancy is reduced to 4%.

Descrepancies of two-to-one are reported for simulated and as-built buildings [44]. Energy usage by the occupants accounted for 64% of the two-fold discrepancy. Equipment being operated for more than the predicted 10 hours per weekday contributed 24% of the underprediction. The remaining 12% is attributed to equipment that did not operate to standard.

These comments are not necessarily intended as criticism of the simulation tool, in this case DOE-2, but as a warning to users of these tools not to rely blindly on the results obtained.

From the discussion in this section it could be seen that no tool exists that satisfies all the specifications of the engineer as set out in section 1.2.1.

Component models

Now that we have discussed HVAC simulation methods it is time to investigate the models for the HVAC components.

The detailed energy transfer processes in HVAC components are well known. Heat transfer coefficients for various situations can be determined from theory and empirical data. To model the transfer processes at this level however will result in models that require lots of numerical effort to solve. Instead, fairly accurate correlation equations can be used to estimate the response of the major HVAC components. These simplifications can reduce the numerical effort to solve the various models. It would thus require less numerical effort to predict the interaction among various components.

Component models for various components were presented by Rousseau [22]. Rousseau classifies models according to the following categories:

1. Purely empirical models.
2. Semi-empirical models.
3. Semi-theoretical models.
4. Fundamental principle models.

The models presented are steady-state models that use correlation coefficients. Correlation coefficients are obtained from regression of the model equation on performance data from the supplier's data sheets, or if these are lacking, from experimental results.

A toolkit has been developed by Brandemuehl and Gabel [45], sponsored by the ASHRAE technical committee TC 4.7. The toolkit reported on provides simplified and complex models of the various HVAC components. The routines are written in ANSI FORTRAN 77 and standard variable names are given. Unfortunately the authors do not mention if the models are dynamic or steady state in nature.

Having considered the models and the integrated simulation, we next consider the control state-of-the-art.

1.2.4 New controller initiatives in building and HVAC systems

In the simulation tool presented in this study, the basic controls that are in common use in practice are modelled. In this section, some of the latest developments in the HVAC control field will be mentioned and will be considered as suggestions for further work.

There have been a proliferation of papers and articles applying new controller technologies to HVAC systems. These include neural nets and fuzzy logic control.

Neural net technology uses the concept of neurons that are connected in a network topology. The neurons have a number of internal parameters called weights. These weights can be "trained" to produce a relation between the input and output.

Curtiss et al. [46] present a proof of concept experiment for local and global control of HVAC systems. Their conclusions are that considerable savings are possible when ANN methods are used to adapt the plant setpoints to match the current loads.

Mistry and Nair [47] propose the use of neural nets for the calculation of non-linear HVAC computations. The authors claim that the neural networks are computationally faster than standard methods to calculate typical psychrometric functions and PMV calculations.

Sebald and Schlenzig [48] discuss the application of neural net controllers for highly uncertain plants. HVAC applications are given as an example where the techniques can be implemented fruitfully.

Neural control of a non-linear HVAC plant is presented by Hepworth and Dexter [49]. The authors compare standard PI (proportional plus integral) control performance with that achieved by neural control. The response is characterised by the maximum absolute error. For their example, the error is 0.6 °C for a well-tuned PI controller, while the neural controller produces errors of 0.32 °C.

Fuzzy logic controllers use a set of *if-then* rules to model the system under consideration. Fuzzy set theory was first introduced by Zadeh [50] in 1965, and is an extension of classical set theory.

Applying the fuzzy control theory and decision support to HVAC system control is the subject of two papers [51, 52]. The conclusions by Kajl et al. [51] are that building loads can be predicted satisfactorily. They compared their modelling to results obtained with DOE-2. Such predictions may be useful for the purposes of HVAC diagnostics, identification, control and energy management optimisation.

Arima et al. [52] do not compare results to standard HVAC control methods. They do however show that the techniques could be applied successfully to HVAC control applications.

After discussing the building model, HVAC component models, controls and the integration of these models, the need for this study, based on the literature survey, will be summarised.

1.2.5 A summary: needs identified from the literature

The need for this project can probably best be paraphrased in the words of LeBrun [53]. He discusses the simulation of building, HVAC systems and its control and notes that '*The dream of many engineers is to find simulation software allowing them to go, without any discontinuity, through all steps of a technical production: early design, selection and sizing of components, system optimization, control design and testing, system balancing and commissioning, control tuning, system management, audit and monitoring, retrofits, etc ...*'

Further according to LeBrun: *'The main challenges from now (1994) are:*

1. *to propose models easy to understand, easy to use and improve whenever necessary;*
2. *to produce reference data allowing the user an easy parameter identification;*
3. *to introduce the simulation in earliest design stages and develop the simulation models in such a way that they can be used all along the "life" of the system.'*

The aim of this project is to address all the issues as stated by LeBrun [53], by developing a tool with the consultant's and LeBrun's specifications in mind.

1.3 THE NEED, OBJECTIVES AND CONTRIBUTIONS OF THIS STUDY

1.3.1 introduction

It was shown, through practical examples and trough a literature review, that fully integrated simulation is a helpful tool for retrofit studies to obtain energy saving suggestions, and to perform problem finding in existing HVAC systems. These techniques could also be of great benefit to the engineer at the design stage, for equipment size and energy consumption reduction.

Although the author has shown that there are a myriad of partially integrated building, HVAC system and control simulation tools available to the researcher, it has been our experience that none of these tools are used on a day-to-day basis by practicing engineers.

There is a need for a fully integrated user-friendly building energy simulation tool developed to the specification of the consulting engineer. The tool should be easy to master and at the same time, give representative answers to the questions that are usually answered with simulation tools.

In order to contribute to the field of user-friendly simulation tools that are also fully integrated, the following objectives are set for this study.

1.3.2 First objective: a building model

Firstly, building models are usually extremely complex and require long computer execution times to solve. Secondly, these building models are not flexible enough to allow direct integration with the rest of the plant and system models.

The first objective of this study is thus to establish a building thermal model that would be simple enough to incorporate into an integrated simulation tool. This building thermal model will also have to be sufficiently accurate and substantially verified.

1.3.3 Second objective: integrated simulation

The overall objective of this study is to accomplish integrated simulation. The simulation should be efficient so that several design and retrofit options can be investigated in one day. The results should be verified sufficiently.

Component modelling

Various component models have already been established. Inadequacies in some of these models have been identified and the models will be enhanced.

Control modelling

Control modelling is also improved to simulate reality more closely.

1.3.4 Contributions of this study

The major contributions of this study are:

1. A new building thermal model.
2. Extending component models to incorporate dynamics and part-load performance.
3. Implementation of energy management systems.
4. A user-friendly simulation tool.

1.4 OUTLINE OF THIS STUDY

The new thermal model for predicting heat transfer in building zones is presented in chapter 2. This provides a basis for the integrated thermal modelling of the building and HVAC system. The model makes provision for the main aspects that need to be treated in building passive simulation as well as a convenient interface between the building and an HVAC system.

In chapter 4 an application of the passive model is presented. This application is currently being used to certify all the official low-cost houses that are built in South Africa as part of the Reconstruction and Development Programme (RDP). The program used the proposed thermal model in chapter 2 to predict the indoor air temperature. Prediction of condensation is done by solving the heat flow through each surface in order to obtain the surface temperature.

A detailed discussion on the implementation of integrated design is given in chapter 5. Aspects covered are the solution approach and optimisation, the extensions to existing models and the introduction of new models.

Modern Direct Digital Control (DDC) systems provide the control engineer with many Energy Management Systems (EMS). It would be extremely useful if a simulation tool could predict the potential savings of such systems. The implementation of EMS is discussed in chapter 6.

An application of integrated simulation and how it can be used to predict energy savings in buildings is presented in chapter 7. This illustrates the usefulness of integrated simulation to HVAC scientists.

Finally in chapter 8, recommendations for future work are presented.

Bibliography

[1] P.G. Richards. *A Design Tool for the Thermal Performance of Buildings*. PhD thesis, Mechanical Engineering, University of Pretoria, 1992.

[2] CENT. *User's and Reference Manual for QUICK A Thermal Design Tool and Load Calculation Computer Program*. Centre for Experimantal and Numerical Thermoflow, P.O.Box 32011, Faerie Glen, 0043, Republic of South Africa, 4.0 edition, July 1991.

[3] H. Hens. Hvac and the building: Siamese twins (an integrated design approach). *HVAC&R*, 1(4), October 1995. Editorial.

[4] P.G. Rousseau and Mathews E.H. Needs and trends in integrated building and HVAC thermal design tools. *Building and Environment*, 28(4):439–452, 1993.

[5] B. Birdsall, W.F. Buhl, Ellington K.L., Erdam A.E., and F.C. Winkelmann. Overview of the DOE-2 building energy analysis program. Technical report, Simulation Research Group, Lawrence Berkeley Laboratory, University of California, Berkeley, California, 94720, 1990.

[6] D. Pedreya and V. Bush. PC-CUBE simulates hourly electric demand and energy consumption. *Energy Engineering*, 89:23–37, 1992.

[7] R.H. Howell and H.J. Sauer. Energy efficiency and conservation of building HVAC system using the AXCESS energy analysis. In *Second Annual Conference on Energy*, Rolla, 7-9 October 1975.

[8] K.E. Fuller and I. Rohmund. COMTECH for commercial building system analysis. *Energy Engineering*, 89:6–22, 1992.

[9] Climatisation and Development Group. *Overview of the Hourly Analysis Program*. CARRIER, 12 Rue de Paris - 78230, LE PECQ, 1992. Available from Carrier SA.

[10] L.K. Lawrie. Day-to-day use of energy analysis software. *Energy Engineering*, 89:41–51, 1992.

[11] M.C.B. Gough. Component based building energy system simulation. *International Journal of Ambient Energy*, 7:137–143, 1986.

[12] J. Althof. Marketing and productivity opportunities of computer aided system design. *Energy Engineering*, 84:4–29, 1987.

[13] S.J. Irving. APACHE - an integrated approach to thermal and HVAC system analysis. *International Journal of Ambient Energy*, 7:129–136, 1986.

[14] A.E. Samual and T.H. Chia. Simulation of the full and part load energy consumption of HVAC system of building. *Building and Environment*, 18:207–218, 1983.

[15] C. Park, D.R. Clark, and G.E. Kelly. *HVACSIM Buildings Systems and Equipment Simulation Program: Building Loads Calculation.* Gaithersburg, MD 20899, February 1986.

[16] C.R. Hill. Simulation of a multizone air handler. *ASHRAE Transactions*, 91(Part1B):752–765, 1985.

[17] O. Ogard, V. Novakovic, and G. Brustad. HVAC-DYNAMIC - a training simulator for dynamic analysis of HVAC plants. In *Selected Papers IFAC Symposium on Computer Aided Design of Control Systems*, Beijing, PRC, 23-25 August 1988.

[18] M. Heintz, O. Ogard, V. Novakovic, and G. Brustad. HVAC-DYNAMIC - a training simulator for dynamic analysis of HVAC plants. *Modeling, Identification and Control*, 10:159–164, 1989.

[19] W.A. Beckman, L. Broman, Fiksel A., S.A. Klein, E. Lindberg, M. Schuler, and J. Thornton. TRNSYS the most complete solar energy system modeling and simulation software. In A.A.M. Saying, editor, *Renewable Energy Climate Change Energy and the Environment: World Renewable Energy Congress*, Reading, U.K., September 1994. Pergamon.

[20] A.K. Athienitis, M. Stylianou, and J. Shou. A methodology for building thermal dynamics studies and control applications. *ASHRAE Transactions*, 2:839–848, 1990.

[21] American Society for Heating Refrigeration and Air Conditioning Engineers, Inc. *ASHRAE Handbook*, 1992.

[22] P.G. Rousseau. *Integrated Building and HVAC Thermal Simulation.* PhD thesis, Mechanical Engineering, University of Pretoria, 1994.

[23] J.F. Kerrisk, N.M. Schnurr, J.E. Moore, and B.D. Hunn. The custom weighing-factor method for thermal load calculations in the DOE-2 computer program. In *ASHRAE Transactions*, volume 87, 1981.

[24] C. Park. Private telephone conversation tel. (301) 975-5879. Conversation concerning modelling of building and central plant in HVACSIM+, 20 May 1997.

[25] V.I. Hanby and A.J. Dil. Error prediction in Markov models of building/HVAC systems. *Applied Mathematical Modelling*, 20(8):608–613, August 1996.

[26] A. Tindale. Third-order lumped-parameter simulation method. *Building Services Engineers Research and Technology*, 14:87–97, 1993.

[27] R. Zmeureanu, P. Fazio, and F Haghighat. Analytical and inter-program validation of a building thermal model. *Energy and Building*, 10:121–133, 1987.

[28] G. Walton. Thermal analysis research program. In *Proceedings of the Second International CIB Symposium*, Copenhagen, Denmark, 28 May to 1 June 1979.

[29] F. Winkelmann. Advances in building energy simulation in North America. *Energy and Buildings*, 10:161–173, 1988.

[30] R. Benton, J.K. MacArthur, Mahesh, and Cockroft J.P. Generalized modeling and simulation software tools for building systems. *ASHRAE Transactions*, 88(II), 1982.

[31] G.N. Walton. *Thermal Analysis Research Program Reference Manual*. National Bureau of Standards, NBSIR 83-2655, 1983.

[32] D. Seth. BESA, Canada's solution to the user interface. In *Proceedings of the Building Energy Simulation Conference*, Seattle, August 1985.

[33] J.L.M. Hensen. Towards an integrated appoach of building HVAC system. *Energy and Building*, 19(4):297–302, 1993.

[34] J.M. Ayres and E. Stamper. Historical development of building energy calculations. *Ashrae Journal*, pages 47–55, February 1995.

[35] P. Nilsson, S. Aronsson, and L. Jagemar. Energy-efficient retrofitting of office buildings. *Energy and Buildings*, 21(3):175–185, 1994.

[36] J. Staib, M. Syal, and D. Peters. Computer based energy analysis for mechanical retrofit of buildings. In *Proceedings of the 1st Congress on Computing in Civil Engineering*, volume 2, Washington, DC, 1994.

[37] A.K. Athienitis. A methodology for integrated building - HVAC system thermal analysis. *Building and Environment*, 28(4):483–496, October 1993.

[38] R. Amor, J. Hosking, and M. Donn. Integrating design tools for total building evaluation. *Building and Environment*, 28(4):475–482, October 1993.

[39] J. Donnelly, J. Flynn, and P.F. Monaghan. Integration of energy simulation and ventilation design tools via an object oriented data model. *Renewable Energy*, 5(5):1190–1192, August 1994.

[40] J. Kennington and P.F. Monaghan. COMBINE: the HVAC-design prototype. *Building and Environment*, 28(4):453–463, October 1993.

[41] C. Robin, J. Brau, and J.J Roux. Integration of expert knowledge and simulation tools for the thermal design of buildings and energy systems. *Energy and Buildings*, 20(2):167–175, 1993.

[42] S. Wang, P. Haves, and P Nusgens. Design, construction, and commissioning of building emulators for emcs applications. In *ASHRAE transactions: Proceedings of the ASHRAE Winter Meeting*, volume 100, New Orleans, LA, 1994.

[43] J.S. Haberl, J.D. Bronson, S.B. Hinchey, and D.L. O'Neal. Graphical tools to help calibrate the DOE-2 simulation program. *ASHRAE Journal*, 35(1):27–32, January 1993.

[44] L.K. Norford, R.H. Socolow, E.S. Hsieh, and G.V. Spadaro. Two-to-one discrepancy between measured and predicted performance of a 'low-energy' office building: Insights from a reconciliation based on the DOE-2 model. *Energy and Buildings*, 21(2):121–131, 1994.

[45] M.J. Brandemuehl and S. Gabel. Development of a toolkit for secondary HVAC system energy calculations. In *ASHRAE Transactions: Proceedings of the ASHRAE Winter Meeting*, volume 100, New Orleans, LA, USA, 1994.

[46] P.S. Curtiss, J.F. Kreider, and Brandemuehl. Artificial neural networks proof of concept for local and global control of commercial building HVAC systems. In *Solar Engineering 1993:ASME International Solar Energy Conference*, New York, NY, 1993. ASME.

[47] S.I. Mistry and S.S. Nair. Nonlinear HVAC computations using neural networks. *ASHRAE Transactions*, 99:775–784, 1993.

[48] A.V. Sebald and J. Schlenzig. Minimax design of neural net controllers for highly uncertain plants. In *IEEE Transactions on Neural Networks*, volume 5, January 1994.

[49] S.J. Hepworth and A.L. Dexter. Neural control of non-linear HVAC plant. In *IEEE Conference on Control Applications*, volume 3, Glasgow, UK, 1994. IEEE.

[50] A.L. Zadeh. Fuzzy sets. *Information Control*, 8:338–353, 1965.

[51] S. Kajl, P. Malinowski, E. Czogala, and M. Balazinski. Prediction of building thermal performance using fuzzy decision support system. In *Proceedings of the 1995 IEEE International Conference on Fuzzy Systems*, volume 1, Yokohama, Japan, 1995. IEEE.

[52] M. Arima, E.H. Hara, and J.D. Katzberg. Fuzzy logic and rough set controller for HVAC systems. In *Proceedings of the 1995 IEEE WESCANEX Communications, Power, and Computing Conference.*, volume 1, New York, 1995.

[53] L. LeBrun. Simulation of HVAC system. *Renewable Energy*, 5(5):1151–1158, August 1994.

Part I

Passive Building Modelling

Chapter 2

NEW THERMAL MODEL FOR BUILDING ZONES

An accurate and efficient thermal model of the heat transfer processes in a building is essential for the accurate prediction of the thermal performance of buildings. The model presented in this chapter is a compromise between simplicity and accuracy. Although comprehensive finite difference techniques are available to determine the thermal performance of buildings, these are often computationally time consuming. A simple yet accurate model is needed if integrated building and HVAC system simulation is to be achieved.

Eventually the model presented here will be incorporated into an integrated simulation. The model would however also be applicable to passive simulations.

NOMENCLATURE

a	$\sqrt{\omega k \rho c_p}$
Area	Area, m^2
A,B,C,D,	
E,F,G,H	Elements in the transfer matrix
acs	Air changes per second
c_p	Thermal capacity of building material, J/kgK
C	Thermal capacity, J/kgK
h	Convection heat transfer coefficient, W/m^2K
i	Imaginary unit operator
k	Thermal conductivity of the slab, W/mK
q	Heat flow, W
Q	Heat source, W
R	Thermal resistance across the surface, K/W
T	Absolute temperature, K
Vol	Volume, m^3
Z	Impedance, K/W
Δ x	Thickness of slab, m
ε	Error
ρ	Density, kg/m^3
τ	$\sqrt{\frac{\omega \rho c_p (\Delta x)^2}{2k}}$
ω	Excitation angular frequency, rad/s

Subsripts

a	air
c	convective
e	envelope
hm	high mass
i	inside
im	inside mass
lm	low mass
o	outside
r	radiative
s	surface
ss	steady state
t	total
v	ventilation
z	zone

2.1 INTRODUCTION

The aim of this chapter is to develop a new thermal building model. Previous work done by Richards [1], which resulted in a first-order building model. was used as a point of departure. The aim of his study was to accurately predict the behaviour of passive buildings.

A thorough investigation into the applicability of a first-order model to building zones showed that first-order models do not adequately represent the thermal response of thermally thick elements. It was found that the first-order model, as proposed by Richards [1], gives very good results for passive buildings where no heat sources are present inside the building zone.

Results for buildings with air-conditioning equipment installed are however not accurate enough. In validation calculations, differences of up to 80 % were found in peak load predictions, and up to 50 % difference in average loads predicted by the first-order model and numerical methods. This prompted further investigation.

The philosophy used here is similar to that used by Richards. Here the building transfer properties (expressed as transfer matrices) are obtained numerically. Elements in the transfer matrix of the model are compared to corresponding elements in the building transfer matrix, and the sum of the square of the differences of the corresponding elements is minimised.

2.2 BUILDING TRANSFER PROPERTIES

A theoretically rigorous procedure will be followed here to find the heat flow in a building zone. First the heat flow through a single wall will be discussed. The heat flow through various walls can then be added to find the heat flow in a zone as a whole. At this stage, the radiative and convective heat generated in the zone will not be included. The theory is established here to facilitate the finding of parameters for use in the electrical analogy to be introduced later.

2.2.1 Wall transfer matrices

The heat flux through a single homogeneous element is well established and can be written as a transfer matrix, given by

$$\begin{bmatrix} T_{os} \\ q_{os} \end{bmatrix} = \begin{bmatrix} A & B \\ C & D \end{bmatrix} . \begin{bmatrix} T_{is} \\ q_{is} \end{bmatrix} . \tag{2.1}$$

Walls consisting of different layers can be represented by multiplying the individual layers to obtain

$$\begin{bmatrix} A & B \\ C & D \end{bmatrix} = \begin{bmatrix} A_1 & B_1 \\ C_1 & D_1 \end{bmatrix} \cdot \begin{bmatrix} A_2 & B_2 \\ C_2 & D_2 \end{bmatrix} \cdots \begin{bmatrix} A_n & B_n \\ C_n & D_n \end{bmatrix}. \tag{2.2}$$

For a homogeneous slab of any thickness, the elements are given by:

$$A = \cosh\tau\cos\tau + i\sinh\tau\sin\tau \tag{2.3}$$

$$B = (\cosh\tau\sin\tau + \sinh\tau\cos\tau)/(a\sqrt{2}) + i(\cosh\tau\sin\tau - \sinh\tau\cos\tau)/(a\sqrt{2}) \tag{2.4}$$

$$C = (-\cosh\tau\sin\tau + \sinh\tau\cos\tau)a/\sqrt{2} + i(\cosh\tau\sin\tau + \sinh\tau\cos\tau)a/\sqrt{2} \tag{2.5}$$

$$D = \cosh\tau\cos\tau + i\sinh\tau\sin\tau \tag{2.6}$$

where

$$\tau = \sqrt{\frac{\omega\rho c_p(\Delta x)^2}{2k}} \tag{2.7}$$

and

$$a = \sqrt{\omega k\rho c_p}. \tag{2.8}$$

Further

- ω is the excitation frequency, Hz
- ρ is the density of the slab, kg/m^3
- c_p is the thermal capacity of the slab, J/kgK
- k is the thermal conductivity of the slab, J/mK, and
- Δx is the thickness of the slab, m.

The transfer matrix for the film resistance is

$$\begin{bmatrix} T_{os} \\ q_{os} \end{bmatrix} = \begin{bmatrix} 1 & \frac{1}{h_i Area} \\ 0 & 1 \end{bmatrix} \cdot \begin{bmatrix} T_{is} \\ q_{is} \end{bmatrix} \tag{2.9}$$

Here h_i is the convective heat transfer coefficient for the inside of the slab, J/m^{2}K.

Obtaining the overall transfer properties for a single non-homogeneous wall consisting of several homogeneous layers is then a matter of complex matrix multiplication.

2.2.2 Zone transfer matrices

Equations 2.1 - 2.6 then describe the thermal response for a wall of any construction. Various walls then have to be combined to obtain the overall transfer properties for a zone. The transfer presented in equation 2.1 can be rewritten as

$$\begin{bmatrix} q_{os} \\ q_{is} \end{bmatrix} = \begin{bmatrix} D/B & -1/B \\ 1/B & -A/B \end{bmatrix} . \begin{bmatrix} T_{os} \\ T_{is} \end{bmatrix} = \begin{bmatrix} E & F \\ G & H \end{bmatrix} . \begin{bmatrix} T_{os} \\ T_{is} \end{bmatrix} . \tag{2.10}$$

The total heat flow into the zone can then be added

$$\begin{bmatrix} q_{oz} \\ q_{iz} \end{bmatrix} = \begin{bmatrix} q_{os1} \\ q_{is1} \end{bmatrix} + \cdots + \begin{bmatrix} q_{osn} \\ q_{isn} \end{bmatrix} = \begin{bmatrix} E_1 & F_1 \\ G_1 & H_1 \end{bmatrix} . \begin{bmatrix} T_{os1} \\ T_{is1} \end{bmatrix} + \cdots + \begin{bmatrix} E_n & F_n \\ G_n & H_n \end{bmatrix} . \begin{bmatrix} T_{osn} \\ T_{isn} \end{bmatrix} . \tag{2.11}$$

For the complete zone the various walls can be combined by

$$E = E_1 + E_2 + \ldots + E_n \tag{2.12}$$

with similar expressions for F, G and H.

After the zone matrix has been obtained, equation 2.10 has to be rewritten in the form of equation 2.1. The elements are given by:

$$B = 1/G \tag{2.13}$$

$$D = EB \tag{2.14}$$

$$A = -HB \tag{2.15}$$

$$C = \frac{AD - 1}{B} . \tag{2.16}$$

Equation 2.16 results from the fact that the determinants of the transfer matrices are unity with no complex component, i.e. 1 + i0.

2.2.3 Equivalent forcing temperature

Equating the right-hand side of equation 2.10 and equation 2.11 results in an equivalent temperature forcing function.

$$\begin{bmatrix} T_{oz} \\ T_{iz} \end{bmatrix} = \begin{bmatrix} E & F \\ G & H \end{bmatrix}^{-1} \left\{ \begin{bmatrix} E_1 & F_1 \\ G_1 & H_1 \end{bmatrix} . \begin{bmatrix} T_{os1} \\ T_{is1} \end{bmatrix} + \cdots + \begin{bmatrix} E_n & F_n \\ G_n & H_n \end{bmatrix} \begin{bmatrix} T_{osn} \\ T_{isn} \end{bmatrix} \right\}. \quad (2.17)$$

This equation, in conjunction with equation 2.10, would result in the complete solution for a building zone. The matrix representation is in the frequency domain, and to get the complete solution, transforming this solution into the time domain would be necessary. This is a simple procedure, but it will not be pursued here.

2.3 AN ELECTRICAL ANALOGY

The question can rightfully be asked: if we have an analytical solution for the heat flow into a building zone, why is an electrical analogy necessary? There is really only one reason. In the analytical solution provided in the previous section, it is assumed that the spectra of all the relevant parameters are known beforehand.

This is not generally true, e.g. when an air-conditioning unit is used in the unit that is controlled, implying that the operation is dependent on the solution to the equations given in the previous section. Thus, for a simulation model that endeavours to simulate the building zone with the air-conditioning plant and its controls, another approach is required.

The transfer matrix for a building zone consists of four complex elements for a given frequency. The real and imaginary parts are counted as separate quantities, resulting in eight elements for which the values have to be determined. There is however a relation between the elements, i.e. the determinant of the matrix, $AD - BC$, is equal to $1 + i0$, thus reducing the number of independent values to six.

Theoretically, six independent parameters would be adequate to exactly predict the thermal response for a building zone for a given frequency excitation (see Davies [2]). Keeping with the philosophy that the thermal model has to be physically interpretable, negative values of the thermal capacities and resistances cannot be allowed. This restricts the values of the model and thus the six parameters cannot generally adequately describe the transfer matrix. Further physical restrictions on the values of C_i and R_i are:

1. the steady state thermal resistance used in the model must be equal to the total thermal resistance of the building; and

2. the total capacity used in the model must be equal to the thermal capacity of the building. This reduces the number of independent parameters by two. (The second restriction will be relaxed later.)

Any model to represent the actual transfer matrix at a given frequency would thus need six independent parameters. An asymmetric T-section (first-order model) would have only one independent parameter, i.e. the ratio of the resistance placed on the outside of the mass. A second-order model would have five parameters, three of which are independent and can be chosen within the constraints of total resistance and total capacitance. A third-order model would have five independent parameters, seven in all. Higher order models could thus be used, but the calculation procedure would then become progressively more complex.

The frequency of the excitation also has to be considered. Richards [1], Davies [2], Tindale [3] and other workers in the field have all used 24 hours as the dominant period. That approach was thought to be sound but, adequate accuracy was not obtained. Taking only 24 hours as a dominant period is justifiable for passive buildings, but for active buildings the assumption is not generally valid.

2.3.1 Third-order model

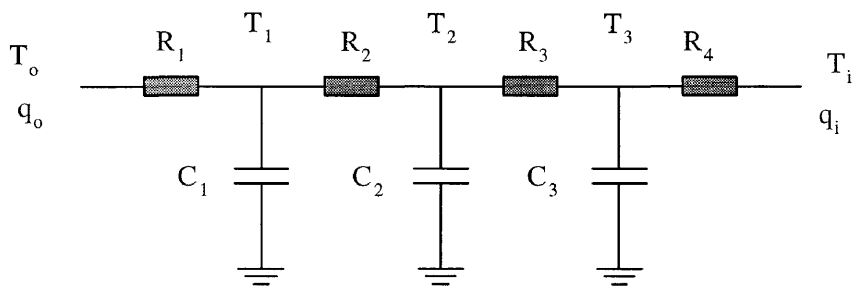

Figure 2.1: Three-capacitor representation of a building element.

The third-order model is treated first since the lower order models are just special cases of this more general model. Equation 2.1 is equally applicable to the model of three masses and four resistances. The elements for the matrix can be obtained for a 3-T configuration (shown in figure 2.1), by multiplying the matrices for three single T sections. They are:

$$Re\{A_{3rd}\} = 1 - \omega^2[C_1C_2R_1R_2 + C_1C_3R_1(R_2+R_3) + C_2C_3R_3(R_1+R_2)] \tag{2.18}$$

$$Im\{A_{3rd}\} = \omega[C_1R_1 + C_2(R_1+R_2) + C_3(R_1+R_2+R_3)] - \omega^3C_1C_2C_3R_1R_2R_3 \tag{2.19}$$

$$\begin{aligned} Re\{B_{3rd}\} = \quad & (R_1+R_2+R_3+R_4) \\ & -\omega^2[C_1C_2R_1R_2(R_3+R_4)+C_1C_3R_1(R_2+R_3)R_4+C_2C_3(R_1+R_2)R_3R_4] \end{aligned} \tag{2.20}$$

$$\begin{aligned} Im\{B_{3rd}\} = \quad & \omega[C_1R_1(R_2+R_3+R_4)+C_2(R_1+R_2)(R_3+R_4)+C_3(R_1+R_2+R_3)R_4] \\ & -\omega^3C_1C_2C_3R_1R_2R_3R_4 \end{aligned} \tag{2.21}$$

$$Re\{C_{3rd}\} = -\omega^2[C_1C_2R_2+C_1C_3(R_2+R_3)+C_2C_3R_3] \tag{2.22}$$

$$Im\{C_{3rd}\} = \omega[C_1+C_2+C_3]-\omega^3C_1C_2C_3R_2R_3 \tag{2.23}$$

$$Re\{D_{3rd}\} = 1-\omega^2[C_1C_2R_2(R_3+R_4)+C_1C_3(R_2+R_3)R_4+C_2C_3R_3R_4] \tag{2.24}$$

$$Im\{D_{3rd}\} = \omega[C_1(R_2+R_3+R_4)+C_2(R_3+R_4)+C_3R_4]-\omega^3C_1C_2C_3R_2R_3R_4 \tag{2.25}$$

and $R_1 + R_2 + R_3 + R_4 = R_t$, and $C_1 + C_2 + C_3 = C_t$.

2.3.2 Second-order model

The second-order model's transfer matrix elements can be obtained from the equations above by setting C_3 and R_4 equal to zero. For the second-order model the elements are:

$$Re\{A_{2nd}\} = 1-\omega^2C_1C_2R_1R_2 \tag{2.26}$$

$$Im\{A_{2nd}\} = \omega[C_1R_1+C_2(R_1+R_2)] \tag{2.27}$$

$$Re\{B_{2nd}\} = (R_1+R_2+R_3)-\omega^2C_1C_2R_1R_2R_3 \tag{2.28}$$

$$Im\{B_{2nd}\} = \omega[C_1R_1(R_2+R_3)+C_2(R_1+R_2)R_3] \tag{2.29}$$

$$Re\{C_{2nd}\} = -\omega^2 C_1 C_2 R_2 \tag{2.30}$$

$$Im\{C_{2nd}\} = \omega(C_1 + C_2) \tag{2.31}$$

$$Re\{D_{2nd}\} = 1 - \omega^2 C_1 C_2 R_2 R_3 \tag{2.32}$$

$$Im\{D_{2nd}\} = \omega[C_1(R_2 + R_3) + C_2 R_3]. \tag{2.33}$$

Again $R_1 + R_2 + R_3 = R_t$, and $C_1 + C_2 = C_t$.

2.3.3 First-order model

For the first-order model a further simplification can be made. Setting C_2 and R_3 equal to zero would reduce the model to the solution as proposed by Richards [1]. For the sake of completeness the elements are given here:

$$A_{1st} = 1 + i\omega C_1 R_1 \tag{2.34}$$

$$B_{1st} = R_1 + R_2 + i\omega C_1 R_1 R_2 \tag{2.35}$$

$$C_{1st} = i\omega C_1 \tag{2.36}$$

$$D_{1st} = 1 + i\omega C_1 R_2. \tag{2.37}$$

The responce of the transfer matrix description and that of the electrical analogy can be compared, and the differences can be minimised.

2.3.4 Forcing functions

The procedure outlined above results in a single thermal network representing the building. The various surfaces of the building experience different outdoor conditions. A representative forcing function thus has to be obtained if more than one wall is being modelled. A procedure similar to that suggested by Mathews [4] will be adopted. The outdoor temperatures for the various walls will be weighed by the steady state thermal resistance.

2.4 VALIDATION OF THE WALL MODEL

The model validation studies were first performed for single walls. The walls were taken from the ASHRAE handbook [5]. Outdoor design conditions for Pretoria were used in these studies. In all cases zones with the same walls throughout were used. The results from the model simulations were compared to full numerical simulations. For the numerical simulations the diffusion equation was solved using a Crank-Nicolson algorithm. Three different cases are described.

2.4.1 Passive studies

For the first case the building was simulated as a passive building, i.e. the inside temperature was permitted to float as heat was transferred to and from it. For these studies, passive parameters were used to compare the data. A mean temperature, the average of the 24-hour values, was used, as a first parameter. The temperature swings, the difference between the minimum and maximum temperature during any 24-hour period, were used as a second parameter. A phase shift was also used. This is the average of the difference in time between the model and numerical maxima and minima.

For this passive case the means are not compared because they will always be correct. In fact, the deviations that were present were probably from numeric errors rather than inaccurate models. In figure 2.2 and figure 2.3 the swings predicted by the third- and first-order predictions are compared to those obtained by the numerical procedure. The next figure (figure 2.4) shows the average and one standard deviation of the phase errors.

2.4.2 Constant inside air temperature

For the second set of studies, the inside temperature was kept constant at 22 °C. For this study the energy usages over a 24-hour period for the models were compared to that predicted numerically. The results are shown in figure 2.5 and figure 2.6. The correlation between the third-order model

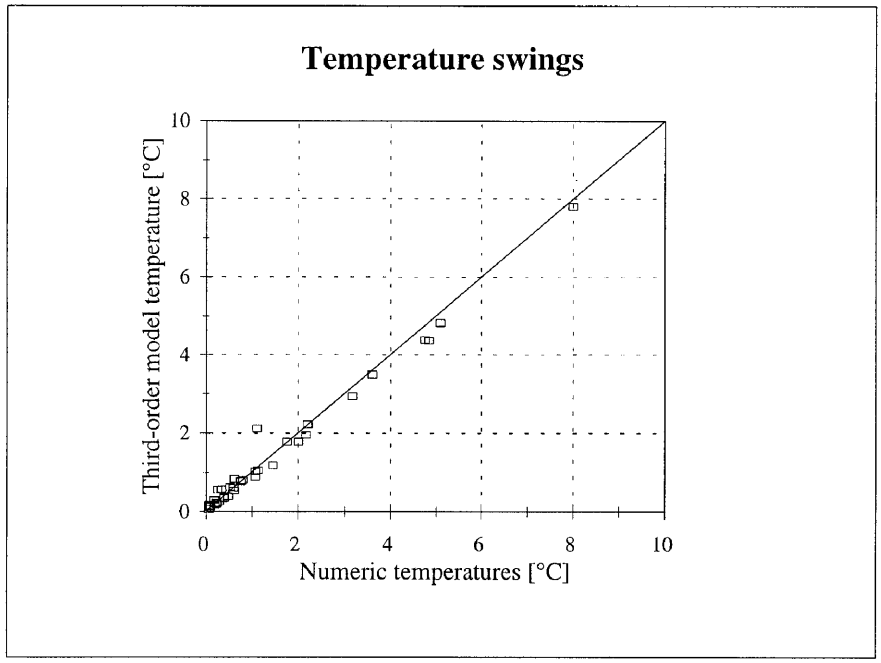

Figure 2.2: Comparison between third-order model and numerically determined inside temperature swing predictions.

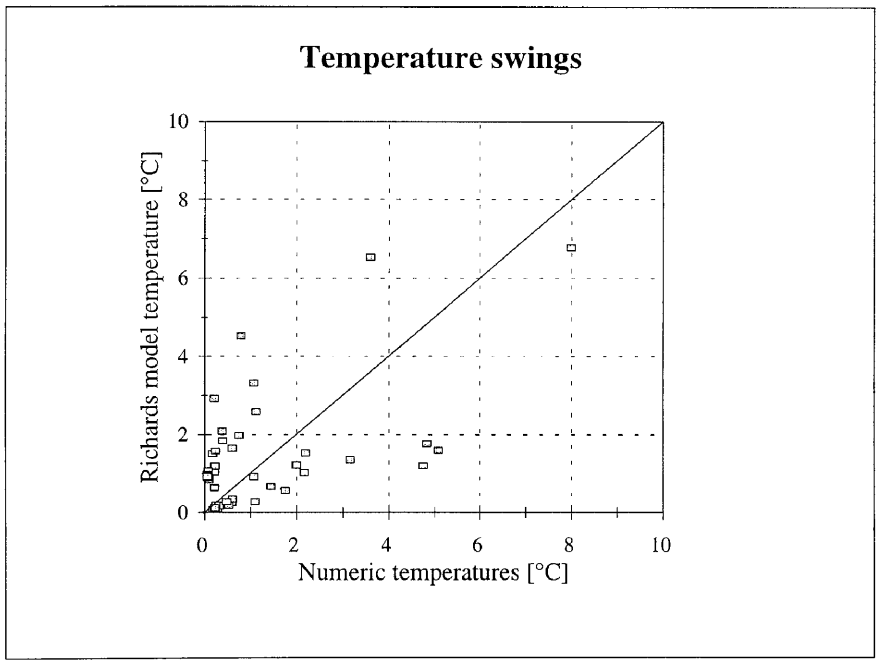

Figure 2.3: Comparison between first-order model and numerically determined inside temperature swing predictions.

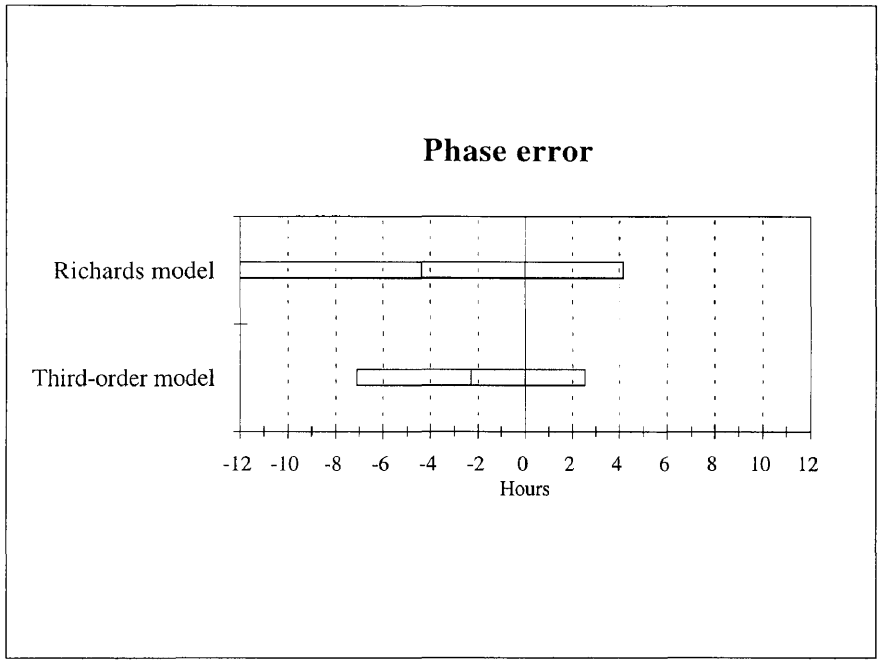

Figure 2.4: Comparison between the third-order and first -order model phase errors. The average and one standard deviation are shown.

and the numerical values is very good (0.9999). The correlation for the first-order model is almost as good (0.9994). The difference is really academic.

Next, the swing in the load is compared. Figure 2.7 shows the comparison for the third-order model, while in figure 2.8 the first-order model is compared. Here one can clearly see that the third-order model is superior to the first-order one. The correlation coefficient for the third-order model is 0.993 compared to the 0.945 for the first-order model. Figure 2.9 shows the mean phase error and one standard deviation for the two models.

2.4.3 Intermittent plant operation

The reason for investigating a new model is that the first-order model does not perform well when sudden changes occur in the inside air. This behaviour is investigated in this paragraph. Predicted energy usage is compared in the first two figures (figure 2.10 and figure 2.11). The energy usage as predicted by the first order model is, on average, 21.3 % lower than the numerically predicted values. In contrast to this, the maximum error predicted by the third order model is 14.7 % (see appendix A).

Maximum predicted loads are compared next (figure 2.12 for the third-order model, and figure 2.13 for the first-order model). Here we can see that the first-order model fails dismally (correlation coefficient of 0.477). The results obtained by the third order model are considerably better. The maximum error here is still 53.1 % (see appendix A), but the correlation between the third-order model and the numeric values is 0.904. This gives us confidence in the loads predicted for intermittent plant operation.

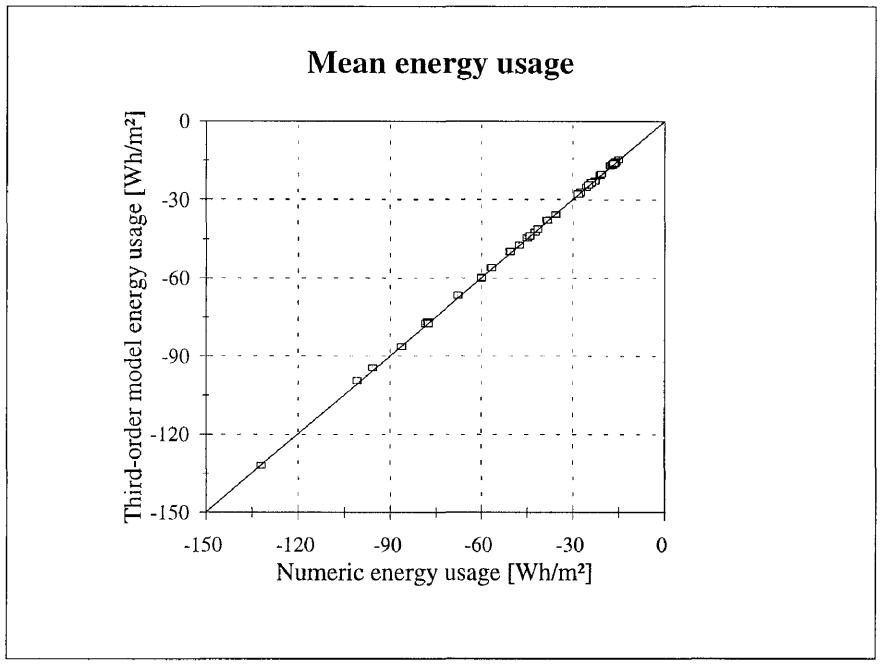

Figure 2.5: Comparison between the energy usage as predicted by the third-order model and the numeric procedure.

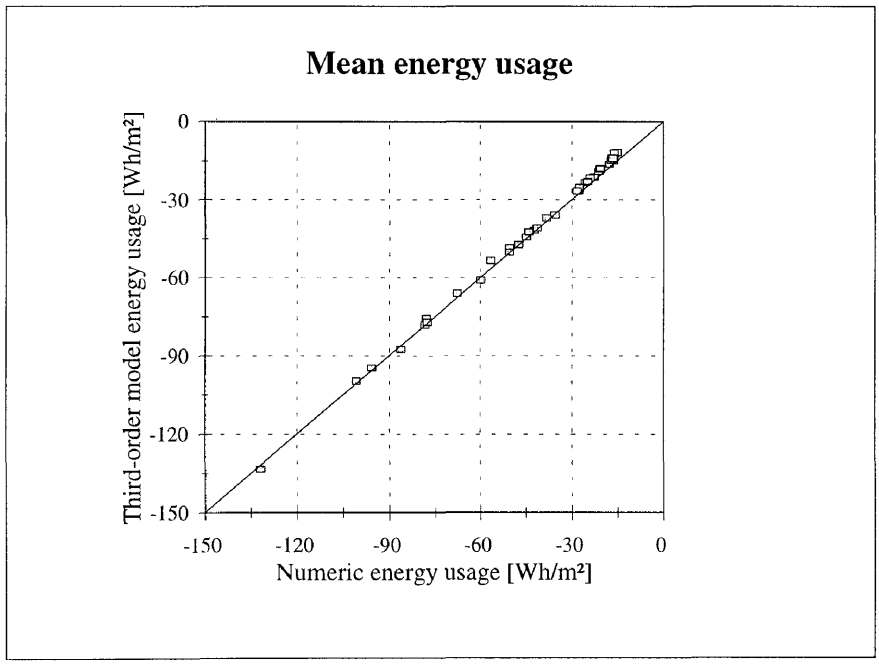

Figure 2.6: Comparison between the energy usage predicted by the first-order model and the numeric procedure.

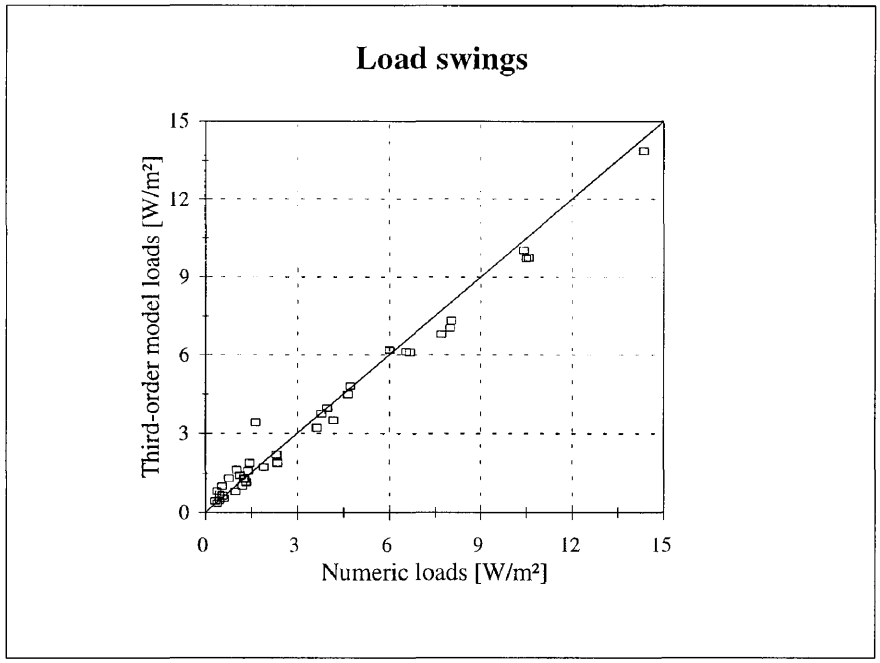

Figure 2.7: Comparison between the load swings as predicted by the third-order model and the numeric procedure.

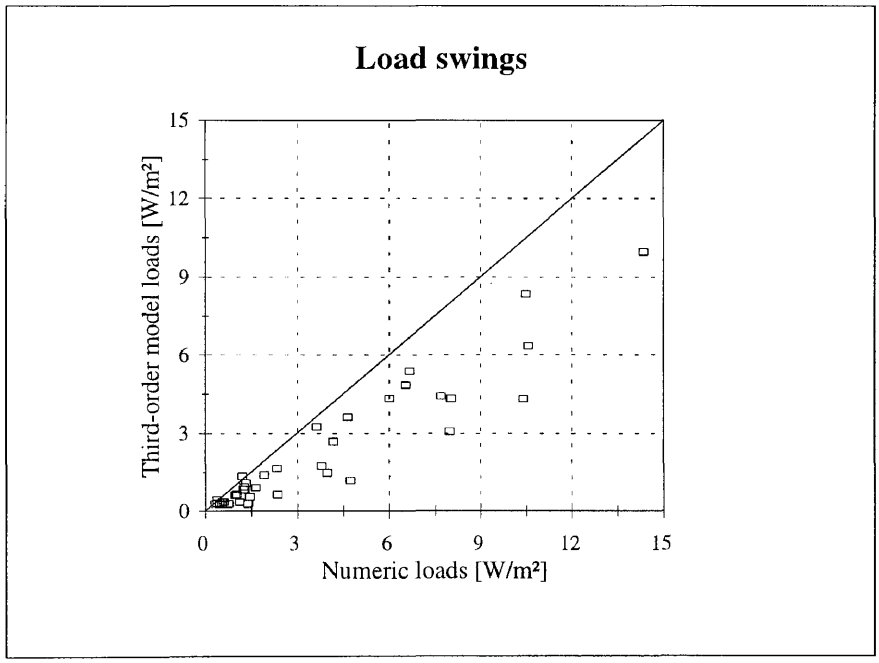

Figure 2.8: Comparison between the load swing as predicted by the first-order model and the numeric procedure.

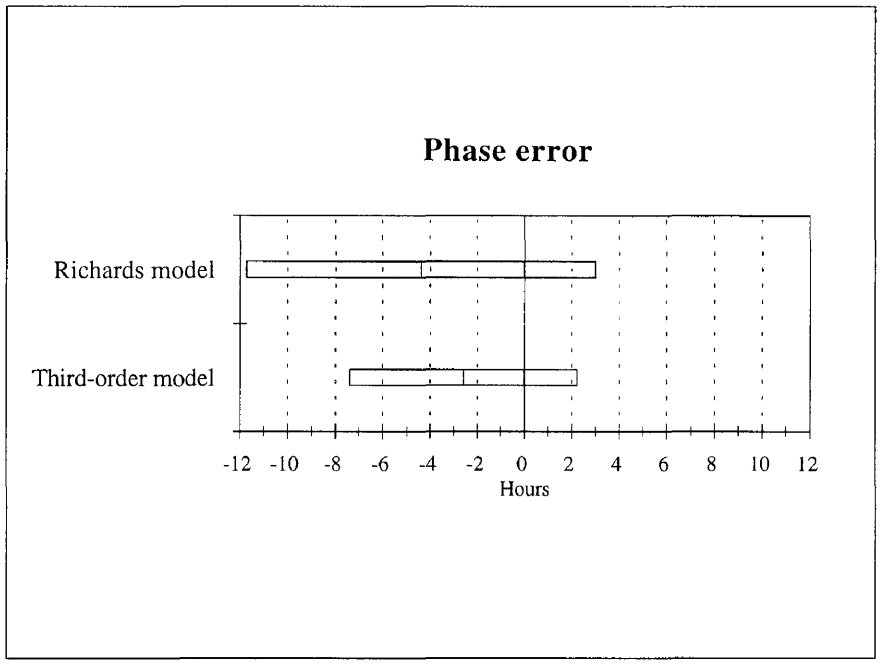

Figure 2.9: Comparison between the phase errors for the third-order model and the first-order model. The average and one standard deviation are shown.

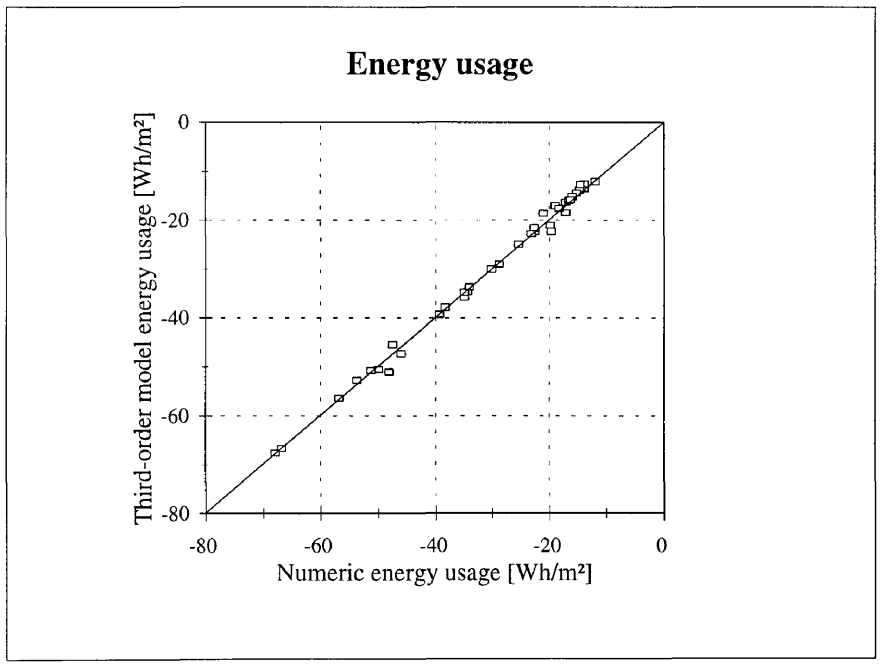

Figure 2.10: Comparison between the energy usage for intermittent plant operation as predicted by the third-order model and the numeric procedure.

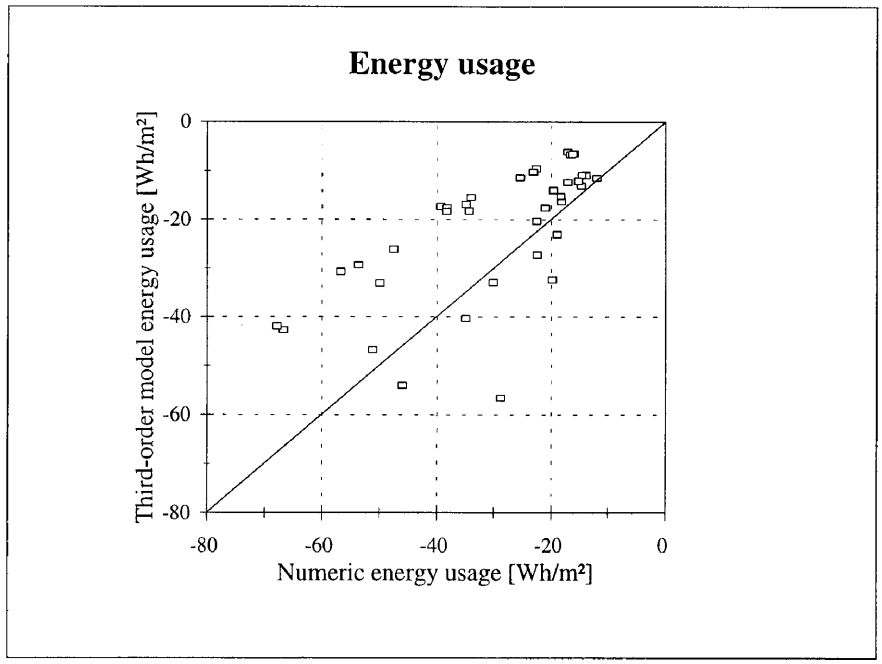

Figure 2.11: Comparison between the energy usage for intermittent plant operation as predicted by the first-order model and the numeric procedure.

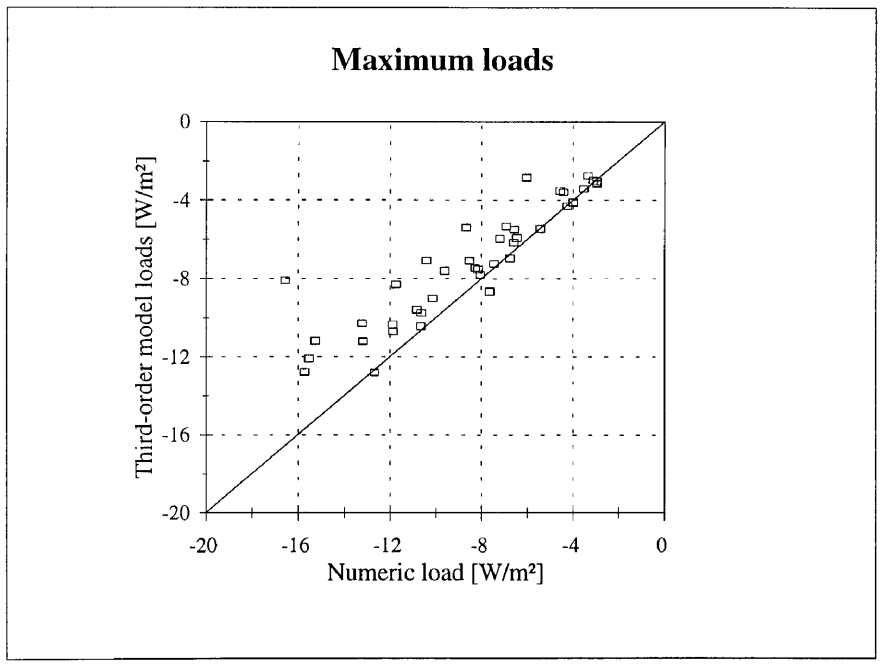

Figure 2.12: Comparison between the maximum load for intermittent plant operation as predicted by the third-order model and the numeric procedure.

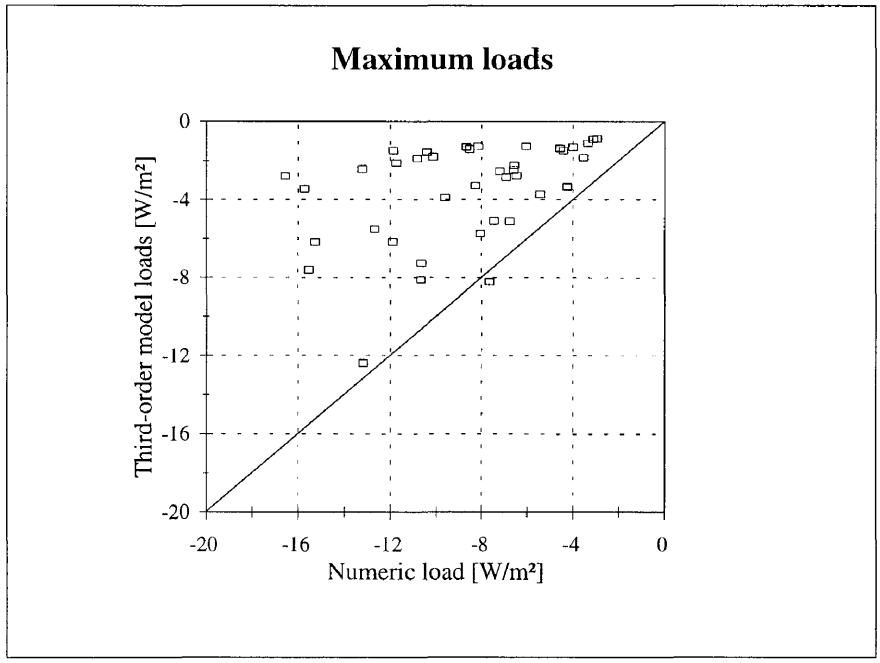

Figure 2.13: Comparison between the maximum load for intermittent plant operation as predicted by the first-order model and the numeric procedure.

Real-life buildings have more than one type of wall, and each wall is usually exposed to various outdoor conditions. A complete validation study of 70 test cases will be discussed in detail after the complete zone electrical analogy is given.

2.5 COMPLETE ZONE MODEL

The following procedure is recommended.

- The air node is treated as a separate node, its capacitance is simply $C_i = Volc_p$.
- The ventilation, infiltration and environmental control are treated separately, i.e. the resistance is given as 1/air changes per second (acs).
- Any internal masses are combined and treated as one capacitor.
- Provision is made for two structural heat flow paths:
  1. Glass, fenestration in general, and other low mass structures (low mass path, single node);
  2. A heavy mass path (triple node).
- The heat gains through the floor are treated separately, or incorporated into the internal mass.
- Convective heat gains act directly on the air node.

- Radiative heat gains are weighed according to surface area and act directly on the surface.

This would result in six capacitances or temperatures that must be solved simultaneously at each time step. Although this is a considerable complication (from a single-order model such as Richards'), the increase in accuracy should justify the effort.

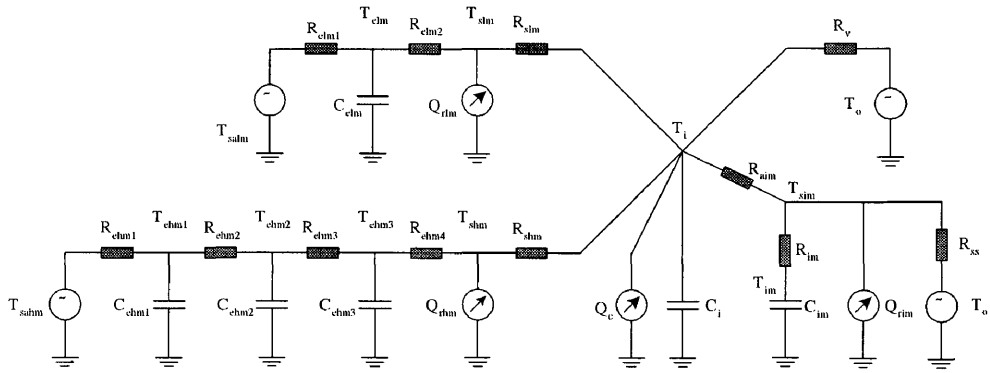

Figure 2.14: Electrical analogy for a zonemodel.

The governing equations for the given circuit can be solved by adding the currents at each node. The resultant equations are:

$$C_{ehm1}\frac{dT_{ehm1}}{dt} = \frac{T_{sahm} - T_{ehm1}}{R_{ehm1}} + \frac{T_{ehm2} - T_{ehm1}}{R_{ehm2}} \tag{2.38}$$

$$C_{ehm2}\frac{dT_{ehm2}}{dt} = \frac{T_{ehm1} - T_{ehm2}}{R_{ehm2}} + \frac{T_{ehm3} - T_{ehm2}}{R_{ehm3}} \tag{2.39}$$

$$C_{ehm3}\frac{dT_{ehm3}}{dt} = \frac{T_{ehm2} - T_{ehm3}}{R_{ehm3}} + \frac{T_{shm} - T_{ehm3}}{R_{ehm4}} \tag{2.40}$$

$$C_{elm}\frac{dT_{elm}}{dt} = \frac{T_{salm} - T_{elm}}{R_{elm1}} + \frac{T_{islm} - T_{elm}}{R_{elm2}} \tag{2.41}$$

$$C_{im}\frac{dT_{im}}{dt} = \frac{T_{sim} - T_{im}}{R_{im}} \tag{2.42}$$

$$C_i\frac{dT_i}{dt} = \frac{T_{shm} - T_i}{R_{ahm}} + \frac{T_{slm} - T_i}{R_{alm}} + \frac{T_{sim} - T_i}{R_{aim}} + \frac{T_o - T_i}{R_v} + Q_c. \tag{2.43}$$

This concludes the nodes that involve a capacitor. Expressions for the surface temperatures still need to be derived. They are:

$$Q_{rhm} = \frac{T_{shm} - T_{ehm3}}{R_{ehm4}} + \frac{T_{shm} - T_i}{R_{ahm}} \tag{2.44}$$

$$Q_{rlm} = \frac{T_{slm} - T_{elm}}{R_{elm2}} + \frac{T_{slm} - T_i}{R_{alm}} \tag{2.45}$$

$$Q_{rim} = \frac{T_{sim} - T_{im}}{R_{im}} + \frac{T_{sim} - T_i}{R_{aim}} + \frac{T_{sim} - T_o}{R_{ss}}. \tag{2.46}$$

From equations 2.44 through 2.46 the surface temperatures can be substituted into equations 2.40 through 2.43. This would eliminate three equations. However, these temperatures have to be calculated later anyway, and eliminating them results in very messy equations for the remaining temperatures.

The differential equations resulting from the nodes containing a capacitor can be discretisised using a forward-in-time differencing scheme. This results in nine equations that have to be solved simultaneously. At first this might sound like a formidable task, but fortunately the resultant matrix is sparse with an almost tri-diagonal structure. Most of the coefficients remain constant thus allowing that the matrix be inverted only once, and the data stored. At each time step only the backward substitution needs to be done. This can be done very efficiently.

2.6 CLOSURE

Using a theoretically rigorous approach an expression for the thermal performance of a building zone was obtained. An electrical analogy was used to approximate the analytical response. This was done by matching the frequency domain response of the electrical analogy to that of the analytical solution. From the model for a single wall, an extension was made to a number of walls.

The resultant thermal model makes provision for all the structural heat flow paths, i.e. a high mass flow path, a low mass flow path, internal mass, floors in ground contact, and convective heat flow by ventilation. Internal loads are also accounted for in the form of convective and radiative heat gains. Convective heat gains act on the air node directly, while radiative heat gains act on the surfaces.

The model is solved using a forward-in-time differencing scheme. The resultant simultaneous equations can be solved very efficiently. All that remains is to comprehensively verify the model. This is done in the next chapter.

Bibliography

[1] P.G. Richards. *A Design Tool for the Thermal Performance of Buildings*. PhD thesis, Mechanical Engineering, University of Pretoria, 1992.

[2] M.G. Davies. Transmission and storage characteristics of walls experiencing sinusoidal excitation. *Applied Energy*, 12:269–316, 1982.

[3] A. Tindale. Third-order lumped-parameter simulation method. *Building Services Engineers Research and Technology*, 14:87–97, 1993.

[4] E.H. Mathews and P.G. Richards. A tool for predicting hourly air temperatures and sensible energy loads at sketch design stage. *Energy and Buildings*, 14:61–80, 1989.

[5] American Society for Heating Refrigeration and Air Conditioning Engineers, Inc. *ASHRAE Handbook*, 1992.

Chapter 3

EXPERIMENTAL VERIFICATION OF THE BUILDING MODEL

In order to establish confidence in a simulation model, the model needs to be verified extensively. In this chapter, one hundred and three verification studies from fifty six different building zones are presented.

The comparisons are drawn to empirical data which, if successful, give us confidence that the underlying assumptions are in fact valid.

NOMENCLATURE

ach	Air changes per hour
C	Ventilation constant
T	Absolute temperature, K
V	Velocity, m/s

Subscripts

i	inside
o	outside

3.1 INTRODUCTION

The success of a building thermal model lies in successful verification studies. Analytical or numerical verification goes a long way to ensure that a building model is error free. Comparisons between models could prove helpful to verify a new model, but at this stage no absolute model is available to which one can compare. Comparisons to actual measured data are however, invaluable to provide confidence in the predictions made by a model.

The advantages and disadvantages of these approaches are given by Bowman et al. [1] and Irving [2]. Bowman also gives a comprehensive list of errors that can be introduced when validating a building model. In this chapter, a comparison is made between measured and predicted values for a wide range of buildings.

3.2 VENTILATION RATES

Direct convective heat exchange between the outdoor environment and the building interior can be divided into two categories, i.e. ventilation and infiltration. Ventilation occurs deliberately when windows and doors are opened to ensure an inflow of outside air. Infiltration is an unintentional effect due to openings under doors and between window frames.

The model used for the infiltration rates as given by Richards [3] will be used here in this validation study. The model is an empirical one also used by the thermal analysis program HVACSIM+ [4].

$$ach = C(0.215 + 0.042V + 0.013|T_0 - T_i|) \tag{3.1}$$

The constant C depends on the tightness of the building (the degree to which the building is sealed), and is given as follows

tight building	$C = 0.5$
standard building	$C = 1.0$
leaky building	$C = 1.5$
very leaky building	$C = 2.0$.

Ventilation rates can be more cumbersome to determine. Ventilation is usually achieved by either natural flow of air or, for a larger building, mechanical ventilation. These ventilation rates would depend inter alia on thermal effects, i.e. the temperature difference between inside and outside, the nature of ventilation openings, and the wind velocity and direction.

Unfortunately, the data required to calculate the ventilation rates were not available for the seventy case studies described by Richards. The results for the ventilation rates obtained by Richards [3] for the case studies were used in the cases where windows and other ventilation openings were open. Richards obtained his ventilation rates by the procedure described in ASHRAE Handbook [5].

For the remainder of the studies (study71 to study103), the ventilation model presented by P.G. Rousseau [6] was used. The infiltration rates were determined using equation 3.1. Where mechanical ventilation was used, the ventilation rates were determined by direct measurements. The procedures are described by Weggelaar [7].

3.3 DESCRIPTION OF THE 56 BUILDING ZONES

Validation studies were performed in 56 different building zones in various types of buildings. To extend the study some of these zones were modified by adding insulation, changing exterior colours, opening and closing windows, generating heat, and so forth. This section only describes the basic 56 building zones, while the following section describes the modifications made to arrive at a total of 103 case studies.

Most of the data pertaining to the building zones and validation studies are provided on a magnetic disk included at the back of this study. The data is given in project files which can be read with the provided program. The files are organised into various directories that will be explained in the text where applicable. To follow the discussions given in this chapter, the data on the disk is not necessary since relevant data is sufficiently described in the text. The data is given on the magnetic disk to facilitate future use by other developers of design tools.

The thermal properties of the building materials used in the analyses are given in the material and climatic database in Directory A of the included magnetic disk. These properties were obtained from tables available in the literature [5, 8], and were thus not measured. Although measuring these properties could have eliminated some uncertainties in the validation, the same information usually available to designers is again used.

Directory B on the disk contains a self-extracting file with 103 projects files. To facilitate future use, a brief description of each building zone and its environment is also given here. The names used for buildings correspond to the description of the project in Directory B of the magnetic disk.

Experim 1 (study1, study5, study9, study13, study17, study21, study25), Experim 2 (study2, study6, study10, study14, study18, study22), Experim 3 (study3, study7, study11, study15, study-19), Experim 4 (study4, study8, study12, study16, study20, study23, study 24): These single-zone experimental huts are all situated in close proximity and it can be assumed that they are subjected to approximately the same outdoor environment. The buildings are surrounded by a few other low-rise buildings on a fairly open test terrain of the National Building Research Institute in Pretoria.

The construction of the huts is nearly identical except for the roofs. The first two huts have identical corrugated iron roofs, the third hut has a tiled roof, and the fourth hut has a high-mass concrete slab as a roof. Various studies were conducted in the buildings by modifying the construction, exterior colour and window operation. The buildings were not furnished.

Bedroom 1 (study26 to study31): This furnished room forms part of a townhouse in a residential area in Verwoerdburg. Adjacent rooms are a study and a dining-room. The door leading into the rest of the building was left open while measurements were taken but the room was not occupied.

Bedroom 2 (study32): This furnished room forms part of a house in a residential area in Wingate Park, Pretoria. Adjacent rooms are a living area and another bedroom. The exposed facade is shaded by a big tree. The door was closed and the room was unoccupied during the validation study.

Bedroom 3 (study33): This furnished room is situated on the first floor of a house in a residential area in Moreleta Park, Pretoria. Adjacent rooms are two bathrooms. The door was closed and the room was unoccupied during the validation study.

Bathroom (study34): This room forms part of a house in a residential area in Faerie Glen, Pretoria. Adjacent rooms are a bedroom and living area. The door was closed and the room was unoccupied during the validation study. The exposed southern wall is covered by plants. Large mirrors are attached to some indoor surfaces.

Dormit 1 (study35 to study37) and Dormit 2 (study38 to study40): These precast concrete units form part of an arrangement consisting of twenty units. The buildings are situated in the Negev Desert in Israel. Indoor partition walls divide the units into four smaller zones. Indoor temperature measurements are however representative of the whole unit. The large windows are fitted with external openable PVC louvres acting as a shading device. During monitoring the units were unoccupied.

Prefab (study41 to study43): This low-mass prefabricated unit is situated in an open area in the Negev Desert in Israel. The building consists of two similar zones, separated by a dividing wall

without a door. Only one of the zones was monitored. During monitoring the units were unoccupied. The building is placed on steel beams approximately 20 cm above the ground. Windows are fitted with external shading devices consisting of openable PVC louvres.

Garage (study44 and study45): This empty garage is attached to a townhouse similar to the description given for Bedroom 1. No ceiling is provided and the southern wall mainly consists of a steel door.

Shop (study46 to study48): The vacant shop is located in a single-storeyed shopping mall in the low-rise city centre of Verwoerdburg. Exposed glazing is well protected by building eaves. The interior walls are shared by an adjoining restaurant and a loading zone.

School 1 (study49 and study50): The monitored classroom is on the third floor of a school situated in a residential area in Menlo Park, Pretoria. Adjacent rooms are another classroom and a storeroom. Measurements were taken during the holidays and the rooms were therefore not occupied. The room is furnished with school desks and chairs.

School 2 (study51): The walls of this single-storeyed classroom are made from prefabricated asbestos cement panels. An adjacent classroom was occupied during validation but the room under consideration was used to store various pieces of furniture. The school is situated in a residential area in The Willows, Pretoria.

Store 1 (study52): The storeroom is attached to another storeroom and a classroom at the same school described as School 2. Clothing was stored on shelves against the walls and on parts of the floor.

Store 2 (study53): This single-zone corrugated iron store is situated on an open area in the industrial area of the rural town of Volksrust. The store was vacant and closed during the validation study, and ventilation was achieved by means of ventilation openings in the roof.

Studio (study54): The southern and western external walls of this studio consist of very large glazing areas allowing solar penetration. Walls are fairly high and a ventilation opening is located in the roof. Interior partition walls form a smaller zone inside the main building. The studio is used as a showroom for furniture and is situated in a residential area in Brooklyn, Pretoria. Validation was done on a Sunday when the building was closed.

Church (study55): The church was designed with the aim to achieve sound human comfort and hence incorporates various techniques enhancing natural ventilation. The main zone of the church can be considered as a single zone with fairly high walls. It is situated in a residential area in Arcadia, Pretoria, and is surrounded by various high trees. Monitoring was done on a Sunday and consequently includes church services in the morning and in the evening.

Factory (study56): The building is situated on an exposed terrain in Groenkloof, Pretoria, with no surrounding buildings. It is naturally ventilated by means of roll doors at ground level and

roof-mounted ventilators. The factory was used for the assembly of mechanical components with no significant heat generation during monitoring. At least half of the roll doors were kept open during the day. The south wall is a partition between the zone under consideration and another factory.

Office l (study57 and study58): This office is on the second floor of a naturally ventilated office block on the grounds of the Council for Scientific and Industrial Research in Pretoria. The building is situated on an open terrain but is sheltered by other buildings. High-mass beams are located in the roof. The office was vacant during monitoring.

Office 2 (study59), Office 3 (study60 and study61) and Office 4 (study62): These three adjacent offices are on the first floor of the air-conditioned G H Marais building in the city centre of Pretoria. Office 2 faces east, Office 3 is on the corner of the building facing north-east, and Office 4 faces north. The floors of Office 2 and Office 4 are exposed to an open parking area, while Office 3 is above the air-conditioning plant room. The offices were furnished but vacant, and closed during monitoring. The air-conditioning was also inoperative for validation purposes.

Office 5 (study63): This office is in the naturally ventilated Central Governments Offices building in the city centre of Pretoria. The office was occupied during the day.

Office 6 (study64): This office is on the 22nd and top floor of the Liberty Life building in the city centre of Pretoria. The office was occupied during the day but air-conditioning equipment was inoperative.

Office 7 (study65): This office is on the 16th floor of the Poyntons building in the city centre of Pretoria. The office was furnished but vacant and closed during monitoring. Air-conditioning equipment was inoperative.

Office 8 (study66): This office is on the fourth floor of the UNISA building near the city centre of Pretoria. The office was furnished but vacant and closed during monitoring. Air-conditioning equipment was in operation.

Office 9 (study67) and Office 10 (study68): These offices are on the 9th floor of the air-conditioned Engineering Tower Block on the campus of the University of Pretoria. The offices were furnished but vacant and closed during monitoring. Air-conditioning equipment was inoperative.

Office ll (study69) and Office 12 (study70): These offices are on the second floor of the J G Strijdom building on the campus of the University of Pretoria. Office ll was empty and Office l2 was furnished but vacant and closed during monitoring. Air-conditioning equipment was inoperative.

Lightweight (study71 and study73) and Heavyweight (study72 and study 74): These are two buildings at the Desert Architecture Unit of the Jacob Blaustein Institute for Desert Architecture at the Ben Gurion University in Israel. The lightweight building is a prefabricated building. The

heavyweight building is a demonstration building of heavy construction. For this study the model presented by Rousseau [6] was used to determine the ventilation rates.

The next 23 studies were conducted at animal laboratories on the Onderstepoort campus of the University of Pretoria. Three separate facilities on the campus were included in the case studies namely, the conventional laboratory-animal facility, the infectious-diseases facility and the metabolic facility.

Room 1-79 (study79), Room 1-80 (study80), Room 1-82 (study81), Room 1-83 (study82), Room 1-90 (study76), Room 1-91 (study75), Room 1-93 (study78), Room 1-94 (study77): These rooms housed cats, dogs and rodents and were supplied with two constant volume direct expansion units. The supply air flow rate and temperature were measured and entered as the ventilation data for these rooms.

Room 1-122 and 1-123, Room 1-125 to 1-127, Room 1-141 to 1-143 and Room 1-145 (study83 to study91): These are the infectious-diseases laboratories. The laboratories were all supplied with air from an evaporative cooler. The temperature after the evaporative cooler and the flow rate to each room was again measured and used in the program as input.

Room 1-7 (study93 and study95), Room 1-9 (study92 and study94): The metabolic facilities were supplied with fresh air, and conditioning of the air was done by ceiling-mounted cassette units. Each room was also equipped with a heater bank.

Sasol-e (study96), Sasol-f (study97), Sasol-n (study98 and study99), Sasol-s (study100 and study101), Sasol-w (study102 and study103): The zones make up an administrative building. These specific zones were only serviced with mechanical ventilation.

Clearly a wide range of building types and construction techniques are covered. A validation study of these buildings should thus help to achieve a high level of confidence in the applicability of the design tool in practice. The following section describes the 103 validation studies carried out in these buildings.

3.4 DESCRIPTION OF 103 VALIDATION STUDIES

A summary of the 103 validation studies is provided in Appendix B. The building zone names, location and date of each experimental study, and additional information are listed. The building zone names correspond to the descriptions given in the previous section.

Although most of the building zones formed part of multi-zoned buildings, only thirty-eight studies are listed as multi-zone experiments. The indoor air temperatures in these thirty-eight zones differed considerably from the air temperatures in adjacent zones. In all other cases, the assumption of similar temperatures in the zone under consideration and adjacent zones was acceptable.

Seventy-nine of the 103 studies were performed in single-storeyed buildings, and thus incorporate the ground contact model described earlier.

Forty-four studies were monitored with open windows. The ventilation rates in these studies are determined by the procedure given in ASHRAE [5], except for studies 71 to 74 where the model presented by Rousseau [6] was used. The infiltration rates in the other studies are determined by means of equation 3.1. Six studies are listed as YN, indicating that the windows were open and closed during monitoring. The window operation of these six studies is discussed later in this section. The heat generation column lists forty-seven studies which included interior heat generation by means of small domestic heaters.

Solar penetration occurred in most of the 103 studies and is thus not listed here under heat generation.

Climatic data for each of the 103 validation studies are provided in the data base in Directory A. The 103 file names in the directory are STUDY1 to STUDY103. Climatic data and air change rates are given for all the studies but internal loads and occupancy are only given where applicable. The climatic data includes hourly outdoor air temperatures, as well as global and diffuse solar radiation measured on a horizontal surface. The longitude and latitude of the location are also given. It is important to note that studies 35 to 43 and 71 to 74 were performed in the Northern Hemisphere, and the rest in the Southern Hemisphere.

It was explained earlier that 103 studies were performed in 56 buildings by modifying the construction and operation in some buildings. The following discussion describes the modifications to obtain the 103 studies. Studies not described here were handled exactly as described in Directory B on the magnetic disk, and in Appendix B.

Twenty-five validation studies were performed on the experimental huts. Studies 1 to 4 were carried out in the huts without any change to the construction. In studies 5 to 8 the floors of the four huts were insulated with 25 mm thick expanded polystyrene. Studies 9 to 12 were again carried out in the buildings without any change to the construction, but the windows were open as opposed to the closed windows in studies 1 to 8.

In studies 13 to 16 the windows were again open but the floors were insulated with 25 mm thick expanded polystyrene. The floors were not insulated in studies 17 to 20, but the ceiling was insulated with 25 mm thick expanded polystyrene. No floor or ceiling insulation was incorporated in studies 21 to 25, only the exterior colours of the buildings were modified. For studies 21 and 23 the roofs were painted black and the walls painted dark brown. The colour of the huts in studies 22, 24 and 25 was unchanged from the descriptions in Directory B of the magnetic disk.

The validation studies carried out in the Negev Desert were a joint project between the University of Pretoria and the Desert Architecture Unit of the Jacob Blaustein Institute of Desert Research [9]. Primarily the twelve studies differ only in window operation.

For studies 35, 38 and 41, the windows were closed for the whole duration of monitoring while the windows were open for the whole duration in studies 37, 40, 43, and 71 to 73. For studies 36, 39, 42 and 74 the windows were opened during the night from 20:00 to 8:00 and closed for the rest of the period.

Study 56 involving the factory also employs open and closed window operation. Although the building did not have openable windows, some of the doors were kept open during the day between 7:00 to 19:00. Ventilation was achieved by means of these open doors and roof-mounted ventilators.

3.5 EVALUATION OF THE PROPOSED THERMAL MODEL

When validating the thermal model, considering each study individually is impossible, therefore criteria need to be established to facilitate the evaluation of the model. In this section several global parameters are defined (following the approach of Richards [3]). This enables us to evaluate all the data at once and make comparisons between different models.

Three global thermal parameters are defined, i.e. the mean indoor temperature, the indoor temperature swing, and the phase shift between the measured and predicted indoor air temperatures. The mean indoor air temperature is simply the mean of the 24-hourly values. The temperature swing is determined by taking the difference between the maximum and minimum indoor temperatures. In this study the phase shift is determined by first calculating the difference in time between the measured and predicted indoor maxima.

Secondly, the difference in time between the measured and predicted indoor minima are determined. The phase shift is then the mean of these two values. The phase lags are defined to be negative, and phase leads to be positive. Maxima and minima were determined using a spreadsheet for all cases and not by inspection as Richards suggested. Although global parameters can be considered representative of the thermal response of the indoor temperature, hourly values will also be compared, but in an aggregated form.

In this study, the model suggested by Mathews and Richards will be used as a reference study for the first 70 case studies. Only the final model presented by Richards will be referred to here. The data presented by Mathews and Richards were not recalculated, but their simulated values were used.

Figure 3.1 shows a comparison between measured and predicted indoor temperature means for the first 70 validation studies using Ridhards' model. In figure 3.2 the same data for the new third-order model is shown. The graphs compare well, with the new model performing better than the one by suggested by Richards. The correlation coefficients for the two models are 0.979 and 0.994 respectively.

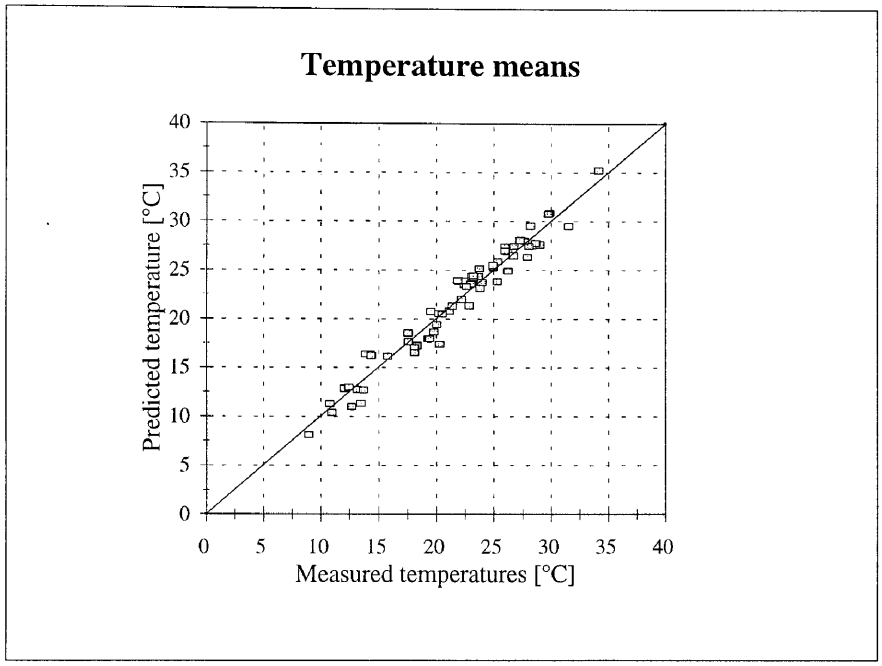

Figure 3.1: Comparison between the measured and predicted air temperature means for the thermal model as proposed by Richards.

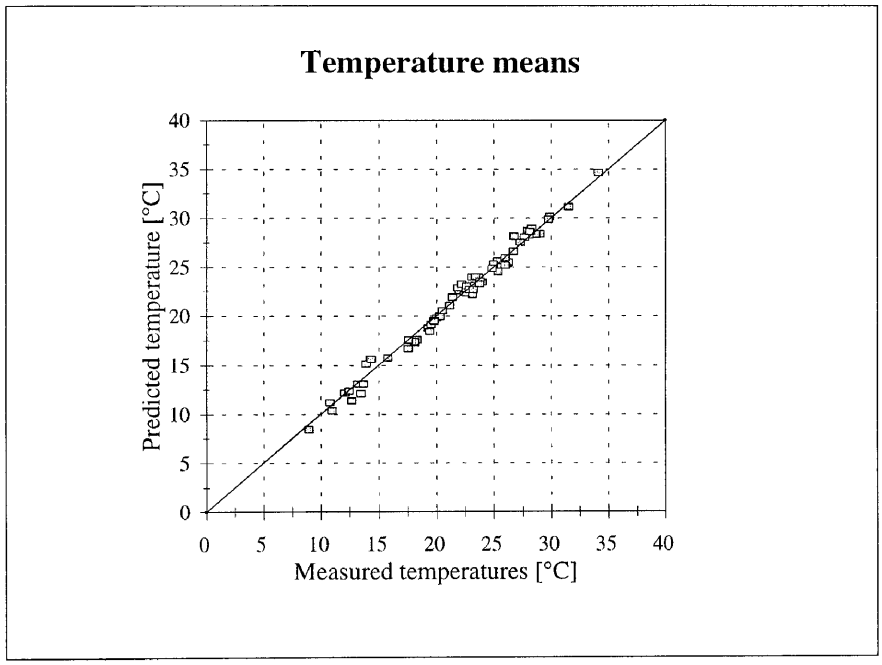

Figure 3.2: Comparison between the measured and predicted indoor air temperature means for the third-order model.

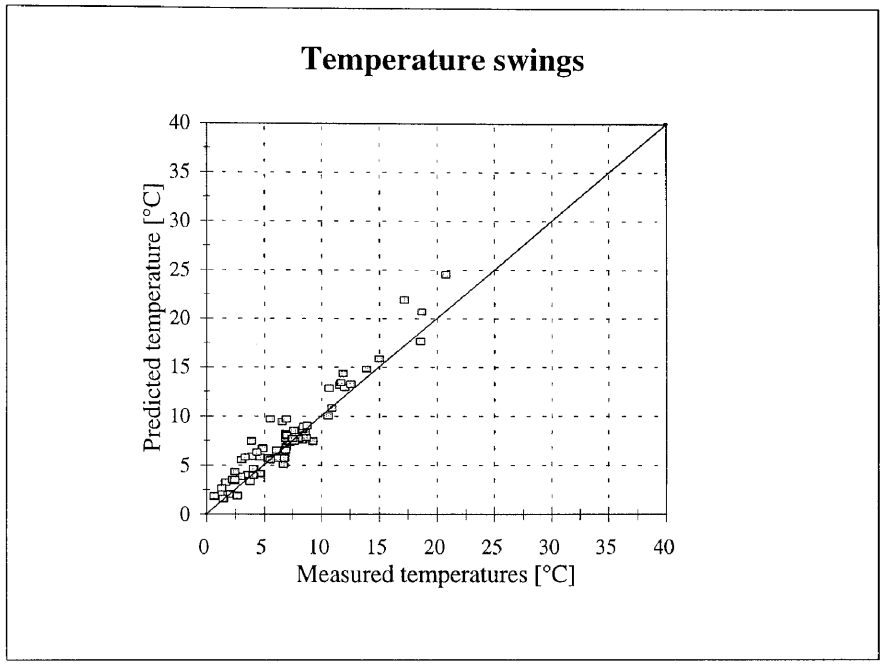

Figure 3.3: Comparison between the measured and predicted inside air temperature swing for the model of Richards.

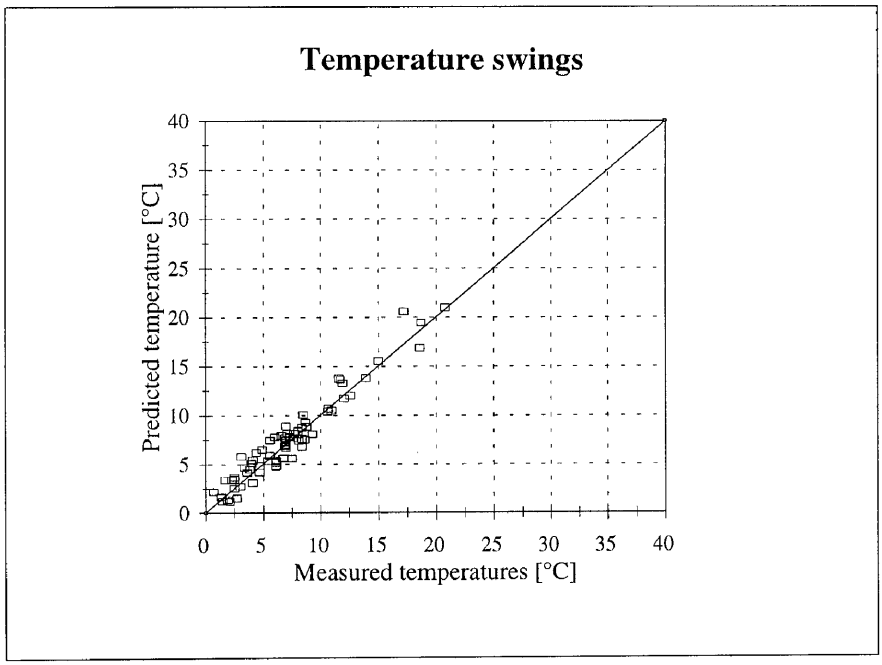

Figure 3.4: Comparison between the measured and predicted indoor air temperature swings for the third-order model.

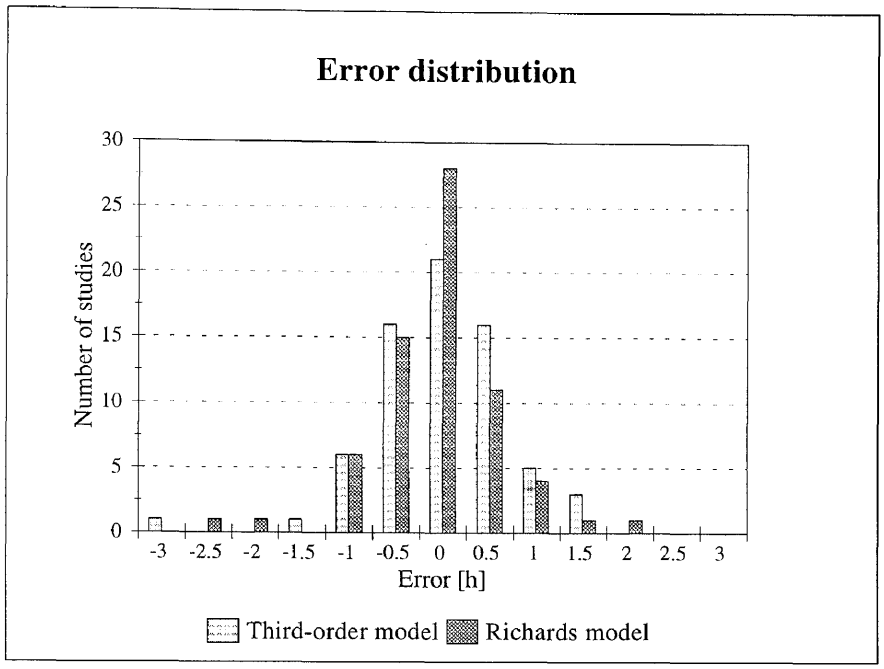

Figure 3.5: Comparison between the phase shifts for the model of Richards and the third-order model.

A similar comparison between the measured and predicted temperature swings is shown in figure 3.3 (for the Richards model) and in figure 3.4 (for the third-order model). Here the correlation coefficients are 0.968 and 0.959 respectively. Again there is seemingly very little to choose between the two models.

The phase shift errors are directly compared in figure 3.5. From this it seems that the model of Richards compares well (better than the third-order model) to the measured values.

From the presentation of the data in the previous paragraphs it is difficult to choose between the two models. Therefore we are going to look at another statistical method to compare the models. The difference between the predicted and measured values of the parameters defined above is calculated, and the average and standard deviations are calculated. Table 3.5 shows a comparison of these values.

	Means		Swings		Phase shifts	
	Average °C	St.dev. °C	Average °C	St.dev. °C	Average hours	St.dev. hours
Richards model	0.074	1.187	0.709	1.328	-0.095	1.056
Third-order model	-0.060	0.642	0.311	1.103	0.049	0.924

Table 3.1: Comparison between the Richards model and the third-order model.

The same values are presented in visual form in figure 3.6, figure 3.7 and figure 3.8. From these figures the third-order model produces better results than the model by Richards. For the means and the swings, both the average of the error and the standard deviation are smaller. Although the average of the phase error for the model by Richards is smaller than that for the third-order model, this is so by design since the model incorporates a phase correction. The standard deviation for

the third-order model is however smaller, so the margin of confidence in the third-order model is better, as can be deduced from figure 3.8.

The cumulative frequency distribution of the difference between the hourly measured and predicted indoor air temperatures are shown in figure 3.9. From this figure it is evident that the third-order model outperforms the Richards model substantially. Qualitatively, figure 3.9 shows that 72.5 % of the third-order model predicted indoor temperatures fall within 1 °C of the measured values, 96.1 % fall within 2 °C and 98.8 % fall within 3 °C. This is a substantial improvement on the model by Richards.

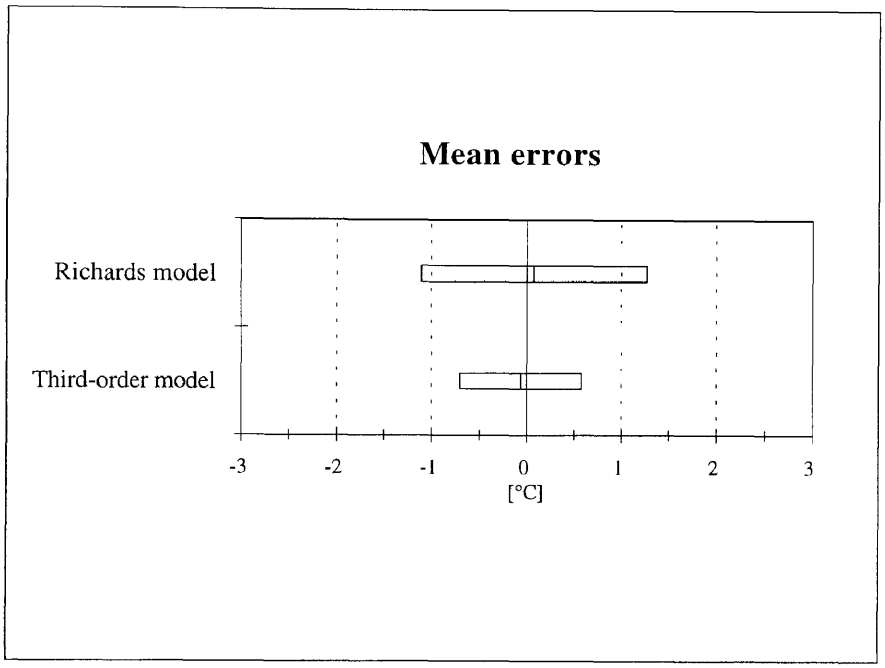

Figure 3.6: Average and one standard deviation of the error of the mean temperature predictions.

The same parameters will be applied for the next 33 case studies. The comparison with the Richards model will however not be pursued. The temperature means as shown in figure 3.10 show a comparison between measured and predicted indoor temperature means for the next 33 validation studies. The correlation coefficient for these studies is 0.947.

A similar comparison between the measured and predicted temperature swings is shown in figure 3.11 (for the third-order model). Here the correlation coefficient is 0.954.

The difference between the predicted and measured values of the parameters defined above is calculated and the average and standard deviations are calculated. Table 3.5 shows these values.

	Means		Swings		Phase shifts	
	Average °C	St.dev. °C	Average °C	St.dev. °C	Average hours	St.dev. hours
Third-order model	-0.561	1.094	0.664	0.944	-1.047	1.810

Table 3.2: Average and standard deviations of the errors for the 33 case studies.

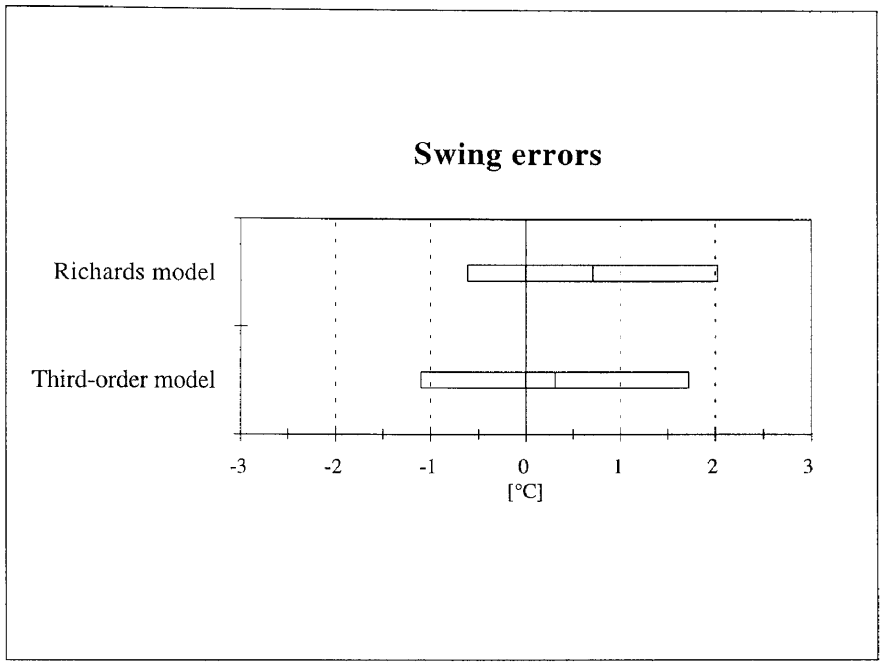

Figure 3.7: Average and one standard deviation of the errors of the temperature swing predictions.

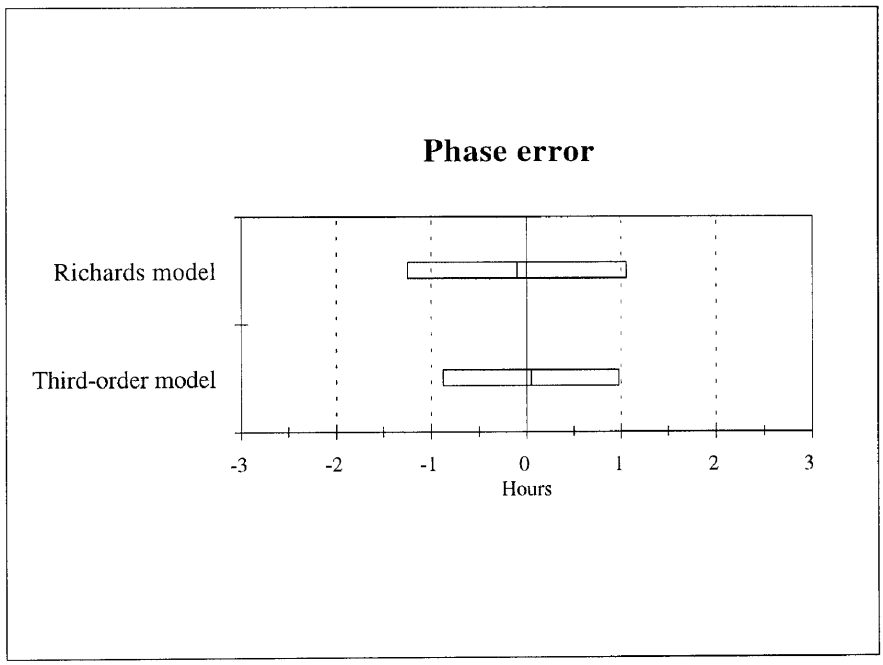

Figure 3.8: Average and one standard deviations for the errors of the temperature phase shift predictions.

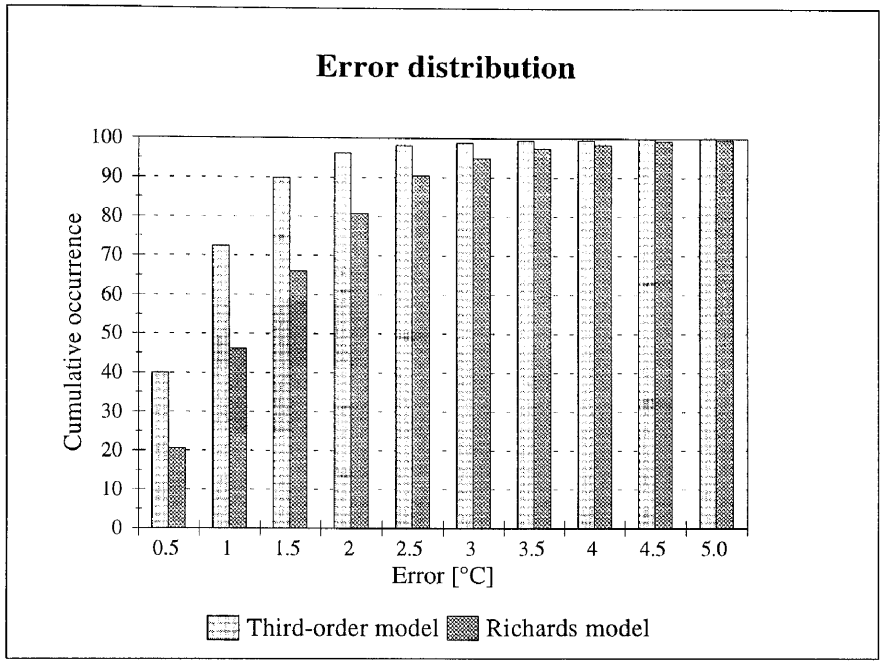

Figure 3.9: Cumulative frequency distribution for the difference between hourly measured and predicted indoor air temperatures for the validation studies.

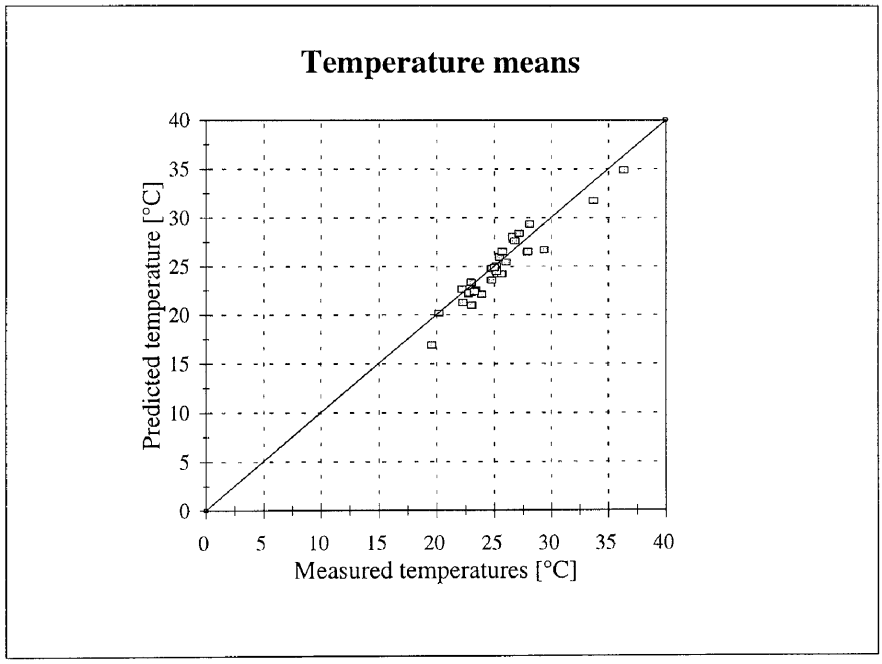

Figure 3.10: Comparison between the measured and predicted indoor air temperature means for the third-order model.

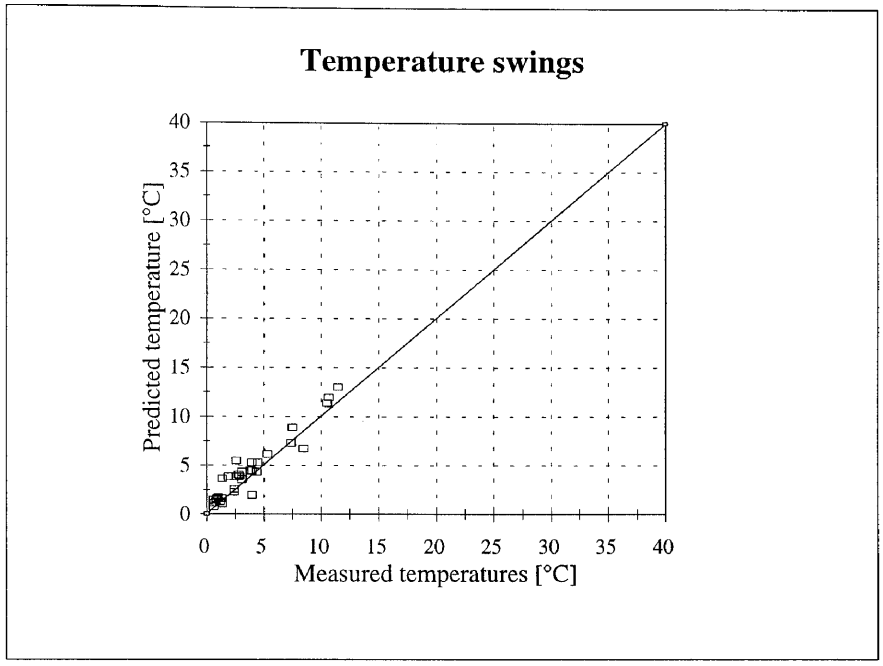

Figure 3.11: Comparison between the measured and predicted indoor air temperature swings for the third-order model.

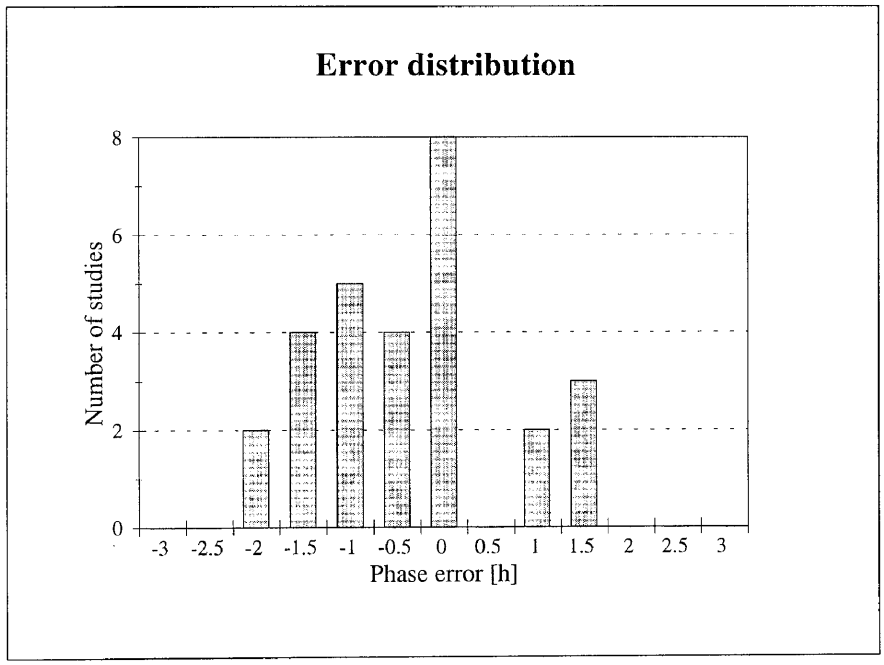

Figure 3.12: The phase shifts between the measured and predicted temperature profiles.

The cumulative frequency distribution of the difference between the hourly measured and predicted indoor air temperatures for the last 33 case studies is shown in figure 3.13. Qualitatively, figure 3.13 shows that 47.1 % of the third order model predicted indoor temperatures fall within 1 °C of the measured values, 87.2 % fall within 2 °C and 96.8 % fall within 3 °C.

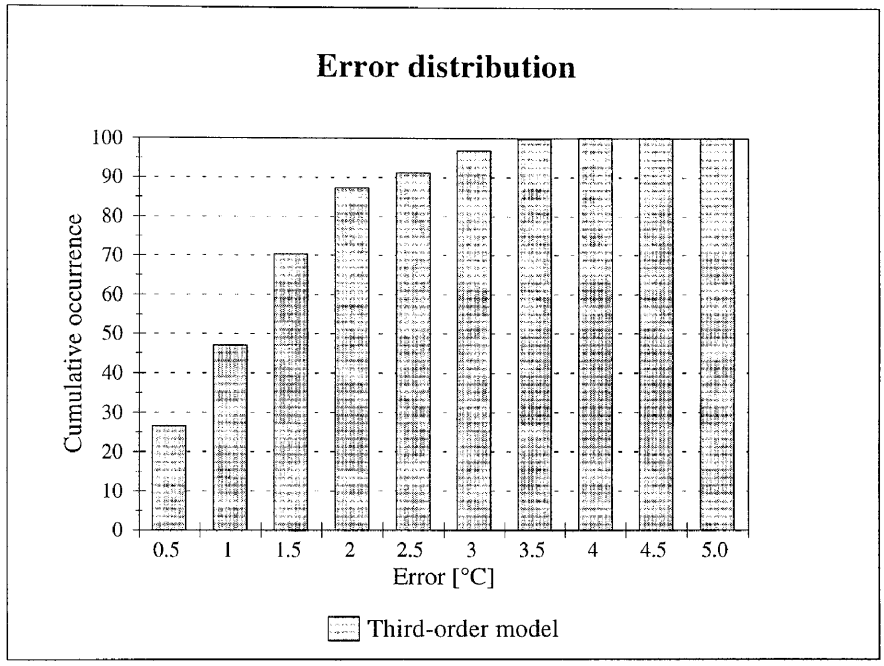

Figure 3.13: Cumulative frequency distribution for the difference between hourly measured and predicted indoor air temperatures for the last 33 validation studies.

3.6 CLOSURE

As described in the previous section, the verification of the third-order model can be considered successful. A wide range of buildings under a wide range of ventilation rates and internal loads were considered. Of all the predicted temperatures, none were more than 5 °C from the measured data. This gives us confidence that the model is an accurate representation of the actual thermal transfer processes that occur in buildings.

Bibliography

[1] N.T. Bowman and K.J. Lomas. Emperical verification of dynamic thermal computer models of buildings. *Building Services Engineers Research & Tegnology*, 13:133–144, 1986.

[2] A.D. Irving. Validation of dynamic thermal models. *Energy and Buildings*, 10:213–220, 1988.

[3] P.G. Richards. *A Design Tool for the Thermal Performance of Buildings*. PhD thesis, Mechanical Engineering, University of Pretoria, 1992.

[4] C. Park, D.R. Clark, and G.E. Kelly. *HVACSIM Buildings Systems and Equipment Simulation Program: Building Loads Calculation*. Gaithersburg, MD 20899, February 1986.

[5] American Society for Heating Refrigeration and Air Conditioning Engineers, Inc. *ASHRAE Handbook*, 1992.

[6] P.G. Rousseau. *Integrated Building and HVAC Thermal Simulation*. PhD thesis, Mechanical Engineering, University of Pretoria, 1994.

[7] S. Weggelaar. Verification, application and extension of a novel thermal simulation model. Master's thesis, Mechanical Engineering, Pretoria, 1996.

[8] J.D. Wentzel and J.A. Page-Ship, R.J. Venter. The prediction of the thermal performance of buildings by the CR-method, NBRI research report BRR 396. Technical report, CSIR, Pretoria, RSA, 1981.

[9] E.H. Mathews, Y. Etzion, E. Errol, P.G. Richards, and P.G Rousseau. Simplified analysis of naturally ventilated desert buildings. *Building and Environment*, 27(4):423–432, 1992.

Chapter 4

THERMAL MODEL APPLICATION: LOW-COST HOUSING DESIGN NORMS

With the coming of the new dispensation in South Africa came the promise from government that every South African is entitled to a house to live in. This promise is a means of establishing a better livelihood for all South Africans.

It is thus important to establish norms for such houses in order to secure a healthy and comfortable indoor climate. The reasons are numerous: health, comfort and economics are all important. There is no sense in providing a cheap house that requires much heating in the winter, or is unbearable to live in in summer.

This is a second field where the expertise of a consulting engineer could be called for. In this chapter, norms are established and the criteria that should be considered from a thermal design perspective are identified.

NOMENCLATURE

A	Area, m^2
A,B,C,D	Elements in the transfer matrix as defined in chapter 2
ACH	Air Changes per Hour
c_p	Thermal capacity, J/kgK
C	Cloudiness coefficient
d	Declination, ^{o}
F	Shape factor
h	Hour angle, ^{o}
h	Convection heat transfer coefficient, W/m^2K
h_{fg}	Latent heat of evaporation (or condensation), J/kg
h_m	Mass transfer coefficient, m/s
I	Radiation, W
J	Radiosity, W
k	Thermal conductivity of the slab, W/mK
l	Latitude, ^{o}
L	Longitude,^{o}
LCT	Local Civil Time
LST	Local Standard Time
p	Pressure, Pa
q	Heat flow, W
Q	Heat source, W
R	Gas constant for vapour, 461 J/kgK
R	Thermal resistance, K/W
SCT	Standard Civil Time
T	Absolute temperature, K
w	Total rate of condensation (or evaporation), kg/m^2s
Δx	Thickness of slab, m
α	Tilt angle of surface, ^{o}
β	Solar altitude, ^{o}
γ	Wall solar azimuth, ^{o}
ε	Emissivity
ρ	Density, kg/m^3
σ	Stefan-Boltzmann constant 5.669×10^{-8} W/m^2 K^4
ϕ	Relative humidity
ϕ	Solar azimuth, ^{o}
ψ	Wall azimuth, ^{o}
θ	Angle of incidence, ^{o}

ω Excitation angular frequency, rad/s

Subscript

a air
i inside
is inside surface
l long wave
o outside
r radiation
s surface, saturation
sa solar air
t total
v vapour

4.1 INTRODUCTION

With the new dispensation in South Africa came the promise of houses for everyone. This implies that a large number of houses would have to be erected in the shortest time and at the lowest overall cost. A number of important issues need to be addressed. Houses have to be erected, energy utilisation has to be optimised, and a better life for everyone has to be realised.

Providing houses and electricity to everyone are two of the key objectives of the Reconstruction and Development Program (RDP). Here in lies an exciting opportunity to contribute to the overall energy efficiency of the country, and in particular, to minimise the costs of individual households.

When designing houses for mass production, it is very tempting to minimise the capital cost of the unit without giving any consideration to other criteria such as comfort, health and heating cost. These costs will greatly determine the quality of life of the occupants, and should be the primary consideration for the developer. It is therefore important to have norms for the evaluation of proposed dwellings.

In this chapter a number of criteria will be established to facilitate the evaluation of building designs. From a thermal design perspective, a number of factors need to be considered, for example the energy consumption required to keep the dwelling comfortable in winter, a means of determining whether condensation will occur on surfaces, and the comfort of the occupants in warm months.

4.2 EXTENSIONS

All the objectives mentioned above can be met if a tool exists to accurately predict the thermal performance and the internal wall temperatures of a building. To this end, a number of extensions to the existing tools have been implemented. They are:

1. A new thermal model of which the extensive verification is given in appendix B.
2. The correct treatment of radiation in heat load estimations.
3. The accurate determination of loads through individual surfaces.
4. Inside wall temperature determination.
5. Prediction of condensation on specific surfaces.
6. A new Windows-based user interface was also developed. The interface provides user-friendly input utility and a summarised table of the important results.

The theoretical base for these extensions will be provided in subsequent sections. In the next section, the treatment of slanted surfaces will be treated in some detail. Most of the results are well known and will be repeated for the sake of completeness.

Load determination and inside wall temperatures will be considered together as they are closely related. Condensation will only then be treated, as it can only be predicted if an accurate assessment of the inside surface temperatures is available.

4.3 RADIATION BUILDING HEAT GAINS

Estimating the effect of solar radiation is an important part of any calculation procedure to determine the total space heat gain. Both the external air temperature and the incident solar radiation change drastically during the day. Many researchers have treated this topic in the past, Parker and McQuiston [1] among others.

In this reference, a complete discussion of the topic is provided and it will therefore not be repeated here. Both authors give a procedure for estimating the direct and diffuse radiation intensity based on general meteorological data as presented in ASHRAE [2]. In this work it will be assumed that the values for direct and diffuse radiation are available. Values for direct and diffuse radiation can usually be obtained from meteorological institutions.

Radiation from building surfaces are not treated as extensively and commonly in the literature as incident radiation. An attempt will be made to quantify the heat loss due to night-time thermal radiation from building surfaces.

4.3.1 Requirements

To calculate the solar radiation incident on a given surface a number of parameters are required. Information concerning radiation intensities, sun angles, surface orientation, etc., will now be discussed in turn.

Radiation data. Radiation incident on a given surface can be divided into three categories: direct radiation from the sun, diffuse radiation that is scattered by atmospheric gases, and radiation reflected from other surrounding surfaces. Reflected radiation is almost impossible to determine in the design phase of a building. If there are highly reflective surfaces in the proximity of the building, this radiation can not be ignored. For now however, it will be assumed that there are no such bright surfaces.

In this work it is also assumed that the direct and diffuse radiation are known for the location of the building. This information is available from the local meteorological offices. Data given by these institutions is usually measured on a horizontal surface on the ground, and the values quoted are total and direct radiation. The diffuse radiation can then be calculated.

Solar angle data. To treat the direct radiation correctly we need the position of the sun in the sky relative to the position at which the building is located. The orientation of the surface with respect to some reference orientation is also required.

For the sun position we need the longitude, L, and the latitude, l, of the building location on the earth's surface, the time of year, and the time of day. From this we can determine the sun hour angle, h, the latitude, l, and the declination, d. These angles are shown in figure 4.1.

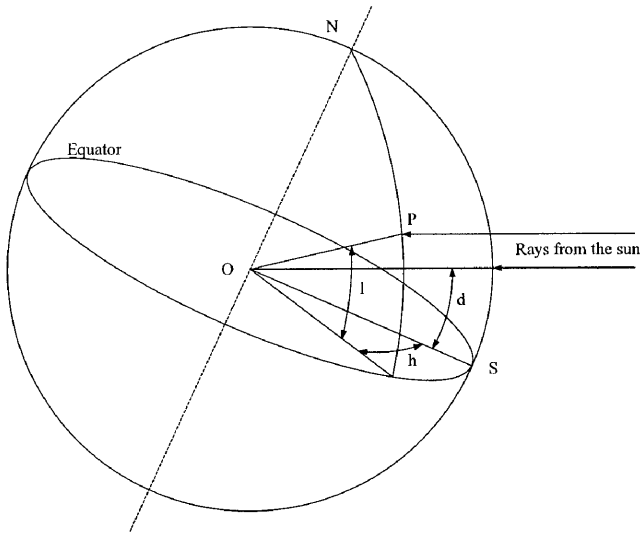

Figure 4.1: Latitude, hour angle, and sun's declination.

It is convenient to specify the sun's position for a given observer in terms of the solar altitude, β, and the solar azimuth, ϕ. These angles are relative to a horizontal surface, and ϕ is measured from south through west to north to east. See figure 4.2. The relation between these quantities will be given in the next section.

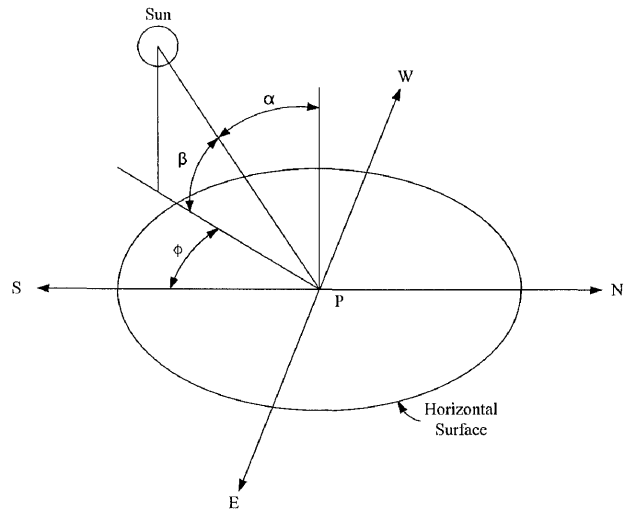

Figure 4.2: Solar altitude, β, and azimuth angle, ϕ.

Surface orientation. The surface orientation can be completely specified by two angles. These are the wall azimuth angle, ψ, and the tilt angle, α. The wall azimuth angle is the angle between the projection of the normal to the surface on the horizontal and the south direction. The tilt angle is the angle between the normal to the tilted surface and the vertical. See figure 4.3.

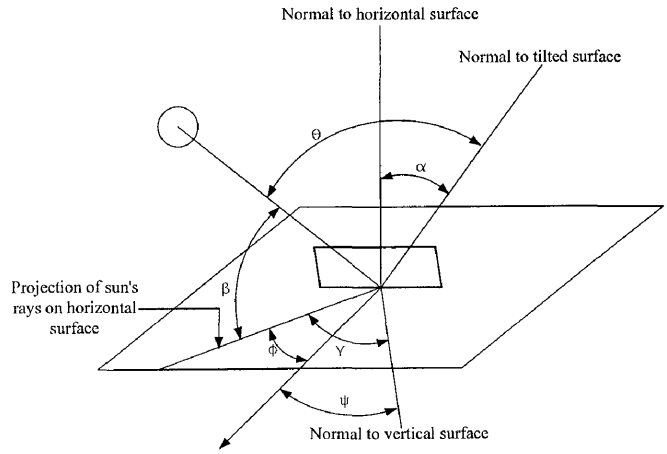

Figure 4.3: Wall azimuth angle, ψ, and angle of tilt, α, for an arbitrary tilted surface.

For any arbitrary oriented surface with no shading, these parameters fully describe the radiation incident on such a surface. We now need the relation between these parameters.

4.3.2 Analytical relations

We need to be able to determine the hour angle, h, and the latitude, l, and the sun's declination from the given data, i.e. the location on earth and the time of year and time of day.

The hour angle can be determined from the longitude, the time of day and the equation of time. First, the Local Civil Time, LCT, must be determined. This is given by the difference between the Standard Civil Time, SCT, (i.e. the time given by your watch), and the time equivalent of the distance from the current location to the standard meridian.

$$LCT = SCT + (longitude - standard\ meridian) \times 4^{o}. \tag{4.1}$$

Local Standard Time, LST, is obtained from Local Civil Time by adding the Equation of time, i.e.

$$LST = LCT + Equation\ of\ time. \tag{4.2}$$

This accounts for the obliquity of the earth's orbit and the fact that the orbit is elliptic. Finally the hour angle is:

$$h = (LST - 12h) \times 0.25. \tag{4.3}$$

The Equation of time is given in McQuiston [1] for a number of days in each month (Table 6.1, p 182). A simple curve can be fitted through the data to give the equation of time for any date.

The sun's declination is a function of the time of year only. This data is also tabulated for a number of days in each month in McQuiston [1] (Table 6.2, p 184). A curve was fitted through this data and is given by

$$d = 0^{o}21' + 23^{o}15' \cos(2\pi X - 2.9830) - 0^{o}23' \cos(4\pi X + 0.1172) - 0^{o}11' \cos(6\pi X + 0.4433) \tag{4.4}$$

where $X = (dayofyear)/365.25$. This expression is accurate within $4'$ (i.e. four arc minutes). If the last cosine term is ignored then it is accurate to within $15'$, and if only the first cosine term is used then a value of the declination can be determined within $45'$.

The latitude is simply the geographic latitude.

The solar altitude can be determined from analytical geometry to be

$$\sin\beta = \cos l \cos h \cos d + \sin l \sin d. \tag{4.5}$$

The solar azimuth can then be found from

$$\cos\phi = (\sin\beta \sin l - \sin d)/(\cos\beta \cos l). \tag{4.6}$$

Here, problems are encountered if $\beta = 90^o$ (i.e. the sun is not visible) or l is close to $\pm 90^o$ (close to the North or South Pole) as the numerator becomes very large. Any design engineer that designs a building for those conditions will obviously appreciate that he should use a value close to but not equal to $\pm 90^o$. As for $\beta = 90^o$ we can take the limit as β approaches $\pm 90^o$.

The wall solar azimuth, γ, is $\gamma = \phi \pm \psi$. For morning hours, with walls facing east of south and afternoon hours for walls facing west of south:

$$\gamma = |\phi - \psi|. \tag{4.7}$$

For morning hours, with walls facing west of south and afternoon hours for walls facing east of south:

$$\gamma = |\phi + \psi|. \tag{4.8}$$

And obviously if $\gamma > 90^o$ then the surface is in the shade!

The angle of incidence, θ , is given by the geometric relation

$$\cos\theta = \cos\beta \cos\gamma \sin\alpha + \sin\beta \cos\alpha. \tag{4.9}$$

Shape Factor One further consideration is the shape factor for diffuse radiation for tilted surfaces. The shape factor for a tilted surface is

$$F = \frac{(1+\sin\alpha)}{2}. \tag{4.10}$$

4.3.3 Long wave radiation

Until now the discussion was only based on the radiation from the sun. It is generally known that the radiation from the sun is at a short wavelength when compared to the earthbound radiation (see for example Holman [3], Mills [4]). The short-wave radiation incident on a surface is absorbed, and an increase in surface temperature results. The surface then emits radiation due to its temperature. Long- wave radiation from the sky is also incident on the surface. For horizontal surfaces receiving radiation from the sky, the radiation intensity is approximately 63 W/m^2 [2, 5].

This effect is negligible during the daytime. At night however, when there is a large difference between ambient temperature and building surface temperature, this effect can become important. Experimental data based on measurements for vertical surfaces were obtained at the NBRI [6]. An average value for sky long-wave radiation based on this study is 40 W/m^2. Joubert [7] suggested using this value as a constant in his thermal model. A theoretically more rigorous approach will be taken here.

Mills [4] suggests that the radiosity of the sky can be given in terms of the air temperature near the surface of the earth as

$$J_{sky} = \varepsilon_{sky}\sigma T_e^4. \tag{4.11}$$

Brunt [8] recommended the following approximate correlation for the emissivity of the sky

$$\varepsilon_{sky} = 0.55 + 1.8(P_{H_2O}/P)^{0.5} \leq 1 \tag{4.12}$$

where P_{H_2O} is the partial pressure of the water in the air and P is the total atmospheric pressure. For the surface, the radiosity is given by

$$J_s = \varepsilon_s\sigma T_s^4 \tag{4.13}$$

where the subscript s is for surface.

In the thermal analysis of buildings we will always have the case (for horizontal surfaces) that the surface 'sees' only the entire sky, and that the area of the sky is much larger that the surface of the building. In this case the radiation heat transfer is simply

$$\frac{q_{rs}}{A_s} = \varepsilon_s \sigma (T_s^4 - T_{sky}^4). \tag{4.14}$$

The net long-wave radiation heat transfer for a surface is thus a function of the difference between the effective temperatures, and the emissivities of the surfaces, as expected. However, the fact that the sky 'area' is much larger than the building surface renders the emissivity of the sky redundant.

To use the radiation transfer equation it is customary to linearize the equation in order to treat the radiative and convective heat transfer together.

$$h_r = \varepsilon_s \sigma (T_s^2 + T_{sky}^2)(T_s + T_{sky}). \tag{4.15}$$

Obviously this heat transfer coefficient is a very strong function of temperature, but if the range of temperature differences are small compared to the absolute temperature, one can assume this coefficient to be constant.

In the CIBSE Guide [9], data for long-wave radiation are given as a function of the cloudiness, and not as a function of the surface temperatures at all. The values for horizontal surfaces are

$$I_l = 93 - 79C \tag{4.16}$$

and for vertical surfaces

$$I_l = 21 - 17C \tag{4.17}$$

where I_l is the long-wave radiation loss, and
C is the cloudiness (C = 0 implies clear skies).

The sol-air temperature is defined as:

$$T_{sa} = T_{oa} + (\alpha I_{es} - \varepsilon I_l)/h_o \tag{4.18}$$

where ε is the long-wave emissivity and
α is the absorptivity.

4.3.4 Closure

In the previous section a procedure was outlined to calculate the radiation incident on a arbitrary tilted surface. If the information for vertical and horizontal surfaces are available, the only additional information needed would be the tilt angle, α, and for horizontal surfaces we also would need the orientation.

The treatment of radiation heat transfer in the night, especially from horizontal surfaces, could be done purely according to Stephan-Boltzmann's law. The radiation transfer coefficient is obtained from linearisation of the radiation transfer equation. Consensus on the treatment of long-wave radiation heat transfer from building surfaces seems to be to use a constant value. It is suggested that the relation from ASHRAE is used instead of the Stephan-Boltzmann approach because it is extremely easy to implement.

4.4 SURFACE LOAD DETERMINATION AND CONDENSATION

4.4.1 Surface temperature and load estimates

Inside wall temperatures for a given zone are important for two reasons. Radiation off these surfaces influences the comfort perception inside the room or zone and these surfaces will be the most likely place where condensation will occur. To this end it is important to have an accurate estimation of these surface temperatures.

Mcquiston [1] uses steady state conduction theory as a simplification to calculate the heating load in cold climates. It is well known that this approach will give larger loads than when the storage effect is taken into consideration. A safety factor is thus built into the calculation procedure, since the steady state values constitute an upper limit of the heating load.

If the steady state resistance was used to determine estimates of inside wall temperatures so that the occurrence of condensation can be predicted, conservative estimates will again be obtained. The result would thus be that condensation is predicted but would not actually occur.

For thermally low-mass elements this approximation is a valid one, and would result in temperatures that are very close to reality. For such a thermally low-mass element (such as windows, doors, and low-mass structures) the inside wall temperatures are given by:

$$T_{is} = T_{ia} - (T_{ia} - T_{sao})/(R_{ts} h_{is} A_s) \tag{4.19}$$

where T_{is} is the inside surface temperature, ^{o}C

T_{ia} is the inside air temperature, °C
T_{sao} is the sol-air temperature outside that specific surface, °C
R_{ts} is the total thermal resistance over the surface, K/W
h_{is} is the inside convection heat transfer coefficient, W/m^{2}K.

R_{ts} can be calculated from

$$R_{ts} = \frac{1}{h_{os}A_s} + \sum_{j=1}^{n} \frac{\Delta x_j}{k_j A_s} + \frac{1}{h_{is}A_s} \tag{4.20}$$

where Δx_j is the thickness of layer j, m
k_j is the thermal conductivity of layer j, W/mK.

Calculating the surface temperature for a thermally low-mass element is thus comparatively easy. For a thermally thick element, the procedure is somewhat more involved. To calculate the heat transfer rate into the surface in this case, a procedure based on transfer matrices is used. This procedure was first proposed by Pipes [10] in 1957. A detailed discussion of the method was more recently given by Davies [11].

4.4.2 Wall transfer matrices

The heat flux through a single homogeneous element is well established and can be written as a transfer matrix given by equation 2.1 in chapter 2.

If the heat flow at a surface on which radiation is incident is considered (see also [12]), the following relations apply:

$$T_{is} = T_i - q_i R_a \tag{4.21}$$

and

$$q_i = -Q_r - q_{is}. \tag{4.22}$$

If equation 4.22 is substituted into equation 4.21 we can rewrite them in matrix form as:

$$\begin{bmatrix} T_i \\ q_i \end{bmatrix} = \begin{bmatrix} 1 & R_a \\ 0 & 1 \end{bmatrix} \cdot \begin{bmatrix} T_{is} \; q_{is} \end{bmatrix} - Q_r \cdot \begin{bmatrix} R_a \\ 1 \end{bmatrix}. \tag{4.23}$$

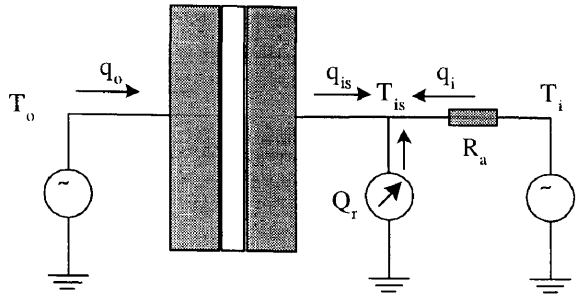

Figure 4.4: Energy balance at the inside surface of a wall.

Now equation 2.1 can be substituted and simplified to obtain the heat flux into a zone in terms of the outside conditions:

$$\begin{bmatrix} T_i \\ q_i \end{bmatrix} = \begin{bmatrix} (D+R_aC) & -(R_aA+B) \\ C & -A \end{bmatrix} \cdot \begin{bmatrix} T_o \\ q_o \end{bmatrix} - Q_r \cdot \begin{bmatrix} R_a \\ 1 \end{bmatrix}. \tag{4.24}$$

Finally, solving for q_i:

$$q_i = CT_o - A\frac{(D+R_aC)T_o - Q_rR_a - T_i}{R_aA+B} - Q_r. \tag{4.25}$$

This representation of the conduction through a building element is in the frequency domain and the elements are therefore a function of frequency. To obtain a solution for passive buildings, a frequency of 1 in 24 hours is usually assumed.

For passive buildings this is an assumption that results in an accurate estimate of building thermal performance. However, if the building temperature is regulated or other sudden changes occur, there are other important frequencies. The actual building performance is then a superposition of a number of responses at different frequencies.

Time domain solutions then can be obtained from adding the solutions of the various frequency components. Once the heat flux is known the surface temperature can be determined from

$$T_{is} = T_i - q_{is}/(h_{is}A_s). \tag{4.26}$$

For thermally thin structures this expression is equally valid.

4.4.3 Thermal bridged constructions

There is an exception to the way in which the temperatures and loads were determined in section 4.4.1. In the case of walls consisting of hollow bricks a part of the brick will transfer heat as

a solid brick while for the rest of the brick the heat will be transferred through brick, air gap and brick.

This phenomenon will be referred to as thermal bridges. The bridge is the part of the brick that is solid, thus having the lowest thermal resistance. In this case it could happen that the average temperature of the wall is above the dew-point temperature of the air in contact with it. However, there are local surface temperatures that are below the dew-point temperature of the air, allowing condensation to occur.

A correct treatment of this problem would be to resort to three- dimensional heat flow solutions. This is costly however and a simplified solution is suggested. The problem could be solved using an area-weighted method. In most cases treating the heat flow through the thermally bridged construction by the area-weighted method would lead to conservative estimates of condensation occurring. That is, condensation will be predicted although it would not actually occur.

It will be assumed that the wall has a solid area and the remainder of the wall area to be composed of brick - air space - brick. The results from section 4.4.1 can then be used directly.

4.4.4 Condensation mechanism

Condensation will occur if the temperature of the air or part thereof is below the saturation temperature corresponding to the vapour pressure in the air. There are basically two ways in which condensation can occur. Firstly, the air can become more saturated by increasing the amount of water vapour in the air (e.g. through breathing), and secondly by reducing the air temperature or part thereof.

In the latter case, it is obvious that heat will have to be transferred. For this to happen there must be a temperature gradient. There must thus be one or more surfaces that are colder than the air inside the zone or room of interest. The air closest to these surfaces would be the coldest. Condensation is then most likely to occur on these surfaces.

If the temperature of the air at the cold interface is below the saturation temperature, water droplets will form on the cold surface. This will cause the vapour pressure to decrease. Mass diffusion will take place to equalise the vapour pressure throughout the air vapour mixture.

For water vapour in air, the surface mass transfer coefficient is related to the surface convective heat transfer coefficient by the Lewis relation:

$$h_m = \frac{h_c}{\rho_a c_p} \tag{4.27}$$

where h_m is the mass transfer coefficient of water vapour at the surface, m/s
h_c is the convective heat transfer coefficient, W/m^{2}K
ρ_a is the density of the air, kg/m^3
c_p is the specific heat capacity at constant pressure, J/kgK.

An approximation of the total condensation rate would be:

$$w = \frac{h_m}{RT}(p_{va} - p_s) \tag{4.28}$$

where w is the total rate of condensation (or evaporation) at surface, kg/m^{2}s
R is the gas constant for vapour, 461 J/kgK
T is the temperature of the surface, K
p_{va} is the vapour pressure, Pa
p_s is the saturation pressure at surface temperature, Pa.

CIBSE [9] presented an expression for the saturation pressure as a function of the absolute temperature, T

$$\log_{10} p_s = 33.59 - 8.2\log_{10} T + (2.48 \times 10^{-3})T - 3142/T. \tag{4.29}$$

Condensation and evaporation are always accompanied by latent heat absorption or rejection. This energy transfer has to be taken into consideration when doing the energy balance at the interface between the surface and the air. The heat transfer is given by

$$q = wh_{fg} \tag{4.30}$$

where h_{fg} is the latent heat of evaporation (or condensation) of water at the surface temperature.

Kröger [13] suggested a correlation for the latent heat of evaporation (or condensation) as a function of the absolute temperature between 273.16 and 380 K as

$$h_{fg} = 3.4831 \times 10^6 - 5.8628 \times 10^3 T + 12.140T^2 - 1.4029 \times 10^{-2}T^3. \tag{4.31}$$

The energy that is rejected during the condensation process will need to be transferred away into the surface or else the surface temperature will rise.

Most calculation procedures have the dry bulb temperature and the relative humidity as part of the solution. To obtain the vapour pressure of the water under these circumstances we need a relation between the saturation pressure and the relative humidity at a given temperature:

$$p_{va} = \phi p_s. \tag{4.32}$$

Knowing the dry bulb temperature and the relative humidity, it is sufficient to calculate the vapour pressure of the water in the water air mixture. Further, using the surface temperature we can predict whether condensation will occur or not. All that remains is to calculate the surface temperature for the given structure. This procedure is provided in section 4.4.2.

In this section a procedure for the prediction of condensation is outlined. Empirical relations for properties such as saturation pressure and latent heat of evaporation is given for the ease of implementing the calculation procedure. It is assumed that the internal air temperature and the external sol-air temperature are known. These are not obtained by the calculation procedure given in this section.

4.5 NORMS EVALUATION

A number of parameters could be used to compare different designs to one another. They are:

1. Energy consumption for space heating.
2. The possibility of condensation, and on which surfaces it will occur.
3. Dry Resultant Temperature for summer comfort comparisons.

The energy consumption for space heating to keep the environmental temperature inside the dwelling at acceptable levels in winter is a direct result from the design tool. The prediction of condensation is described above.

The Dry Resultant Temperature (see CIBSE [9]) can be determined from the already available results. It is given by

$$T_{res} = 0.5T_i + 0.5T_r \tag{4.33}$$

where T_r is the mean radiant temperature of the surfaces under consideration, and
T_i is the dry-bulb temperature.

For each of the buildings under consideration, an assessment of all these parameters will be made for each of the major areas in the country, and tabulated according to performance.

4.6 AN EXAMPLE OF THE NORMS EVALUATION

In this section we will consider the application of the thermal design norms to a house that was previously considered difficult to analyse. The house under consideration is a dome-shaped house, with single brick partition walls. The dome is made of corrugated mild steel. In cold climates the dome is insulated with a minimum of 12.5 mm polystyrene and 4 mm hardboard. The doors and windows are standard equipment. Two options exist for the floor construction: 75 mm poured concrete onto a damp-proofed membrane or 150 mm compacted earth.

A schematic of the general construction is given in figure 4.5. For the evaluation of this house the dome was divided into five panels, all the same size, and at various tilt angles. The areas were chosen so that the total area is the same as the area of the dome. This is an approximation, but the results should be adequately accurate.

Using the norm evaluation tool based on the work in this chapter and chapter 2, the following results are then obtained. The buildings used for comparisons were chosen by the Board that provides certification for the proposed building designs. Five buildings are used for comparisons. They differ mainly in floor area except for the shack. The brick buildings are constructed with double brick walls and a pitched tile roof with a ceiling.

The results for this test house are shown in Appendix D.

4.7 CLOSURE

In this chapter, the theory for the necessary parameters to predict comfort, condensation and energy usage in buildings is reported. A thermal model that predicts the indoor temperatures as well as the mean wall temperatures is used to determine the overall thermal performance of buildings.

This thermal model includes aspects such as ventilation, radiation on tilted surfaces, and internal loads. From the resultant indoor temperature profile and the internal radiation loads, an accurate assessment of the wall temperatures can be made. This can then be used to determine whether condensation occurs.

The theory is implemented in a user-friendly program that has the user-profile of typical dwellers as default values in the program. These default valued are provided in Appendix C. One hundred and five verification studies are included in Appendix B to provide the user with the assurance that the program can predict building thermal performance with a large degree of certainty.

The evaluation of a building is not done in an absolute manner, but rather by comparing the performance of a given building to standard buildings of which the performance is known. A table of the data for all the regions for which the evaluations of standard buildings have been performed is included with the program.

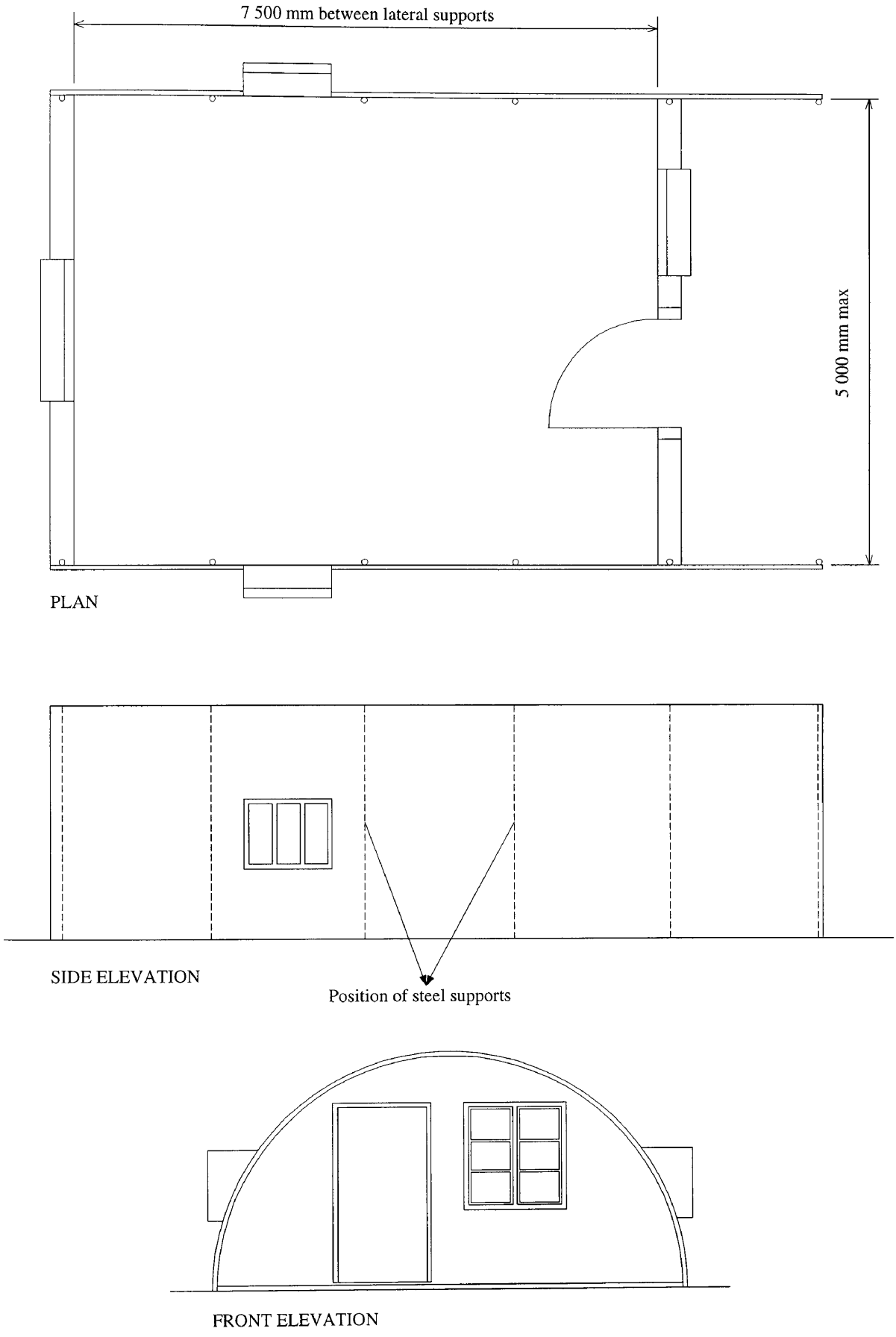

Figure 4.5: Plan and elevations of the test house.

Bibliography

[1] F.C. McQuiston and J.D. Parker. *Heating Ventilation and Air Conditioning, Analysis and Design*. John Wiley and sons, New York, fourth edition, 1984.

[2] American Society for Heating Refrigeration and Air Conditioning Engineers, Inc. *ASHRAE Handbook*, 1992.

[3] J.P. Holman. *Heat Transfer*. McGrawHill, Singapore, sixth edition, 1986.

[4] A.F. Mills. *Heat Transfer*. IRWIN, Concord, 1992.

[5] R.W. Bliss. Atmospheric radiation near the surface of the ground: a summary for engineers. *Solar Energy*, 5(3):103–120, 1961.

[6] A.J.A. Roux. Periodic heat flow through building components - heat exchange at the outside surface, with special reference to the application of sol-air temperature. National building research report dr 8, CSIR, Pretoria, 1950.

[7] P.H. Joubert. Numerical simulation of the thermal performance of naturally ventilated buildings. Master's thesis, University of Pretoria, 1987.

[8] D. Brunt. Radiation in the atmosphere. *Quarterly Journal of the Royal meteorological Society*, 66:34–40, 1940.

[9] Chartered Institution of Building Services Engineers, London. *CIBSE Guide, Volume A, Design Data*, 1986.

[10] L.A. Pipes. Matrix analysis of heat transfer problems. *J. Franklin Institute*, 18:195–206, 1957.

[11] M.G. Davies. Transmission and storage characteristics of walls experiencing sinusoidal excitation. *Applied Energy*, 12:269–316, 1982.

[12] C. Lombard. Two-port simulation of HVAC systems, an object oriented approach. Master's thesis, Mechanical and Aeronoutical Engineering, University of Pretoria, PRETORIA, January 1996. Chapter 4.

[13] D.G. Kroger. *Dry Cooling Towers for Power Stations*. University of Stellenbosch, Stellenbosch, 1988.

Part II

Integrated System Simulation

Chapter 5

INTEGRATED SIMULATION

Integrated simulation is a powerful means of determining the performance of a system without actually taking measurements at the site. Using the building thermal model, and models for system components derived by Rousseau [1], the integrated simulation can be accomplished.

The purpose is to predict beforehand what the influence of control parameters is, and to accurately determine the combined performance of the building and HVAC system. This should be done in a user-friendly and effective way.

NOMENCLATURE

A	Area, m^2
a_i	Regression coefficients
C	Fraction of full-load capacity
C_p	Thermal heat capacity J/kg K
CS	Control signal
c	Concentration, ppm
e	T_{SP} - $T_{measured}$
f	Fractions of rated power consumption for full-load conditions
h	Convective heat transfer coefficient, W/m^2K
K	Gain constant
K_d	Derivative gain constant
K_i	Integral gain constant
K_p	Proportional gain constant
L	Time lag, s or length, m
M	Metabolic rate, W
$\dot{m}$	Mass flow rate, kg/s
N	Number
n	number of air changes
Q	Volume flow rate, m^3/s
RQ	Respiratory quotient (rate of CO_2 produced to the rate of O_2 consumed)
s	LaPlace complex plane variable
T	Temperature, ^oC
TF	Transfer function
t	Time, s
V	Velocity, m/s or volume flow rate, m^3/s
τ	Time constant, s

Subscripts

a	air
hc	heating coil
s	sensor
SP	setpoint
td	time delay
z	building zone

5.1 INTRODUCTION

Integrated simulation is a powerful means of determining the performance of a system without actually measuring at the site. Using the building thermal model as introduced in chapter 2, and models for system components derived by Rousseau [1], the integrated simulation can be accomplished. The purpose is to predict beforehand what the influence of control parameters is, and to accurately determine the combined performance of the building and HVAC system.

To accomplish this, the solutions to the model predictions have to be obtained. This is described in the following section. In determining the solution one has to ensure that it can be obtained as efficiently and effectively as possible. This is discussed in section 5.3. Examples of the system dynamics are provided in section 5.4.

Further, it is extremely important that the simulation tool is easy to use and can simulate most of the processes occurring in real life. Further extensions to accomplish this are introduced in section 5.5.

5.2 SIMULATION PROCEDURE

After the models for all the components have been found, they need to be solved numerically and in the correct order. To set up a given configuration, a graphical user interface is used. The various components that make up a system can be dragged and dropped into position. Connections between these can then be established by graphically inserting the connections.

This establishes the configuration but the solution order still needs to be determined. To facilitate this, graph theory will be used. Tarjan [2] devised a recursive algorithm to transform any graph into a spanning tree. This algorithm will be adapted to determine the order in which the components that constitute a HVAC system need to be solved. The algorithm proposed by Tarjan can be adapted easily to accomplish two objectives, i.e. any ducting or piping system can be transformed into a tree, and the minimum unknowns can be identified.

In this context a graph is a number of nodes connected by a number of edges. In this application the edges are directed, i.e. a flow direction is associated with each edge. A tree is a representation of the graph showing in which order each node can be visited.

The procedure is as follows:

1. Store all components into a list, *Component List*. Ignore the controllers at first.
2. All the components in the HVAC system of which the properties are known are stored in a separate list, *Initial List*. Delete them from *Component List*.

3. Apply the Tarjan Depth-First-Search algorithm with each component in the *Initial List* as starting points. During this process all the components that make up a tree are deleted from the *Component List* and stored in the stack associated with each tree, *Tree[j]*.

4. At this stage all the components that remain in the *Component List* will be part of closed loops. Choose any component and apply the DFS algorithm to the graph that it forms part of. Repeat until *Component List* is empty. The first pipe in any given *tree* can be chosen as the unknown pipe in the *Unknown List*.

After this algorithm is applied, each *Tree* will consist of the components in a given duct or pipe network. The trees can be transversed and the network thus solved. Interactions among the various trees have however not been taken into account. These interactions will occur at components that form part of two or more trees, e.g. a cooling coil will be part of a duct network and of a pipe network.

To solve this problem we will employ the following algorithm:

1. Insert all pipes and ducts leaving the *Initial List* into a *Known List*.

2. Transverse a *Tree*, and insert the components we encounter in a *Visited List*, and the pipe leaving it into the *Known List*, provided that all incoming pipes and ducts are in the *Known List*. Delete each component inserted into the *Visited List* from the present *Tree*.

3. If all incoming pipes or ducts are not in the *Known List* then select the next *Tree*.

4. Repeat the steps until all the trees are empty.

Eventually each component will be visited and inserted into the *Visited List*. The components can now be solved in the order in which they occur in the *Visited List*.

5.2.1 An illustrative example

To illustrate the procedure introduced above consider the following example. Figure 5.1 shows a diagrammatic presentation of a simple HVAC system. Applying the algorithm gives the tree structure as shown in figure 5.2.

After applying the second algorithm the contents of the Visited List are:

1. Climate

2. Temperature sensor (air loop)

3. Air diverge

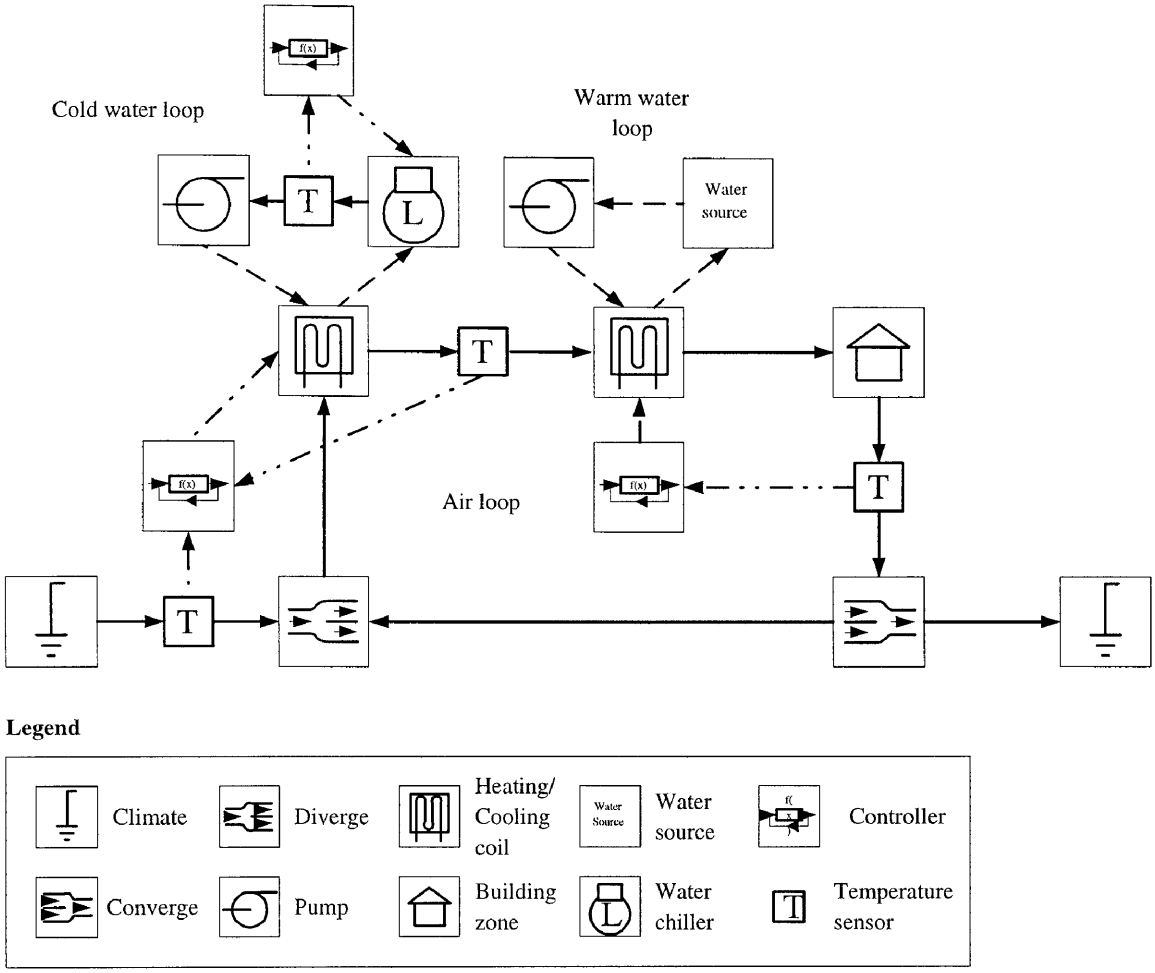

Figure 5.1: Diagram of an HVAC system.

4. Liquid chiller
5. Temperature sensor (cold water loop)
6. Cold water pump
7. Cooling coil
8. Temperature sensor (air loop)
9. Water source
10. Warm water pump
11. Heating coil
12. Building zone
13. Temperature sensor
14. Air converge
15. Climate.

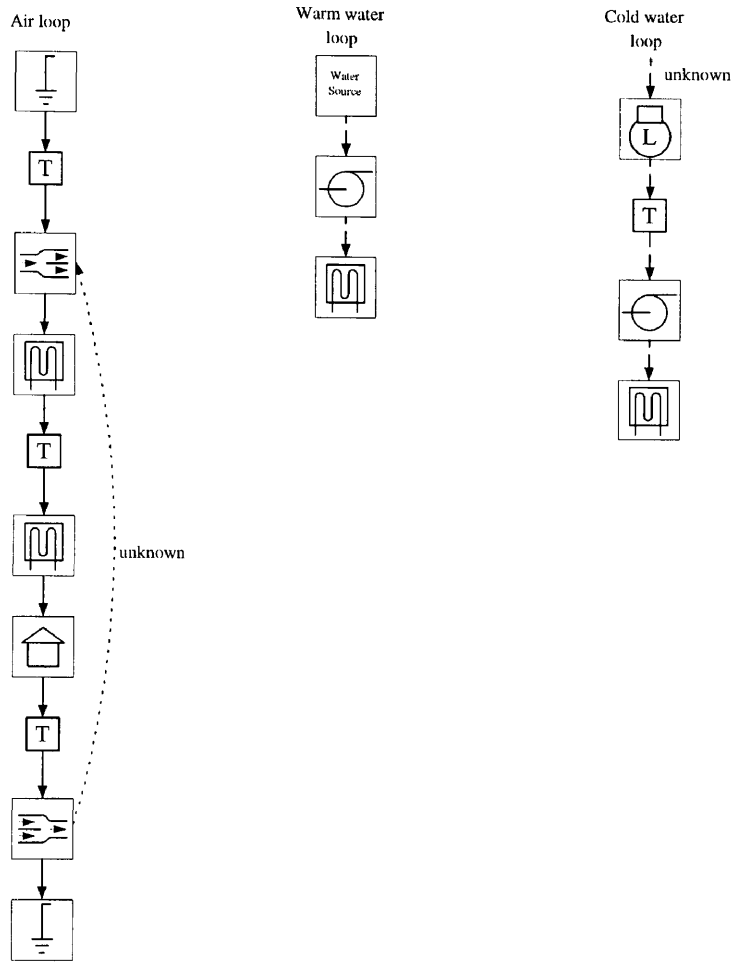

Figure 5.2: Resulting tree structures after applying the algorithm introduced in the text. See figure 5.1 for symbol definition.

And the contents of the *Unknown List* are:

1. Duct from converge to diverge
2. Pipe from cooling coil to chiller.

The number of unknowns that need to be solved simultaneously would be three, i.e. the pipe temperature, the enthalpy and the humidity ratio of the air. The procedure to solve these will be presented in the next section.

The value of the controller output at the current time step will depend only on the value of the controller input from the previous time step. This implies that the controller simulation is explicit, while the rest of the variables are solved implicitly.

This simulation procedure can be adapted to include the controller output. This would however increase the number of variables to be solved. An additional complication is the instabilities which are associated with the iterative solution of the system and control dynamics.

5.3 SOLUTION OPTIMISATION

Solution optimisation will consist of two major components, i.e. numerical methods and code optimisation. Most of the topics in this section are well known, but it is informative to consider each in some detail. A balance between simplicity and efficiency is attempted throughout.

5.3.1 Numerical methods

As discussed in section 5.2, the solution of the simultaneous equations resulting from the component models and configuration description has to be solved. The solution procedure is inevitably an iterative procedure. Most of the equations begin with one or more of three type of variables.

In water loops, the water temperature is the variable used. In air loops there are two variables, i.e. the enthalpy of the air and the humidity ratio. One can choose any two independent variables for the purpose of solving the equations. Energy is a convenient choice since it is easy to relate to. The other variable is also fairly easy to relate to, and results from the maintenance of mass.

Let $\mathbf{X}_i$ be the starting values of the variables for the first iteration. Let $\mathbf{X}_f$ be the value of the variables after the first iteration. Then we can define the functions $\mathbf{F}(\mathbf{X}_i) = \mathbf{X}_f - \mathbf{X}_i$. The purpose of any solving algorithm will then be to solve for $\mathbf{X}_i$ so that $\mathbf{F}(\mathbf{X}_i) = 0$. Methods to find these roots are discussed next.

Successive approximation

By successive approximation we mean that the first value at a given time step solution is chosen arbitrarily. In successive iterations the value obtained in the previous iteration is used as guess to the next iteration. This procedure is not guaranteed to converge, and even if it does it can do so extremely slowly. It is thus obvious that this method is not the most efficient and should therefore be avoided.

Linear interpolation

Linear interpolation here is a special application of the secant method. The first iteration value is again chosen arbitrarily, and then two or more successive approximation steps are taken in order to approximate the first derivative of the functions. Once two or more values of the function evaluations are available, interpolation or extrapolation can be done to approximate the zero of the function values. Clearly, linear interpolation will result in an effective solution algorithm if two conditions hold:

1. The functions do not deviate substantially from linearity. If this is not so the method could, in fact, result in diverging solutions.

2. The individual functions are only weakly dependent on the parameters that are ignored in the linear shooting method.

Newton's method

It is well known that Newton's method is quadratically convergent for starting values close to the root of the functions. A further major advantage is that Newton's method takes the dependencies of all functions with all variables (parameters) into account when shooting for the next approximation.

Unfortunately, the method is not guaranteed to converge for starting values far from the roots. Secondly, the Jacobian for the given problem has to be calculated at each iteration. A solution to a number of simultaneous linear equations also has to be obtained at each time step. This results in a large number of function evaluations, and thus a lot of computer execution time.

Quasi-Newton methods

Quasi-Newton methods use an approach similar to the Newton's method, but use an approximation of the inverse of the Jacobian (Hessian). Probably the most famous of these is the Broyden updating algorithm. (See for instance R.L. Burden and J.D. Fairs [3].) The Quasi-Newton methods do not converge as fast as Newton's, but the number of function evaluations more than compensates for this. There is also the added advantage that Quasi-Newton methods converge in some cases where pure Newton methods do not [3].

A variation of the Newton method was implemented, i.e. the Jacobian was calculated and inverted at the first step. Then the inverse was used until the predicted changes in the variable were more than ten per cent of their previous value, or when convergence did not occur in five iterations. This reduces the number of function evaluations dramatically.

5.3.2 Code optimisation

The solution procedure was implemented in Pascal. Most of that which is discussed hereafter is particular to Pascal, although the principles are generally true.

Number types

Historically, Borland Pascal implemented their floating point number types as eight-byte *reals*. Borland Pascal compilers have the option of compiling code with or without numeric co-processor emulation. The *real* number type provided an effective twelve-digit floating point number type for computer without math coprocessors. Borland Pascal also provide three other floating point number types, i.e. *single* (six bytes), *double* (ten bytes) and *extended* (twelve bytes). In contrast to the *real* number type the others do conform to the IEEE standard for floating point number types.

This has the advantage that the math co-processor present in most PCs today handles these number types much more effectively than the Pascal *real* type. The IEEE standard provides for a ten-byte floating point number type, so one would expect the *double* type to be the best choice. There are however other considerations such as the number of memory accesses required to load each variable from memory.

5.4 SYSTEM DYNAMICS

The models established by Rousseau [1] are steady-state models, i.e. the dynamics of the components and the flow in the pipes and ducts are not considered. These dynamics cannot be ignored if the purpose is to simulate the effect of control parameters. There are a number of factors that contribute to the dynamics of the individual components and the combined system, inter alia

1. Mechanical inertia, especially at start-up and shut-down (pumps, fans and compressors).
2. Time delays associated with fluid flow in ducts and pipes.
3. Thermal capacities. Elements such as coils and heat exchangers and the fluids in them have finite capacity and therefore take time to heat up or cool down.
4. Sensors will typically respond exponentially to a step change in the fluid properties being measured.
5. The controller itself if it has non-zero integral or differential constants.

Each of the contributing factors discussed above will be discussed in detail in the following sections.

5.4.1 Mechanical inertia

All rotating equipment will take time to reach its operating speed due to the polar moment of inertia of the motor and other rotating elements being non-zero. Modern motor starters also limit

the start-up current in order to increase the motor life. Thus, if a fan or pump is controlled by controlling the rotational speed of such component, that component will take time to respond to the control signal that has changed.

The same argument holds for linear mechanical elements such as proportionally controlled valves. Linear displacement of these elements also takes time due to the fact that the masses of the elements are non-zero. By physical argument one can deduce that these transients will happen on very short time-scales.

5.4.2 Time delays

Time delays can be attributed to the fact that a fluid takes time to move from point A to point B in a duct or a pipe. Here the time-scales are a function of the length of the duct or pipe, and the fluid velocity.

As an example, the time it takes for air moving at 2 m/s to travel from a cooling coil to a building zone 20 m away will be 10 s. In a variable air volume (VAV) system this time delay is a function of the volume flow rate, and can vary with time. This could lead to difficulty in modelling VAV systems.

5.4.3 Thermal capacity

Thermal equipment with a high thermal mass and high thermal resistance will take considerable time to reach the equilibrium temperature after a change in the setpoint has been made by the controller.

There are a number of potential contributors to this dynamic response, for example, the material from which the coil or heat exchanger is made, and the cooling/heating fluids e.g. water, glycols and refrigerants. These all have thermal capacities that could be high. The other factor is the rate at which heat can be transferred to and from the metal and fluids. Notoriously, the heat transfer coefficients for water and refrigerants are high. The thermal conductance of most metals is also generally high.

It is very difficult to predict how much time it will take for equilibrium to be reached in such equipment.

5.4.4 Sensor dynamics

Temperature sensors also take time to reach the temperature of the medium of which they are measuring the temperature. This is again a function of the thermal capacity of the sensor and the heat transfer coefficients between the sensor and the fluid.

Sensors typically used for measuring air temperatures have diameters of approximately 12 mm. The convective heat transfer coefficient for air flow at 2 m/s is approximately 20 W/m^{2}K.

Assuming that the sensor is made of steel, this would result in a time constant in the region of 200 to 500 seconds for that sensor. (This is admittedly a relatively large sensor, but it does illustrate the point.)

If the same sensor is used in water, where the convective heat transfer coefficients are approximately 1000 to 2000 W/m^{2}K, the time constants are in the region of 2 to 5 seconds.

5.4.5 Controller dynamics

The purpose of the controller is to adapt to the dynamics of the system being controlled, in order to produce the required response. Therefore the controller dynamics are 'tuned' to get the best or at least an acceptable response from the system.

In most HVAC applications, PID, On/Off or step controllers are used. The controller dynamics that we are discussing here include only the integral and derivative components of the PID controller.

5.4.6 An example of system dynamics

To illustrate the concepts discussed in the previous section, consider the following simplified yet typical situation in figure 5.3. The block diagram of this system is shown in figure 5.4. In the block diagram the physical controller is represented by the reference input, the subtractor and the controller block.

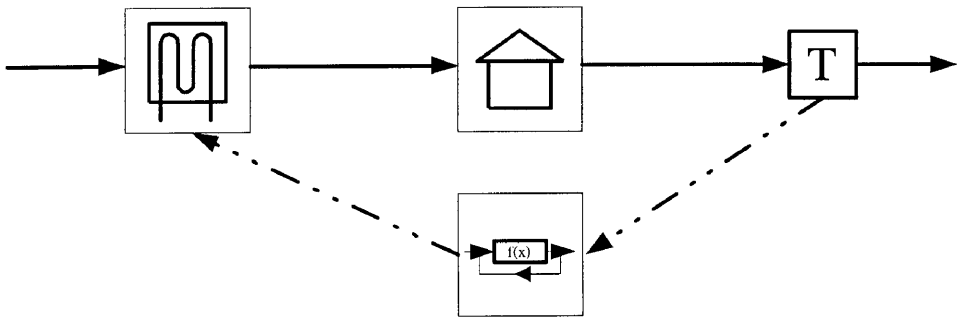

Figure 5.3: Diagram of a control loop.

Determining the gain and setpoint in the physical controller is done by specifying the temperature (in this case) at which the valve (in this case) must be fully open, as well as the temperature at which the valve must be fully closed. The integral and the differential factors are determined by specifying their numerical values.

The controller dynamics can be represented by the following:

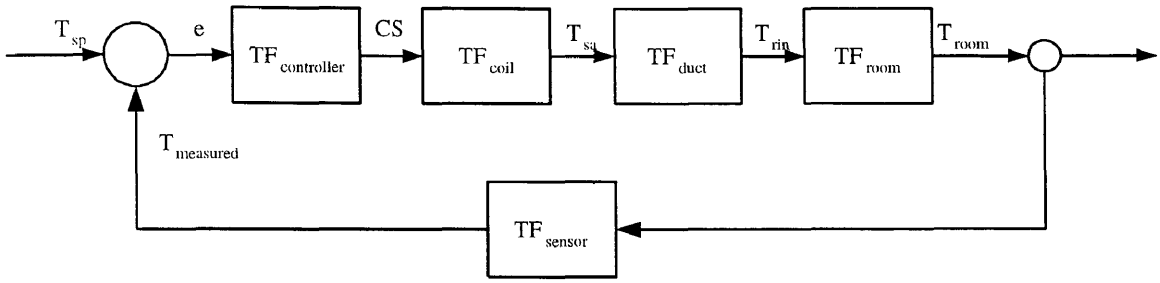

Figure 5.4: Block diagram of the control loop shown in figure 5.3.

$$CS = K_p e + K_i \int e dt + K_d \frac{de}{dt} \tag{5.1}$$

or, equivalently, by

$$CS = K\left(e + K_i' \int e dt + K_d' \frac{de}{dt}\right). \tag{5.2}$$

Here e is T_{SP} - $T_{measured}$
CS is the Control signal
K_p is the proportional gain constant
K_i is the integral gain constant
K_d is the derivative gain constant.

The resultant transfer function for the controller is

$$TF_c = K_p + \frac{K_i}{s} + K_d s. \tag{5.3}$$

Modelling the sensor will be done by a first-order differential equation:

$$\frac{dT_s}{dt} = \frac{(T_s - T_f)A_s h_f}{m_s C_{ps}}. \tag{5.4}$$

The resultant transfer function for the sensor is

$$TF_s = \frac{1}{1 + \tau_s s} \tag{5.5}$$

where $\tau_s = \frac{m_s C_{ps}}{A_s h_f}$.

For the building zone, only the air node will be considered. All the heat gains from the walls and convective gains will be ignored to simplify the analysis. Thus the building zone air node can be modelled as follows:

$$m_a C_{pa} \frac{dT_a}{dt} = \frac{(T_{in} - T_a)}{\dot{m}_{in} C_{pa}}. \tag{5.6}$$

Simplifying the equation and taking the La Placian results in

$$sT_a(s) = \frac{\dot{m}_{in} C_{pa}}{m_a C_{pa}} T_{in}(s) - \frac{\dot{m}_{in} C_{pa}}{m_a C_{pa}} T_a(s). \tag{5.7}$$

The resultant transfer function for the building zone is

$$TF_z = \frac{1}{1 + \tau_z s}. \tag{5.8}$$

Here $\tau_z = \frac{m_a C_{pa}}{\dot{m}_{in} C_{pa}} = \frac{1}{air\ changes\ per\ second}$.

The time delay for the air to flow from the coil to the building zone will be considered. We will assume that the air flows at 2 m/s and has to cover a distance of 40 m, thus a time delay of L = 20 s.

$$TF_{td} = e^{-Ls} \approx \frac{2 - sL}{2 + sL}. \tag{5.9}$$

The approximate relation in equation 5.9 is the Padé polynomial approximation in the La Place domain of a time delay.

All that remains is to model the heating coil. As this is a formidable task we will again assume that the coil can be modelled using a first-order differential equation. We will not endeavour here to model the coil completely. Instead we will follow a similar approach to that of J.F. Kreider and A. Rabie [4], and will write the transfer function directly in the La Place domain:

$$TF_{hc} = \frac{K_{hc}}{1 + \tau_{hc} s}. \tag{5.10}$$

Here K_{hc} is the efficiency of the coil and τ_{hc} is the coil time constant.

From the control block diagram, the overall transfer function can be found to be

$$TF_{overall} = \frac{G(s)}{1 + G(s)H(s)}. \tag{5.11}$$

G(s) represents the dynamics of the feed forward elements, and H(s) is the sensor dynamics.

The characteristic equation is thus

$$0 = 1 + G(s)H(s)$$

$$0 = 1 + \left[\left(\frac{K_p s + K_i + K_d s^2}{s}\right)\left(\frac{K_{hc}}{1+\tau_{hc}s}\right)\left(\frac{2-sL}{2+sL}\right)\left(\frac{1}{1+\tau_z s}\right)\right]\left[\frac{1}{1+\tau_s s}\right]. \tag{5.12}$$

If we make the derivative constant zero, and factor out the open loop gain, the resultant characteristic equation is

$$0 = 1 + \frac{K_p K_{hc} K_i'(1+\frac{s}{K_i'})(1-0.5sL)}{s(1+\tau_{hc}s)(1+0.5sL)(1+\tau_z s)(1+\tau_s s)}. \tag{5.13}$$

For our example we can now study the stability of the system, and the effect of the proportional gain and the integral and derivative constant. We must first obtain, or where this is not possible, assume values for the other parameters:

τ_{hc}	= 30	seconds	(assumed)
τ_z	= 450	seconds	(corresponds to 8 air changes per hour)
τ_s	= 300	seconds	(typical value as derived above)
L	= 20	seconds	(corresponds to 40 m duct and air flowing at 2 m/s)
K_{hc}	= 20		(throttling range assumed).

Figure 5.5 shows the Root-Locus diagram for the system described above. For this diagram the derivative and integral control constants are set to zero. One can deduce that for moderate values of the proportional gain the control loop is stable.

There are other poles and zeros that are not shown in this diagram due to the fact that they are very far from the origin. There is one zero on the right hand side of the imaginary axis (at 0.1) and a pole on the left hand side (at 0.1). This is a result of the Padé-approximation.

Studying the response of the system to a unit change in the setpoint we find that the settling time is very long and that the rise time too is long (See figure 5.6). An important point to be made here is that the setpoint is never reached. This is due to the fact that we only have a proportional gain controller.

The purpose of a controller is to modify the dynamic response in order to get a better response time, shorter settling time, and smaller overshoot. This is illustrated in the second root-locus plot (figure 5.7), and the step response for this controller is shown in figure 5.8.

For the PID compensated system, the overshoot has been reduced to less than 20% (compared to 32% of the final value in the case of the proportional only control). The settling time too has been reduced to approximately 1000 seconds (compared to approximately 3000 seconds).

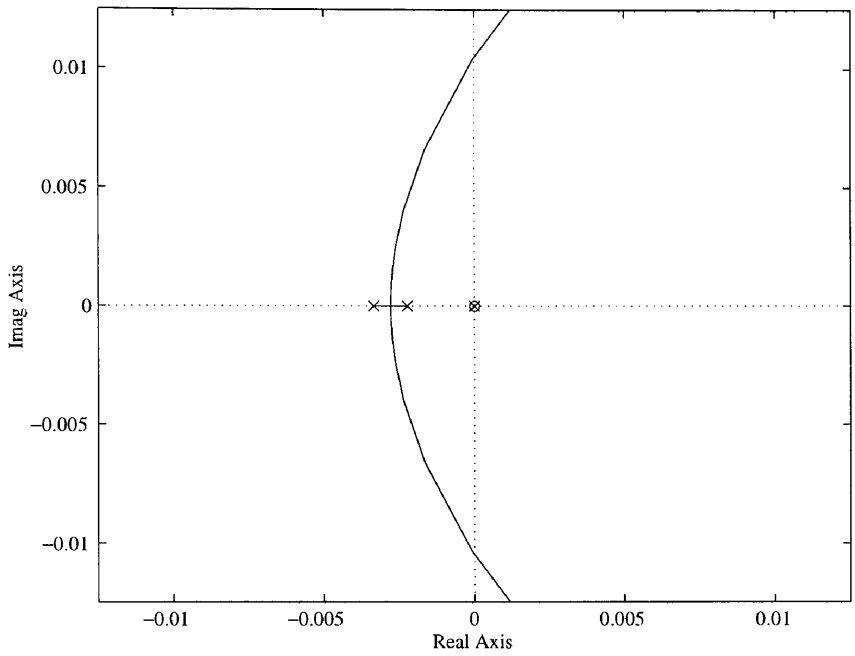

Figure 5.5: Root-Locus diagram for the system described in the text. ($K_i = K_d = 0$)

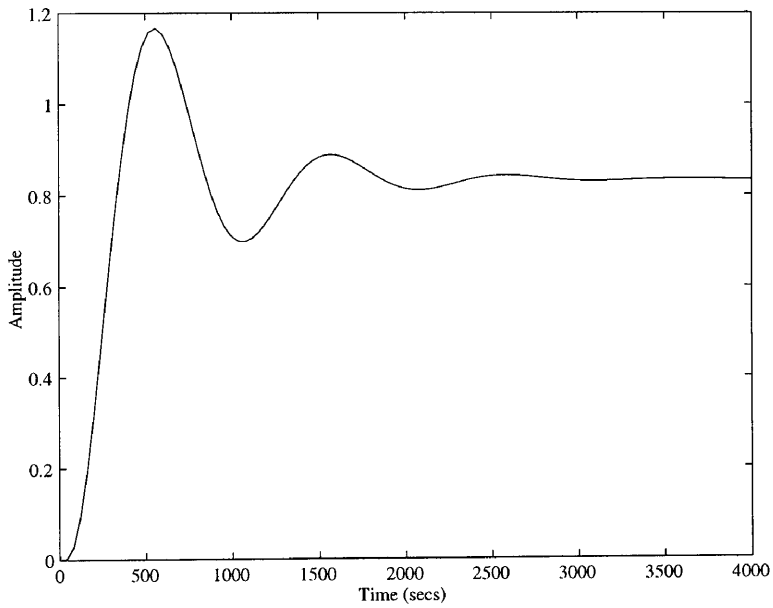

Figure 5.6: Step response of the system with proportional gain only. ($K_i = K_d = 0$)

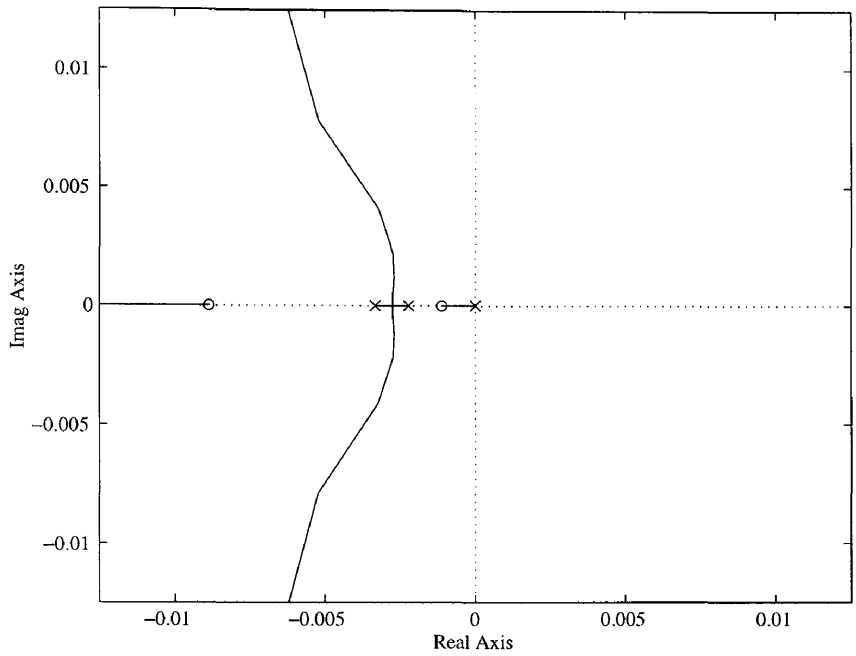

Figure 5.7: Root-Locus diagram for the system described in the text. ($K_i = 0.01, K_d = 1000$)

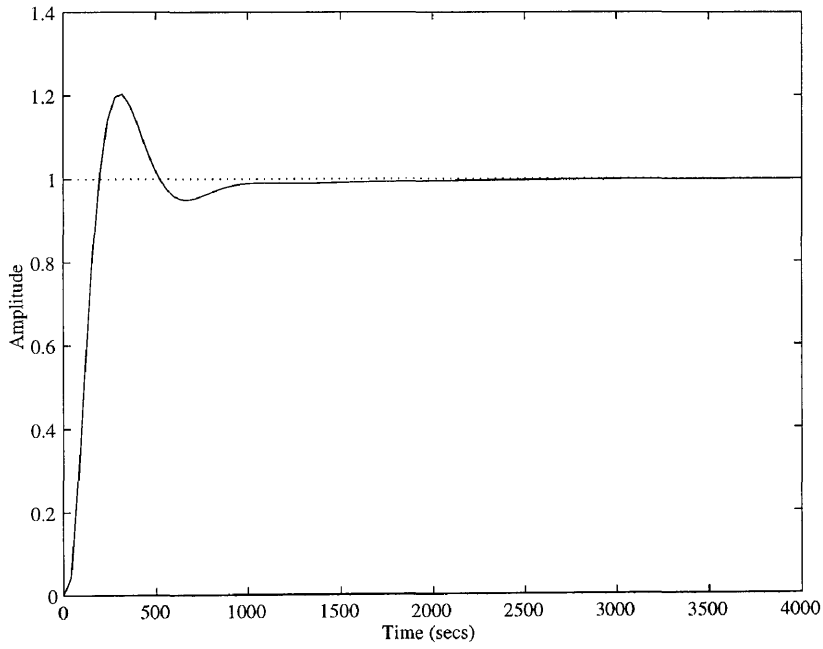

Figure 5.8: Step response of the PID compensated system. ($K_i = 0.01, K_d = 1000$)

It should be pointed out that the new loop will also become unstable at large values of the proportional gain constant.

For a recent discussion on the tuning of PID controllers in HVAC systems, refer to Geng and Geary [5]. They propose a modification to the Ziegler-Nichols method for PID controller tuning. This topic will not be pursued here.

Throughout the previous discussion it was passively assumed that the system is linear. As a matter of fact, almost all the theory that is currently available assumes that the system on which it is applied is linear. More correctly, that in the region in which the system is operated it can be assumed to be linear.

In the previous section we do not know if the controller signalled the valve of the heating coil to open more than 100 % or to close beyond 0 %. In fact, in the theory that we used we cannot make provision for these limits, except to limit the gain margin so that the controller would not give a control signal outside these limits.

The discussion is instructive however, seeing that we can theoretically determine whether or not a system is stable, as well as determine control constants to comply to certain criteria. For real systems that are highly nonlinear, the only option is to simulate the system. It is then important to accurately simulate the dynamics of the system.

It should be clear that ignoring the dynamics of the components would result in the incorrect system being simulated. Controller simulation would thus be futile. In the next section, a first attempt at extending the existing models to account for the dynamics will be made.

5.5 NEW MODELS

In order to successfully simulate the dynamics of a system and building, one needs to have accurate models of the individual components. Such models for the various components have been established by Rousseau [1], and in this study (chapter 2), for the building thermal modelling.

As pointed out in the previous section (section 5.4), if control is to be simulated, the system dynamics have to be accounted for. For the various existing steady-state models, an extension needs to be implemented. The time delay introduced by the flow in the ducts and the pipes will have to be approximated.

For many applications, this time delay will be insignificant compared to the overall dynamics of the system. In control loops however, this could be the dominating factor and thus needs to be accounted for.

In the next sections new models will be introduced, and extensions to existing models will be presented. The first extension and new model are due to the system dynamics that need to be accounted for. The remaining models are extensions to the simulation tool.

5.5.1 Dynamics in the existing models

The existing models introduced by Rousseau [1] are steady-state models. The models thus give an indication of the gain of the devices that they are models of. To introduce the dynamic effects one would need a time constant. For the existing models it is suggested that a simple time constant approach is used. The user will thus be responsible for supplying a time constant.

As stated above, first-order models will be assumed for the existing models. This would imply that modelling of the following form would be used:

$$\tau \frac{d\psi}{dt} = function(model\ input\ parameters). \tag{5.14}$$

Here τ is the time constant of the model, and
ψ is one of the output parameters of the model.

The sensors used in the simulation model can also be modelled using the technique introduced above.

5.5.2 Pipe and duct flow dynamics

Dynamic simulation of the flow in a pipe and a duct cannot be accomplished using the technique introduced in the previous section, since the dynamics of a pipe or duct are, to a good approximation, pure time delay. This is especially true for pipes or ducts with large length-to-diameter ratios.

In the time domain, record would have to be kept of where in the pipe or duct the change in property is. This could be a formidable task and could have implementation implications that could become problematic. In the example in section 5.4, the Padé approximation could be used in the La Place domain as an approximation of the time delay.

For the present implementation the direct time domain implementation will be used. This implies that record must be kept of the properties as they enter a pipe. The number of records, N, will depend on the velocity of the fluid in the pipe, V, the length of the pipe, L, and the length of an integration time step, Δt, i.e.

$$N = round(\frac{L}{\Delta t V}) + 1. \tag{5.15}$$

A dynamic data structure will be used to store the time series of the fluid properties. Each new incoming value will replace the previous one that was first in the data structure, and all other values will move up one time space. The value kept in data location N + 1 will contain the value of the fluid's property leaving the pipe or duct.

This implementation by its nature is highly nonlinear, and care should be taken when it is used in a simulation. Very short simulation time steps will be required to maintain a stable simulation. It is suggested that it is only used where the delay effects are thought to have a significant contribution to the overall dynamics of the system.

5.5.3 Part-load modelling

In the models suggested by Rousseau [1], only the full-load characteristics of the HVAC equipment was taken into consideration. To accurately predict the energy consumption under part-load conditions, the following modelling is suggested:

$$f(C) = a_0 + a_1 C + a_2 C^2. \tag{5.16}$$

Here:

a_n Regression coefficients
C Fraction of full-load capacity
f Fraction of rated power consumption for full-load conditions.

The coefficients that are used will depend on the specific component, and if the part-load performance is provided by the manufacturers. If the part-load performance is not provided, the correlations given by Yang et al. [6] are suggested.

5.5.4 CO_2 modelling

The introduction of a CO_2 model in the simulation tool is necessitated by the advantages of controlling on this basis, in the case when occupancy can vary greatly. If the minimum air requirements are supplied to the zone based on the nominal occupancy levels, then it could result in larger cooling or heating loads on the HVAC system. In the building zone, the CO_2 concentration is of utmost importance. High levels of CO_2 could adversely affect the health and productivity of the occupants.

For this reason it is imperative that this very important energy saving potential be modelled in a simulation tool. In this section CO_2 modelling is introduced.

The zone model

In the building zone there are basically only two sources of CO_2:

1. CO_2 is present in the outdoor or supply air, and
2. CO_2 is introduced by the occupants' respiration.

ASHRAE [7] suggests a relation between the metabolic rate of the occupant and the volume rate of

$$V_{CO_2} = \frac{2.76 \times 10^{-6} A_d M}{(0.23RQ + 0.77)} RQ \tag{5.17}$$

where V_{CO_2} is the volume of CO_2 produced in m^3/s
A_d is the outer skin area of a human in m^2
M is the metabolic rate
RQ is the respiratory quotient (rate of CO_2 produced to the rate of O_2 consumed).

Further

$$RQ = \begin{cases} 0.83 & for M \leq 1.5, \\ 0.04857M + 0.757 & for M > 1.5. \end{cases} \tag{5.18}$$

Following a similar procedure to Jones [8], consider a room of volume, V m^3 and a number of people, N inside. Air with a CO_2 concentration of c_a ppm enters the room at a rate of Q m^3/s. Each occupant produces CO_2 at a rate of V_c m^3/s, per person. The concentration of CO_2 in the room at any time is c in ppm.

In a given time increment, Δt, a mass balance for the given room yields:

$$\Delta c = \frac{Q(c_a - c)\Delta t + NV_c \Delta t 10^6}{V}. \tag{5.19}$$

Dividing by Δt and taking the limit as $\Delta t \to 0$

$$\frac{dc}{dt} + \frac{Qc}{V} = \frac{Qc_a + NV_c 10^6}{V}. \tag{5.20}$$

Multiplying throughout with the integration factor $e^{Qt/V}$ and integrating yields:

$$A + ce^{Qt/V} = \frac{Qc_a + NV_c 10^6}{V} \frac{V}{Q} e^{Qt/V} \tag{5.21}$$

where A is the integration constant. If $t = 0$ then $c = c_0$ so that

$$A = c_a - c_0 + V_c N 10^6. \tag{5.22}$$

Thus, with $n = Q\delta t/V$ (the number of air changes):

$$c = \left(\frac{V_c N 10^6}{Q} + c_a\right)(1 - e^{-n}) + c_0 e^{-n}. \tag{5.23}$$

Air converges

In this context, an air converge is any combing-flow duct. From a simple mass balance it follows that:

$$c_{leaving} = \frac{\sum_{i=1}^{N} \dot{m}_i c_i}{\sum_{i=1}^{N} \dot{m}_i}. \tag{5.24}$$

Here c is the concentration of CO_2 [ppm]
N is the total number of inflowing branches
$\dot{m}_i$ is the mass flow rate in duct i [kg/s].

Other components

For all other components, the concentration of CO_2 leaving is simply equal to the concentration entering. The assumption is that no CO_2 is produced or absorbed by any of the HVAC components.

This model has been implemented in the design tool. The same solution procedure as introduced in section 5.2 is used to solve the CO_2 balance in the HVAC system. The potential energy savings using a CO_2 control strategy instead of a standard temperature or enthalpy economiser are illustrated in section 6.4.5.

5.6 CLOSURE

In this chapter, the solution of the models as presented by Rousseau [1] is presented. A modification to the standard Newton method was introduced to solve the energy and mass conservation equations. The solution is very stable and the minimum number of variables are solved at each time step.

A means for introducing dynamics into existing models is also presented, as are dynamics of flows in ducts and pipes. The time constants need to be accurately known if control parameters are to be fine tuned using the simulation tool. For year simulations the dynamics are not as important and no significant errors will be introduced if long time constants are used. Determining accurate values for the time constants will be recommended for future work. Finally, the modelling of CO_2 is introduced.

In chapter 6, further extensions to the control modelling are presented. Substantial verification of the individual models is presented by Rousseau [1]. He also presented verification of an integrated simulation of an office building. Further validation of the integrated simulations will be presented in chapter 7.

Bibliography

[1] P.G. Rousseau. *Integrated Building and HVAC Thermal Simulation*. PhD thesis, Mechanical Engineering, University of Pretoria, 1994.

[2] R. Tarjan. Depth-first search and linear graph algorithms. *SIAM Journal of Computing*, 1(2):146–160, June 1972.

[3] R.L. Burden and J.D. Faires. *Numerical Analysis*. PWS-KENT Publishing Company, Boston, 1989.

[4] J.K. Kreider and A. Rabl. *Heating and Cooling of Buildings, Design for Efficiency*. McGraw-Hill, Singapore, 1994.

[5] G. Geng and G.M. Geary. On performance and tuning of PID controllers in HVAC systems. In *Seccond IEEE Conference on Control Applications*, Vancouver, B.C., 13-16 September 1993.

[6] K.H. Yang, C.H. Su, and R.L. Hwang. An efficient method to calculate annual energy use of buildings. *Transactions of SHASE*, 60:157–164, Febuary 1996.

[7] American Society for Heating Refrigeration and Air Conditioning Engineers, Inc. *ASHRAE Handbook*, 1992.

[8] W.P. Jones. *Air Conditioning Engineering*. Edward Arnold, London, fourth edition edition, 1994.

Chapter 6

ENERGY MANAGEMENT SYSTEMS

There are a vast number of ways to reduce the energy consumption of HVAC systems. These are collectively named Energy Management Programs. They are implemented in what are called Energy Management Systems. With the advances in electronic digital controllers it has become possible to implement advanced control strategies.

Most of the benefits derived from the implementation of these strategies can be predicted qualitatively. One needs an accurate simulation tool to quantify the actual benefits prior to implementing the actual strategy. This chapter describes the extensions to a simulation tool that can provide these answers.

NOMENCLATURE

a_i	Regression coefficients
T	Temperature, °C

Subscripts

in	inside
ma	monthly mean

6.1 INTRODUCTION

In the building and HVAC control industry, there is a need for more energy-efficient control. To this end, a number of features are build into most Direct Digital Controllers (DDC). These features are collectively referred to as Energy Management Systems (EMS). Most manufacturers have, from experience, a good estimation of the payback periods for installation of each control strategy.

Accurate assessments of the potential benefits can only be made once the system is operational or an accurate simulation can be performed. The simulation tool described in this study can be extended to include the simulation of various energy management strategies.

In 1991 Reinold A. Carlson and Robert A. Di-Gandomenico [1] wrote that "Approximately 67% of the energy consumed in an office building is electrical. Thirty-three percent is oil, gas, and purchased steam or hot water. A breakdown of the electrical energy consumed reveals that cooling systems use 40%, lighting systems use 33%, heating 12%, and the remaining 15% is consumed by other means. The energy management strategies, resident in the DDCs, address all of these areas of energy consumption."

It would thus follow that a simulation tool should be able to simulate these control and energy management strategies. There are a number of obvious ways in which energy usage can be reduced, inter alia:

1. Reduced running times.
2. Use of free cooling/heating.
3. Using reset programs to minimise mechanical equipment loads and operation.
4. Reducing lighting levels if they are excessive.
5. Temperature set-backs.

For most of these strategies it is obvious that there will be a potential benefit. However, there are situations where it is not so obvious that there will be benefits. For example, night ventilation is a tried and tested method of using 'free cooling'. If the fans consume more power than the reduction in energy consumption of the mechanical cooling equipment, it is no longer a benefit.

Both the energy saving and effect on comfort cannot always be determined off-hand. For this too a simulation program would be beneficial. There is an added benefit for some of these strategies namely, the size of the initial system can be reduced.

There is a proliferation of various energy management strategies. The most common of these will be discussed in the following sections. Only the imagination of the engineer limits the possibilities. It would be ideal to be able to simulate all possible options, but this will not be attempted here.

It will however, become clear that the facilities implemented are adequate to provide a good indication of the energy savings potential. In the following sections, a simplified but fully integrated HVAC system will be considered to illustrate the facilities implemented.

6.2 SETPOINT-RELATED ENERGY MANAGEMENT STRATEGIES

6.2.1 Temperature reset

A simple constant temperature constant volume reheat system will be introduced here. Consider the HVAC system shown in figure 6.1. The controller parameters are given in table 6.1. As a benchmark, the energy profile and indoor temperature will be given in figure 6.2 and figure 6.3.

Controller	Controlled value		Controlled item	
	Min value	Max value	Min value	Max value
Chilled water controller	7	9	0	1
Cooling coil controller	14	17	0	1
Heater controller	11	14	1	0
Reheater controller	20	22	1	0

Table 6.1: Controller parameters for illustrative example.

There are interesting observations to make from these results.

1. The temperature inside the zone is at the setpoint for 24 hours.
2. The mechanical equipment is operational for 24 hours.

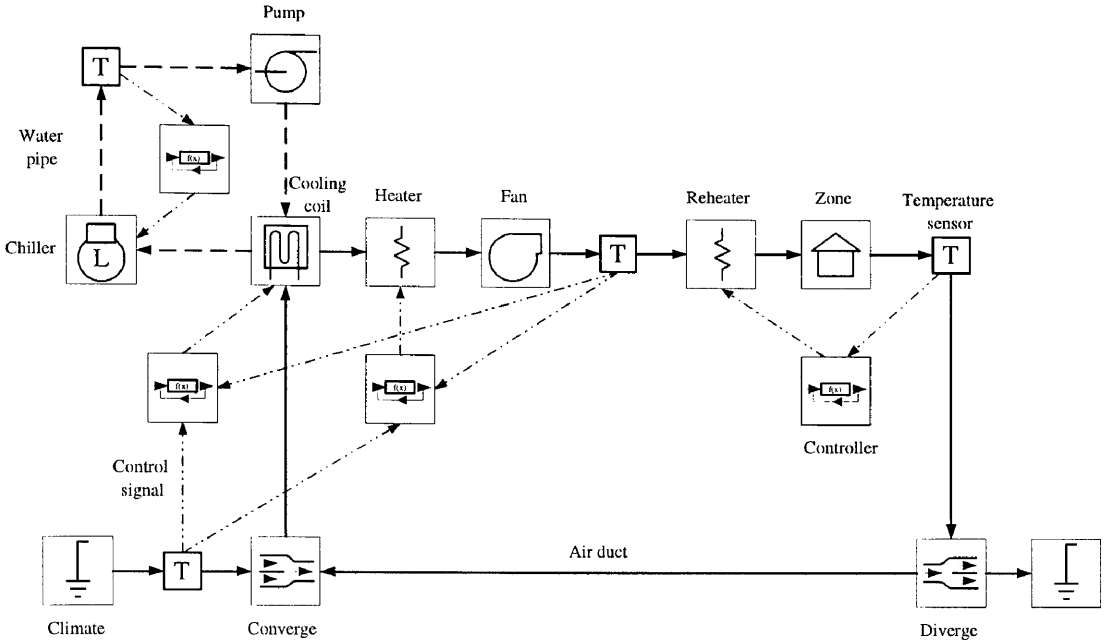

Figure 6.1: Constant temperature constant volume with reheat system used as illustrative example.

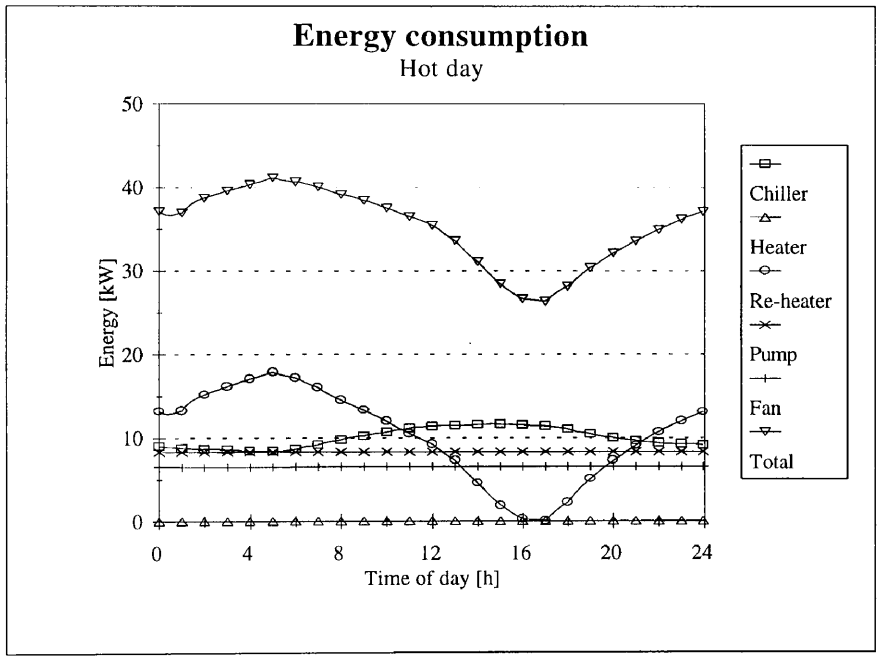

Figure 6.2: HVAC system energy usage. (These results will be used for comparing the next strategy to.)

3. From figure 6.2 it can be seen that heating and cooling is done at the same time.

Here there are two ways in which the energy consumption can be reduced. If it is not imperative that the temperature should be kept constant throughout the 24 hours, the mechanical equipment can be scheduled off overnight. An attempt can also be made to reduce the use of heating and cooling simultaneously.

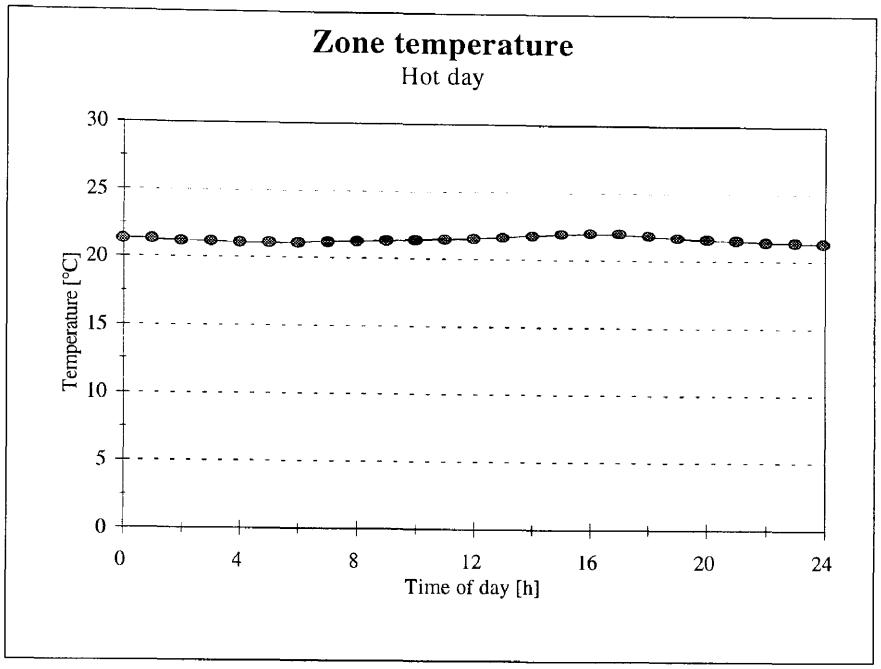

Figure 6.3: Indoor air temperature. (These results will be used for comparing the next strategy to.)

In the following sections, these and other strategies will be introduced in order to show the effects of the strategies. Only the temperature and energy results will be provided in the next sections. Where necessary, the hardware configuration will be given.

Where heating and cooling needs to be done simultaneously, energy is unnecessarily used, to first cool the air, just to heat it up again. One way to reduce the energy consumption is to reset the supply air temperature according to the outdoor temperature.

These parameters need to be determined for each specific building. Using a simulation tool predicting the optimal relation between the supply air and the outdoor air becomes easy. In this example the relations are given in table 6.2.

Controller	Setpoint value		Outdoor air temperature	
	Min value	Max value	Min value	Max value
Cooling coil controller	17	23.5	24	14
Heater controller	13	19.5	24	14

Table 6.2: Reset relation for illustrative example.

From the energy consumption (figure 6.4) it can be seen that very little heating and cooling is done simultaneously. Both the overall energy consumption and the maximum load is reduced significantly. This implies that smaller equipment could be used.

In figure 6.5 the resultant zone temperature is close to the previous result and should be acceptable. This control strategy could have implications if the humidity must also be controlled. In this simple example it is assumed that this will not be a problem.

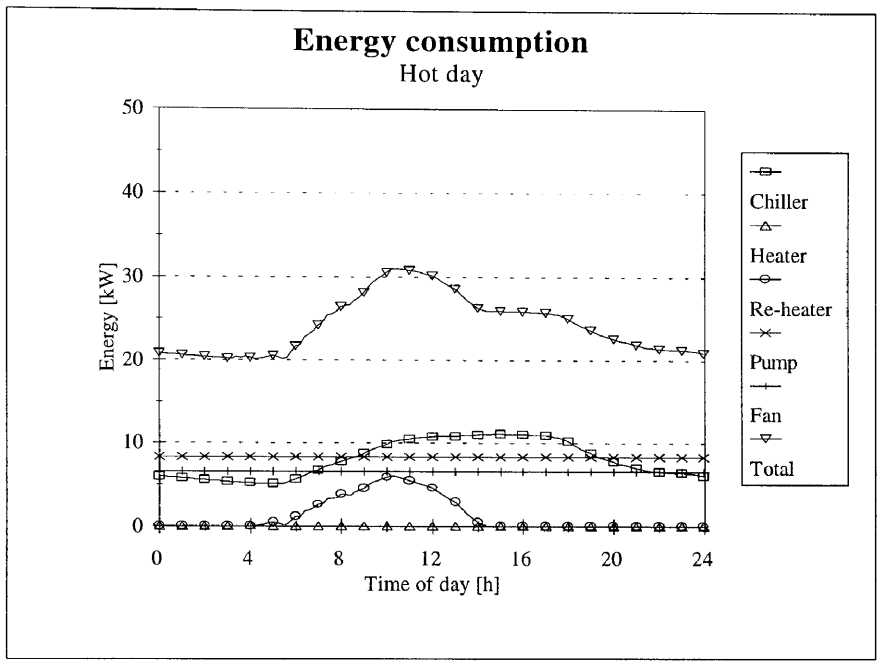

Figure 6.4: HVAC system energy usage after implementing temperature reset.

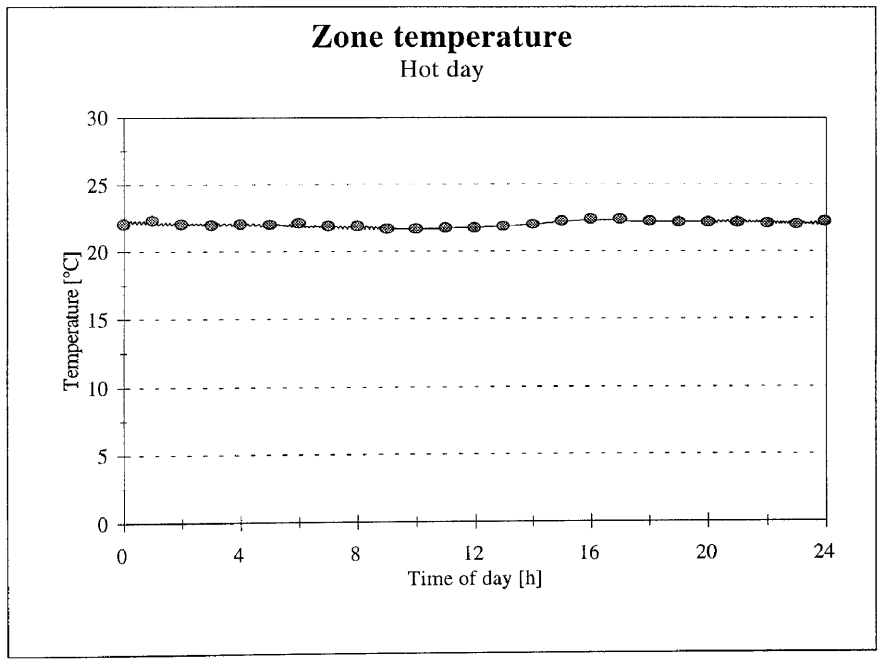

Figure 6.5: Indoor air temperature after implementing temperature reset.

6.2.2 Zero energy band control

As the name suggests, this control option is geared to use no energy under a given set of conditions. It frequently implies that controller parameters are relaxed so that no cooling or heating is used in a given setpoint band. In our application this can be implemented in the system shown in figure 6.6, simply by setting the cooling coil setpoint higher, and the heating setpoint lower. (In this example the enthalpy controller is not active.)

As a benchmark, results for this system will be given with strict control parameters. The energy and temperature results can be seen in figures 6.7 and 6.8. Control parameters for this section can be seen in table 6.3.

Controller	Standard strategy		Zero energy band strategy	
	Min value	Max value	Min value	Max value
Cooling coil controller	21	23	23	25
Heater controller	19	21	18	20

Table 6.3: Control parameters for zero energy control example.

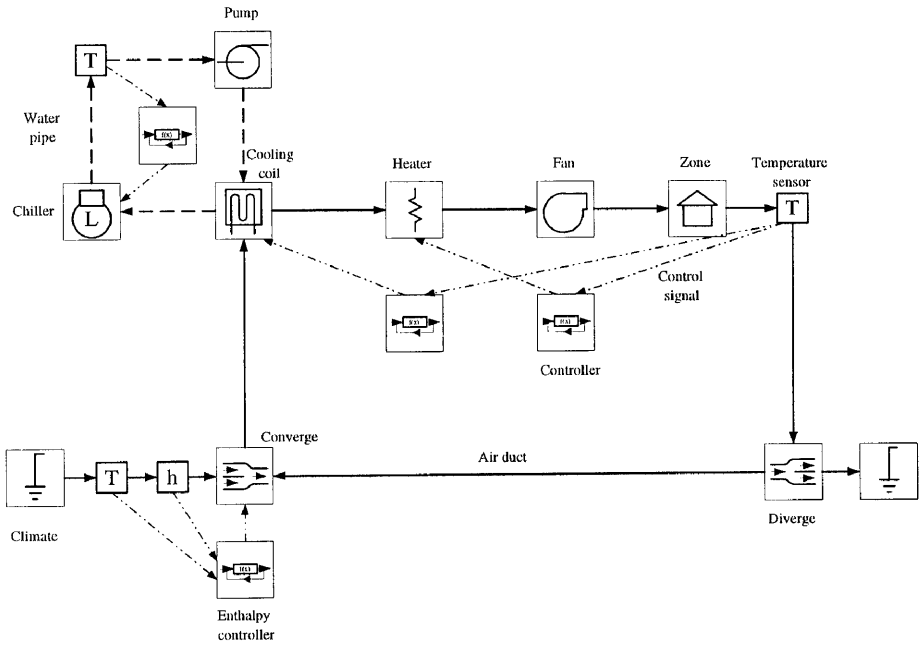

Figure 6.6: Constant volume system with direct zone temperature control used as example for the following sections.

The effect on the indoor environment must also be taken into account. As shown in figure 6.10, there is a large temperature drift in this case. If energy conservation is important, this might be the solution. The energy consumption is lower (see figure 6.9). The maximum load is reduced when compared to figure 6.7. Heating and cooling at the same time during the morning hours are eliminated.

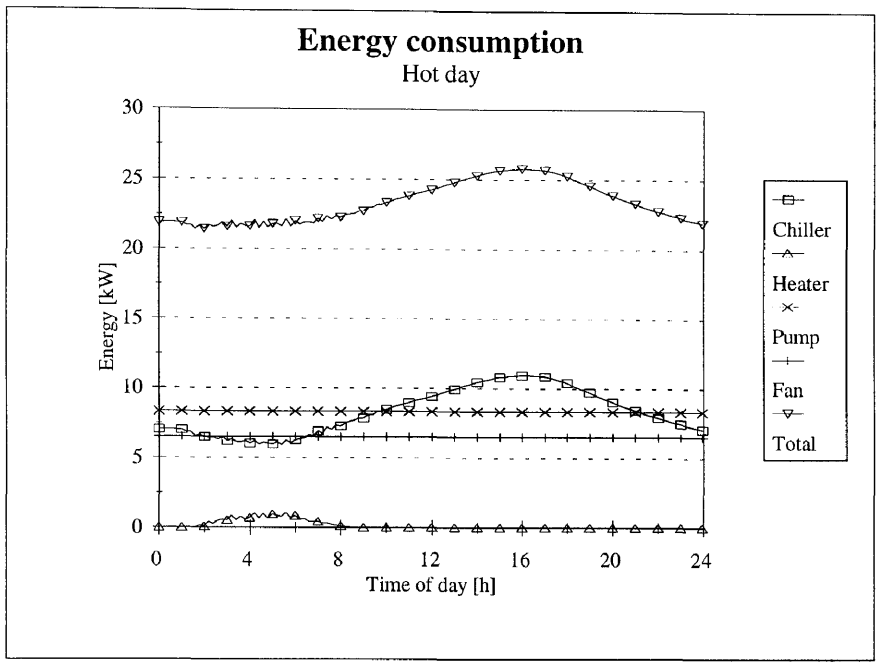

Figure 6.7: HVAC system energy usage. (These results will be used for comparing following strategies to.)

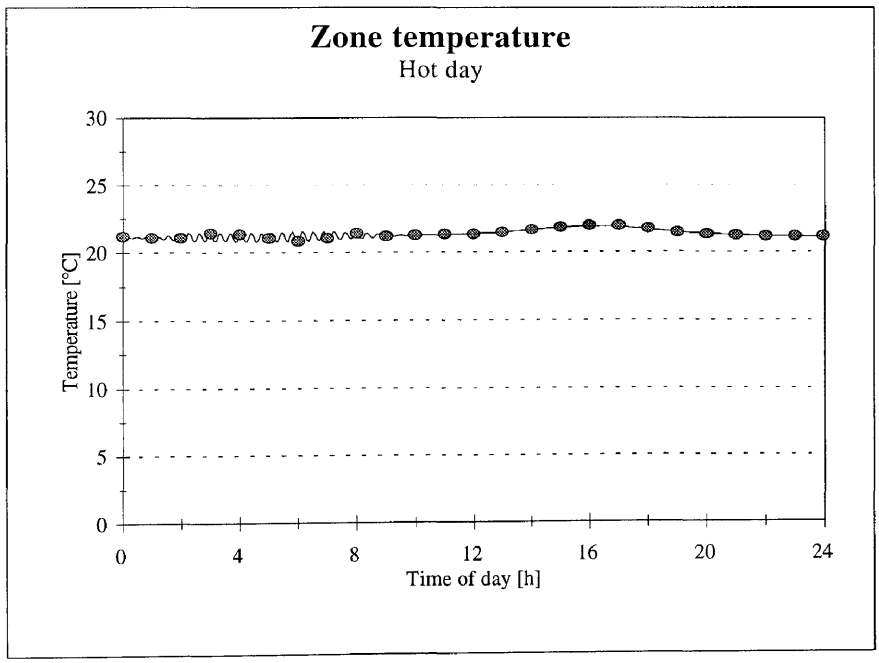

Figure 6.8: Indoor air temperature. (These results will be used for comparing following strategies to.)

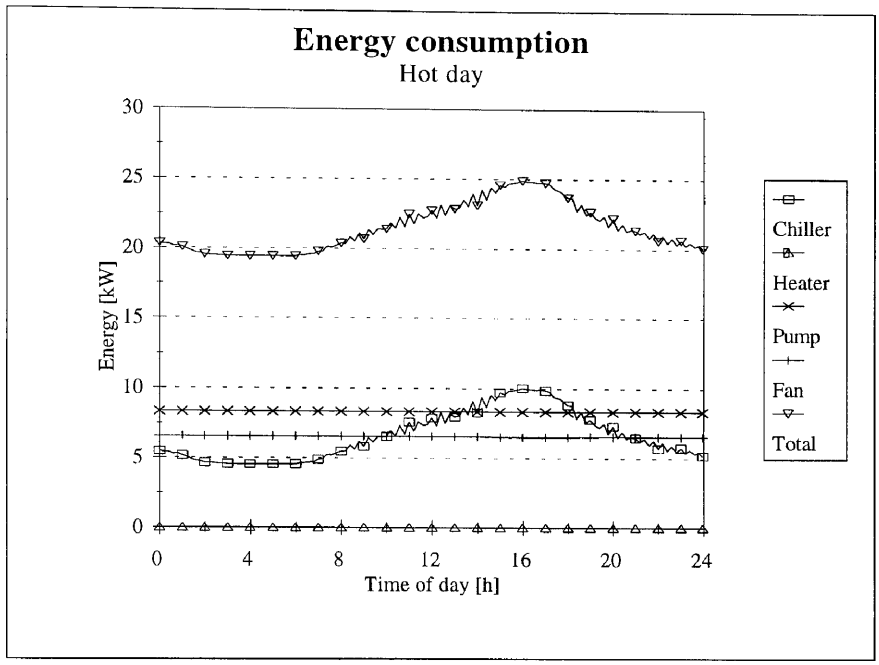

Figure 6.9: HVAC system energy usage for the system with zero energy band control.

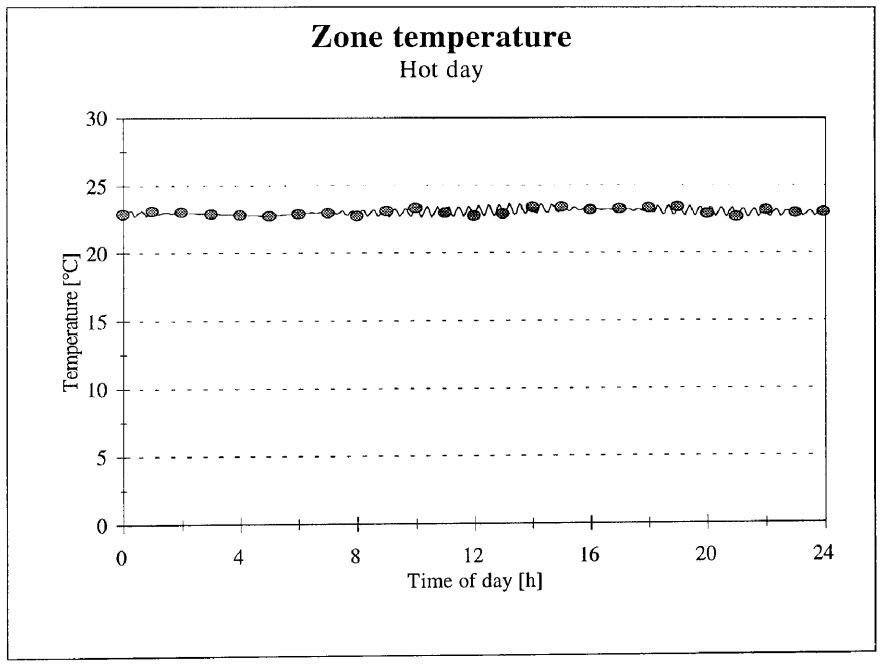

Figure 6.10: Indoor air temperature for the system with zero energy band control.

6.2.3 Enthalpy control

Enthalpy control is a term used to describe the control of an economiser by using the enthalpy as a criteria. If the outdoor enthalpy is higher than the indoor enthalpy, it is more energy effective to use as little outdoor air as possible. If the outdoor air enthalpy is lower than the indoor air enthalpy, less cooling would be required if full fresh air is used. If the outdoor enthalpy is too low, one would again benefit by using less outdoor air.

The controller logic for a modified enthalpy controller can be seen in figure 6.11. The controller logic is as follows: if the outdoor air conditions fall anywhere in region A, then full fresh air is used. At the lower temperature region D, the return air and the fresh air dampers are modulated so that the mixture is as close as possible to the supply air temperature. This would result in the minimum heating been done.

For any outdoor air conditions to the left of region A, the minimum fresh air will be used. This is a modified enthalpy controller. For a standard enthalpy economiser the region C would be included in the full fresh air region. For a standard temperature economiser the region B would be included. A complete discussion of the benefits of this modified approach is given in reference [2].

This strategy would require an additional controller. The new system configuration is shown in figure 6.6 (here the enthalpy controller is active, but not in the following examples).

The energy results can be seen in figure 6.12, and the results for the zone temperature in figure 6.13. The reference simulations were performed for the summer design conditions in Pretoria.

The outdoor conditions are such that very little outdoor air will be used with the enthalpy economiser active. The results would thus not deviate much from the reference case were the minimum fresh air is used throughout.

6.2.4 Adaptive comfort control

Adaptive comfort control is based on the assumption that the comfort perception of people will be dependent on the outdoor climatic conditions. For winter months people will be comfortable if the indoor temperature is lower. The opposite is true in summer. This strategy is suggested in reference [3].

This affords us the opportunity to potentially save energy. If the indoor temperature can be cooler in winter, less heating would be required. In summer, a higher temperature would imply that less cooling would be required.

For the inside air, setpoint the following relation has been implemented in the simulation tool

$$T_{in} = a_0 + a_1 T_{ma} + a_2 T_{ma}^2 + a_3 T_{ma}^3. \tag{6.1}$$

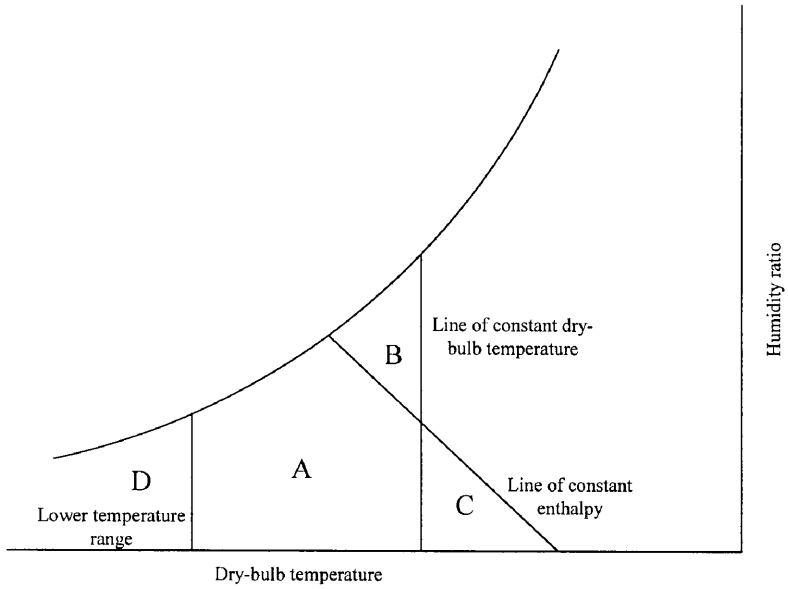

Figure 6.11: Controller logic for enthalpy economiser.

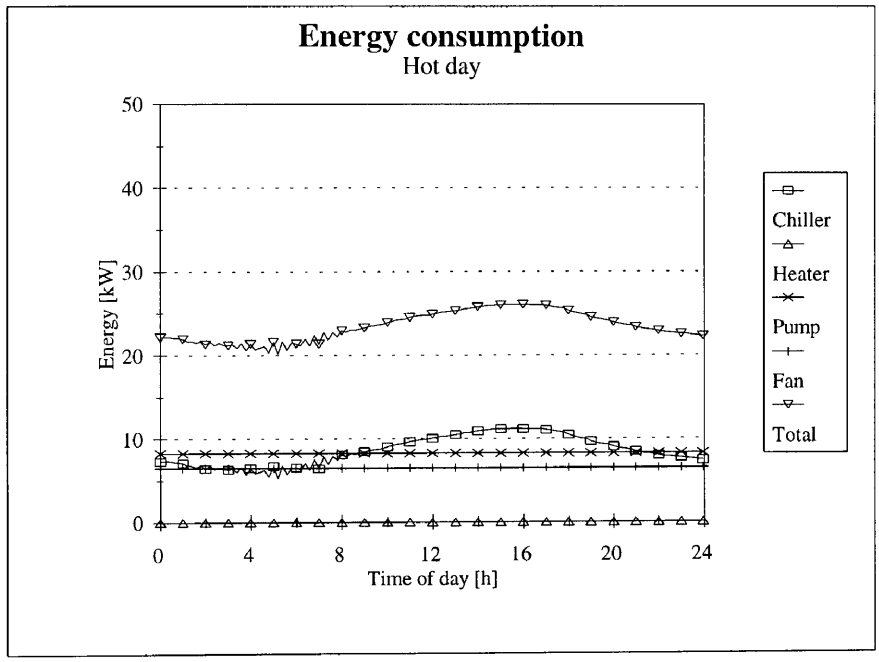

Figure 6.12: HVAC system energy usage for the system with enthalpy-controlled economiser.

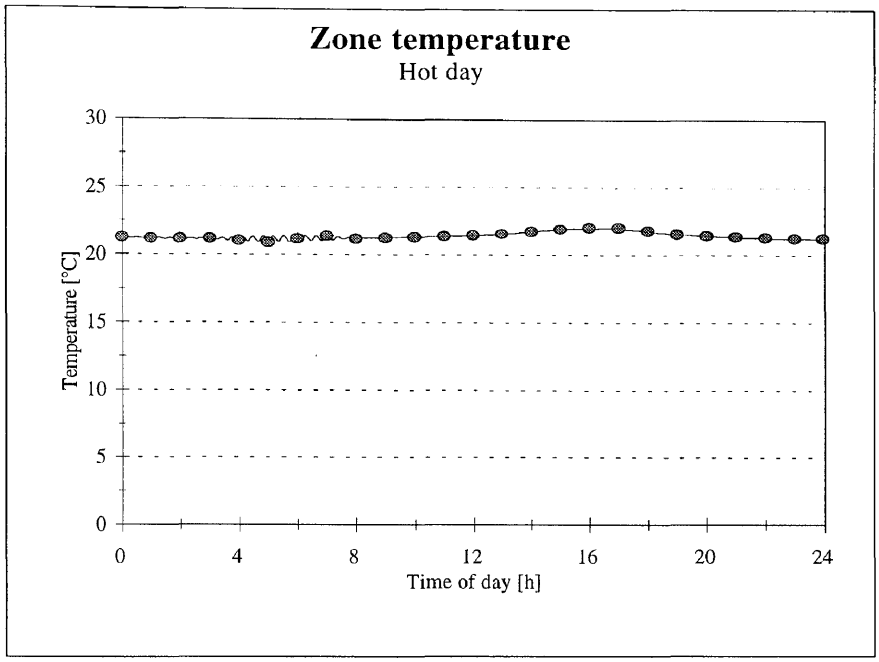

Figure 6.13: Indoor air temperature for the system with enthalpy-controlled economiser.

Here

T_{in} is the setpoint temperature inside the zone, °C
T_{ma} is the monthly mean outdoor air temperature, °C
a_i are correlation coefficients.

If a relation between the indoor air temperature and the monthly average outdoor temperature is (this relation has been assumed (for emperical data consult reference [3]))

$$T_{in} = 21.5 + 0.005T_{ma}^2 \tag{6.2}$$

then we find the energy consumption and indoor temperatures as shown in figures 6.14, 6.15 and 6.16.

It should be noted that the simulations were conducted using the weather data for Pretoria. Although temperatures in Pretoria do not vary as greatly as in other cities, there is still a considerable saving on energy.

If the before and after temperatures are compared (see figure 6.16), it is observed that the summer temperatures after adaptive control are higher than before. The reduction in the power consumed for cooling for these months is considerable, as can be seen in figure 6.15.

Similar observations are applicable to the winter months. In this case the temperatures in the winter months (see figure 6.16) after adaptive control are lower than before. The reduction in the power consumed for heating for these months is considerable as can be seen in figure 6.14.

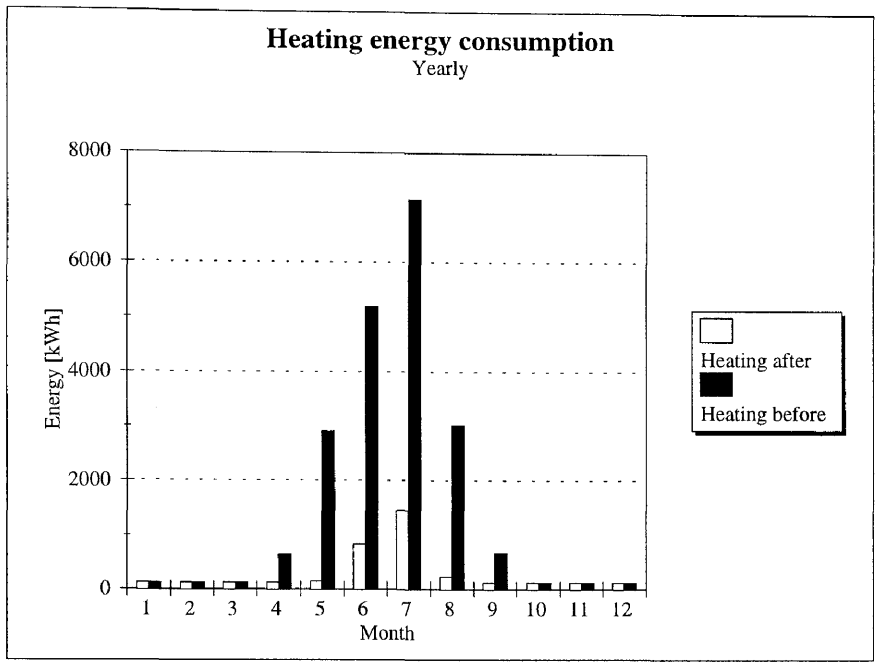

Figure 6.14: Comparison between monthly heating energy usage before and after adaptive comfort control has been implemented.

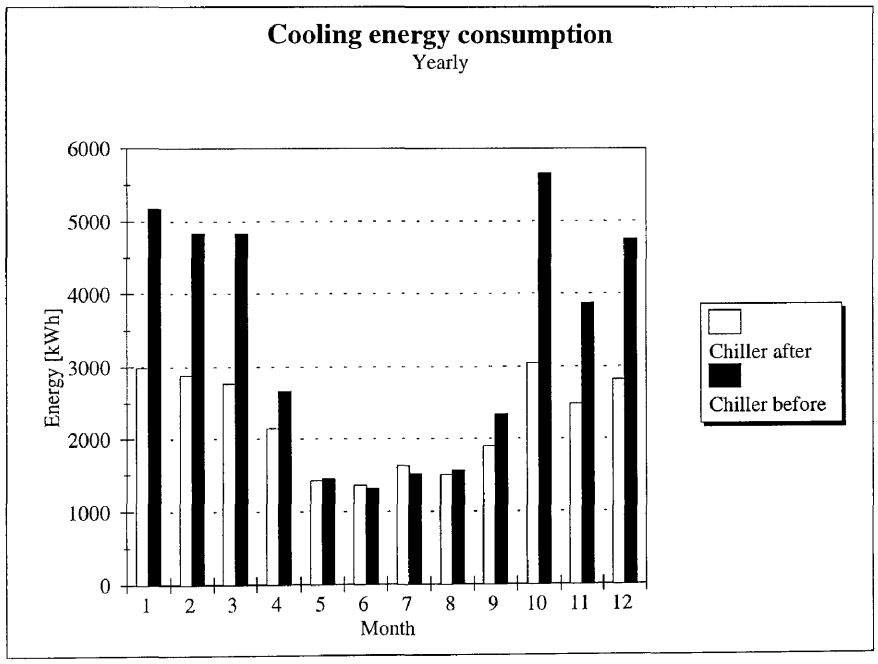

Figure 6.15: Comparison between monthly refrigeration energy usage before and after adaptive comfort control has been implemented.

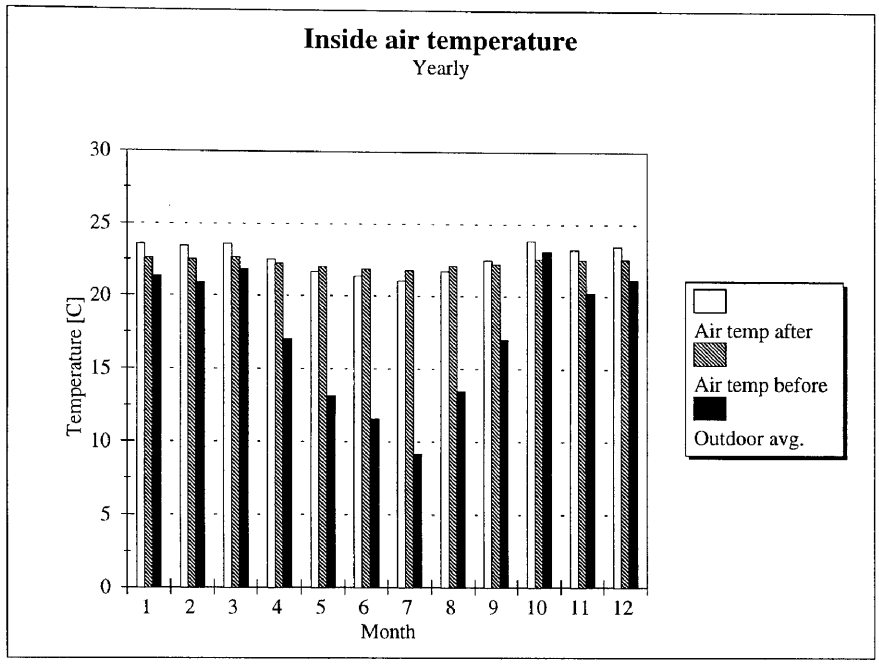

Figure 6.16: Comparison between monthly average indoor air temperature before and after adaptive comfort control has been implemented.

Not all building are candidates for this control strategy. For example, if a building has a large internal load such that cooling is required in winter. If the indoor air temperature setpoint is then reduced it would imply that more cooling would be required to realise the temperature set point. With an intelligent controller this problem could also be resolved.

6.3 SCHEDULE-RELATED ENERGY MANAGEMENT STRATEGIES

6.3.1 Scheduling

Scheduling is a term that refers to the active/inactive or on/off times of the system and equipment. In this example it can be argued that the equipment can be off from 18h00 to 07h00 in the morning. This will have two effects, i.e. the energy consumption will be reduced since the equipment is not operational, and there could be an increase in compressor power due to the larger cooling-down loads.

The resulant zone temperature can be seen in figure 6.18. Obviously here the temperature is allowed to drift during the night-time. The energy consumption is reduced considerably due to the fact that the equipment was off (see figure 6.17). Notice that the compressor power has increased slightly during the first hour due to the pull-down load.

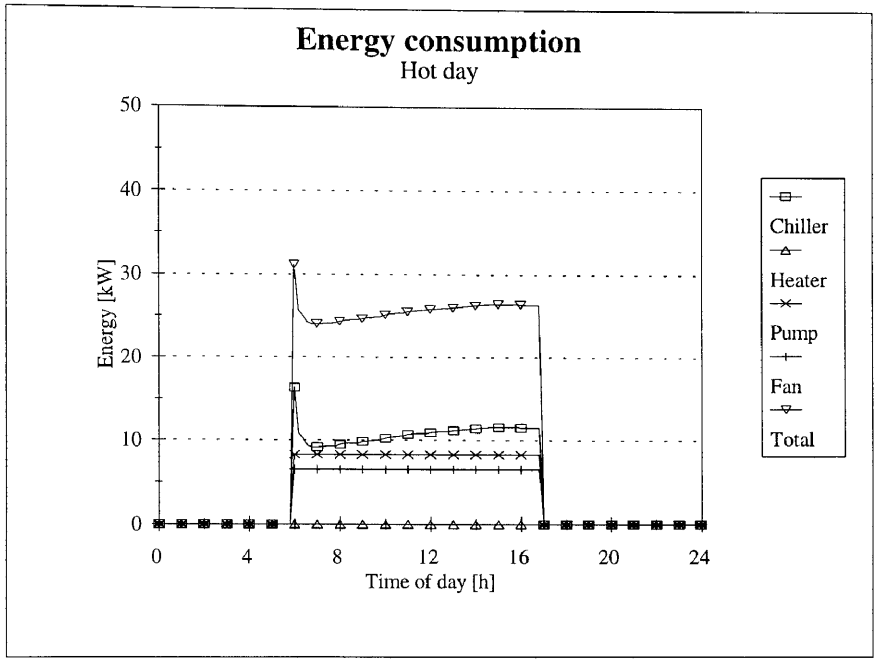

Figure 6.17: HVAC system energy usage after implementing scheduling (all equipment off from 18h00 to 07h00).

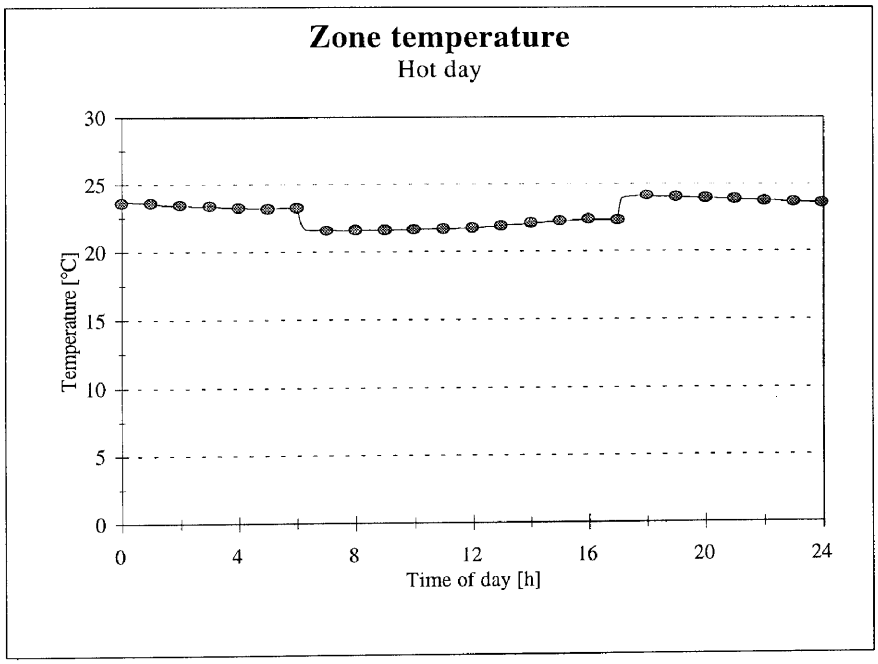

Figure 6.18: Indoor air temperature after implementing scheduling (all equipment off from 18h00 to 07h00).

6.3.2 Unoccupied time set-back

Another alternative to scheduling the mechanical equipment off is to use unoccupied time set-back. This implies that the temperatures are allowed to drift higher or lower if the building is not occupied.

In our current example, the system is already off overnight so we will use this technique as an illustration over lunch-time. The resultant zone temperature and energy consumption are shown in figures 6.19 and 6.20. A two-degree temperature set-back on the cooling coil and the heating coil was implemented.

The effect of this set-back on the indoor temperature is illustrated in figure 6.20. Energy saving benefits resulting from this strategy are also evident from figure 6.19. The compressor power is reduced significantly by the two-degree temperature set-back. The pull-down load seen in figure 6.17 is eliminated.

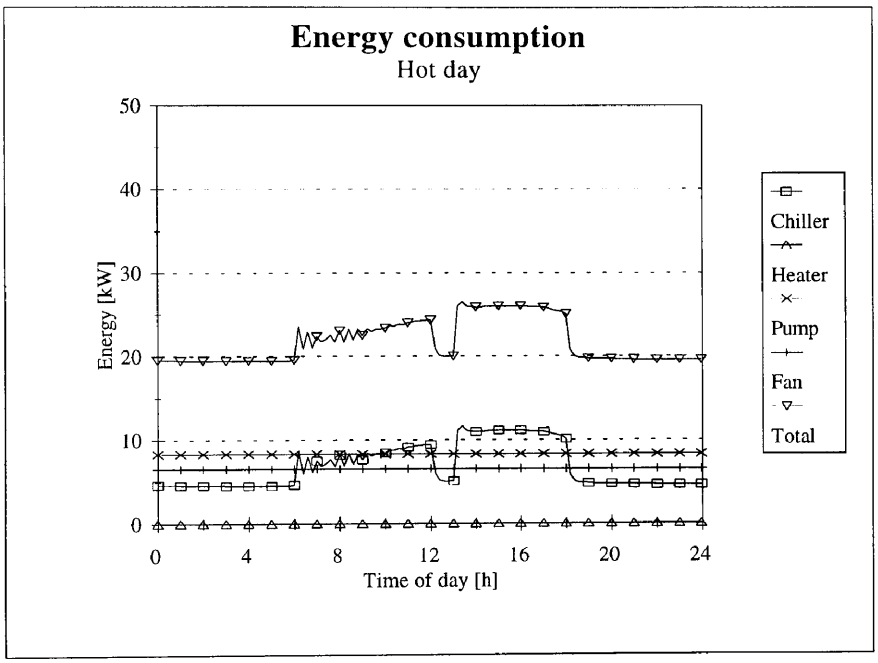

Figure 6.19: HVAC system energy usage using unoccupied time set-back.

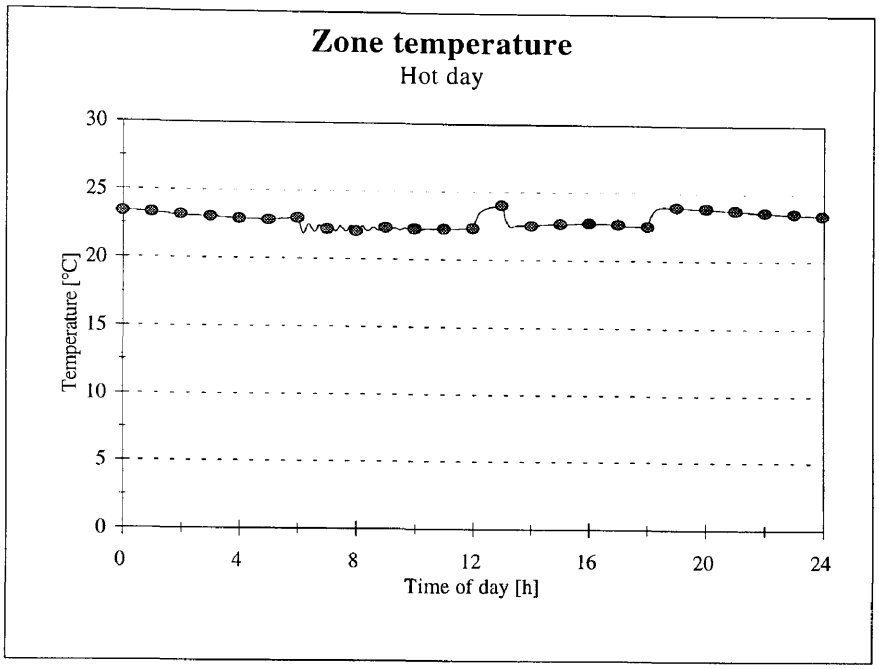

Figure 6.20: Indoor air temperature using unoccupied time set-back.

6.4 ADVANCED ENERGY MANAGEMENT STRATEGIES

6.4.1 Demand limiting

Demand limiting is a very attractive strategy to use if time-of-use tariffs are introduced. This would imply that the utilities charge according to the maximum energy consumed in a given time interval. There are a number of means to reduce the maximum demand. We have exploited some of these options already in the previous sections.

The difference here is that the controller decides to take load reducing action based on the current energy consumption. The designer and building owner/manager will have to decide which loads are sheddable. Ideally one would not like to compromise the internal air conditions but sometimes this is unavoidable.

Priorities will have to be assigned to each action. In the current implementation the order in which the controllers are listed represents the priorities. In this example only temperature set-backs were used. The demand setpoint was set to 25 kW.

From figure 6.22 it is evident that a compromise was required to reduce the demand. Figure 6.21 shows the reduction in energy consumed. Although the power consumed follows the trend for the base case during the time of load reduction, it should be noted that load-measuring equipment usually uses integration times of 30 minutes. Using this convention it is evident that the load as reported to the utility company has been reduced.

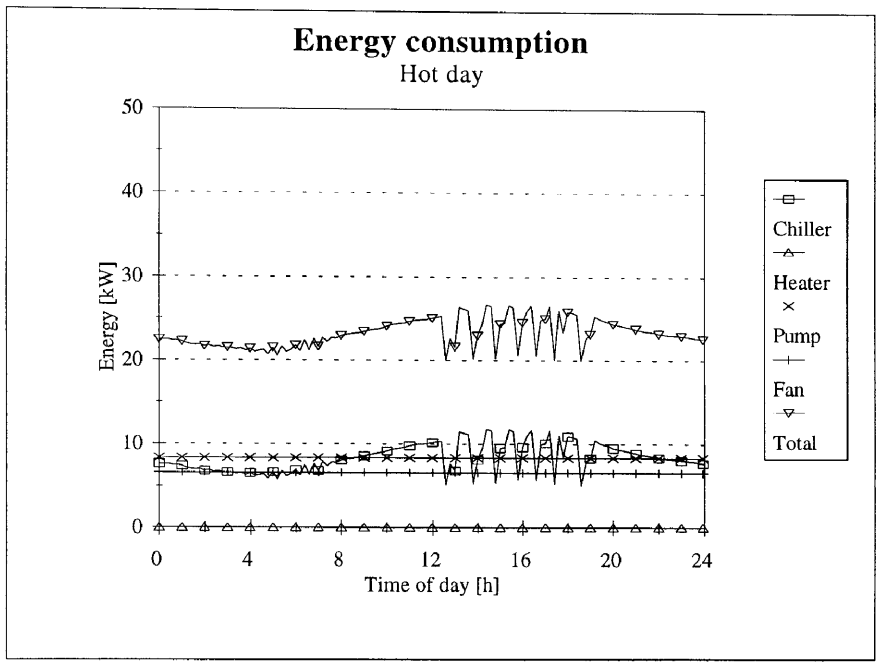

Figure 6.21: HVAC system energy usage using demand limiting strategies.

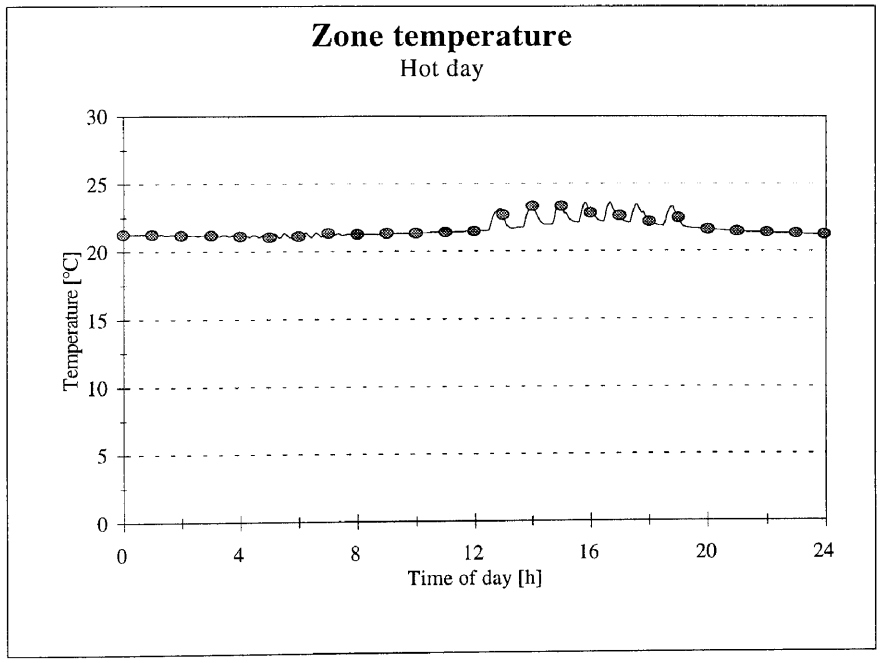

Figure 6.22: The effect of demand limiting strategy on indoor air temperature.

6.4.2 Duty cycling

Duty cycling should be implemented with care. It relies on cycling equipment (the AHU fan for example). Most electrical motors have to be down-rated if switching occurs frequently. Further minimum on/off times need to be specified.

For this example only the AHU fan was cycled. The on/off times were related to the comfort conditions. Averages of the zone temperatures are used to determine the on/off times according to the relation in table 6.4.

Comfort temperature		Off time	
Min value	Max value	Min value	Max value
22	24	10	30

Table 6.4: The relation between on/off times and comfort temperatures.

The energy consumption is shown in figure 6.23. Zone conditions are shown in figure 6.24.

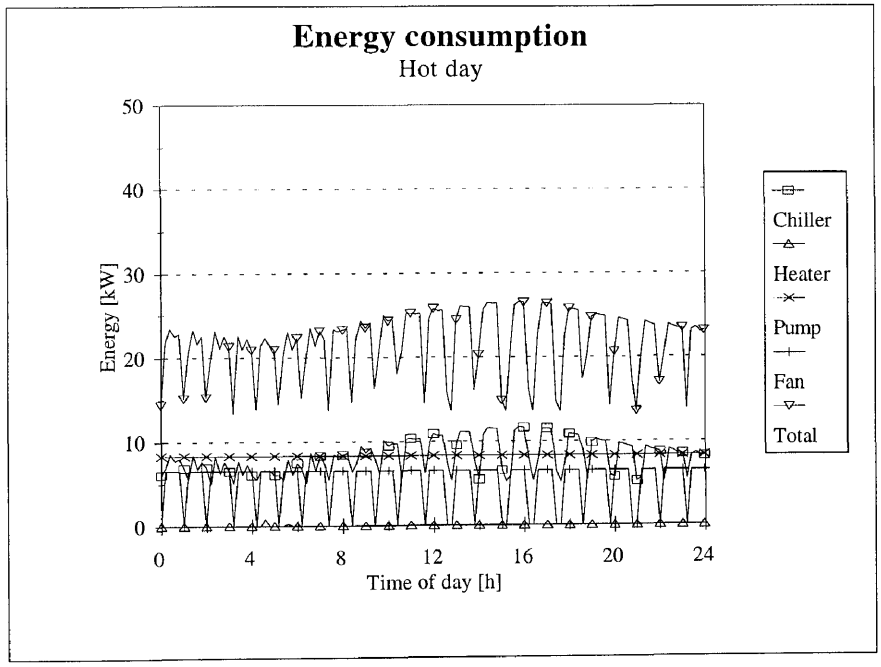

Figure 6.23: HVAC system energy usage after duty cycling has been implemented.

6.4.3 Load resetting

Load resetting is a strategy that only activates a given piece of equipment once the function of the equipment is needed. For example, if a number of cooling coils are supplied with chilled water from a chiller, the chiller will only be activated if the valve of a cooling coil is about to open.

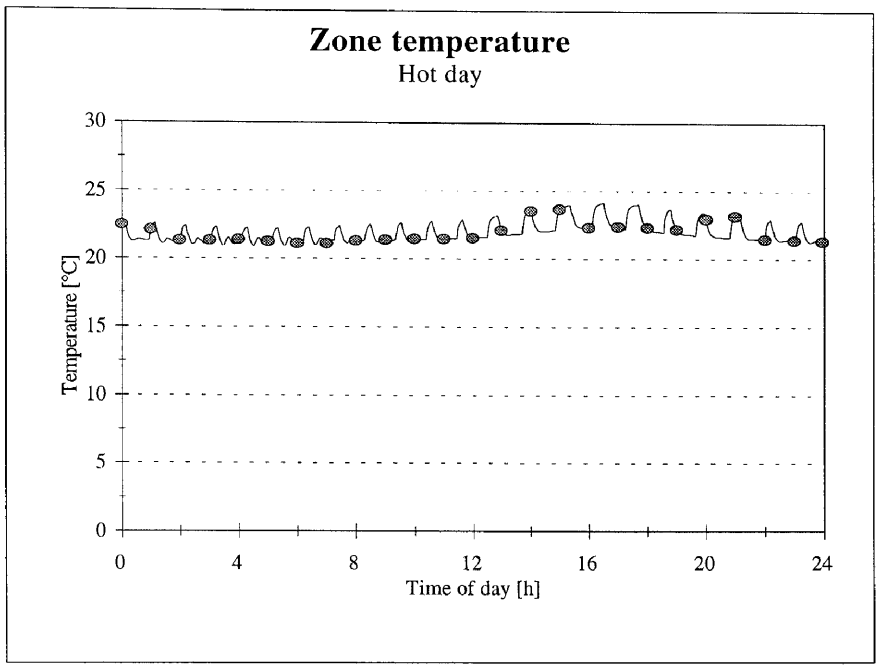

Figure 6.24: Indoor air temperature after duty cycling has been implemented.

In this example only one coil is used, but the principle can still be illustrated. In figure 6.25 we can see that in the morning hours no cooled water is required by the coil and the chiller is off. The indoor air temperature shown in figure 6.26 shows very little or no deviation due to this energy management strategy.

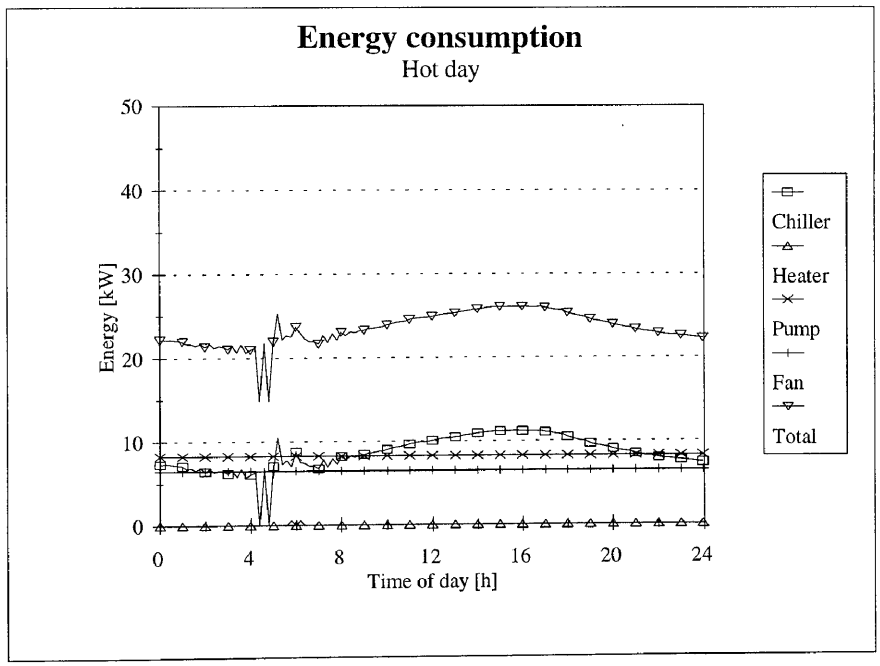

Figure 6.25: HVAC system energy usage with load resetting implemented.

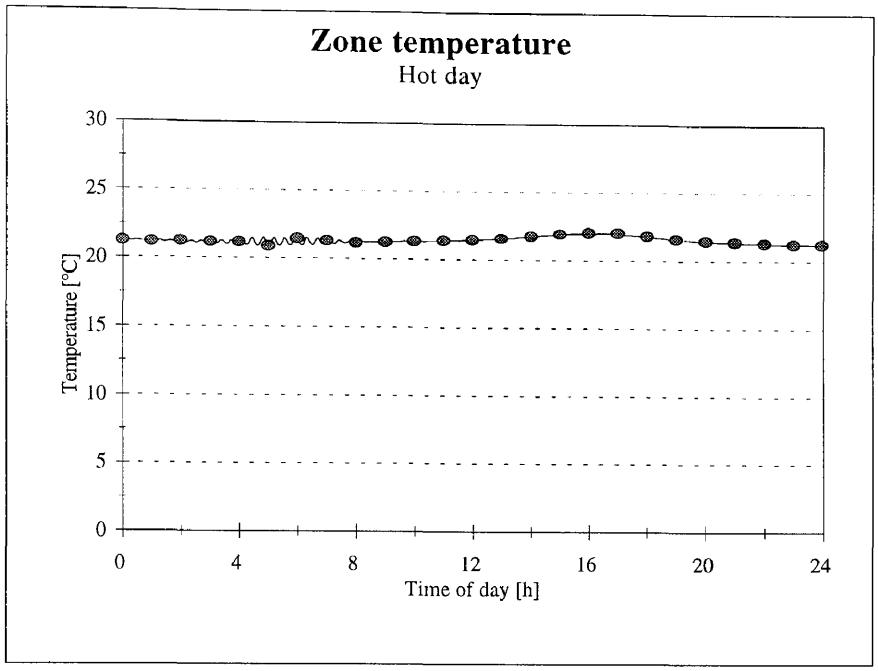

Figure 6.26: Indoor air temperature with load resetting implemented.

6.4.4 Optimal start stop

In applications where the indoor temperature has to be at the correct temperature at a given time one can apply the Optimal Start Stop Strategy. The strategy uses a self-teaching approach to 'learn' how late the equipment needs to be started, in order to have the indoor temperature at setpoint at a given time.

The controller learns from previous experience, and based on this activates the equipment at a given time. If the time proves to be too early, i.e. the indoor temperature is at setpoint before occupation time, then next time under the same set of conditions the controller will activate a little later.

The learning process can be emulated on the simulation tool. At this point it is not considered practical to implement Optimal Start Stop Control. The reason is that the real-life controller adapts the starting and stopping times from day to day. In the simulation tool the climate data for a month are considered not to vary from day to day. No learning process can thus be emulated.

6.4.5 CO_2 control

The modelling of CO_2 in building zones was discussed in section 5.5.4. In this section we endeavour to show the potential benefit of using the CO_2 levels as an indication to determine the fresh air requirements. This is especially useful in lecture halls or movie houses that are not always fully occupied.

The strategy entails measuring the CO_2 concentrations in the return air. The fresh air quantity is then controlled so that these levels do not exceed a predetermined level. In our example 450 ppm was used as an acceptable level in the lecture hall under consideration. Concentrations of 300 ppm in the outdoor air is the norm in Pretoria. The resultant energy consumption and indoor air temperature are shown in figures 6.28 and 6.29.

It should be noted that in this case the minimum air quantity for 80 people was used in the reference case. A constant number of 80 people were used in both the reference (figures 6.28) and the case with CO_2 control. The saving on energy is low but the actual benefit would be when the occupant numbers change and are not the maximum throughout the day.

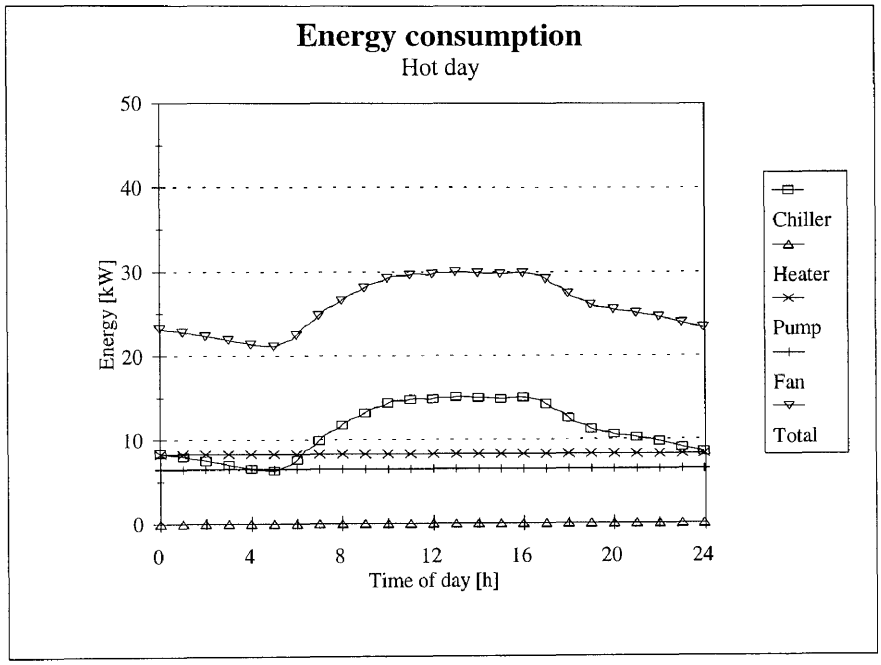

Figure 6.27: HVAC system energy usage before CO_2 control has been implemented.

6.5 CLOSURE

In this chapter, Energy Management Programs were introduced. The majority of the most commonly used strategies were discussed and their potential benefits illustrated. Although any of these strategies can be used in combination with one another, this was not illustrated here. It can be appreciated that the number of permutations precludes this.

The execution time of the simulation was not noticeably affected. This is due to the fact that the manager logic is comparatively simple when compared to the numerical models for the other individual components. Furthermore, many of the strategies rely on deactivation equipment. This has the effect that execution times are reduced since the mathematical model of the specific component is then not solved.

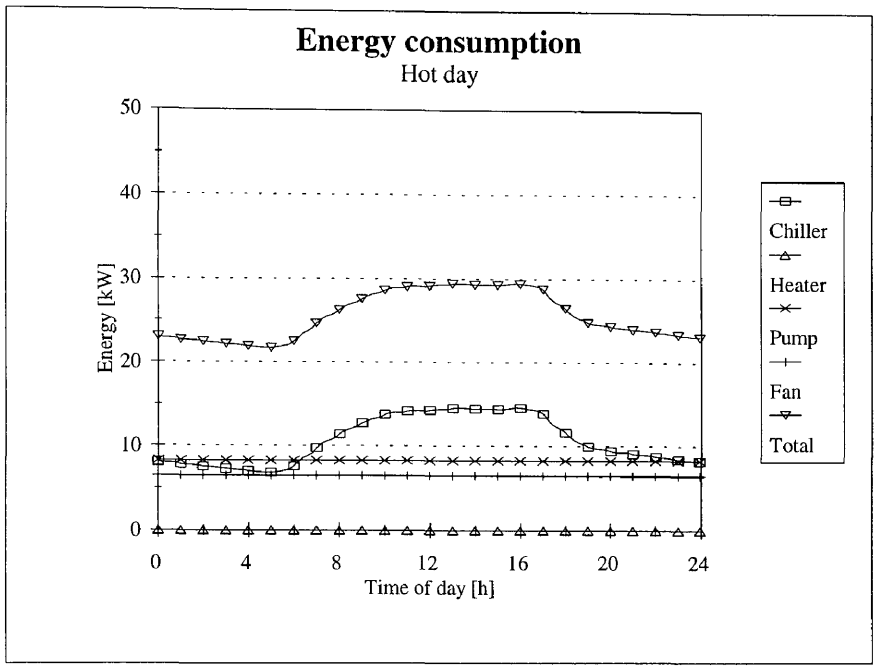

Figure 6.28: HVAC system energy usage after CO_2 control has been implemented.

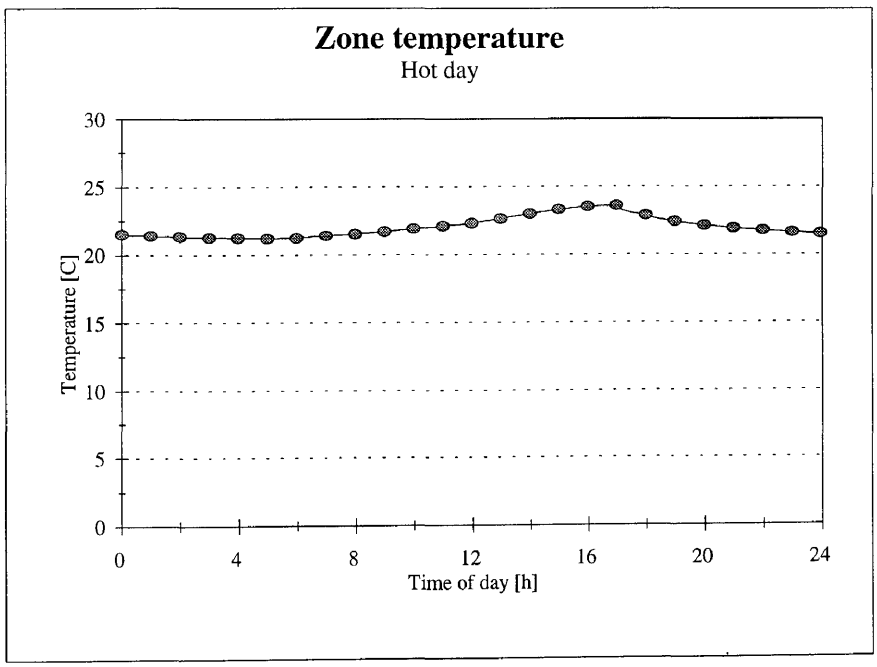

Figure 6.29: Indoor air temperature after CO_2 control has been implemented.

From the examples above it is evident that there is great potential for energy saving by implementing the Energy Management Systems. The proposed simulation tool gives the user, building manager, and control engineer, the ability to quantify the energy reduction and the effect of the various strategies on the indoor temperature.

Bibliography

[1] R.A. Carlson and R.A. Di-Gandomenico. *Understanding Building Automation Systems*. R.S. Mears Company inc., Kingston, 1991.

[2] G. Shavit. Enthalpy control systems: Increase energy conservation. *Heating Piping Air Conditioning*, pages 117–122, January 1974.

[3] M.A. Humphreys. Thermal comfort temperatures and the habits of hobbits. In F. Nicol, M.A. Humphreys, O. Sykes, and S. Roaf, editors, *Standards for Thermal Standards*. Chapman and Hall, London, 1995.

Chapter 7

CASE STUDIES: VERIFICATION AND SIMULATION

The power of integrated simulation lies in the prediction of system performance of an integrated building, HVAC system, and its control configuration. The usefulness of having a computer tool to predict the performance of a system by simulation is illustrated in this chapter.

Three buildings will be used in this chapter as validation studies. Measurements of actual thermal performances are used to verify the simulation tool results.

NOMENCLATURE

$\dot{Q}$	Thermal power consumed for heating, kW
$\dot{m}_w$	Mass flow rate of hot water, kg/s
C_{pw}	Thermal heat capacity of water, kJ/kg K
ΔT	Difference between entering and leaving water temperatures, °C or K.

7.1 INTRODUCTION

Validation of a simulation tool forms an important part of ensuring the applicability of the simulation to real-life situations. To this end, three validation studies will be presented in this chapter. The three buildings are a residential house, an office and studio building and a combined office and laboratory building. Details of the various buildings will be provided in the respective sections.

7.2 CASE STUDY 1: A RESIDENTIAL HOUSE

7.2.1 Introduction

The first case study under consideration is a residential house situated in the east of Pretoria. The house is fitted with a ducted split air-conditioning system. Four of the rooms in the residence are air-conditioned. Construction of the residence was completed in 1996.

In this study, the performance of a single air-conditioning unit to serve four zones is investigated. The effect of having a single temperature sensor in the return air duct is illustrated.

7.2.2 Building and HVAC system description

The building is a double-storeyed building. Four of the rooms in the house namely, the study, main bedroom, play-room and the lounge, are supplied with conditioned air from one ducted split unit. The air quantities supplied to each zone are proportional to the maximum load predicted for each zone.

Temperature is controlled by monitoring the return air temperature. The chiller is switched on and off to regulate the temperature. The purpose of this case study is not to optimise the control for the system, but to verify if this simple system can be simulated reliably.

A ducted split unit with a 14 kW rating at 27 °C indoor air temperature was installed in the house. Details of the system parameters are provided in appendix F. A diagrammatic of the system and the zones it supplies is shown in figure F.1.

7.2.3 Verification results

The power used for the chiller was monitored for a number of days and a verification day was chosen. The climate for that day was used in the project database, and the simulation for the system was performed. The resultant power consumption for the simulated and measured cases are shown in figure 7.1.

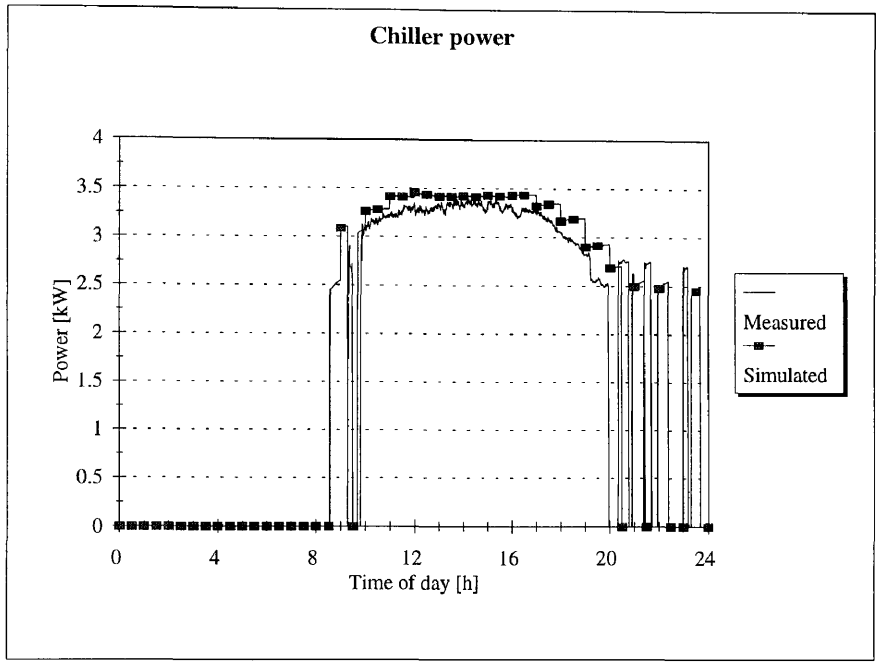

Figure 7.1: Power consumption of air-cooled air-conditioner.

The inside air conditions in each zone were measured and compared to the simulated values. The results can be seen in figures 7.2 to 7.9. Comparing the measured and simulated temperatures we see that the agreement is good. Humidity results are also compared and the results are again in good agreement.

In order to confirm that the building model predicts the correct loads, the supply air temperature was also monitored and the comparison is shown in figure 7.10. The fact that the correlation between the supply air temperature and the zone temperatures is good shows that the building model predicts the heat gain to the zone air accurately.

The good agreement between the measured and simulated humidities reflects on the accuracy of the latent load modelling of the building zone, and the modelling of the air-cooled air-conditioner latent cooling load.

In this section it was illustrated that the simulation tool can accurately predict the energy consumption and the indoor air conditions for the simple system. Furthermore, the effect of using a single temperature sensor as feedback variable was illustrated. If the supply volumes to the individual zones were incorrect they would have been picked up during this simulation. As it turned out, this was not the case.

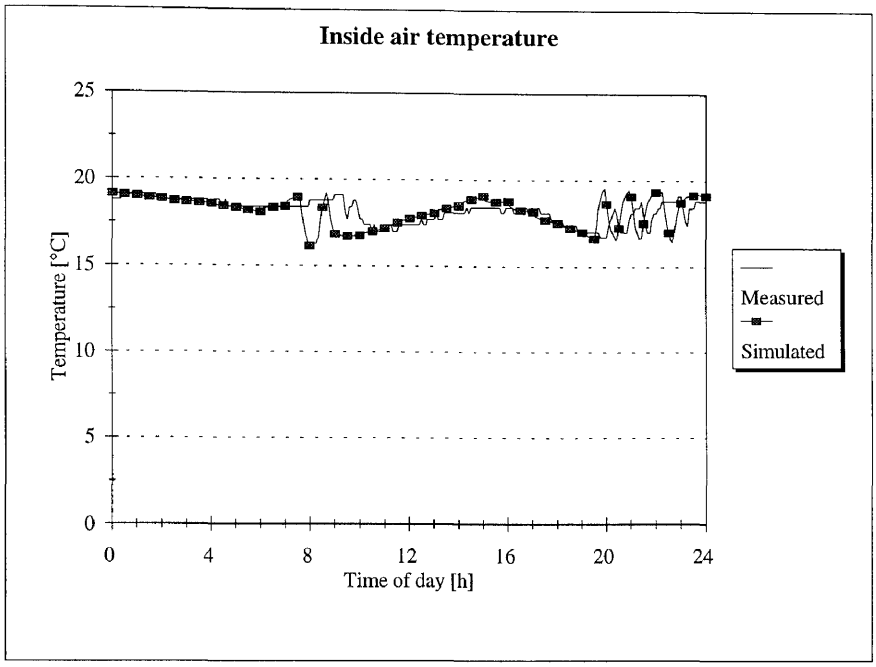

Figure 7.2: Inside air temperature of the play-room.

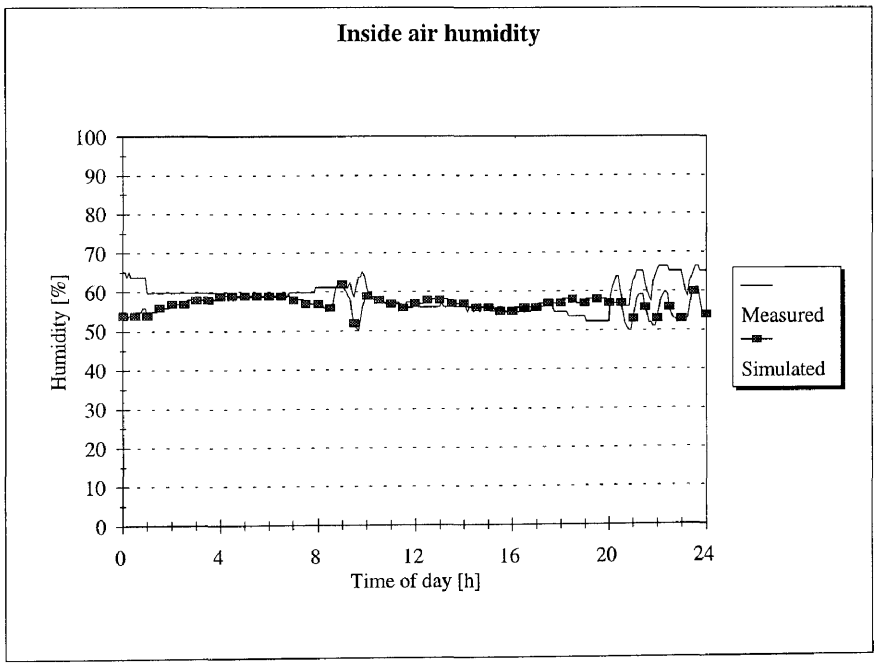

Figure 7.3: Inside air humidity of the play-room.

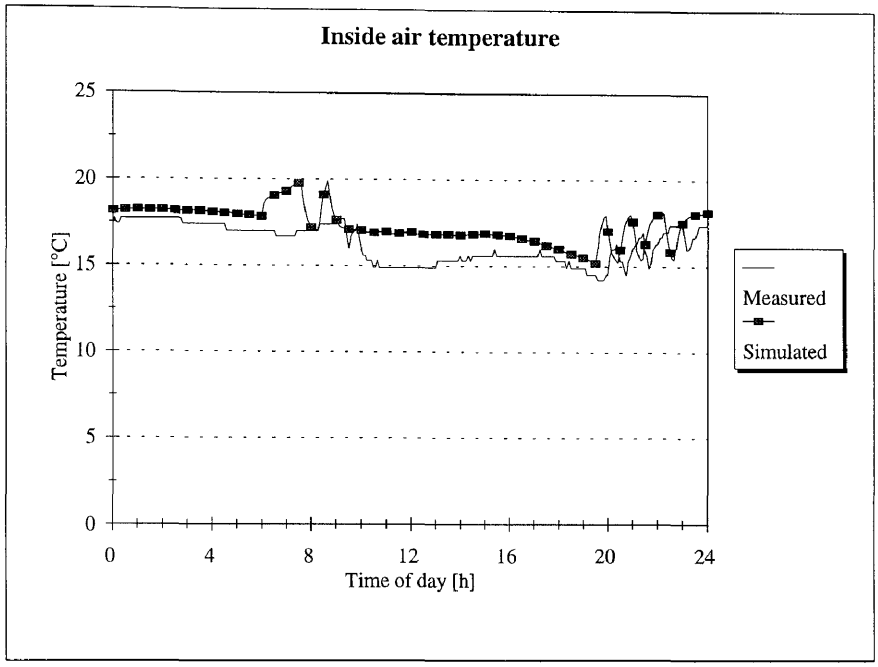

Figure 7.4: Inside air temperature of the study.

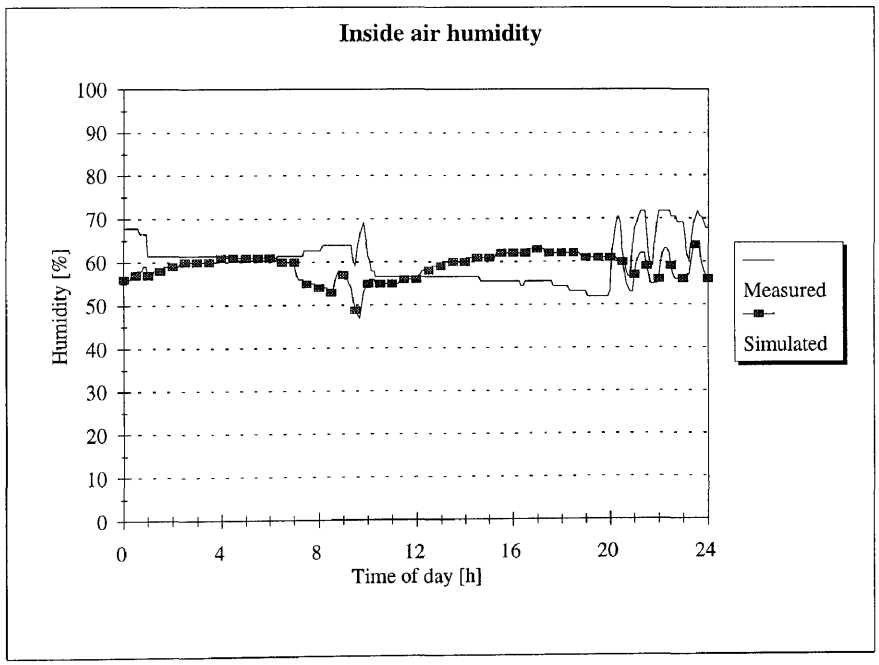

Figure 7.5: Inside air humidity of the study.

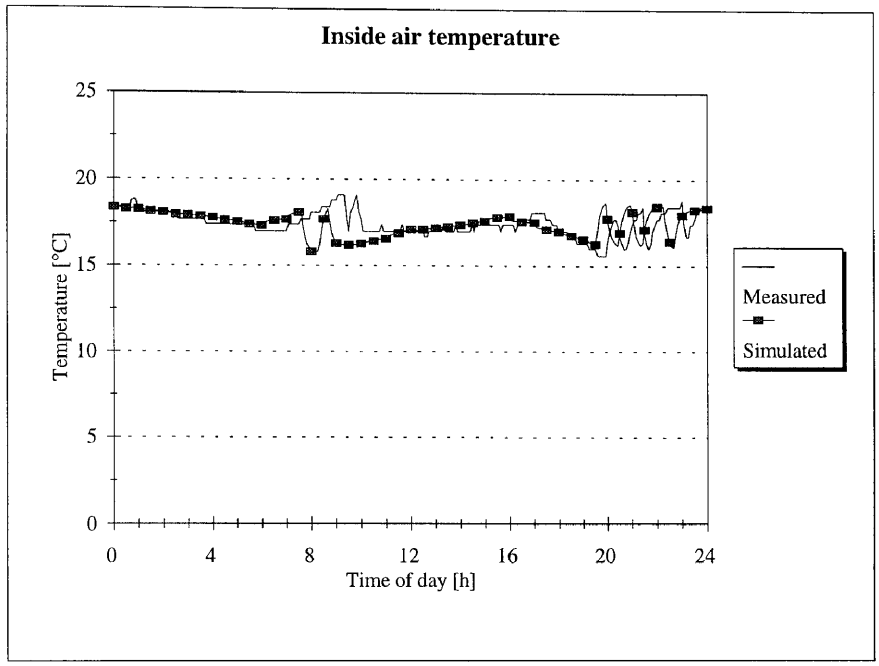

Figure 7.6: Inside air temperature of the bedroom.

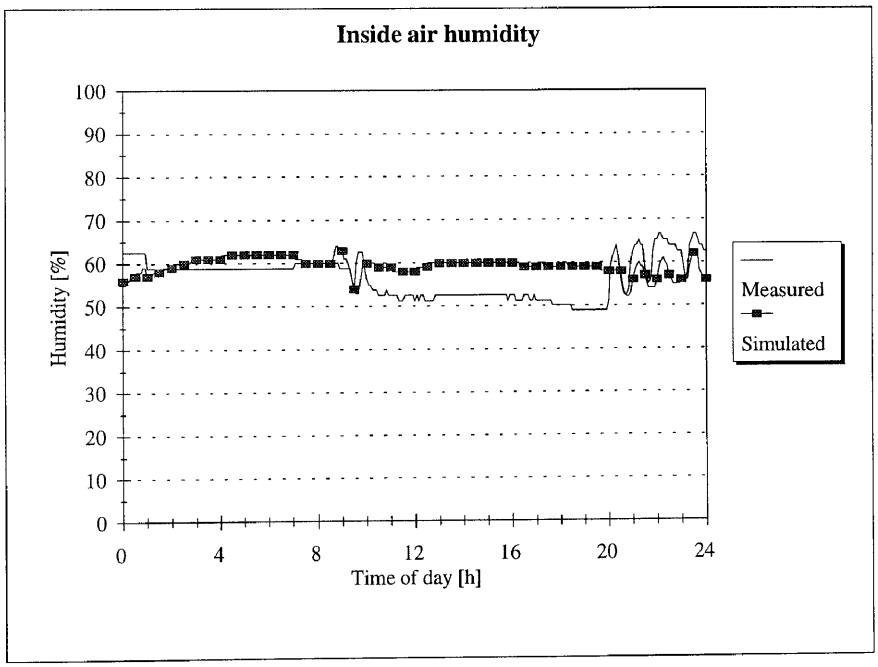

Figure 7.7: Inside air humidity of the bedroom.

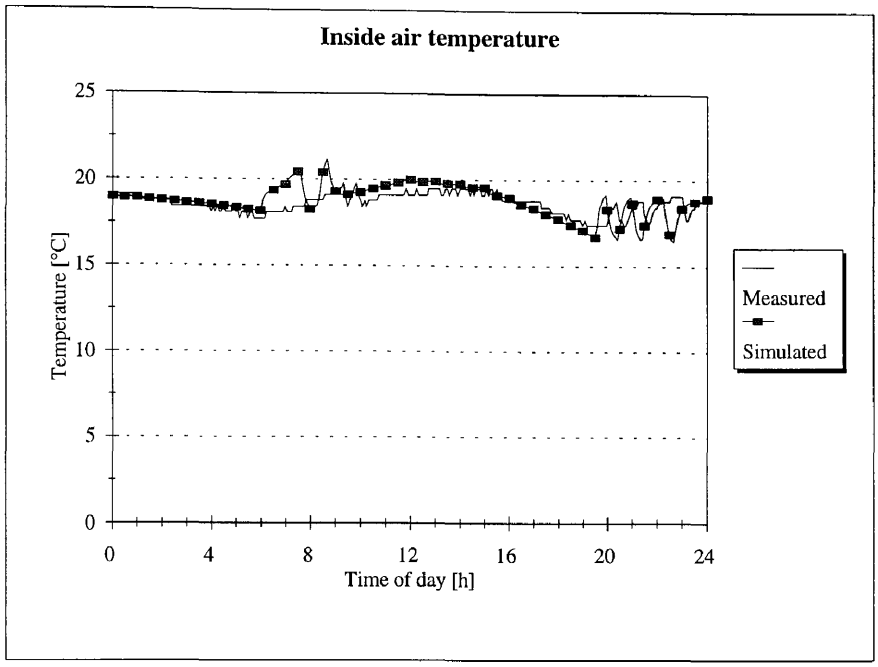

Figure 7.8: Inside air temperature of the lounge.

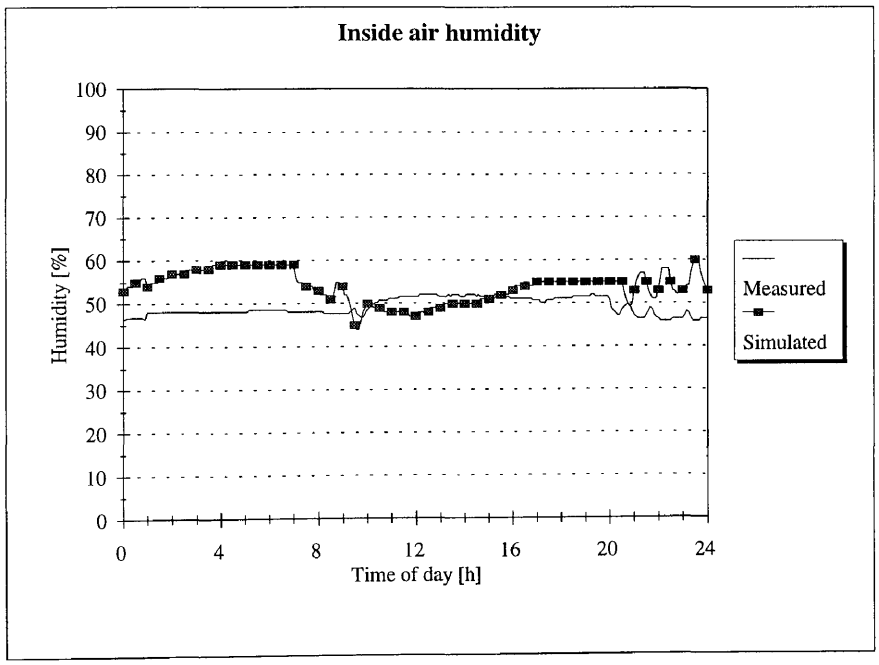

Figure 7.9: Inside air humidity of the lounge.

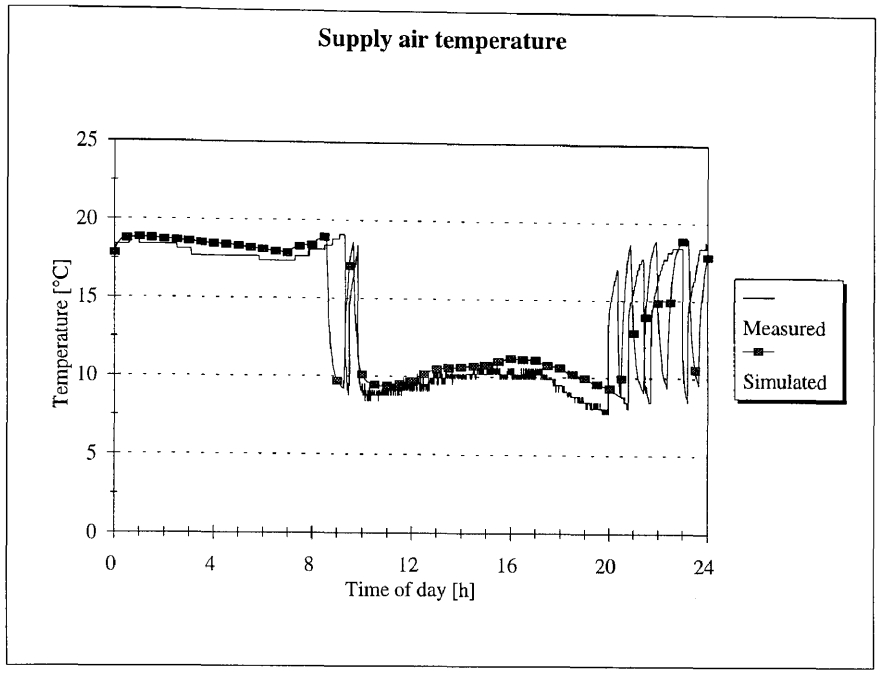

Figure 7.10: Supply air temperature from the evaporator coil.

7.3 CASE STUDY 2: AN OFFICE AND STUDIO BUILDING

7.3.1 Introduction

The second case study is an office and studio building situated on the campus of the University of Pretoria . The building is divided into six zones and each zone is measured separately. The building was used for a comfort study. The aim of this discussion is not to consider the comfort problems, but to verify the results by integrated simulation.

7.3.2 Building and HVAC system description

Four of the zones are supplied by a common air-handling unit. The return air from the four zones is exhausted to the atmosphere. Before the air is exhausted it is mixed and the temperature and humidity are measured.

The additional two building zones are conditioned by their own air-handling units. Each zone is temperature controlled, and dehumidification is performed using the cooling coils.

Primary chilling is done by a modified Trane chiller. The chiller was a water-cooled chiller which was modified to an air-cooled chiller. Further detail of the system is described in appendix G.

7.3.3 Verification results

The chiller power consumption was measured and simulated using a representative set of measurements. Air temperatures at the inlet to the AHUs were measured and specified as the inlet conditions in the simulation tool. Hot water temperatures were measured and specified as inlet conditions to the heating coils.

The simulated and measured chiller power are compared in figure 7.11. Agreement between the measured and predicted power consumption is good. The simulation tool successfully simulated the cycling of the chiller. Chiller cycling is an indication that the chiller capacity is too large for the given application.

Cycling, as observed here, is detrimental to the chiller and would result in high maintenance costs. It would be advantageous if this could be predicted beforehand, and rectified before the plant is in operation.

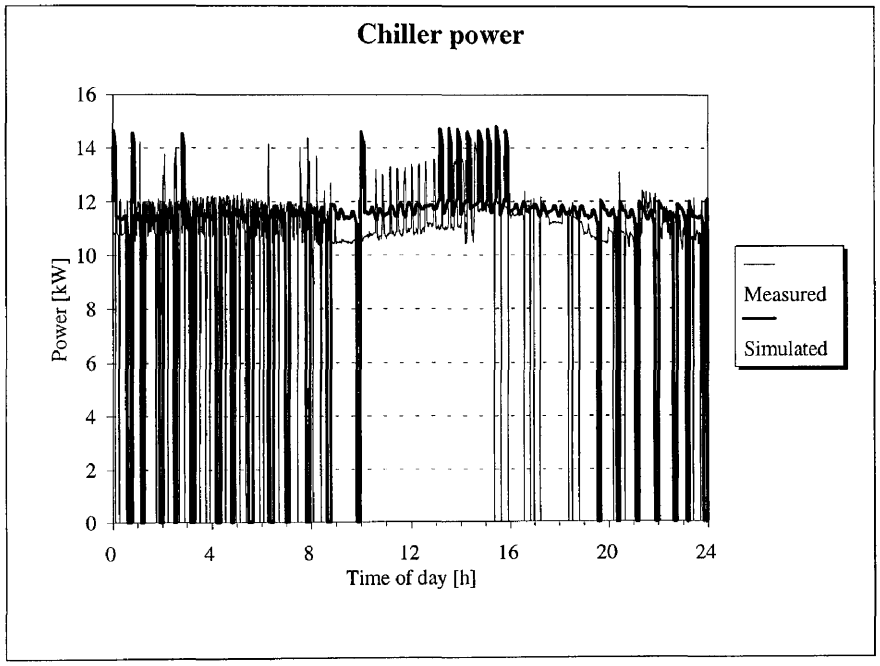

Figure 7.11: Power used by the chiller.

Figures 7.12 to 7.15 show the inside air temperature of the zones supplied by the common AHU. In the next two figures (figures 7.16 and 7.17), the zone temperatures for the two zones supplied by their own AHUs are compared to the measured data. The agreement is again seen to be good.

In figures 7.18 to 7.20, the measured and simulated supply air temperatures are compared. The dynamics of the coils and controller can be observed here. Accurate predictions of the supply and zone air temperatures again give us confidence in the applicability of the building model and the predicted indoor air temperatures.

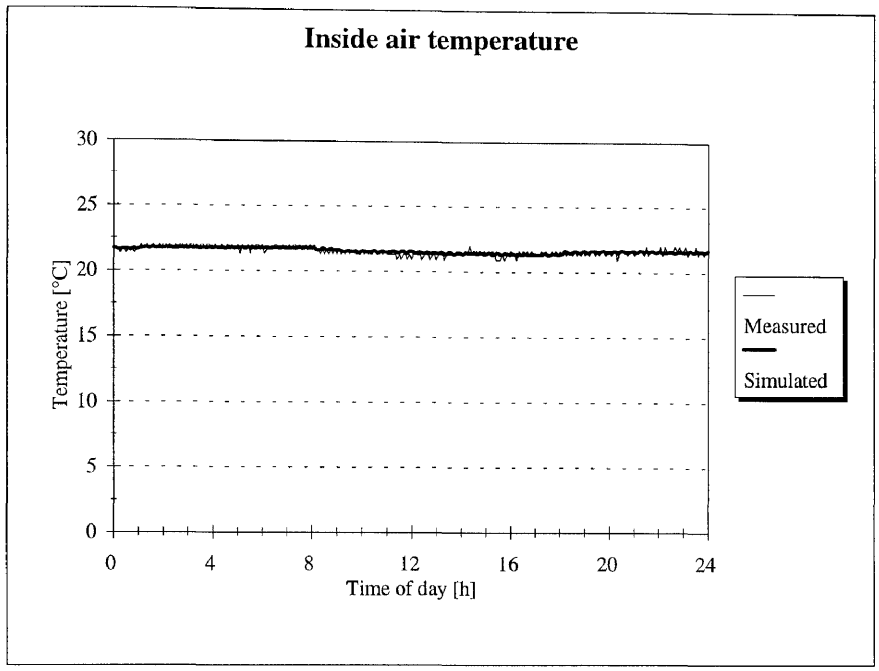

Figure 7.12: Photo laboratory 1 inside air temperature.

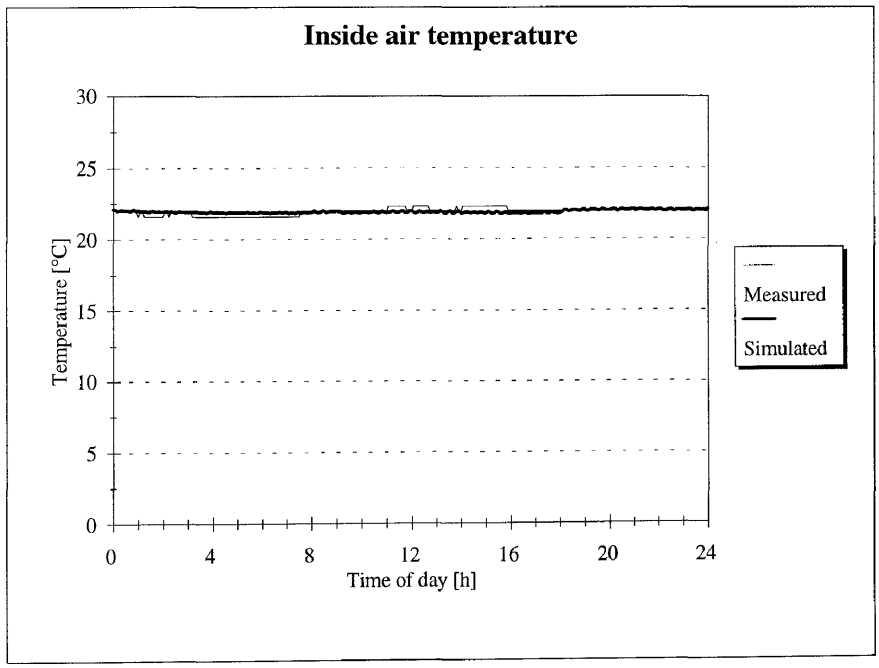

Figure 7.13: Photo laboratory 2 inside air temperature.

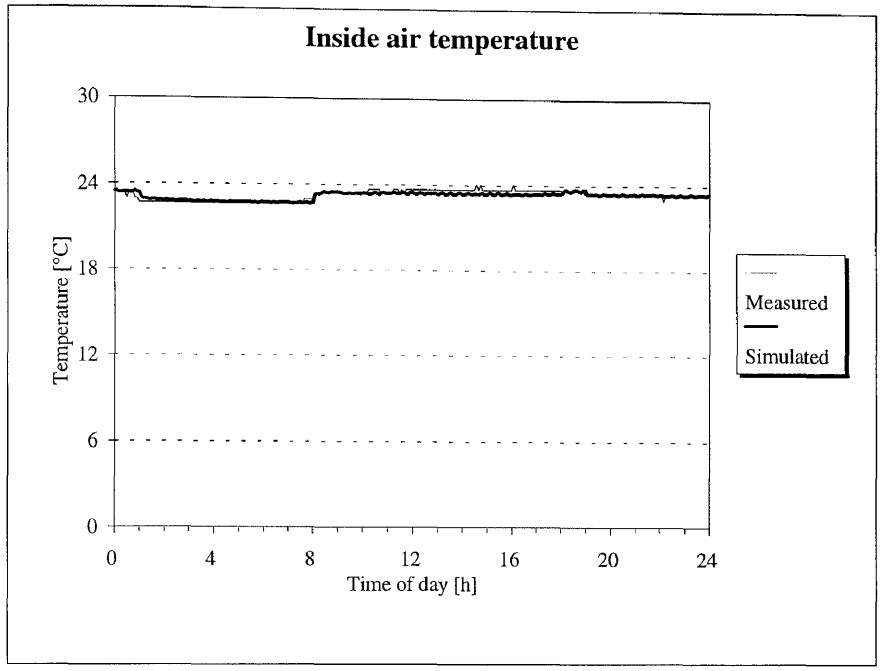

Figure 7.14: Photo laboratory 3 inside air temperature.

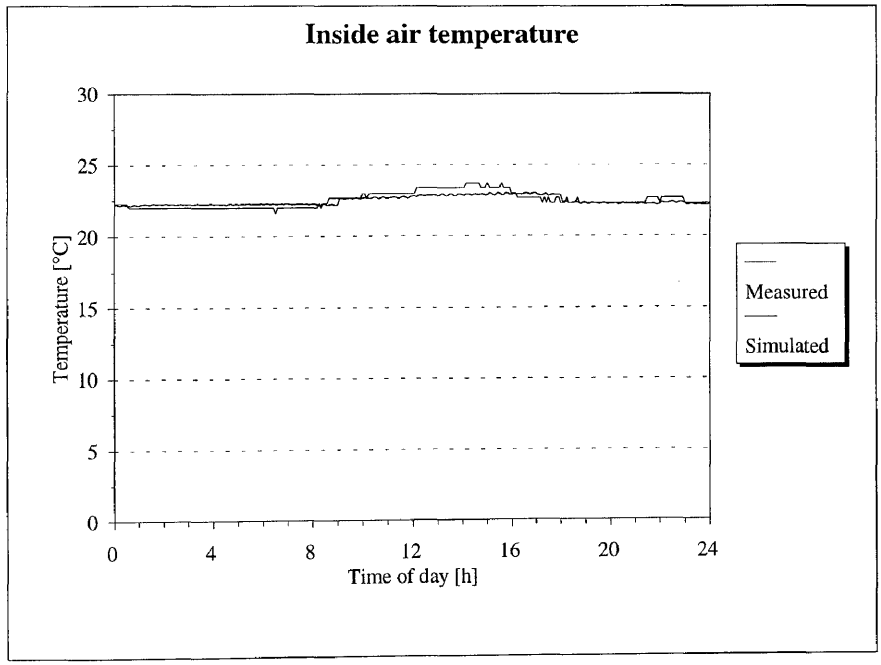

Figure 7.15: Photo laboratory 4 inside air temperature.

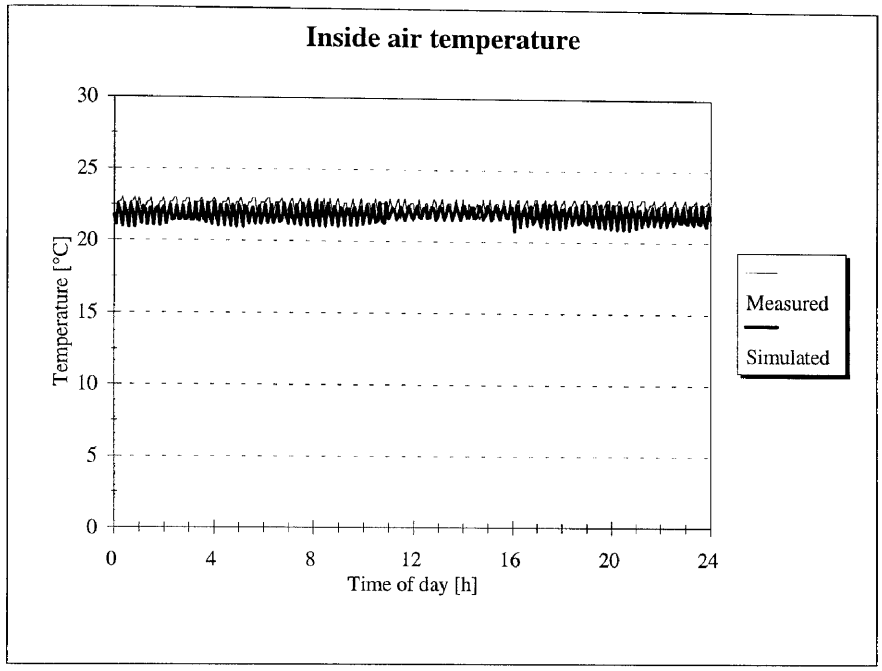

Figure 7.16: Reception inside air temperature.

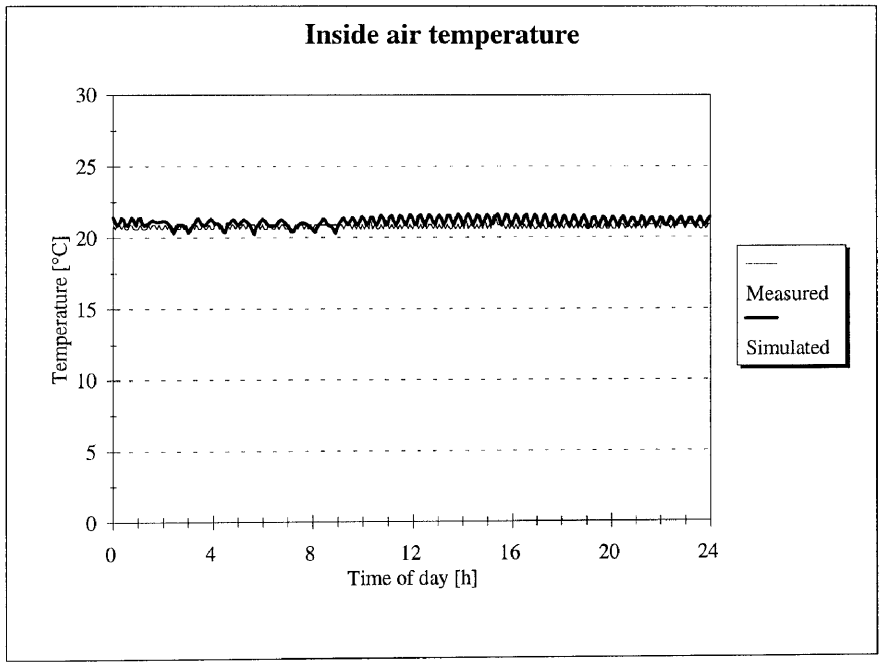

Figure 7.17: Studio inside air temperature.

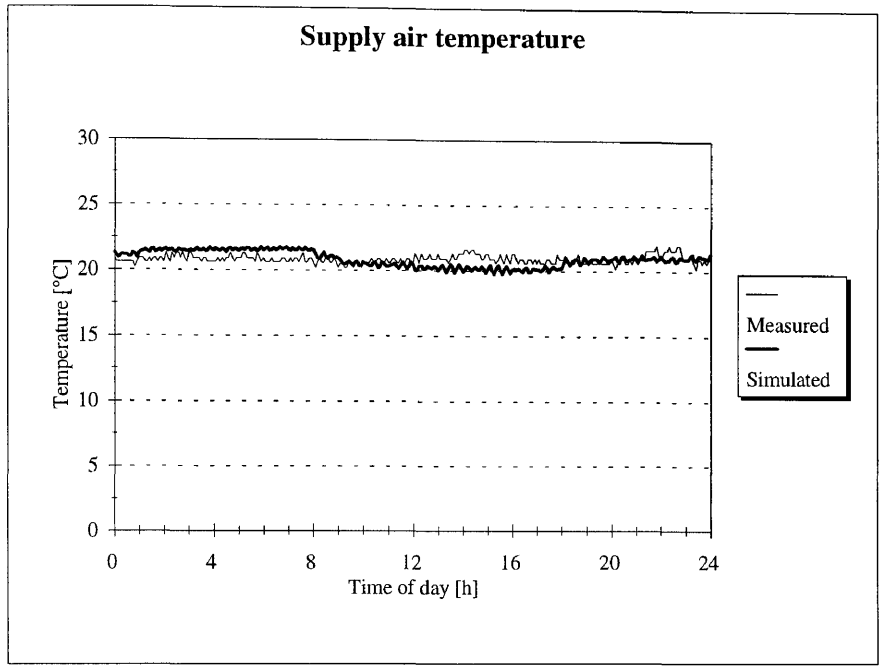

Figure 7.18: Supply air temperature from AHU 1.

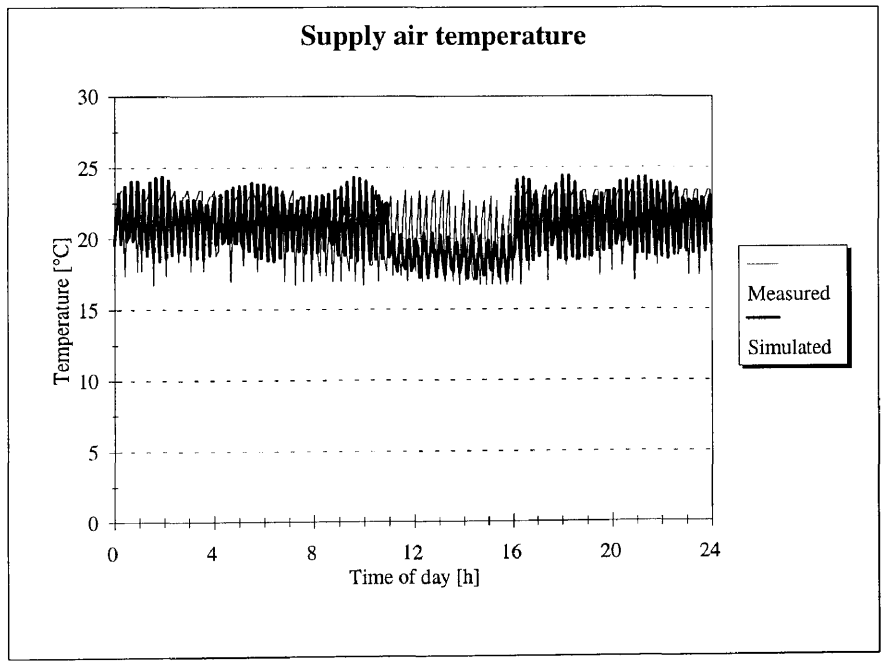

Figure 7.19: Supply air temperature from AHU 2.

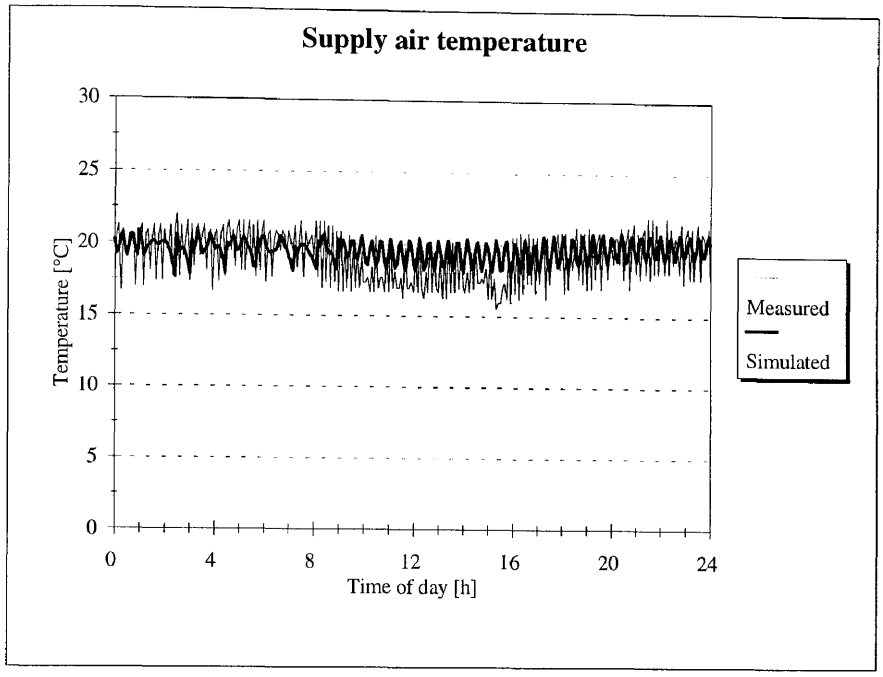

Figure 7.20: Supply air temperature from AHU 3.

7.4 CASE STUDY 3: AN OFFICE AND LABORATORY BUILDING

7.4.1 Introduction

The building is a multi-storeyed combined laboratory and office building situated approximately 35 km west of Pretoria. The building was built in the seventies and supplied with a constant volume reheat HVAC system. Originally, the system was designed as a constant volume system with the supply air temperature fixed for a given zone, irrespective of the load occurring inside the building or of the outside conditions.

During a retrofit study it was found that an enormous amount of energy is wasted on reheating the supply air at the reheat coils. A suggestion that the supply air temperature should be reset according to the outside air temperature was implemented.

7.4.2 Building and HVAC system description

The building is a five-storeyed office and laboratory building. The greatest part of the building is equipped with a once-through HVAC system. This is because the substances used inside the building are hazardous to human life.

A schematic of the building is shown in figures E.1 to E.3 of appendix E. There are nine zones in all, each supplied by its own air-handling unit from the main plant room.

There are three primary chiller units. All of these units reject heat to the atmosphere via cooling towers. The chillers supply nine air-handling units with chilled water. Most of the air-handling units are also equipped with a heating coil. Warm water is supplied from a heat exchanger where steam is used as a source of energy.

The supply air is transported to the various building zones via an air ducting system. Reheat coils at the entrance to each room or zone regulate the temperature in the room or zone.

A complete discussion of the determination of the model parameters is provided in Appendix E.

7.4.3 Verification results

Measured data from the building will be used to ensure that the simulation does reflect that that actually occurs in the building. The measurements were taken over a period of a month. The whole system was not measured simultaneously.

Data from various components in building H1 were added together in order to make the data manageable. Similarly, data from various components of buildings H2 and H5 were also treated together. The grouping is based on the distribution of chilled water from the two chillers that were operational at the time of verification.

Retrofit options were implemented based on previously conducted studies. The retrofit options that were implemented are:

1. Variable off-coil supply air temperature.
2. Scheduling selected pumps and fans on-off times from 17h00 to 05h00.

For the H1 building, all AHUs are switched off over weekends. For buildings H2 and H5, AHU 1 is switched off over weekends. AHUs 3 and 5 circulate air, but no cooling is done.

The variable off-coil air temperature is reset according to the relation given in table E.17.

Verification of daily thermal energy consumption for heating and reheating

In order to determine the thermal energy that was consumed for heating and reheating, the mass flow rate of the hot water and the temperature difference over the heat exchanger were measured. The energy used could then easily be determined from

$$\dot{Q} = \dot{m}_w C_{pw} \Delta T \tag{7.1}$$

where:

$\dot{Q}$ the thermal power consumed for heating, kW
$\dot{m}_w$ the mass flow rate of hot water, kg/s
C_{pw} thermal heat capacity of water, kJ/kg K
ΔT difference between entering and leaving water temperatures, °C or K.

The data obtained from the measurements are compared to the same values obtained from simulation, and are shown in figure 7.21 for building H1 and in figure 7.22 for buildings H2 and H5.

The figures clearly indicate that there is no heating done in building H1 during the unoccupied times. Heating in H2 and H5 does occur throughout the day. Peak power values are in good agreement and although the predicted power values do deviate from the measured values, the trend is predicted to a good degree.

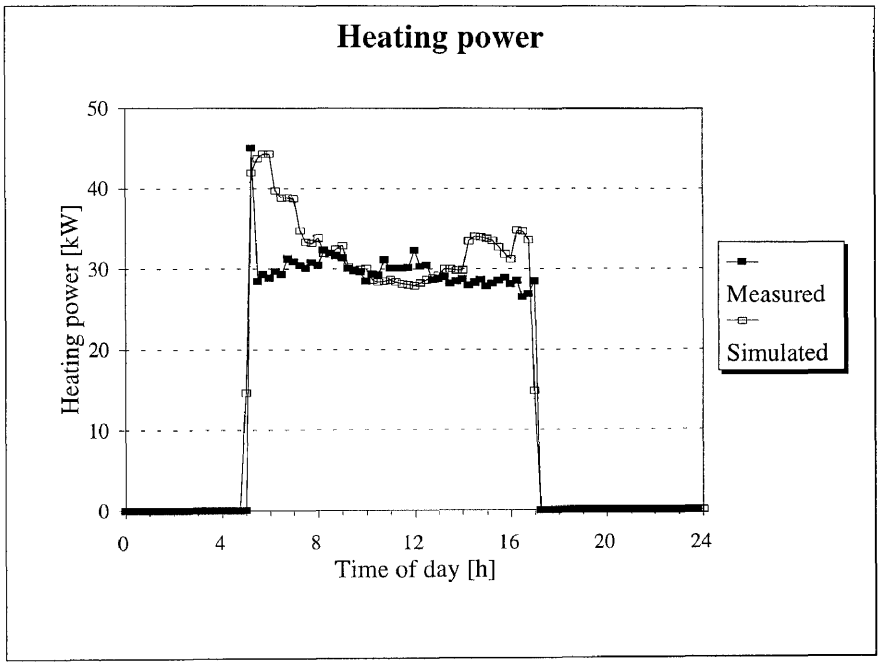

Figure 7.21: Heating power for the system of building H1.

Verification of daily energy consumption of fans and pumps

Figures 7.23, 7.24, 7.25 and 7.26 show good agreement between the predicted and measured pump and fan power for building H1, and buildings H2 and H5 respectively. The graphs again confirm the operation times.

Verification of daily energy consumption of chillers

A centrifugal chiller was present in buildings H2 and H5, while in building H1, the primary refrigeration device is a reciprocating chiller. The measured results confirm the typical trends

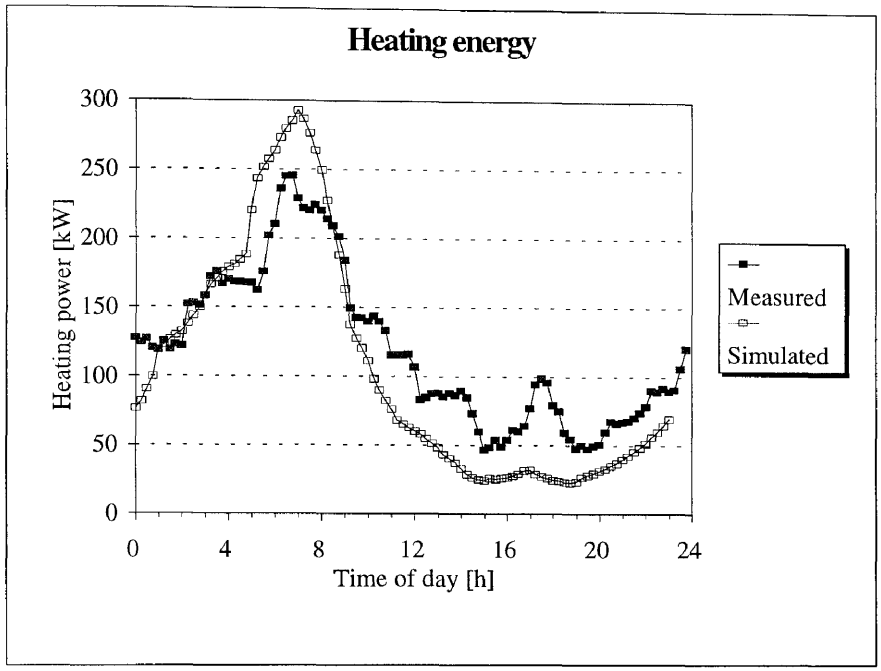

Figure 7.22: Heating power for the system of buildings H2 and H5.

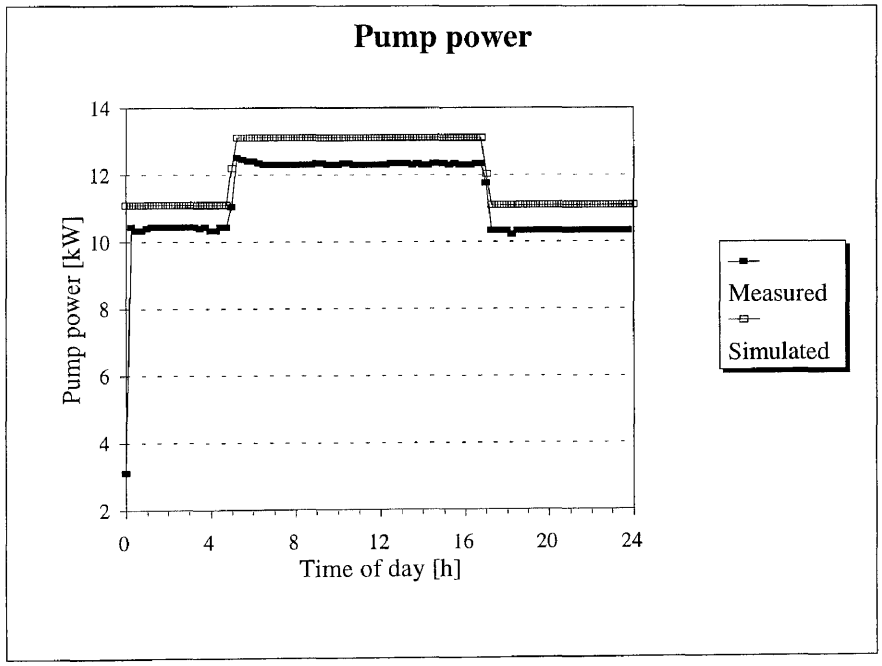

Figure 7.23: Pump power for the system of building H1.

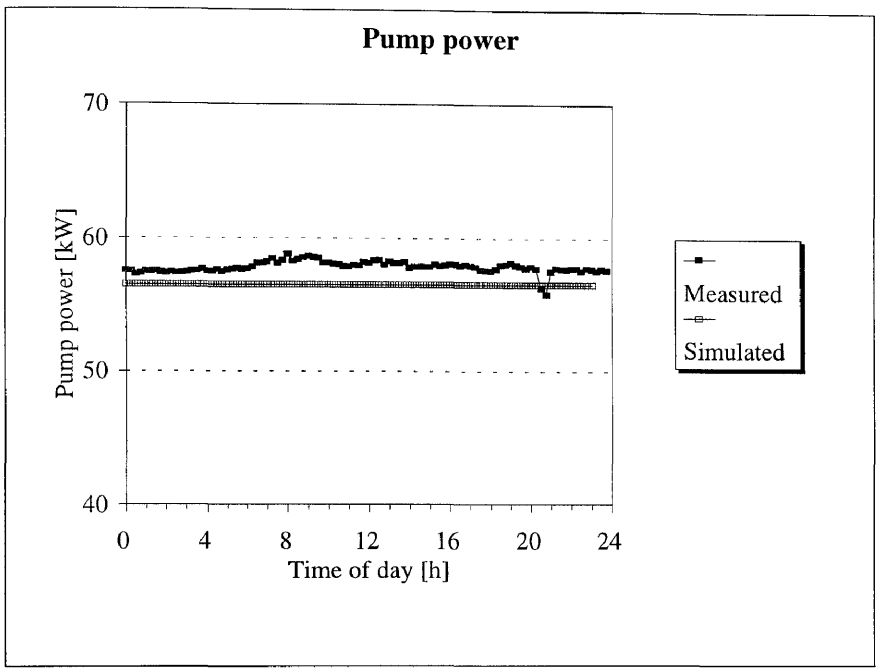

Figure 7.24: Pump power for the system of buildings H2 and H5.

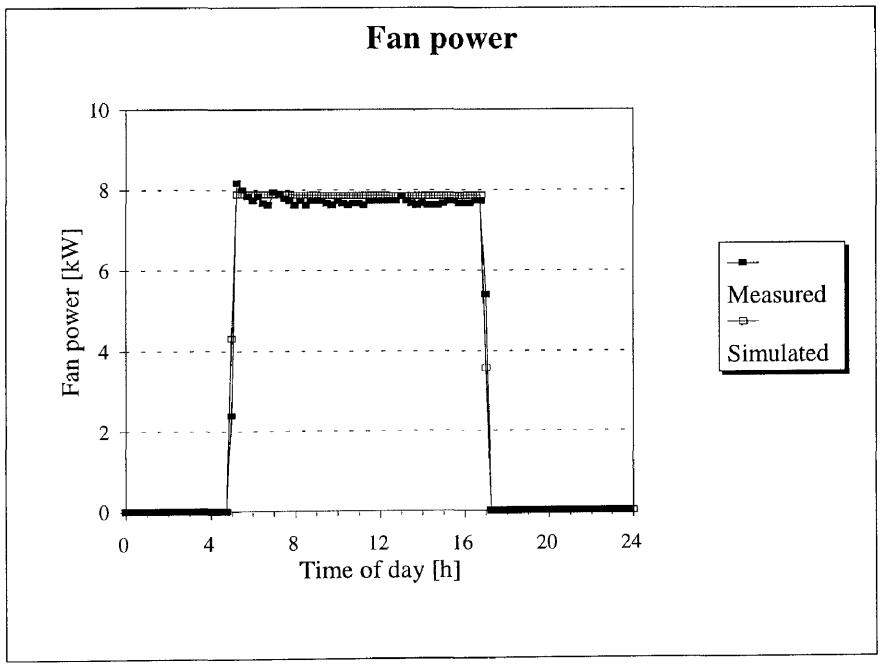

Figure 7.25: Fan power for the system of building H1.

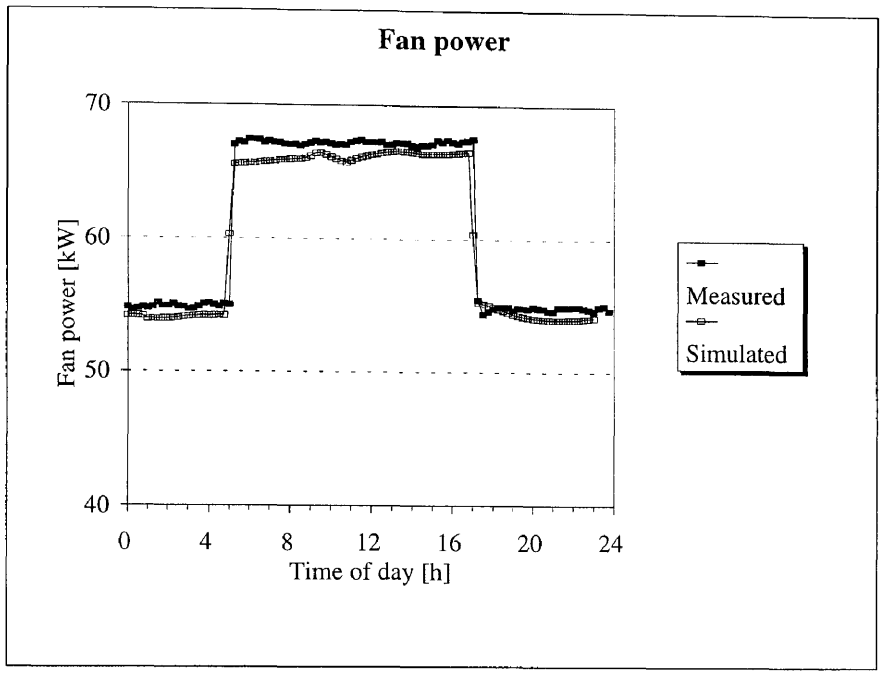

Figure 7.26: Fan power for the system of buildings H2 and H5.

for these machines. The simulated results are shown in figures 7.27 and 7.28.

Agreement between the measured and predicted power consumption is good. It should be noted that the loading and unloading of the reciprocating chiller is predicted to an extent. The discrepancies could be due to a number of reasons. The exact initial conditions were not specified. This could result in switching occurring at the incorrect times. Heat gains to piping are also not taken into account during the simulation. This could result in the chiller of the measured system loading and unloading even though the cooling coils are not operational.

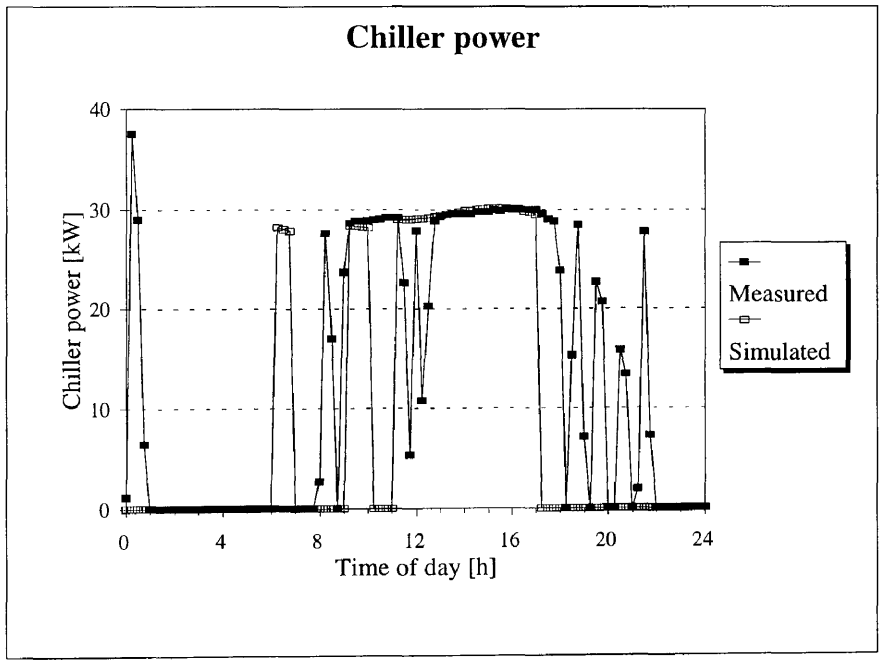

Figure 7.27: Chiller power for the system of building H1.

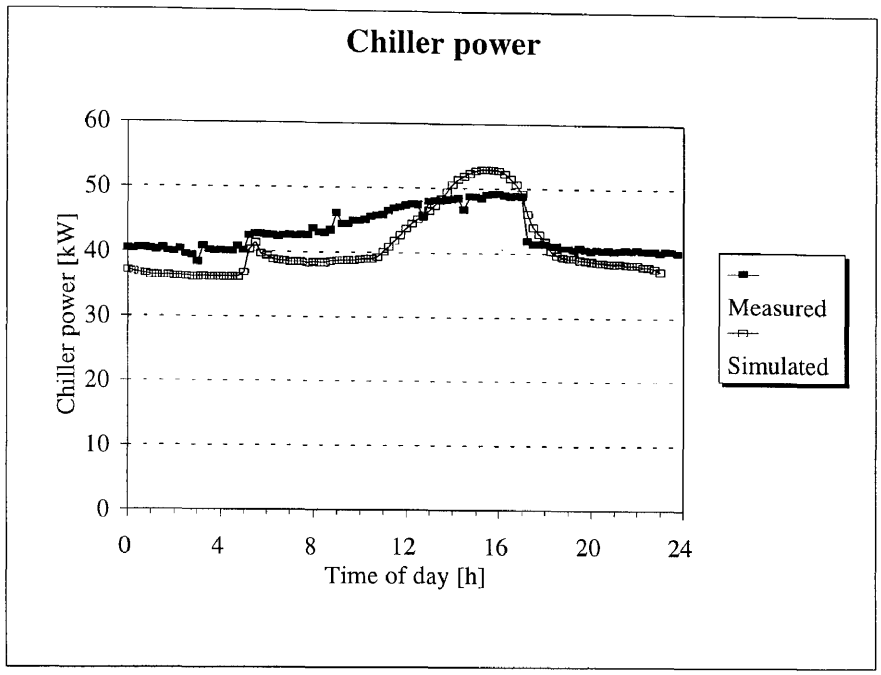

Figure 7.28: Chiller power for the system of buildings H2 and H5.

Verification of daily zone temperature

Accurate prediction of indoor air temperature is essential. For this reason, two typical zones, one each in building H1 and buildings H2 and H5, are given in the next two figures (figures 7.29 and 7.30). Agreement between measured and predicted data is good.

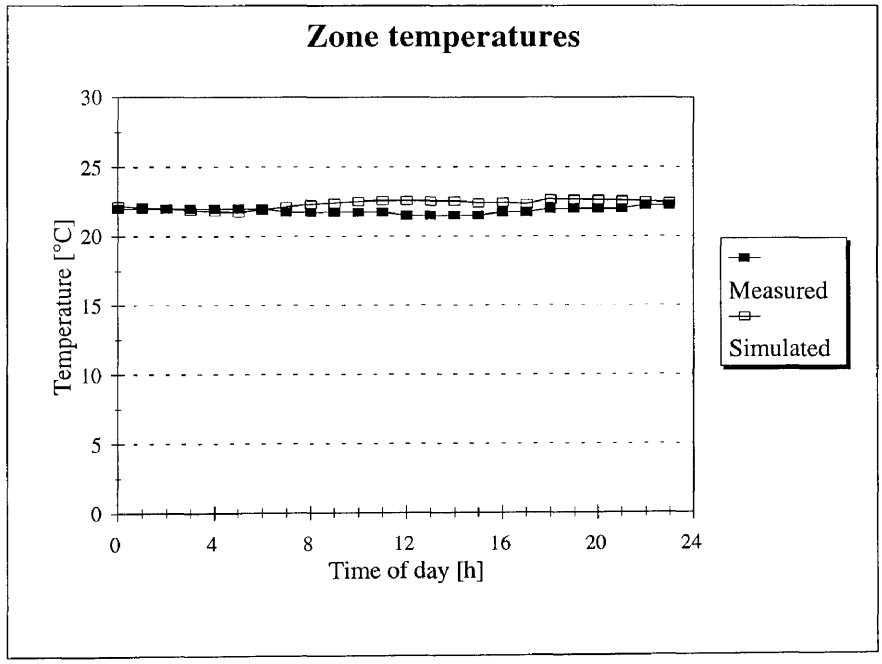

Figure 7.29: Zone temperature for a typical zone in building H1.

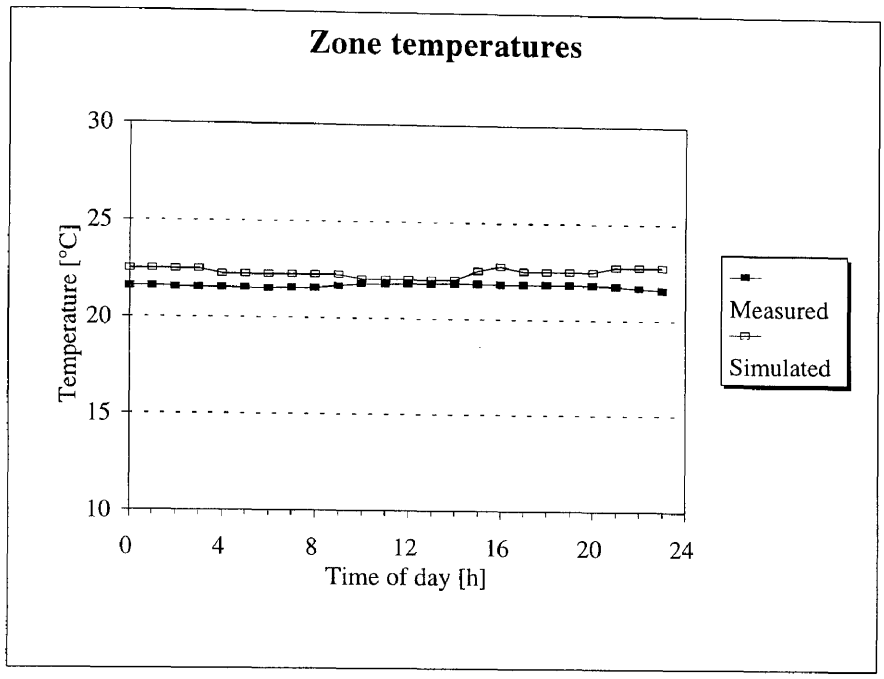

Figure 7.30: Zone temperature for a typical zone in buildings H2 and H5.

7.4.4 Yearly energy consumption simulation results

At this stage, the applicability of the computer model has been established. The tool will now be used to compare the energy consumption before and after retrofit for the same year. Here the value of the simulation tool is clearly shown. If this data had to be obtained experimentally two buildings would be needed, each exposed to the same climatic data. This is clearly not a feasible option.

Climatic data obtained from a weather station on the building site was used. The data for each month was averaged, and used as the climatic database for the project. For each month, two day simulations were done sequentially using the previous month as an initial condition for the first day. This was done to allow the transients, of the building structure primarily, to die out.

Then, the occupancy and the operational schedules for Saturday and Sunday were used, and these days were simulated, after which two weekdays were simulated. This is to emulate the dynamic effects of the building and the HVAC system. The energy consumption for the weekend and the first two weekdays are added, and three additional weekdays are obtained by adding the second simulated weekday values four times in total. Month values are obtained by assuming 4.33 weeks in each month.

Each major component group's data is reported on for the entire building. The data are presented in four graphs, i.e. the heating and cooling power in figures 7.31 and 7.32, and the fan and pump power in figures 7.33 and 7.34.

There is a substatial reduction in the energy required after the retrofit has been implemented. This is expected due to very limited reheating been done in the building zone. Chiller power is also

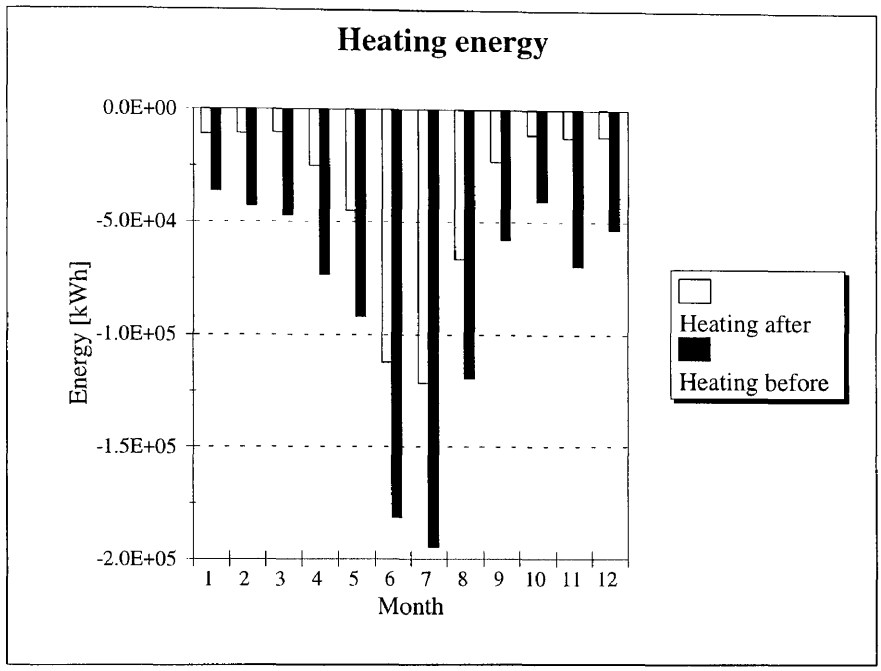

Figure 7.31: Year simulation result for heating power for the entire building.

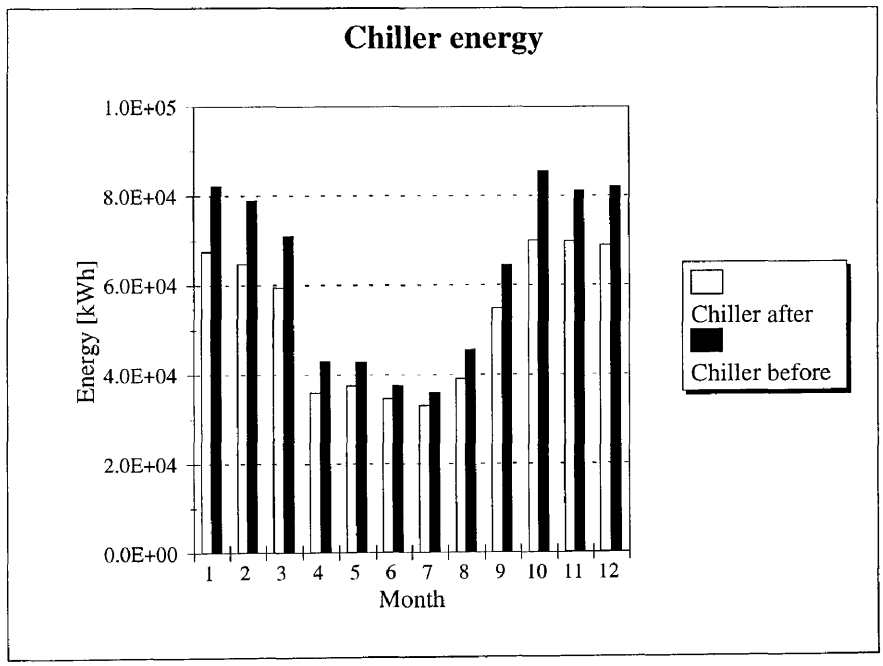

Figure 7.32: Year simulation result for cooling power for the entire building.

reduced. THis is due to the air not beeing cooled down as far as before the retrofit. THe fan power

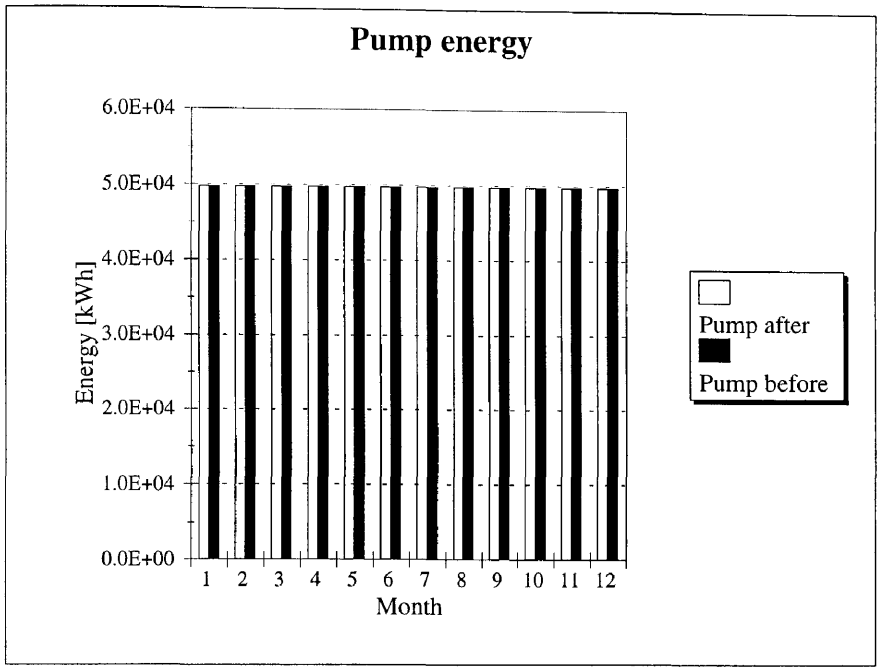

Figure 7.33: Year simulation result for pump power for the entire building.

is not reduced significantly. This is because the larger fans had to be opperational for ventilating the zones. The reduction that was obtained is due to the scheduling of the smaller fans.

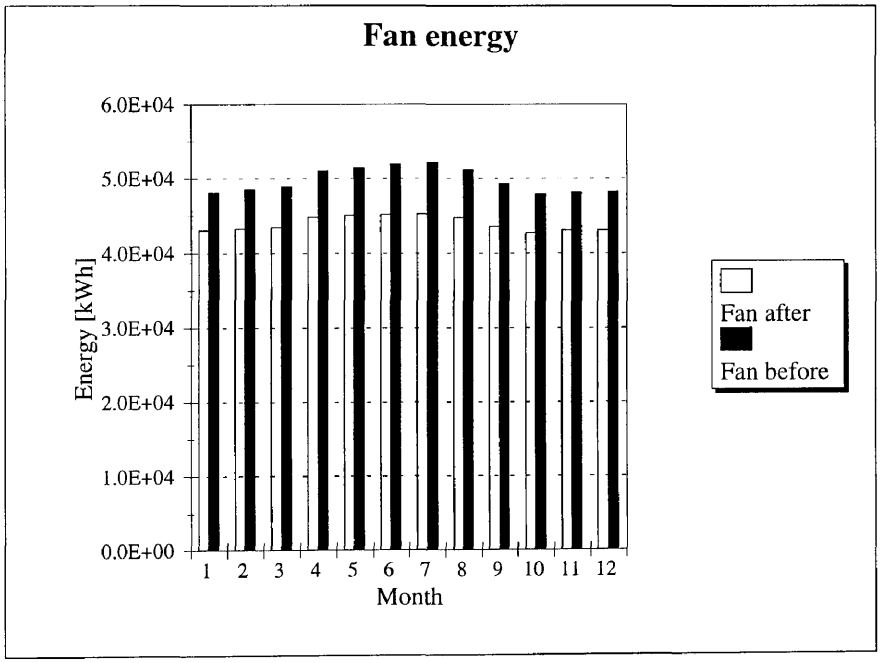

Figure 7.34: Year simulation result for fan power for the entire building.

7.5 CASE STUDY 4: A SIMULATION FOR A NEW DEVELOPMENT

7.5.1 Introduction

This section outlines an analysis, including life cycle costing (LCC), for the HVAC system of a new development. The site for this new development is in Brooklyn, Pretoria. Two systems were considered for comparison purposes, namely console units and split units versus a chilled water system with fan coil units in the ceiling void.

The building was divided into representative zones, and the various systems were simulated with the proposed simulation tool. This was done so that the performance of the system could be predicted. Year analyses were conducted for both systems to determine the energy consumption for each. The initial costs were estimated for both systems.

7.5.2 Requirements

The developer has the following requirements:

1. The system needs to be flexible since the office partitioning could change during the life of the building.
2. The feasibility of console units versus a chilled water system had to be investigated.

7.5.3 Concepts

The following two concepts were considered:

1. Console units and split units. The console units are proposed for the peripheral zones, and the split units for the core zones. A diagrammatic of the system that was simulated can be seen in figure 7.35. The zones and the equipment were lumped together to reduce the simulation time.
2. Chilled water system with ceiling mounted fan-coil units. The fan coil units will be mounted in the ceiling voids and will supply air through ducting and ceiling mounted diffusers. Chilled water will be supplied to the fan coil units from four chillers situated in two plant rooms. Chilled water will be piped to the zones where the pipes will be taken up in the provided service ducts to the ceiling voids. The cooling towers will fit on the roofs of the two buildings where provision has already been made for them. A diagrammatic of the system that was simulated is shown in figure 7.36. Once again, many of the components were

lumped to reduce simulation time. (Note: Two plant rooms, each 8x6 m^2, would be required for this concept. Ideal placement would be in the basement.)

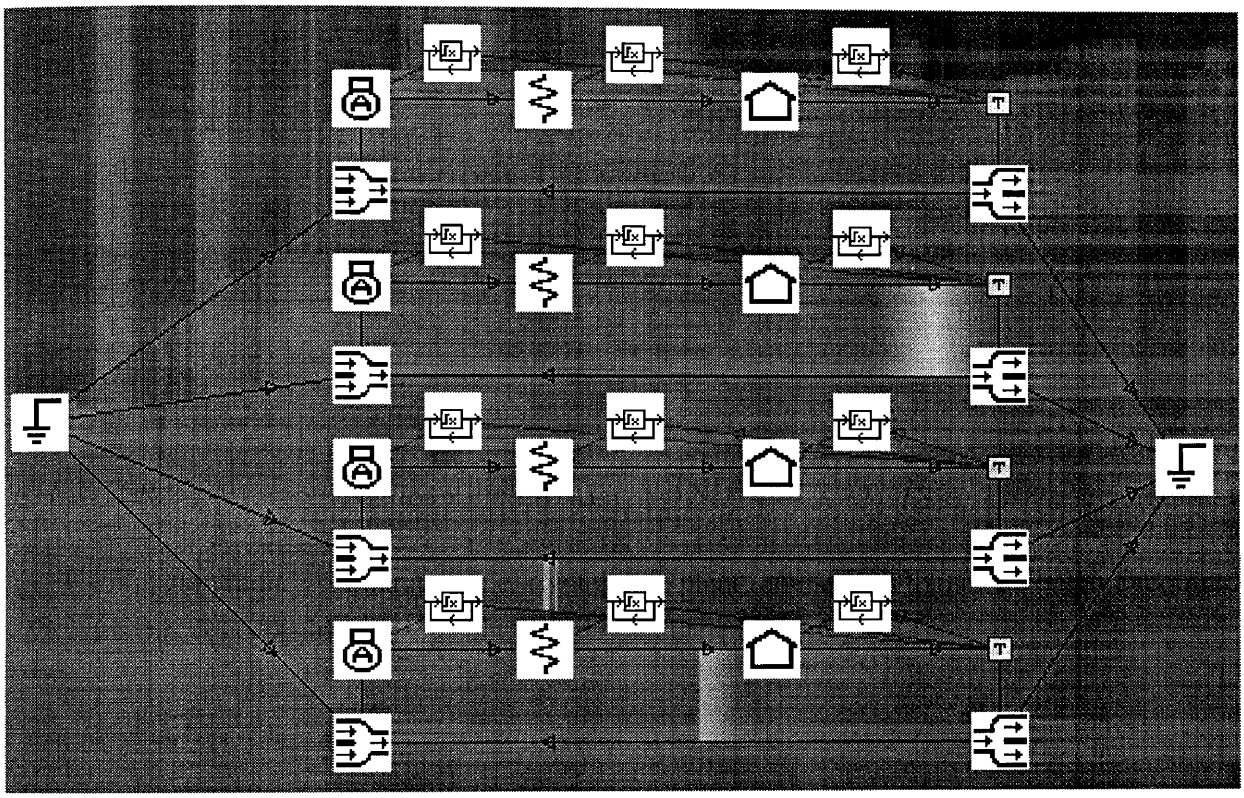

Figure 7.35: Schematic of console units.

Ceiling insulation

As a first step, the building load calculations were performed. Calculations for the top floor were performed with and without ceiling insulation. The loads calculated without insulation were twice as high as the loads calculated with insulation. In the following discussions it is assumed that the insulation would be included in the ceiling on the top floor.

Pros and cons

Various factors need to be considered when deciding which system to choose. The advantages and disadvantages of the various systems will be outlined below.

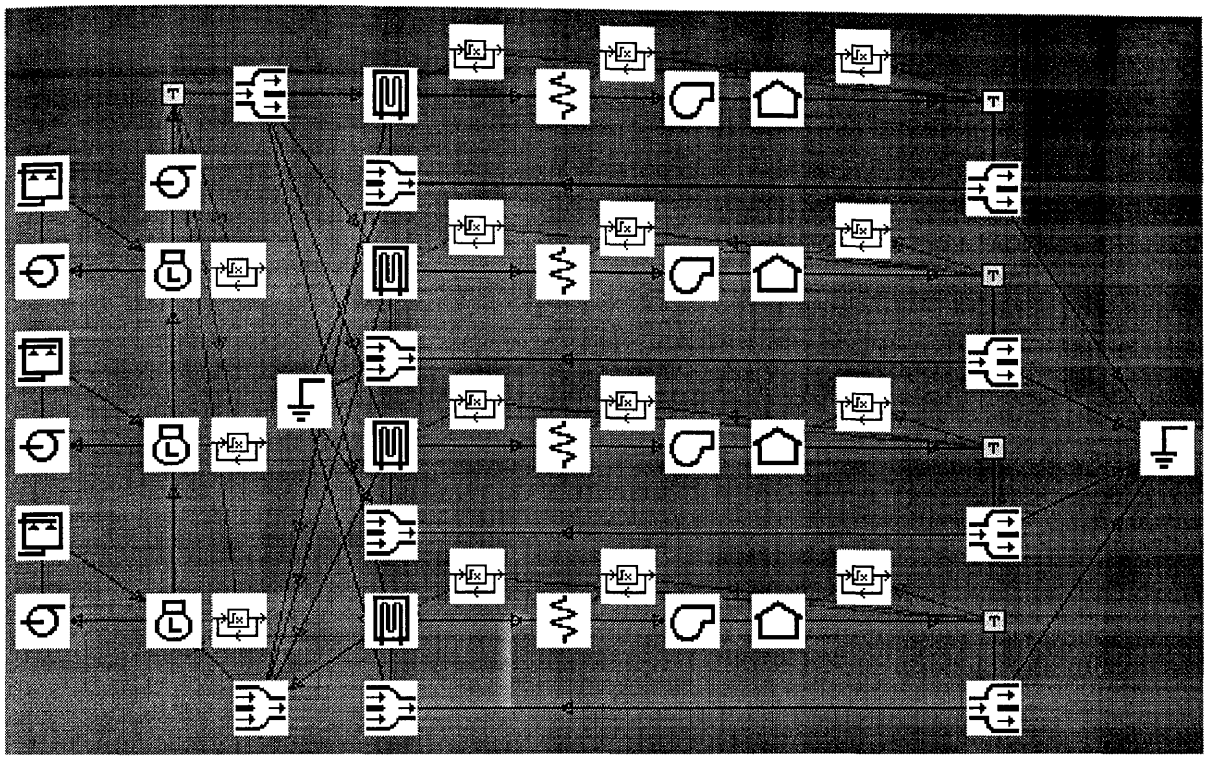

Figure 7.36: Schematic of chilled water system.

Consoles:

Benefits of the console and split units are:

1. Each zone can be individually controlled to a temperature that best suits the occupants.
2. When maintenance is required, only one occupant is affected.
3. Easy access to clean filters in each zone.

Drawbacks of the console and split units are:

1. They occupy space in the conditioned area.
2. The coefficients of performance are lower than that of a central plant, i.e. more energy is used to provide the same cooling.
3. Space would have to be provided for the condensing units of the split units.
4. Maintenance will be required in the conditioned space.

5. Relatively short service life.

Chilled Water Plant:

Benefits of a chilled water plant are:

1. Plant coefficient of performance is higher than that of consoles, i.e. less energy is used to provide the same cooling.
2. Maintenance to the chiller plant will be performed outside the building zone.
3. The diffusers are less obtrusive than the console units.
4. Longer service life.
5. Energy management strategies can be implemented for these systems.

Drawbacks of a chilled water system are:

1. Initial cost is higher.
2. If the plant is out of operation, more people will be adversely affected.
3. Space will need to be provided for the plant rooms.
4. Maintenance to the fan coil units will be required in the zones.

Life cycle cost

An economic analysis was conducted for the two different concepts. The

- initial costs
- annual energy costs, and
- annual maintenance costs

were estimated. These costs were used to conduct a life-cycle cost analysis.

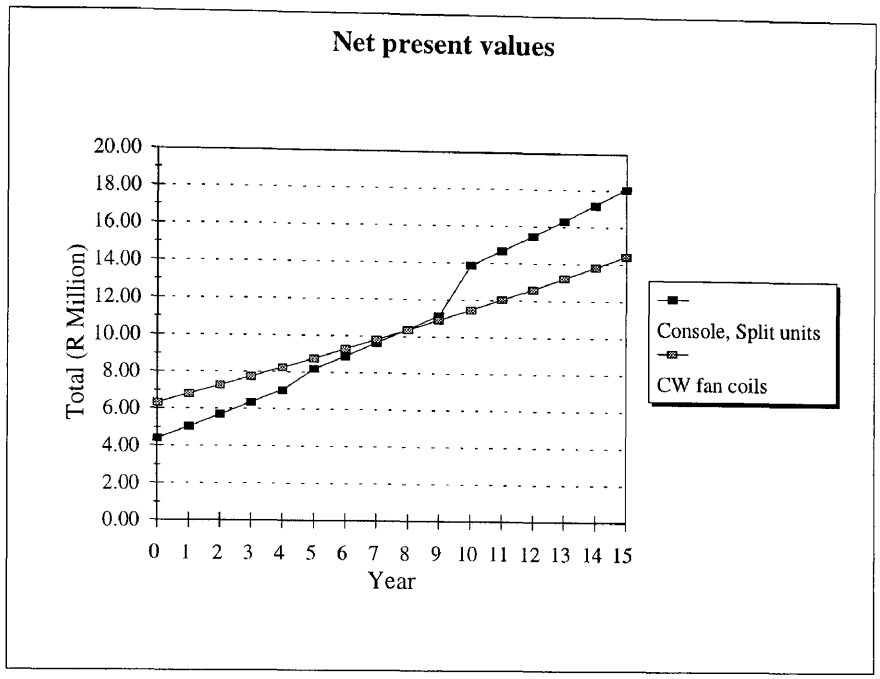

Figure 7.37: Nett present values for the two options described in text.

Results

The results of the economic analysis are described next. The nett present values are given in figure 7.37. A summary of the life cycle costing is shown in table 7.1.

Options	Consoles and split units	Chilled water fan coil units
Initial cost (Year 1)	R 4 450 000	R 6 350 000
Energy cost (Year 1)	R 502 000	R 330 000
Maintenance cost (Year 1)	R 98 000	R 150 700
Life-cycle cost (Year 15)	R 18 070 000	R 15 220 000
Discounted payback	Not applicable	8 years

Table 7.1: Summary of the life cycle costing of the two options.

Assumptions

The assumptions made in the above analysis are shown in table 7.2.

It was further assumed that some of the consoles will need to be replaced. The assumption is summarised in table 7.3.

Electricity tariff

The tariff used for this analysis is shown in table 7.4.

Parameters	Consoles and split units
Life-cycle	15 years
Discount rate	15 %
Energy escalation	18 % per annum
Maintenance escalation	16 % per annum
Initial cost expenditure	Beginning of year 1
Value added tax	Not taken into account
Residual values	None

Table 7.2: Summary of the assumptions made for the life cycle costing.

% of Consoles replaced	Year replaced
10	5
40	10
50	15

Table 7.3: Assumptions for console replacement.

Pretoria Town Council - 11kV Supply	
Energy consumption	8.06 c/kWh
Demand charge	44.44 R/kVA
Basic charge	R 246.30 per supply point

Table 7.4: Tariff structure used in this analysis.

Conclusion

Taking only costs into account it is clear that in the short and medium term, consoles and split units are the best choice. After 8 years, however, at he chilled water fan coil units becomes more economical.

7.5.4 Recommendations

Based on the pros and cons and the life cycle analysis, the selection of the system clearly depends on the building owner and/or the tenant. If the building owner adopts a long term approach, i.e. eight years or longer, then the chilled water system with fan coil units is recommended. For a shorter term approach, the consoles and split units will be the recommended option.

7.5.5 Exclusions

The following items are excluded in the estimates:

1. Service shafts to buildings not directly above the main basement.
2. Parking garage ventilation shafts.
3. Ceiling insulation

7.5.6 Cost summary

The total cost of the system is given in table 7.5.

Item	Costs excluding VAT
Console units	R 4 450 000
Chilled water system	R 6 350 000
Ventilation of basement	R 127 000
Ceiling insulation	R 264 000
Consulting fees (based on Chilled Water System)	R 590 000

Table 7.5: Cost summary for the project.

7.6 CLOSURE

Before the tool could be used for practical integrated simulations it had to be verified.

Verification studies on three buildings were conducted and are described here. The buildings ranged from a five-storeyed office and laboratory building, to a residential house with a ducted split unit. The simulation results are in good agreement with the measured values.

Certain deviations from the measured data were observed, but these could be explained based on the assumptions that have been made in the simulation tool.

Problems concerning the control and capacity of the chiller in the second case study could be predicted to a large degree. This gives us confidence in using the tool as an aid in problem solving.

After the tool was successfully verified it could be applied to the practical problems in sections 1.1.2 and 1.1.3. Firstly the applicability of the tool to retrofit studies is illustrated in the third case study. Secondly the applicability of the tool to design and life cycle costing is illustrated in the fourth case study. This solution to a practical problem introduced in chapter 1, shows that our goal for this study has been met.

Chapter 8

CLOSURE

In this chapter a brief summary of the study is given. Recommendations for future work are given.

8.1 CONCLUSIONS

In this study, the problems of a practicing engineer were stated by the author and confirmed by LeBrun [1]. He stated that: '*The dream of many engineers is to find simulation software allowing them to go, without any discontinuity, through all steps of a technical production: early design, selection and sizing of components, system optimization, control design and testing, system balancing and commissioning, control tuning, system management, audit and monitoring, retrofits, etc ...*'.

It was shown in sections 7.4 and 7.5 that these problems stated by the author and Lebrun [1] were successfully addressed by the study. To achieve this, a number of new developments had to be made.

Firstly, a new thermal model for buildings is presented. The model has been extensively verified with one hundred and three case studies. The thermal model is also used in a program that was custom-made for the board that certifies new low-cost housing.

In the second part of this study, the implementation of integrated simulation was discussed. A solution algorithm based on the Tarjan depth-first search algorithm is implemented. This ensures that the minimum number of variables are solved.

Various extensions to the models and simulation originally suggested by Rousseau [2] were implemented. Firstly, the steady-state models were extended by using a simplified time-constant approach to emulate the dynamic response of the equipment. Secondly, a CO_2 model for the building zone was implemented.

Further extensions to the simulation tool were implemented so that energy management strategies could be simulated. A detailed discussion of the implications of the EMS was given.

Finally, the simulation tool was verified by three case studies. The buildings used here ranged from a five-storeyed office and laboratory building, to a domestic dwelling. The energy consumption and the dynamics of the systems could be predicted sufficiently accurately to warrant the use of the tool for further building retrofit studies.

The resultant energy simulation tool is user-friendly, and will hopefully contribute to further the use of these tools by consulting engineers. A novice user will be able to use the tool confidently after only one day. A day simulation (with twenty time steps per hour) of a single-zone building and a simple HVAC system will take approximately ninety seconds on a 133MHz Pentium running Windows 95 ®.

Simulations of a building consisting of five building zones and a central plant, with a chiller and a cooling tower with forty time steps per hour takes approximately 660 seconds on the same PC.

8.2 RECOMMENDATIONS FOR FUTURE WORK

During this study a number of problems were encountered. These will be discussed here as a basis for future work. This work was based on the initial assumption that quasi-steady-state models for the HVAC components would suffice for the simulation of energy consumption of the HVAC systems.

It was further assumed that the system simulation could be used for the prediction of yearly energy consumption. After implementation of the solution algorithm and the simulation of control dynamics, it was found that the execution time of a simulation is considerably longer than expected.

Based on the summary, the following is suggested for future work:

1. The internal loads that are currently worked out by hand and entered into the passive building interface should be extended. The interface should provide for the specification of the number of computers, the number of specific lighting equipment, and all other equipment that make up the internal loads. Scheduling of this equipment on an individual basis should also be allowed for.

2. Dynamics models should be considered for the modelling of the major HVAC components.

3. At present, the user has to specify the time constants for the various components. The user should be given guidance for the choices of these time constants. It is suggested that existing dynamic models be considered (for example those implemented in HVACSIM+) and parameter studies be performed on these models. This could then assist the user in specifying the time constants. As an alternative the user can be prompted for the relevant parameters from which the time constants can be determined. Where necessary numerical parameter studies based on detailed fundamental principle models will have to be conducted.

4. Although much code optimisation has been done, it is suggested that further code optimisation be considered.

5. The possibility of employing a BIN-type method for yearly energy consumption should be investigated. It is doubtful if dynamic simulation of an entire year is necessary in order to compare various design or retrofit options. The modified method as suggested by Yang [3] could be considered.

6. A first selection algorithm should be devised and implemented in the program. Such a procedure should use the system layout as proposed by the user and make a first selection for the components, based on 'passive' building load calculations. This selection may or may not be modified by the user.

7. Integrating the tool to include building monitoring and audits is also a future task.

Appendix A

THEORETICAL VERIFICATION SUMMARY

Wall no.	Layers: inside to outside Description	First-order load prediction			Third-order load prediction		
		Max load (% error)	Energy (% error)	Wall temp. (90th pers)	Max load (% error)	Energy (% error)	Wall temp. (90th pers)
1	EO A3 B1 B13 A3 AO Steel 2, Air, Ins 100, Steel 2	90.4	11.3	3.0	24.6	-3.0	0.2
2	EO E1 B14 A1 AO Plaster 20, Ins 125, Stucco 25	87.8	39.1	7.5	8.8	0.4	0.2
3	EO C3 B5 A6 AO HD 100, Ins 25, Fin 13	52.3	12.9	2.4	1.3	-0.6	0.2
4	EO E1 B6 C12 AO Plaster 20, Ins 50, HD 50	85.9	34.6	6.9	8.1	-1.5	0.4
5	EO A6 B21 C7 AO Fin 13, Ins 35, LD 200	84.2	30.8	5.8	20.8	-3.3	0.9
6	EO E1 B2 C5 A1 AO Plaster 20, Ins 25, HD 100	79.0	28.6	5.5	13.4	-4.0	0.8
7	EO A6 C5 B3 A3 AO Fin 13, HD 100, Ins 50, Steel 2	26.5	2.5	1.0	-1.2	-3.9	0.2
8	EO A2 C12 B5 A6 AO F/B 100, HD 50, Ins 25, Fin 13	29.6	9.2	1.4	4.4	-0.9	0.3
9	EO A6 B15 B10 AO Fin 13, Ins 150, Wood 50	90.2	46.0	8.4	32.2	0.8	0.6
10	EO E1 C2 B5 A2 AO Plaster 20, LD 100, Ins 25, F/B 100	74.0	40.1	6.7	10.0	0.8	0.4
11	EO E1 C8 B6 A1 AO Plaster 20, HD 200, Ins 50, Stucco 25	51.5	19.4	3.4	4.0	-0.7	0.2
12	EO E1 B1 C10 A1 AO Plaster 20, Air, HD 200, Stucco 25	59.4	17.0	2.1	14.4	-5.7	1.0
13	EO A2 C5 B19 A6 AO F/B 100, HD 100, Ins 15, Fin 13	30.2	9.7	1.3	5.2	-0.7	0.4
14	E0 A2 A2 B6 A6 AO F/B 100, F/B 100, Ins 50, Fin 13	31.7	8.4	1.5	4.8	0.1	0.1
15	E0 A6 C17 B1 A7 AO Fin 13, LD 200, Air, F/B 100	83.7	43.0	7.4	31.7	-1.2	0.9
16	E0 A6 C18 B1 A7 AO Fin 13, HD 200, Air, F/B 100	62.0	28.8	4.4	7.1	-1.5	-0.2
17	E0 A2 C2 B15 AO F/B 100, LD 100, Ins 150	26.1	4.5	1.1	-22.9	3.9	0.4
18	E0 A6 B25 C9 AO Fin 13, Ins 85, Com brick 200	89.8	43.0	7.8	52.8	5.5	2.2
19	E0 C9 B6 A6 AO Com brick 200, Ins 50, Fin 13	44.0	10.9	1.9	3.1	0.3	0.1
20	E0 C11 B19 A6 AO HD 300, Ins 15, Fin 13	30.8	10.4	1.4	0.2	1.4	0.1

Wall no.	Layers: inside to outside description	First-order load prediction			Third-order load prediction		
		Max load (% error)	Energy (% error)	Wall temp. (90th pers)	Max load (% error)	Energy (% error)	Wall temp. (90th pers)
21	E0 C11 B6 A1 AO HD 300, Ins 50, Stucco 25	33.5	10.1	1.9	2.1	0.9	0.1
22	E0 C14 B15 A2 AO LD 100, Ins 150, F/B 100	84.4	49.1	8.9	22.7	-0.3	0.3
23	E0 E1 B15 C7 A2 AO Plaster 20, Ins 150, LD 200, F/B 100	89.2	50.6	9.8	45.0	0.7	0.8
24	E0 A6 C20 B1 A7 AO Fin 13, HD 300, Air, F/B 100	62.2	28.8	4.2	8.9	-0.9	0.1
25	E0 A2 C15 B12 A6 AO F/B 100, LD 150, Ins 75, Fin 13	38.6	12.1	2.9	-29.9	2.8	0.7
26	E0 A2 C6 B6 A6 AO F/B 100, Clay Tile 200, Ins 50, Fin 13	37.2	11.5	2.2	-13.8	2.5	0.5
27	E0 E1 B14 C11 A1 AO Plaster 20, Ins 125, HD 300, Stucco 25	89.8	50.2	9.6	55.3	-3.7	1.0
28	E0 E1 C11 B13 A1 AO Plaster 20 HD 300, Ins 100, Stucco 25	36.7	6.9	1.2	3.4	4.4	0.1
29	E0 A2 C11 B5 A6 AO F/B 100, HD 300, Ins 25, Fin 13	38.3	11.1	1.8	-7.3	3.2	0.5
30	E0 E1 B19 C19 A2 AO Plaster 20, Ins 15, LD 300, F/B 100	85.5	45.3	8.2	36.4	1.8	0.7
31	E0 E1 B15 C15 A2 AO Plaster 20, Ins 150, LD 150, F/B 100	89.7	50.4	9.6	47.6	1.2	0.8
32	E0 E1 B23 B9 A2 AO Plaster 20, Ins 60, Wood 100, F/B 100	87.7	44.4	8.3	50.4	-0.3	0.7
33	E0 A2 C6 B15 A6 AO F/B 100, Clay Tile 200, Ins 150, Fin 13	34.8	4.0	2.4	-27.3	3.4	0.5
34	E0 C11 B21 A2 AO HD 300, Ins 35, F/B 100	45.4	24.0	3.8	0.5	0.7	0.1
35	E0 E1 B14 C11 A2 AO Plaster 20, Ins 125, HD 300, F/B 100	90.0	50.6	9.6	70.1	-1.3	1.2
36	E0 A2 C11 B25 A6 AO F/B 100, HD 300, Ins 85, Fin 13	35.5	4.8	1.7	-13.0	9.2	0.2
37	E0 E1 B25 C19 A2 AO Plaster 20, Ins 85, LD 300, F/B 100	89.6	49.0	9.2	58.9	3.9	0.8
38	E0 E1 B15 C20 A2 AO Plaster 20, Ins 150, HD 300, F/B 100	90.2	50.9	9.6	67.1	2.6	0.9
39	E0 A2 C16 B14 A6 AO F/B 100, LD 200, Ins 125, Fin 13	41.6	11.1	3.2	-70.5	5.5	1.3
40	E0 A2 C20 B15 A6 AO F/B 100, HD 300, Ins 150, Fin 13	35.7	3.1	2.5	46.1	5.0	0.8
41	E0 E1 C11 B14 A2 AO Plaster 20, HD 300, Ins 125, F/B 100	55.4	31.2	4.7	3.2	4.9	0.1

Appendix B

VERIFICATION STUDIES

In this appendix the verification studies results are presented in detail. A summary of the verification study data is given in tabular form. The symbols used in the table are:

- MZ - Multi-zone simulation performed? (Y/N)
- GC - Building zone in ground contact? (Y/N)
- WO - Windows open during monitoring period? (Y/N)
- HG - Heat generation in building zone? (Y/N)
- FA - Floor area of building zone (m^2)

NO	BUILDING	LOCATION	DATE	MZ	GC	WO	HG	FA
1	Experim1	Pretoria	07/06/82-13/06/82	N	Y	N	N	9
2	Experim2	Pretoria	07/06/82-13/06/82	N	Y	N	N	9
3	Experim3	Pretoria	07/06/82-13/06/82	N	Y	N	N	9
4	Experim4	Pretoria	07/06/82-13/06/82	N	Y	N	N	9
5	Experim1	Pretoria	26/07/82-01/08/82	N	Y	N	N	9
6	Experim2	Pretoria	26/07/82-01/08/82	N	Y	N	N	9
7	Experim3	Pretoria	26/07/82-01/08/82	N	Y	N	N	9
8	Experim4	Pretoria	26/07/82-01/08/82	N	Y	N	N	9
9	Experim1	Pretoria	27/09/82-03/10/82	N	Y	Y	N	9
10	Experim2	Pretoria	27/09/82-03/10/82	N	Y	Y	N	9
11	Experim3	Pretoria	27/09/82-03/10/82	N	Y	Y	N	9
12	Experim4	Pretoria	27/09/82-03/10/82	N	Y	Y	N	9
13	Experim1	Pretoria	13/07/82-19/08/82	N	Y	Y	N	9
14	Experim2	Pretoria	13/07/82-19/08/82	N	Y	Y	N	9
15	Experim3	Pretoria	13/07/82-19/08/82	N	Y	Y	N	9
16	Experim4	Pretoria	13/07/82-19/08/82	N	Y	Y	N	9
17	Experim1	Pretoria	14/02/83-20/02/83	N	Y	Y	N	9
18	Experim2	Pretoria	14/02/83-20/02/83	N	Y	Y	N	9
19	Experim3	Pretoria	14/02/83-20/02/83	N	Y	Y	N	9
20	Experim4	Pretoria	14/02/83-20/02/83	N	Y	Y	N	9
21	Experim1	Pretoria	18/04/84-26/04/84	N	Y	Y	N	9
22	Experim2	Pretoria	18/04/84-26/04/84	N	Y	Y	N	9
23	Experim4	Pretoria	18/04/84-26/04/84	N	Y	Y	N	9
24	Experim4	Pretoria	10/02/86-16/02/86	N	Y	Y	Y	9
25	Experim1	Pretoria	01/11/90-03/11/90	N	Y	Y	Y	9
26	Bedroom1	Verwoerdburg	18/08/86-24/08/86	N	Y	N	N	11
27	Bedroom1	Verwoerdburg	04/08/86-10/08/86	N	Y	N	N	11
28	Bedroom1	Verwoerdburg	21/10/85-27/10/85	N	Y	Y	N	11
29	Bedroom1	Verwoerdburg	25/11/85-01/12/85	N	Y	Y	N	11
30	Bedroom1	Verwoerdburg	04/11/85-17/11/85	N	Y	Y	N	11
31	Bedroom1	Verwoerdburg	21/07/86-27/07/86	N	Y	Y	Y	11
32	Bedroom2	Wingate Park	31/10/90-01/11/90	Y	Y	N	Y	11
33	Bedroom3	Moreleta Park	20/10/90-21/10/90	Y	N	N	Y	8
34	Bathroom	Faerie Glen	19/10/90-21/10/90	Y	Y	N	Y	4

35	Dormit1	Negev Desert	11/07/88-16/07/88	N	Y	N	N	23
36	Dormit1	Negev Desert	25/07/88-01/08/88	N	Y	NY	N	23
37	Dormit1	Negev Desert	01/08/88-08/08/88	N	Y	Y	N	23
38	Dormit2	Negev Desert	11/07/88-16/07/88	N	Y	N	N	23
39	Dormit2	Negev Desert	25/07/88-01/08/88	N	Y	NY	N	23
40	Dormit2	Negev Desert	01/08/88-08/08/88	N	Y	Y	N	23
41	Prefab	Negev Desert	11/07/88-16/07/88	N	Y	N	N	13
42	Prefab	Negev Desert	25/07/88-01/08/88	N	Y	NY	N	13
43	Prefab	Negev Desert	01/08/88-08/08/88	N	Y	Y	N	13
44	Garage	Verwoerdburg	27/01/86-02/02/86	N	Y	N	N	18
45	Garage	Verwoerdburg	03/02/86-09/02/86	Y	Y	Y	Y	18
46	Shop	Verwoerdburg	04/08/86-10/08/86	N	Y	N	N	102
47	Shop	Verwoerdburg	21/07/86-27/07/86	N	Y	Y	N	102
48	Shop	Verwoerdburg	27/01/86-16/02/86	Y	Y	Y	Y	102
49	School1	Menlo Park	20/07/87-26/07/87	N	N	N	N	58
50	School1	Menlo Park	13/07/87-19/07/87	N	N	Y	N	58
51	School2	The Willows	17/02/90-18/02/90	N	Y	Y	N	51
52	Store1	The Willows	20/10/90-23/10/90	Y	Y	N	Y	13
53	Store2	Volksrust	29/06/87-04/07/87	N	Y	Y	N	763
54	Studio	Brooklyn	09/11/91-10/09/91	N	Y	N	N	340
55	Church	Arcadia	18/03/90-18/03/90	N	Y	NY	Y	200
56	Factory	Groenkloof	11/11/85-24/11/85	N	Y	NY	N	7755
57	Office1	CSIR Pretoria	09/04/84-15/04/84	N	N	N	N	14
58	Office1	CSIR Pretoria	02/04/84-08/04/84	N	N	Y	N	14
59	Office2	G H Marais	06/05/89-07/05/89	N	N	N	N	34
60	Office3	G H Marais	06/05/89-07/05/89	N	N	N	N	17
61	Office3	G H Marais	18/04/90-20/04/90	N	N	N	Y	17
62	Office4	G H Marais	06/05/89-07/05/89	N	N	N	N	12
63	Office5	Cent. Gov. Off	18/02/89-21/02/89	N	N	N	Y	29
64	Office6	Liberty Life	26/01/88-31/01/88	N	N	N	Y	22
65	Office7	Poyntons	12/04/89-16/04/89	N	N	N	N	21
66	Office8	UNISA Pretoria	11/04/89-14/04/89	N	N	N	N	14
67	Office9	Eng. Block	20/10/90-21/10/90	Y	N	N	Y	18
68	Office10	Eng. Block	20/10/90-21/10/90	Y	N	N	Y	21
69	Office11	J G Strijdom	20/10/90-21/10/90	Y	N	N	Y	10
70	Office12	J G Strijdom	20/10/90-21/10/90	Y	N	N	Y	14
71	Lightweight	Negev Desert	18/08/92-25/08/92	N	N	Y	N	45.9
72	Heavyweight	Negev Desert	18/08/92-25/08/92	N	Y	Y	N	9.7
73	Lightweight	Negev Desert	24/08/92-30/08/92	N	N	Y	N	45.9
74	Heavyweight	Negev Desert	24/08/92-30/08/92	N	Y	NY	N	9.7
75	Room 1-91	Pretoria	20/02/96-23/02/96	Y	Y	N	Y	14.6
76	Room 1-90	Pretoria	20/02/96-23/02/96	Y	Y	N	Y	14.6
77	Room 1-94	Pretoria	20/02/96-23/02/96	Y	Y	N	Y	43.1
78	Room 1-93	Pretoria	20/02/96-23/02/96	Y	Y	N	Y	33.2
79	Room 1-79	Pretoria	23/02/96-27/02/96	Y	Y	N	Y	8.2
80	Room 1-80	Pretoria	23/02/96-27/02/96	Y	Y	N	Y	8.2
81	Room 1-82	Pretoria	23/02/96-27/02/96	Y	Y	N	Y	9.9
82	Room 1-83	Pretoria	23/02/96-27/02/96	Y	Y	N	Y	14.5

83	Room 1-122	Pretoria	30/09/96-03/10/96	Y	Y	N	Y	31.6
84	Room 1-123	Pretoria	30/09/96-03/10/96	Y	Y	N	Y	31.6
85	Room 1-125	Pretoria	03/10/96-07/10/96	Y	Y	N	Y	8.3
86	Room 1-126	Pretoria	03/10/96-07/10/96	Y	Y	N	Y	8.3
87	Room 1-127	Pretoria	03/10/96-07/10/96	Y	Y	N	Y	16.7
88	Room 1-141	Pretoria	01/03/96-05/03/96	Y	Y	N	Y	18.8
89	Room 1-142	Pretoria	01/03/96-05/03/96	Y	Y	N	Y	18.8
90	Room 1-143	Pretoria	01/03/96-05/03/96	Y	Y	N	Y	18.8
91	Room 1-145	Pretoria	01/03/96-05/03/96	Y	Y	N	Y	18.8
92	Room 1-7	Pretoria	12/03/96-15/03/96	Y	Y	N	Y	27.0
93	Room 1-7	Pretoria	15/03/96-18/03/96	Y	Y	N	Y	27.0
94	Room 1-9	Pretoria	12/03/96-15/03/96	Y	Y	N	Y	30.5
95	Room 1-9	Pretoria	15/03/96-18/03/96	Y	Y	N	Y	30.5
96	Sasol-e	Secunda	09/09/95-15/09/95	Y	N	Y	Y	683.9
97	Sasol-f	Secunda	23/09/95-29/09/95	N	Y	Y	Y	135.7
98	Sasol-n	Secunda	16/09/95-22/09/95	Y	Y	Y	Y	911.8
99	Sasol-n	Secunda	09/09/95-15/09/95	Y	N	Y	Y	911.8
100	Sasol-s	Secunda	16/09/95-22/09/95	Y	Y	Y	Y	911.8
101	Sasol-s	Secunda	09/09/95-15/09/95	Y	N	Y	Y	911.8
102	Sasol-w	Secunda	16/09/95-22/09/95	Y	Y	Y	Y	683.9
103	Sasol-w	Secunda	09/09/95-15/09/95	Y	N	Y	Y	683.9

Study 1

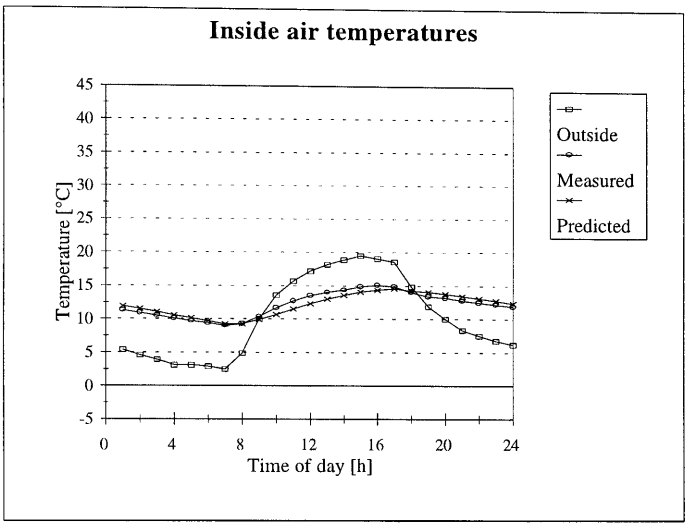

Hour	Measured	Predicted	Hour	Measured	Predicted
1	11.3	11.96	13	14.0	13.02
2	10.9	11.51	14	14.4	13.60
3	10.5	11.04	15	14.9	14.10
4	10.1	10.55	16	15.1	14.40
5	9.7	10.12	17	14.9	14.61
6	9.4	9.70	18	14.0	14.30
7	9.0	9.26	19	13.4	14.08
8	9.3	9.30	20	13.2	13.82
9	10.4	9.90	21	12.8	13.49
10	11.7	10.69	22	12.5	13.15
11	12.7	11.52	23	12.2	12.78
12	13.5	12.31	24	11.9	12.39

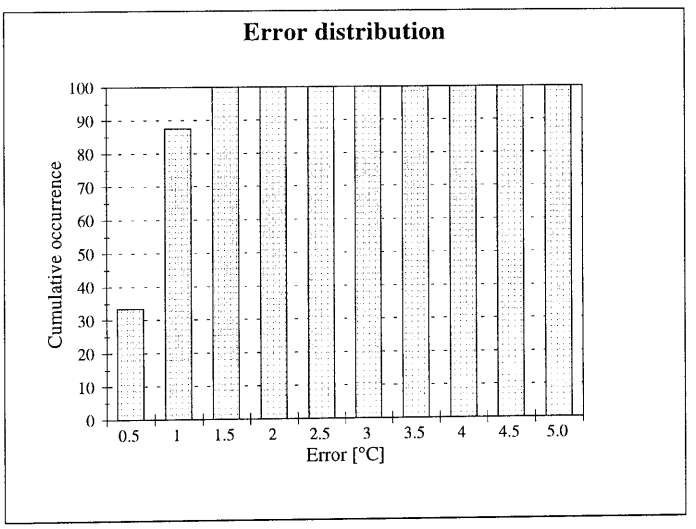

Study 2

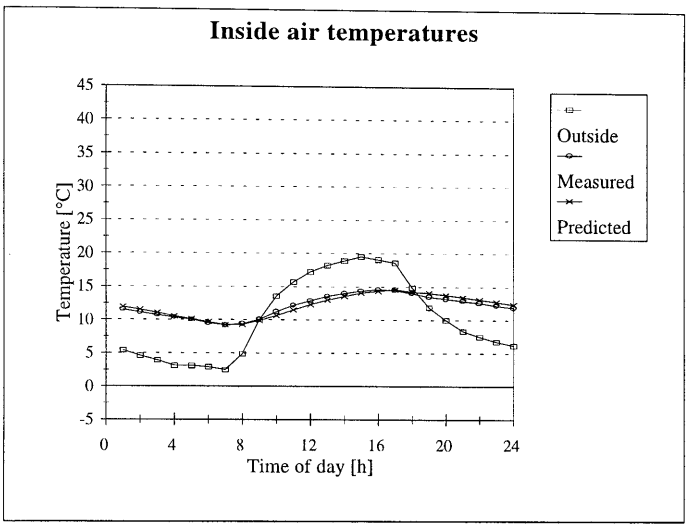

Hour	Measured	Predicted	Hour	Measured	Predicted
1	11.5	11.96	13	13.6	13.02
2	11.1	11.51	14	14.0	13.60
3	10.7	11.04	15	14.4	14.10
4	10.4	10.55	16	14.6	14.40
5	10.0	10.12	17	14.5	14.61
6	9.5	9.70	18	14.0	14.30
7	9.2	9.26	19	13.5	14.08
8	9.4	9.30	20	13.2	13.82
9	10.1	9.90	21	12.9	13.49
10	11.2	10.69	22	12.6	13.15
11	12.2	11.52	23	12.2	12.78
12	12.9	12.31	24	11.9	12.39

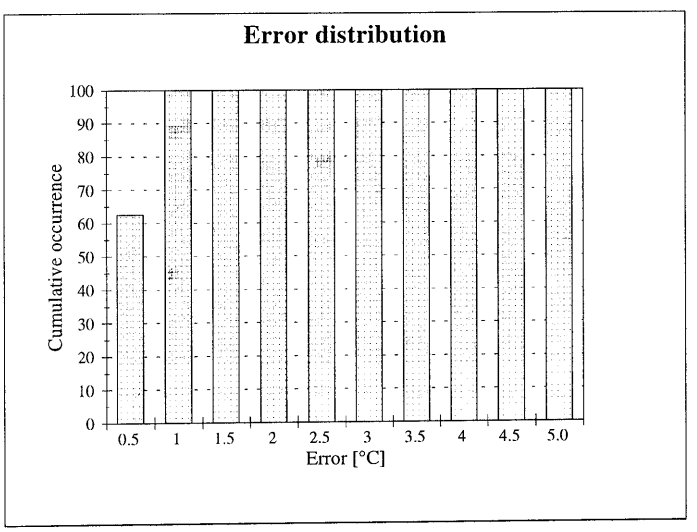

Study 3

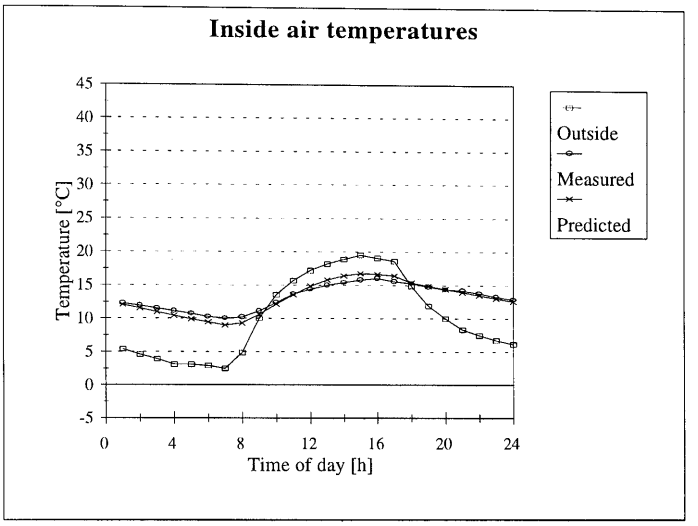

Hour	Measured	Predicted	Hour	Measured	Predicted
1	12.3	12.06	13	15.0	15.84
2	11.9	11.53	14	15.4	16.46
3	11.5	10.99	15	15.8	16.80
4	11.1	10.43	16	16.0	16.66
5	10.7	9.96	17	15.6	16.43
6	10.3	9.49	18	15.3	15.41
7	10.0	9.01	19	14.8	14.89
8	10.2	9.33	20	14.4	14.45
9	11.1	10.61	21	14.2	13.97
10	12.4	12.14	22	13.8	13.52
11	13.7	13.58	23	13.3	13.05
12	14.4	14.87	24	12.9	12.58

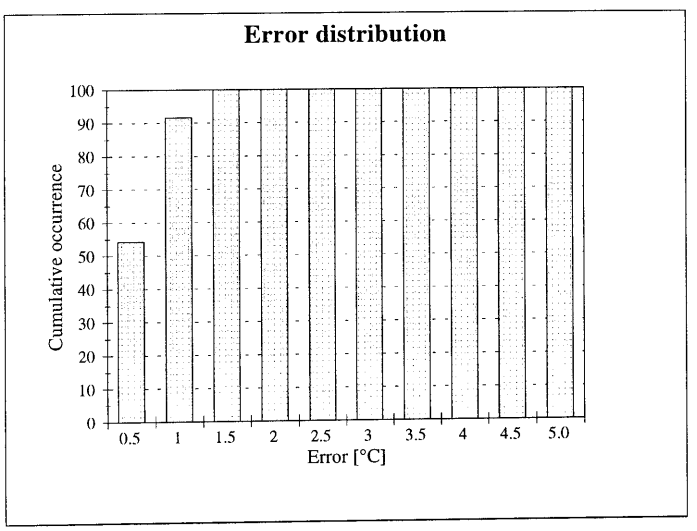

Study 4

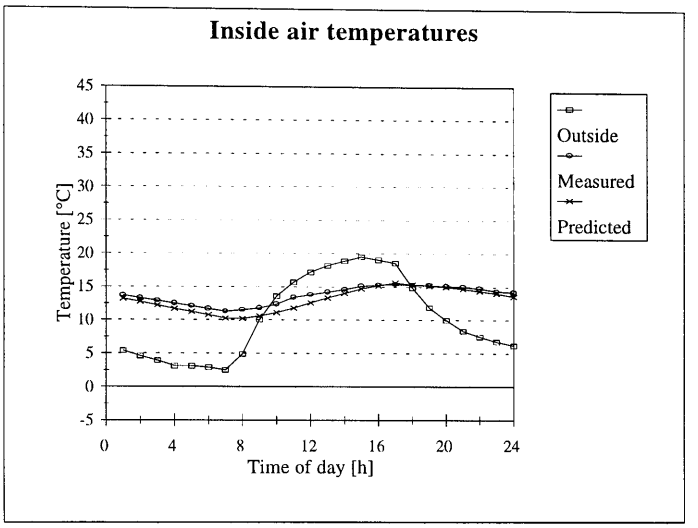

Hour	Measured	Predicted	Hour	Measured	Predicted
1	13.7	13.16	13	14.2	13.33
2	13.3	12.70	14	14.6	14.05
3	12.9	12.21	15	15.1	14.72
4	12.5	11.71	16	15.3	15.21
5	12.1	11.24	17	15.4	15.65
6	11.7	10.77	18	15.3	15.36
7	11.3	10.30	19	15.2	15.23
8	11.5	10.23	20	15.1	15.03
9	11.8	10.59	21	15.0	14.74
10	12.4	11.15	22	14.8	14.40
11	13.4	11.82	23	14.4	14.02
12	13.8	12.58	24	14.2	13.61

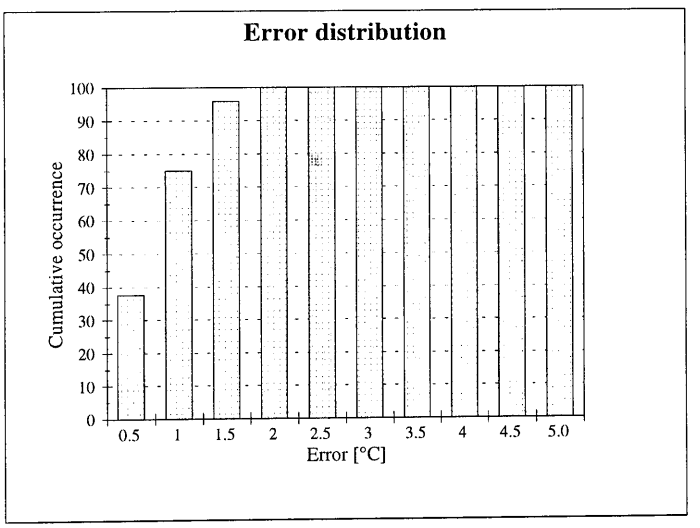

Study 5

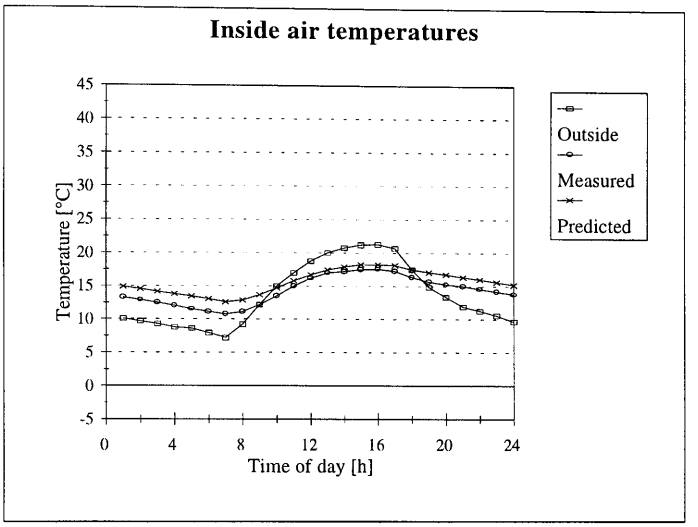

Hour	Measured	Predicted	Hour	Measured	Predicted
1	13.3	14.91	13	17.0	17.47
2	12.9	14.55	14	17.2	17.89
3	12.5	14.18	15	17.5	18.25
4	12.0	13.80	16	17.6	18.28
5	11.5	13.46	17	17.3	18.15
6	11.1	13.05	18	16.4	17.51
7	10.8	12.63	19	15.7	17.11
8	11.1	12.90	20	15.3	16.78
9	12.2	13.68	21	15.0	16.38
10	13.5	14.71	22	14.6	16.03
11	15.0	15.79	23	14.2	15.64
12	16.2	16.72	24	13.8	15.20

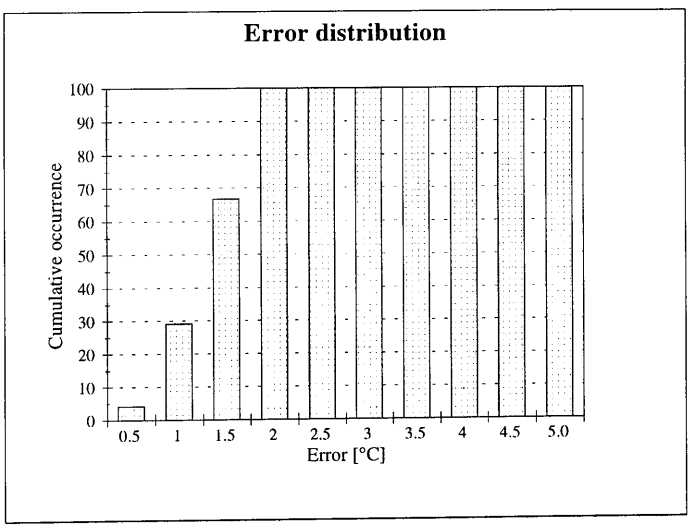

Study 6

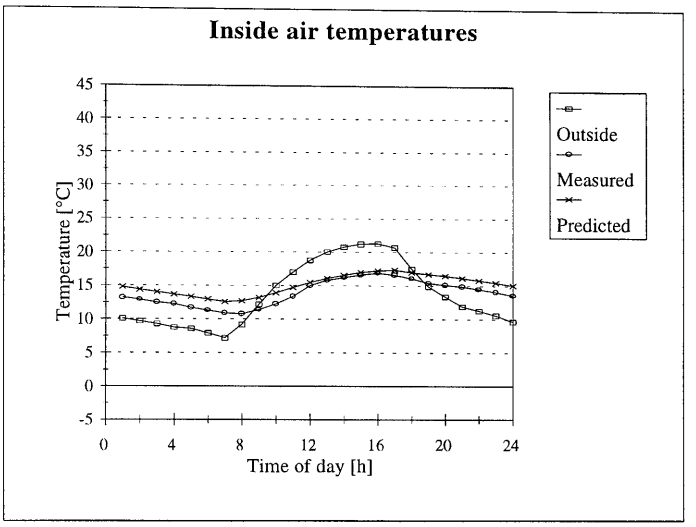

Hour	Measured	Predicted	Hour	Measured	Predicted
1	13.2	14.77	13	15.8	16.09
2	12.9	14.42	14	16.2	16.56
3	12.5	14.07	15	16.6	17.01
4	12.3	13.71	16	16.9	17.26
5	11.7	13.37	17	16.6	17.38
6	11.3	12.99	18	16.1	17.00
7	10.9	12.59	19	15.4	16.73
8	10.8	12.70	20	15.1	16.47
9	11.4	13.20	21	14.9	16.13
10	12.3	13.91	22	14.5	15.81
11	13.4	14.70	23	14.1	15.46
12	15.0	15.44	24	13.6	15.05

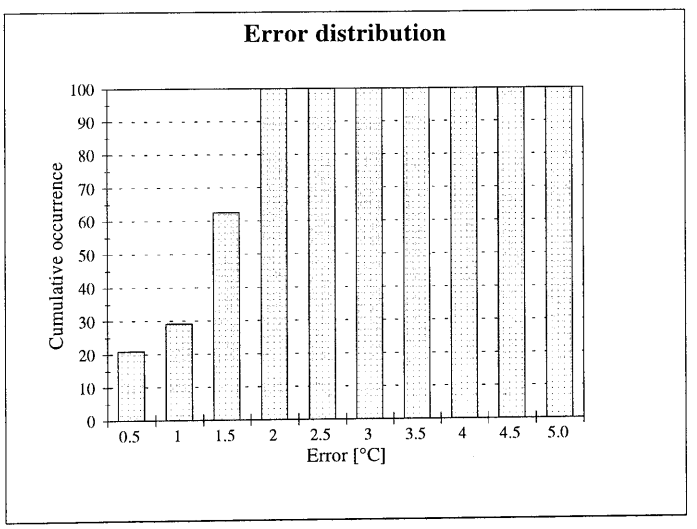

Study 7

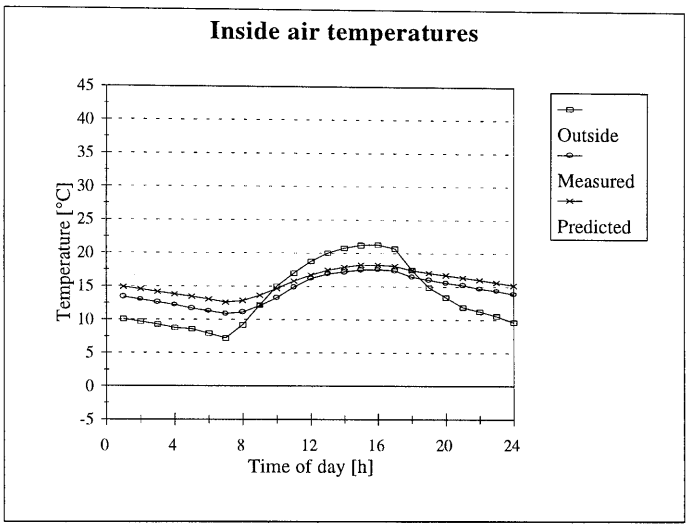

Hour	Measured	Predicted	Hour	Measured	Predicted
1	13.4	14.91	13	16.9	17.49
2	13.0	14.55	14	17.2	17.91
3	12.6	14.18	15	17.5	18.26
4	12.2	13.80	16	17.6	18.25
5	11.7	13.45	17	17.4	18.08
6	11.3	13.05	18	16.5	17.45
7	10.9	12.63	19	16.0	17.06
8	11.1	12.86	20	15.6	16.74
9	12.1	13.63	21	15.2	16.36
10	13.3	14.67	22	14.7	16.02
11	14.9	15.77	23	14.4	15.64
12	16.2	16.73	24	13.9	15.21

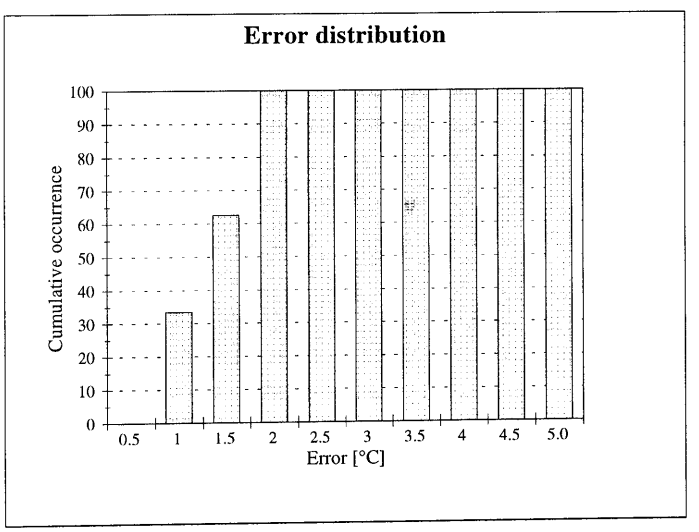

Study 8

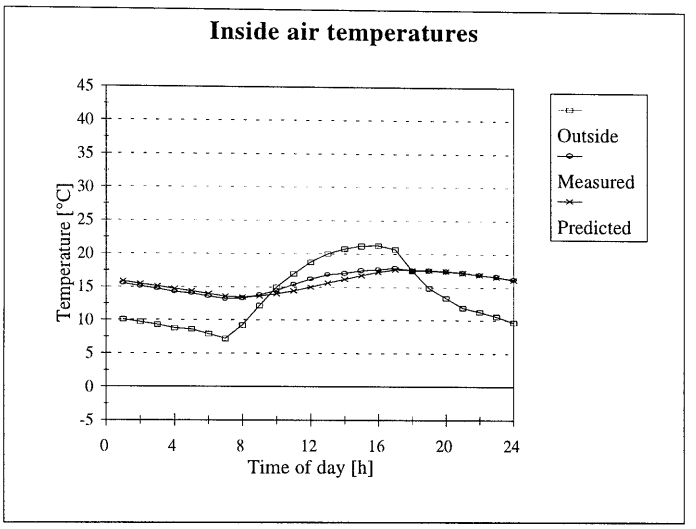

Hour	Measured	Predicted	Hour	Measured	Predicted
1	15.5	15.85	13	16.9	15.63
2	15.1	15.48	14	17.1	16.20
3	14.7	15.10	15	17.5	16.80
4	14.3	14.72	16	17.7	17.29
5	14.0	14.36	17	17.9	17.68
6	13.6	13.97	18	17.6	17.65
7	13.2	13.56	19	17.5	17.60
8	13.3	13.49	20	17.4	17.47
9	13.8	13.64	21	17.2	17.21
10	14.5	13.97	22	16.9	16.92
11	15.4	14.46	23	16.6	16.58
12	16.2	15.03	24	16.2	16.18

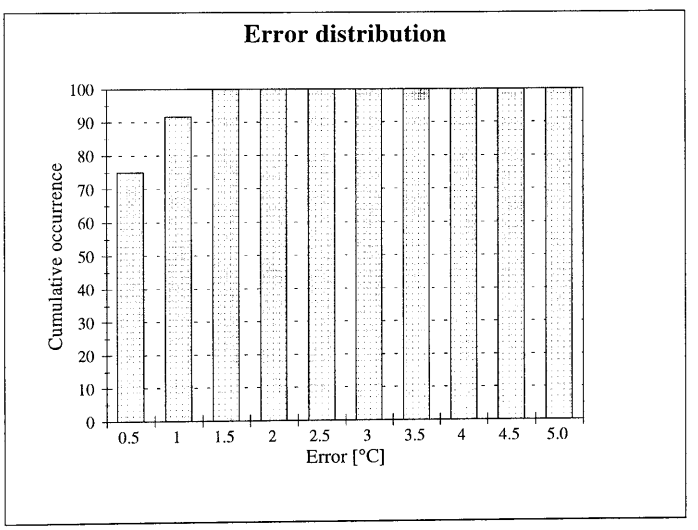

Study 9

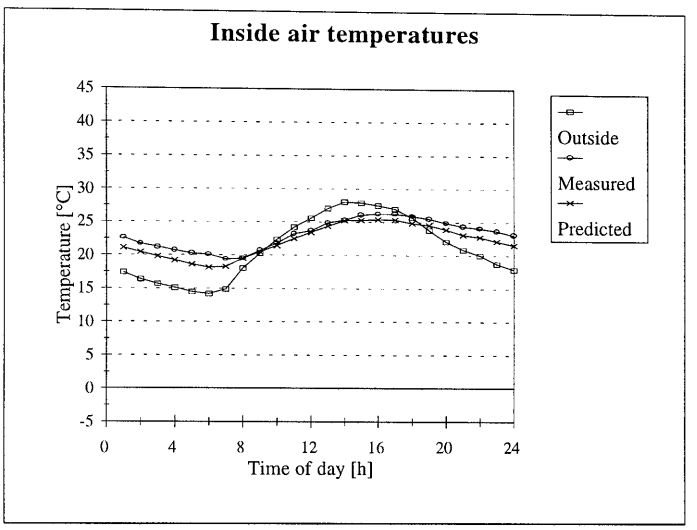

Hour	Measured	Predicted	Hour	Measured	Predicted
1	22.6	21.10	13	24.9	24.42
2	21.7	20.43	14	25.3	25.24
3	21.2	19.82	15	26.1	25.28
4	20.7	19.23	16	26.3	25.41
5	20.3	18.63	17	26.3	25.38
6	20.1	18.16	18	25.9	24.88
7	19.4	18.29	19	25.5	24.54
8	19.5	19.51	20	24.9	23.94
9	20.7	20.47	21	24.4	23.14
10	21.8	21.43	22	24.1	22.79
11	23.2	22.50	23	23.7	22.19
12	23.7	23.44	24	23.1	21.58

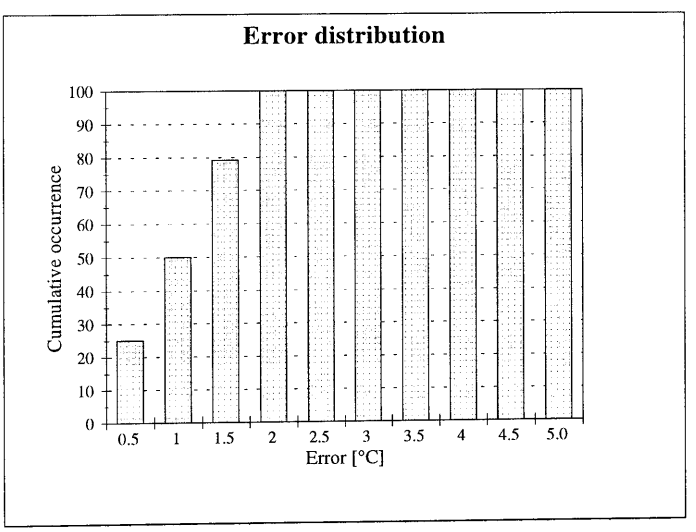

Study 10

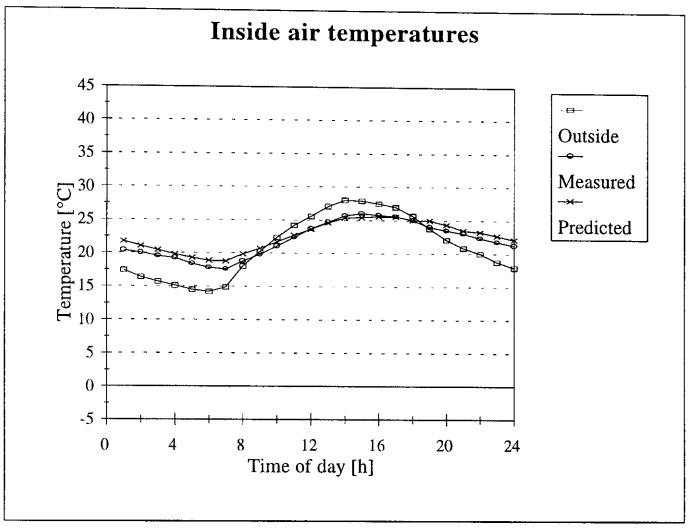

Hour	Measured	Predicted	Hour	Measured	Predicted
1	20.4	21.76	13	24.7	24.60
2	20.0	21.05	14	25.7	25.36
3	19.5	20.44	15	26.0	25.43
4	19.2	19.83	16	25.8	25.57
5	18.4	19.29	17	25.6	25.54
6	17.8	18.86	18	25.1	25.04
7	17.6	18.79	19	24.0	25.01
8	18.8	19.88	20	23.5	24.39
9	19.8	20.75	21	23.1	23.52
10	21.1	21.70	22	22.4	23.29
11	22.4	22.76	23	21.8	22.76
12	23.7	23.63	24	21.3	22.17

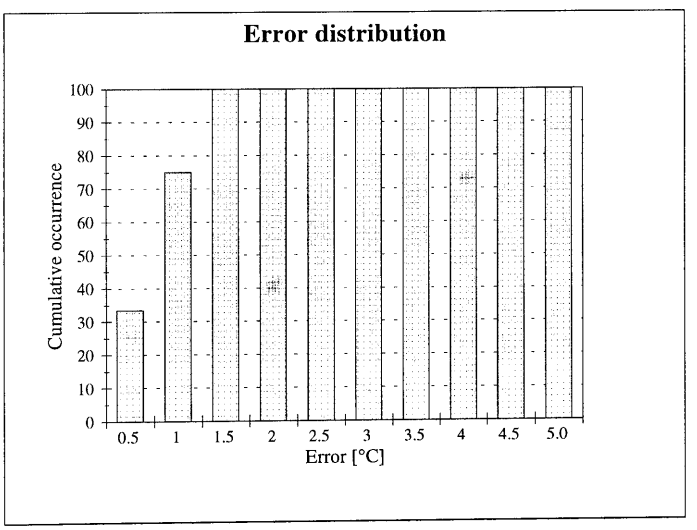

Study 11

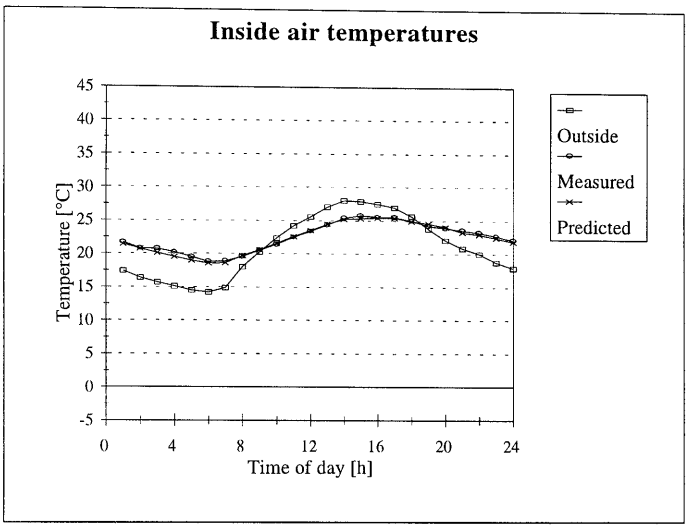

Hour	Measured	Predicted	Hour	Measured	Predicted
1	21.7	21.39	13	24.4	24.50
2	20.8	20.76	14	25.4	25.26
3	20.7	20.11	15	25.8	25.35
4	20.2	19.53	16	25.6	25.49
5	19.5	18.97	17	25.5	25.44
6	18.8	18.54	18	25.0	24.95
7	18.9	18.59	19	24.3	24.65
8	19.6	19.66	20	23.9	24.09
9	20.5	20.60	21	23.6	23.30
10	21.4	21.55	22	23.2	22.99
11	22.5	22.62	23	22.7	22.44
12	23.4	23.53	24	22.1	21.87

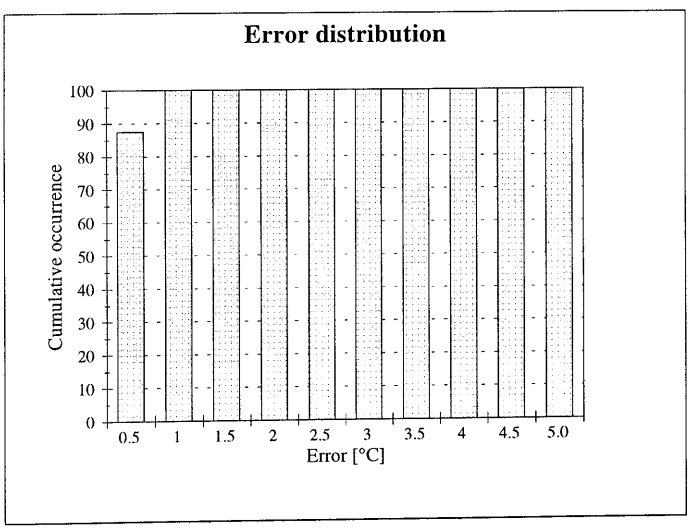

Study 12

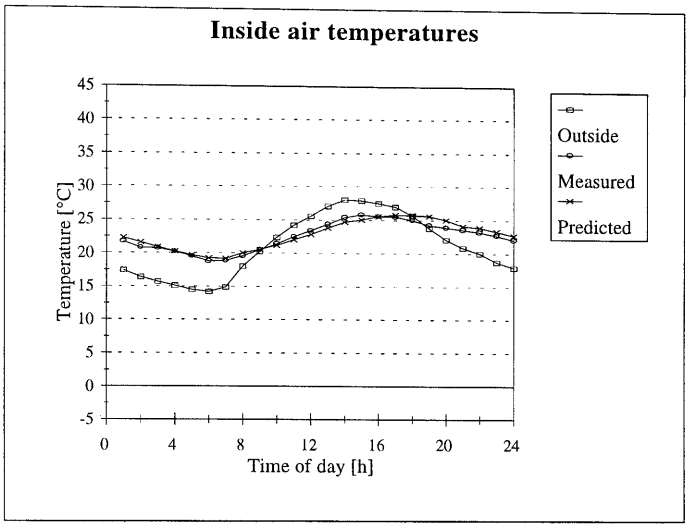

Hour	Measured	Predicted	Hour	Measured	Predicted
1	21.7	22.24	13	24.4	23.84
2	20.8	21.58	14	25.4	24.73
3	20.7	20.90	15	25.8	25.07
4	20.2	20.29	16	25.6	25.54
5	19.5	19.70	17	25.5	25.83
6	18.8	19.25	18	25.0	25.74
7	18.9	19.18	19	24.3	25.63
8	19.6	20.00	20	23.9	25.05
9	20.5	20.55	21	23.6	24.16
10	21.4	21.16	22	23.2	23.90
11	22.5	22.02	23	22.7	23.35
12	23.4	22.82	24	22.1	22.75

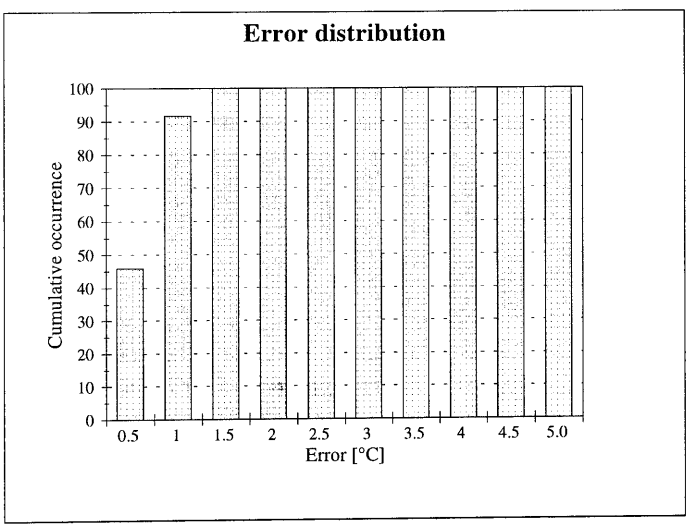

Study 13

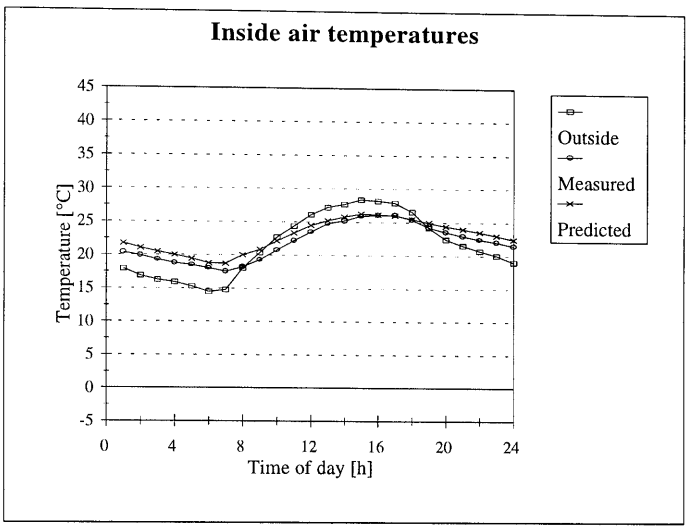

Hour	Measured	Predicted	Hour	Measured	Predicted
1	20.4	21.74	13	24.8	25.23
2	19.9	21.06	14	25.2	25.82
3	19.3	20.49	15	25.9	26.24
4	18.8	20.03	16	26.1	26.18
5	18.5	19.45	17	26.1	26.02
6	18.0	18.77	18	25.4	25.51
7	17.5	18.71	19	24.3	24.98
8	18.2	20.07	20	23.6	24.44
9	19.3	20.85	21	23.0	24.00
10	20.8	22.19	22	22.5	23.58
11	22.2	23.35	23	22.1	23.06
12	23.5	24.49	24	21.5	22.47

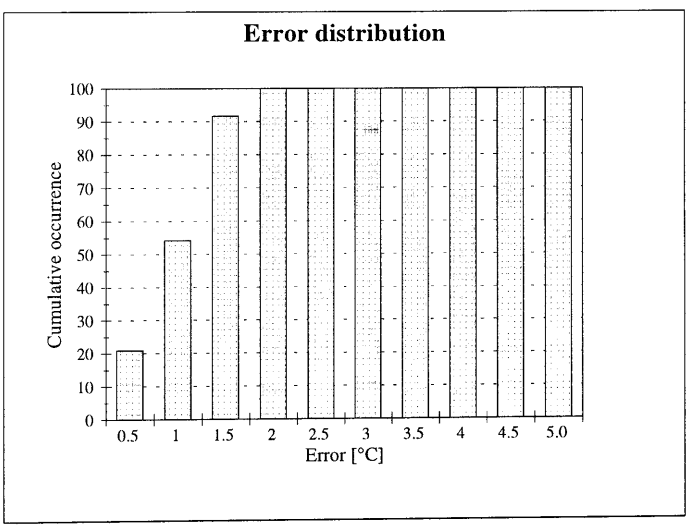

Study 14

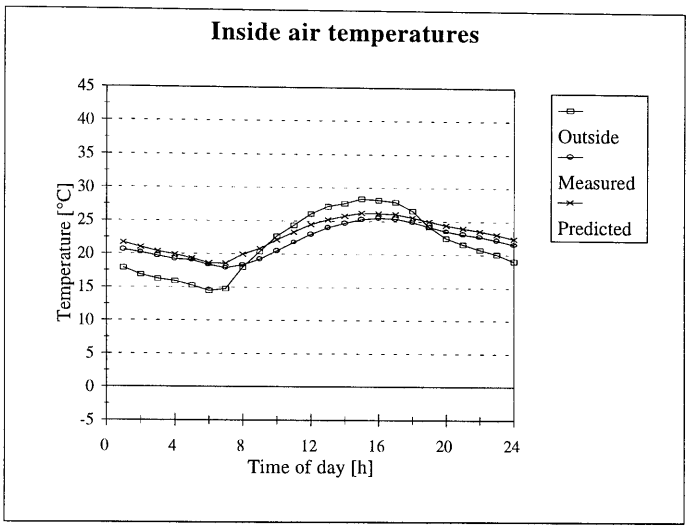

Hour	Measured	Predicted	Hour	Measured	Predicted
1	20.6	21.71	13	24.0	25.25
2	20.2	21.01	14	24.7	25.84
3	19.7	20.41	15	25.3	26.27
4	19.2	19.96	16	25.5	26.21
5	19.1	19.34	17	25.4	26.08
6	18.4	18.68	18	24.9	25.55
7	17.9	18.62	19	24.2	25.00
8	18.4	19.99	20	23.5	24.46
9	19.2	20.83	21	23.1	23.99
10	20.5	22.17	22	22.7	23.56
11	21.8	23.34	23	22.2	23.04
12	23.0	24.49	24	21.6	22.45

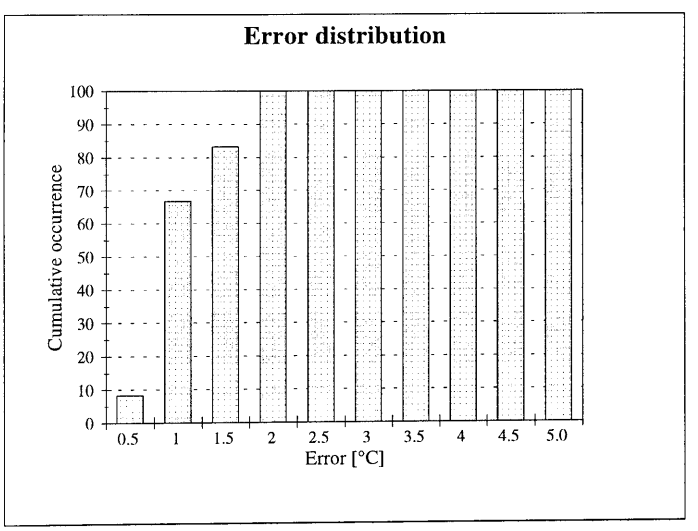

Study 15

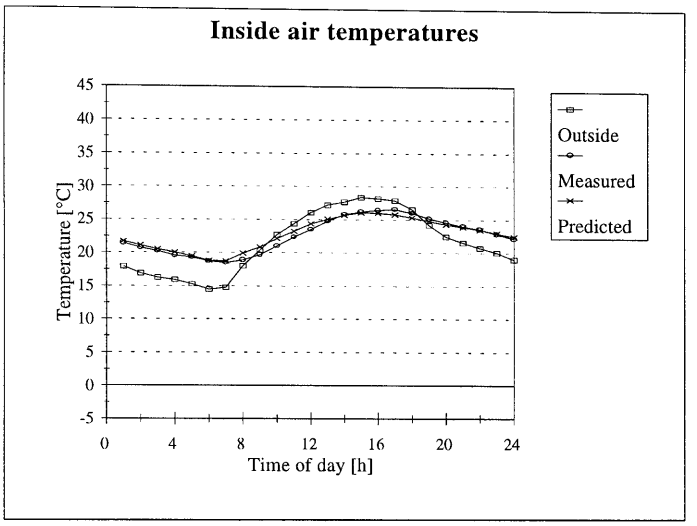

Hour	Measured	Predicted	Hour	Measured	Predicted
1	21.4	21.73	13	24.8	25.11
2	20.7	21.09	14	25.8	25.68
3	20.2	20.50	15	26.2	26.08
4	19.6	20.06	16	26.5	26.00
5	19.3	19.49	17	26.6	25.83
6	18.7	18.83	18	26.0	25.35
7	18.5	18.71	19	25.2	24.87
8	18.9	19.95	20	24.6	24.33
9	19.7	20.83	21	24.0	23.92
10	21.0	22.13	22	23.6	23.50
11	22.4	23.26	23	22.9	23.02
12	23.5	24.38	24	22.2	22.47

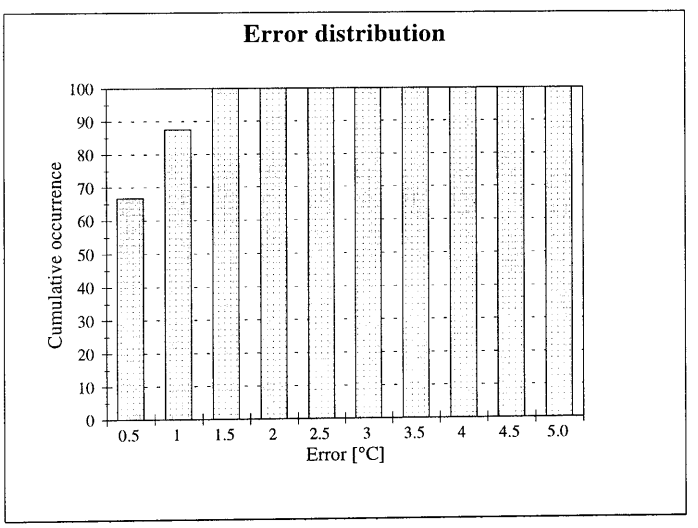

Study 16

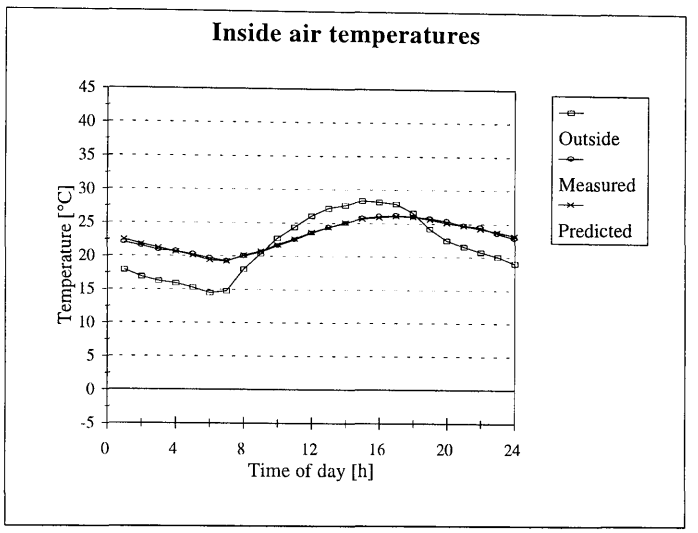

Hour	Measured	Predicted	Hour	Measured	Predicted
1	22.0	22.47	13	24.4	24.37
2	21.5	21.79	14	25.0	25.15
3	20.9	21.20	15	25.8	25.72
4	20.7	20.68	16	26.1	25.94
5	20.3	20.08	17	26.2	26.12
6	19.7	19.41	18	26.0	26.01
7	19.3	19.24	19	25.8	25.65
8	20.0	20.18	20	25.4	25.14
9	20.6	20.77	21	24.8	24.72
10	21.6	21.75	22	24.5	24.28
11	22.5	22.66	23	23.6	23.79
12	23.5	23.65	24	22.9	23.21

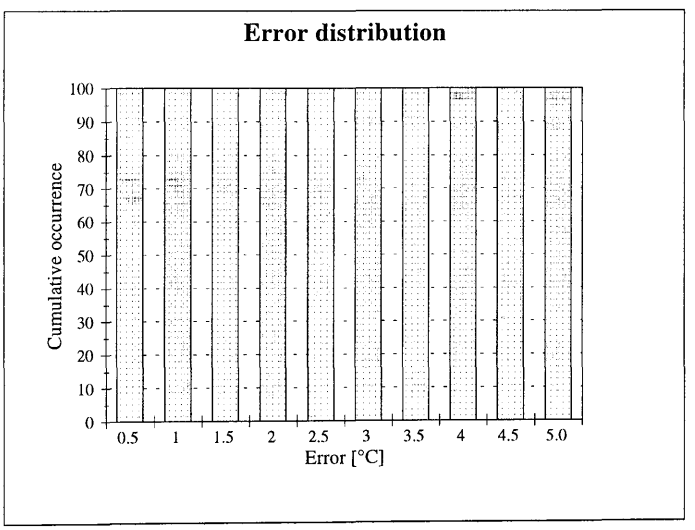

Study 17

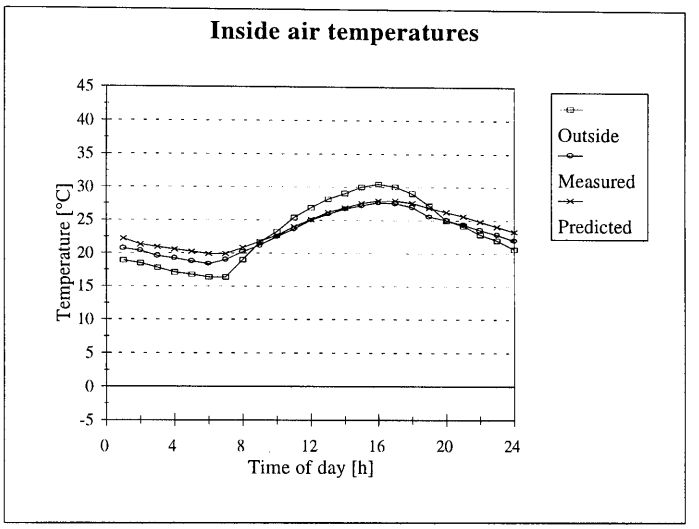

Hour	Measured	Predicted	Hour	Measured	Predicted
1	20.7	22.20	13	25.9	26.20
2	20.4	21.31	14	26.7	26.90
3	19.6	20.95	15	27.2	27.59
4	19.2	20.60	16	27.7	27.97
5	18.8	20.28	17	27.6	27.97
6	18.4	19.92	18	27.0	27.64
7	19.0	19.89	19	25.6	26.91
8	20.2	20.85	20	25.1	26.27
9	21.2	21.82	21	24.4	25.63
10	22.5	22.73	22	23.6	24.81
11	23.7	24.00	23	22.9	24.10
12	25.0	25.15	24	22.0	23.36

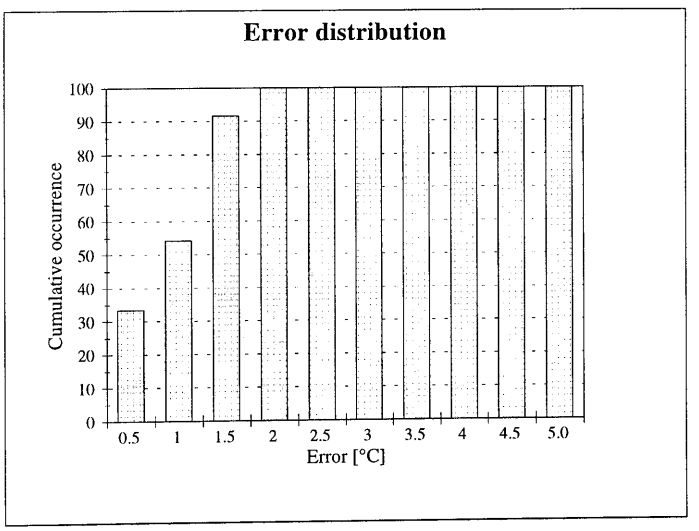

Study 18

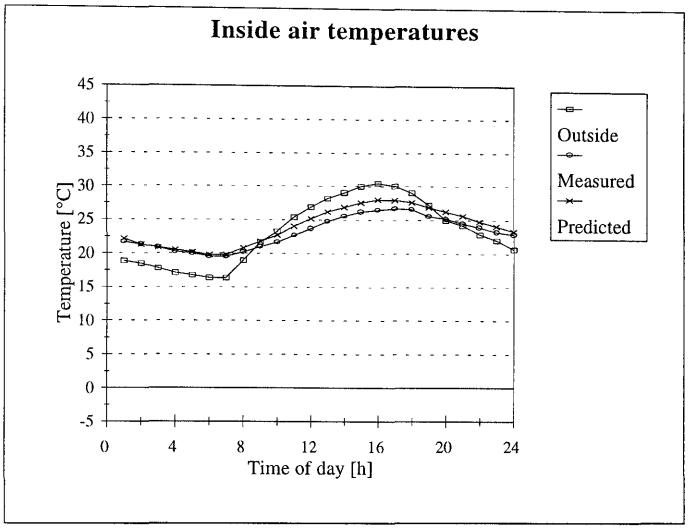

Hour	Measured	Predicted	Hour	Measured	Predicted
1	21.7	22.16	13	24.8	26.21
2	21.3	21.29	14	25.6	26.92
3	20.9	20.90	15	26.2	27.60
4	20.3	20.54	16	26.5	28.00
5	20.0	20.20	17	26.7	27.98
6	19.6	19.83	18	26.6	27.65
7	19.6	19.82	19	25.6	26.91
8	20.2	20.83	20	25.2	26.26
9	21.0	21.81	21	24.5	25.63
10	21.7	22.73	22	23.9	24.80
11	22.7	24.00	23	23.2	24.09
12	23.7	25.16	24	22.9	23.34

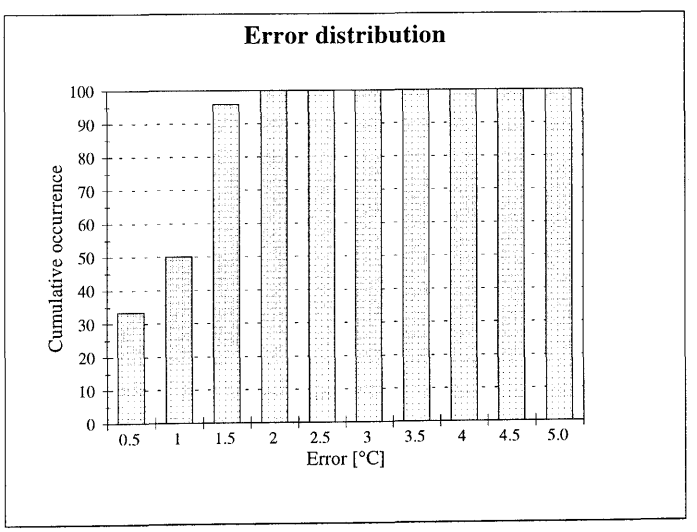

Study 19

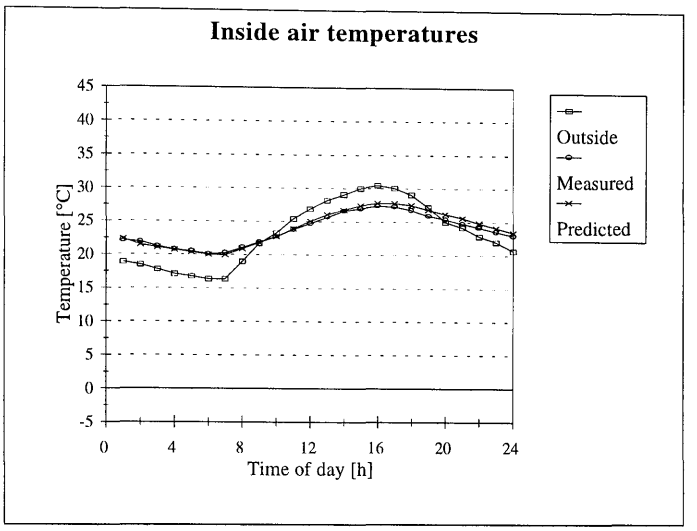

Hour	Measured	Predicted	Hour	Measured	Predicted
1	22.1	22.33	13	25.7	26.08
2	21.9	21.47	14	26.6	26.77
3	21.2	21.09	15	27.0	27.43
4	20.8	20.73	16	27.4	27.80
5	20.5	20.38	17	27.3	27.80
6	20.1	20.01	18	26.8	27.51
7	20.3	19.97	19	25.9	26.82
8	21.1	20.90	20	25.4	26.22
9	21.9	21.84	21	24.8	25.63
10	22.7	22.72	22	24.2	24.85
11	23.8	23.93	23	23.6	24.17
12	24.7	25.06	24	23.0	23.46

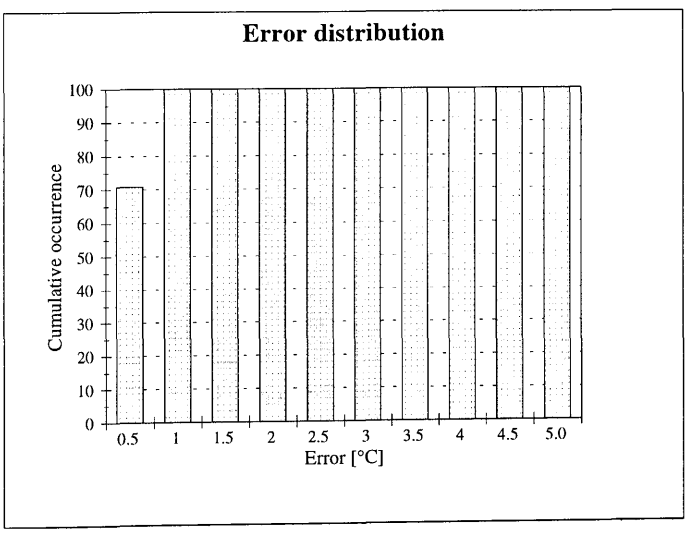

Study 20

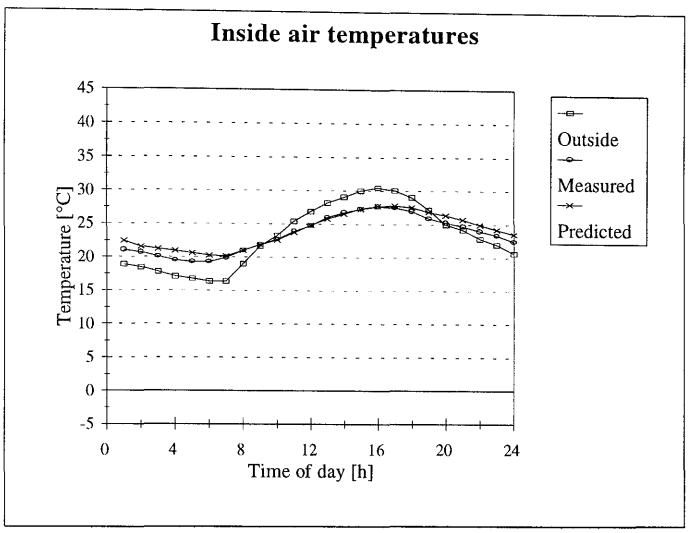

Hour	Measured	Predicted	Hour	Measured	Predicted
1	21.1	22.44	13	26.0	25.84
2	20.7	21.56	14	26.8	26.55
3	20.1	21.22	15	27.3	27.31
4	19.5	20.93	16	27.7	27.75
5	19.3	20.61	17	27.5	27.81
6	19.3	20.25	18	27.0	27.57
7	19.9	20.18	19	25.9	26.92
8	21.0	21.03	20	25.3	26.35
9	21.9	21.85	21	24.7	25.74
10	22.7	22.61	22	24.0	24.95
11	23.9	23.75	23	23.4	24.26
12	24.8	24.83	24	22.5	23.56

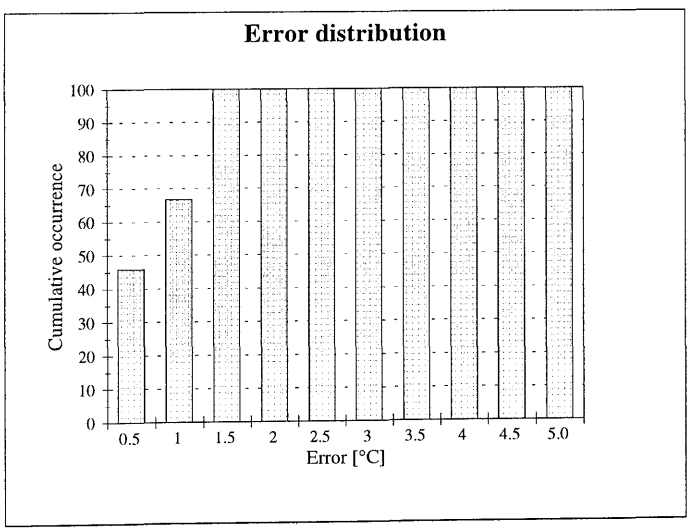

Study 21

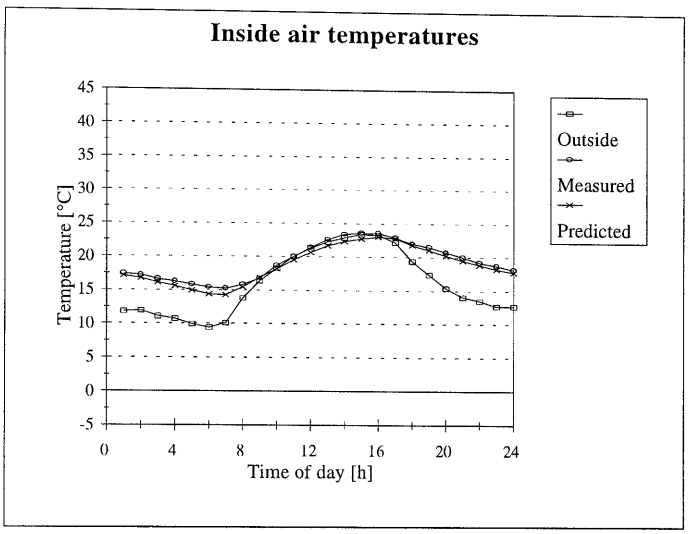

Hour	Measured	Predicted	Hour	Measured	Predicted
1	17.4	17.13	13	22.6	21.69
2	17.2	16.73	14	23.4	22.31
3	16.6	16.10	15	23.6	22.72
4	16.3	15.57	16	23.6	23.00
5	15.8	14.94	17	22.9	22.84
6	15.4	14.38	18	22.0	21.81
7	15.2	14.25	19	21.5	21.09
8	15.8	15.48	20	20.8	20.26
9	16.8	16.92	21	20.0	19.51
10	18.7	18.23	22	19.2	18.92
11	20.0	19.52	23	18.8	18.25
12	21.4	20.68	24	18.2	17.81

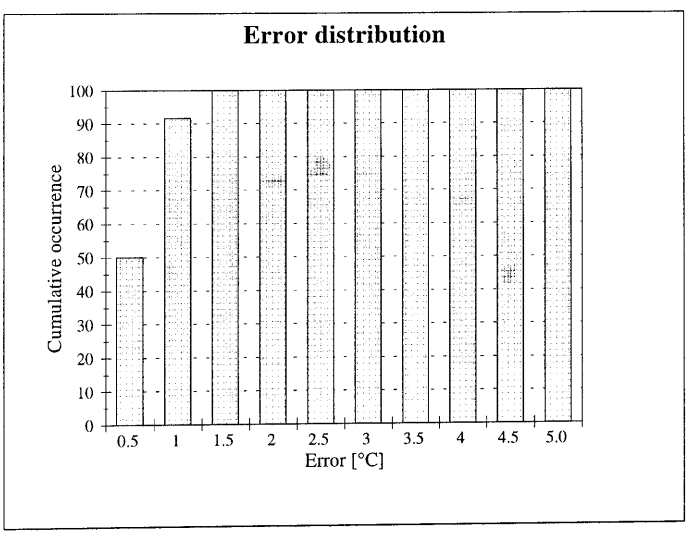

Study 22

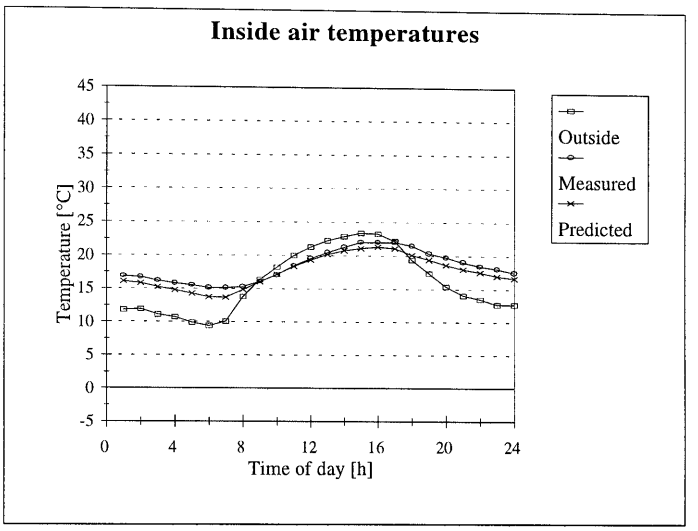

Hour	Measured	Predicted	Hour	Measured	Predicted
1	16.9	16.09	13	20.5	20.23
2	16.7	15.78	14	21.3	20.77
3	16.2	15.24	15	22.0	21.14
4	15.8	14.80	16	22.0	21.38
5	15.5	14.24	17	22.0	21.12
6	15.1	13.75	18	21.5	20.16
7	15.1	13.67	19	20.4	19.44
8	15.3	14.88	20	19.8	18.69
9	16.1	16.04	21	19.1	18.05
10	17.1	17.19	22	18.5	17.56
11	18.5	18.35	23	18.1	17.01
12	19.6	19.37	24	17.5	16.67

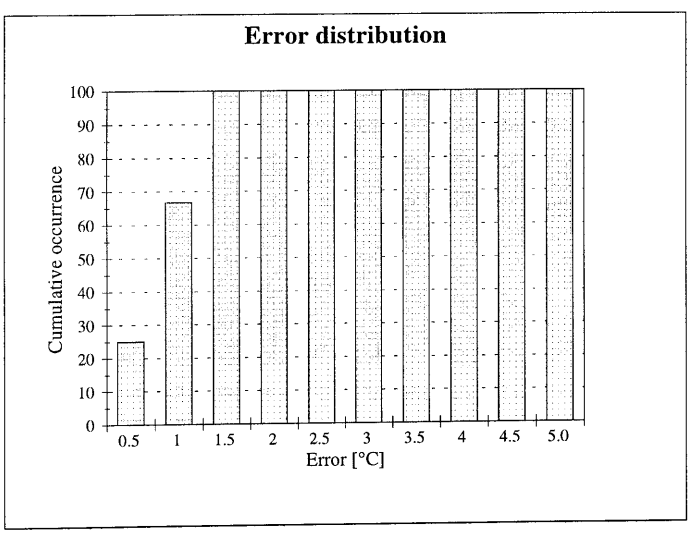

Study 23

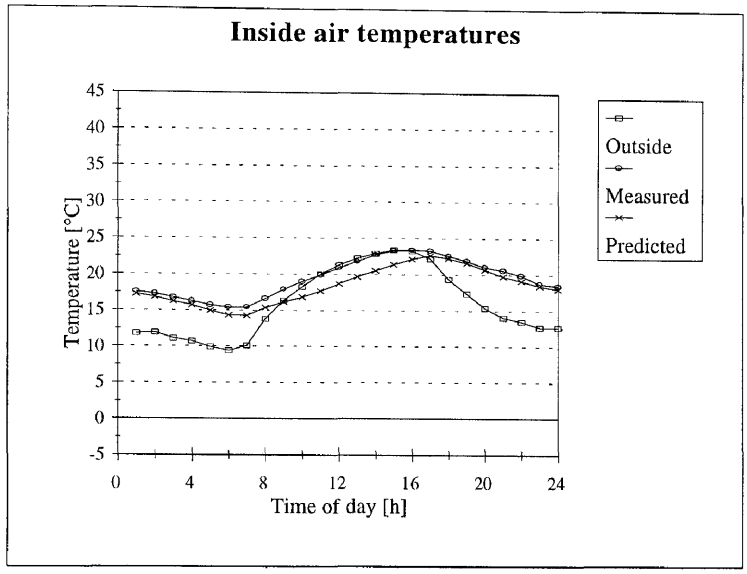

Hour	Measured	Predicted	Hour	Measured	Predicted
1	17.6	17.24	13	21.8	19.69
2	17.3	16.83	14	22.7	20.57
3	16.8	16.22	15	23.3	21.42
4	16.3	15.67	16	23.4	22.18
5	15.7	14.95	17	23.3	22.68
6	15.4	14.32	18	22.6	22.26
7	15.4	14.25	19	21.9	21.63
8	16.6	15.35	20	21.1	20.70
9	17.9	16.15	21	20.6	19.83
10	19.0	16.87	22	19.9	19.19
11	19.9	17.67	23	18.8	18.48
12	20.9	18.74	24	18.5	18.05

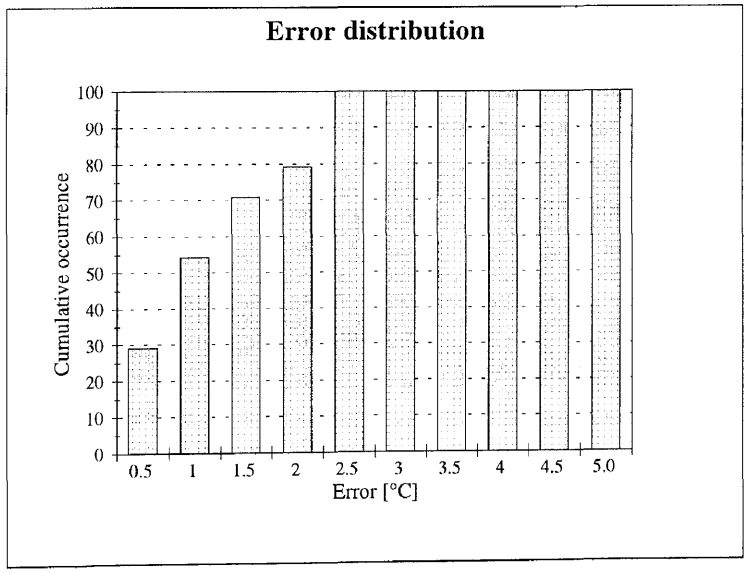

Study 24

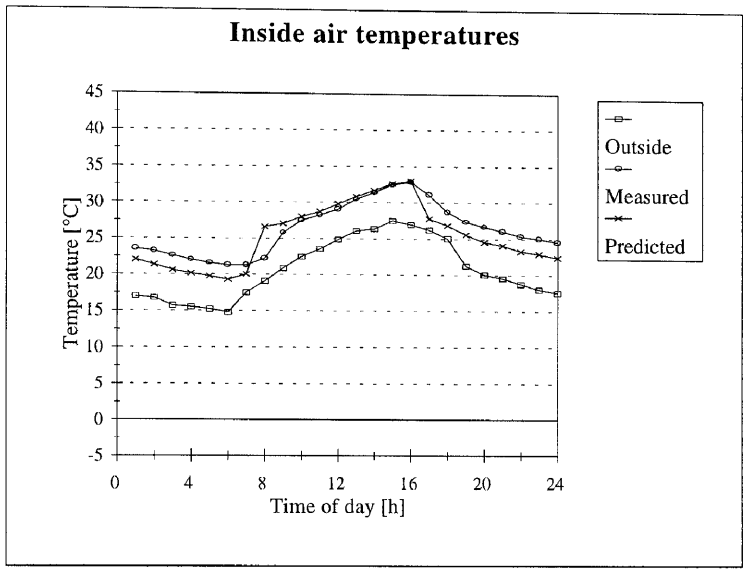

Hour	Measured	Predicted	Hour	Measured	Predicted
1	23.6	22.01	13	30.5	30.88
2	23.2	21.35	14	31.4	31.68
3	22.6	20.62	15	32.5	32.67
4	22.0	20.12	16	32.9	33.03
5	21.6	19.74	17	31.1	27.79
6	21.3	19.29	18	28.7	26.92
7	21.3	20.05	19	27.4	25.63
8	22.2	26.62	20	26.7	24.62
9	25.8	27.06	21	26.1	24.18
10	27.5	28.07	22	25.4	23.32
11	28.3	28.75	23	25.1	22.98
12	29.1	29.77	24	24.6	22.44

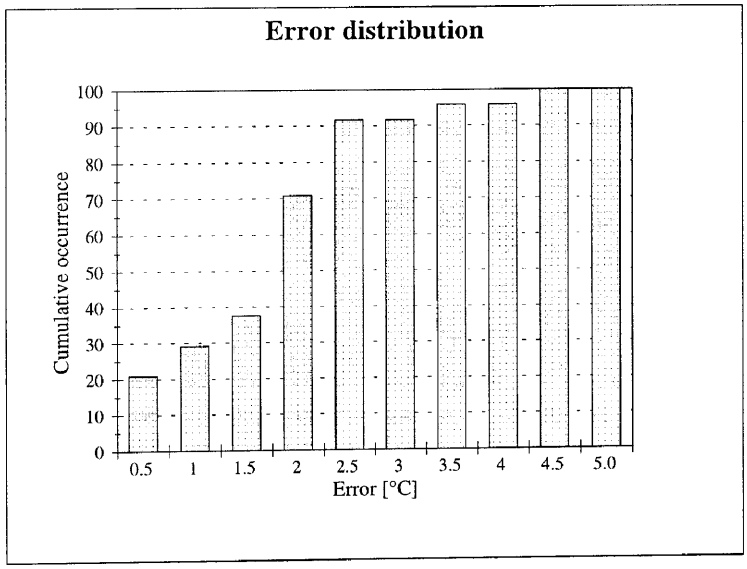

Study 25

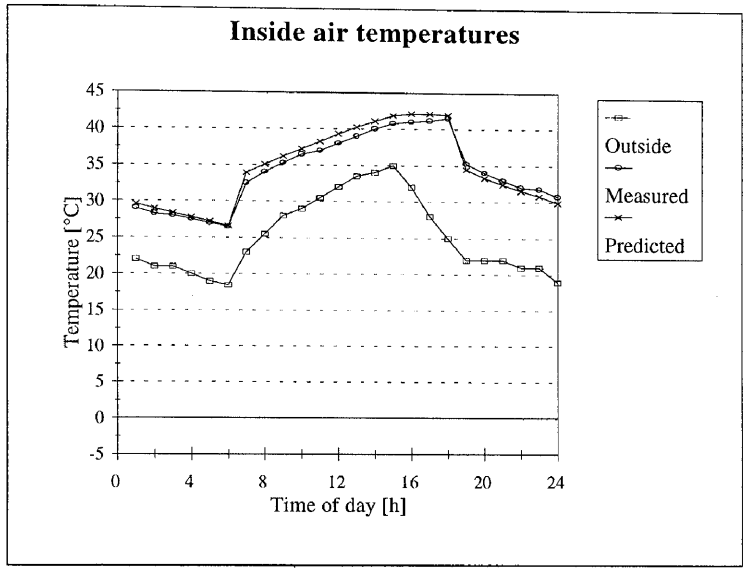

Hour	Measured	Predicted	Hour	Measured	Predicted
1	29.0	29.58	13	39.0	40.28
2	28.3	28.95	14	40.0	41.08
3	28.0	28.42	15	40.8	41.87
4	27.5	27.82	16	41.0	42.19
5	27.0	27.20	17	41.2	42.15
6	26.5	26.63	18	41.5	41.97
7	32.5	33.89	19	35.3	34.48
8	34.0	35.09	20	34.0	33.32
9	35.3	36.22	21	33.0	32.43
10	36.5	37.24	22	32.0	31.56
11	37.0	38.28	23	31.8	30.84
12	38.0	39.31	24	30.8	29.96

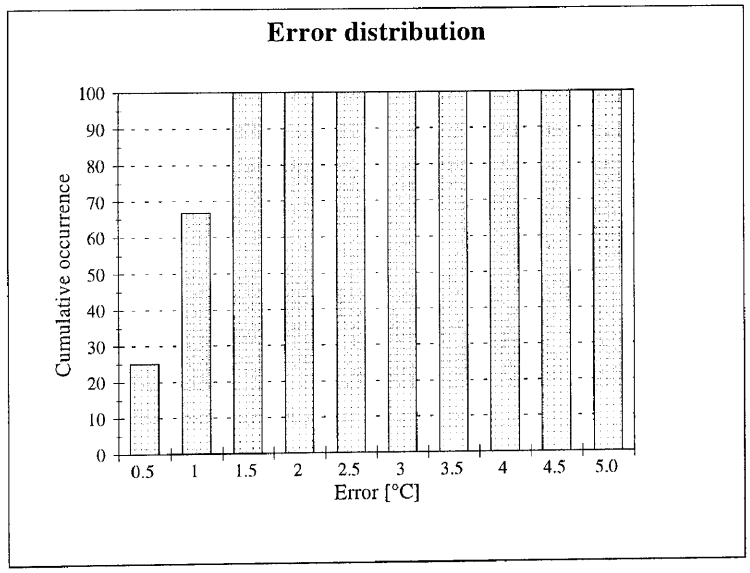

Study 26

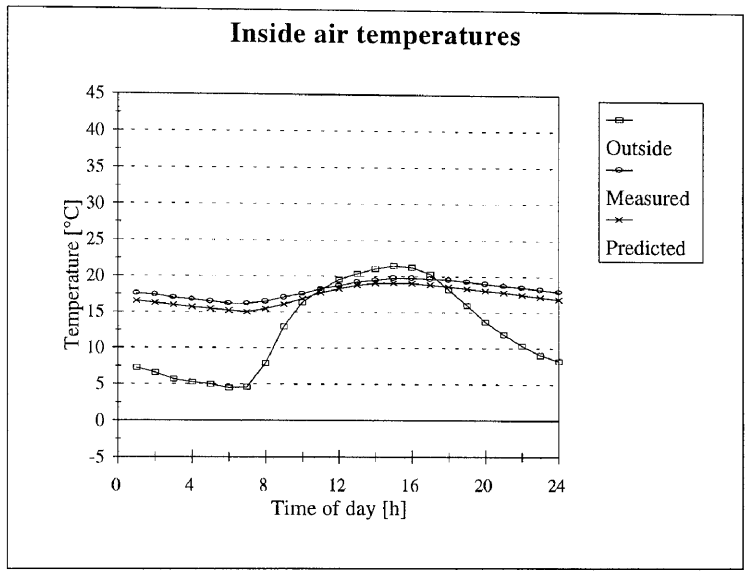

Hour	Measured	Predicted	Hour	Measured	Predicted
1	17.6	16.56	13	19.2	18.79
2	17.4	16.27	14	19.5	19.10
3	17.0	15.99	15	19.8	19.12
4	16.8	15.72	16	19.8	19.06
5	16.5	15.46	17	19.7	18.88
6	16.2	15.22	18	19.6	18.59
7	16.2	15.02	19	19.3	18.34
8	16.5	15.47	20	19.0	18.06
9	17.1	16.10	21	18.7	17.77
10	17.6	16.89	22	18.5	17.47
11	18.3	17.67	23	18.2	17.16
12	18.7	18.30	24	17.9	16.86

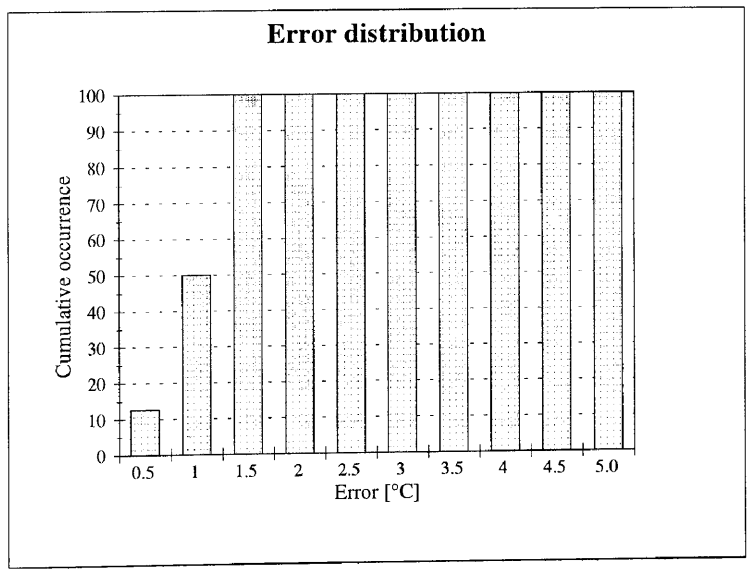

Study 27

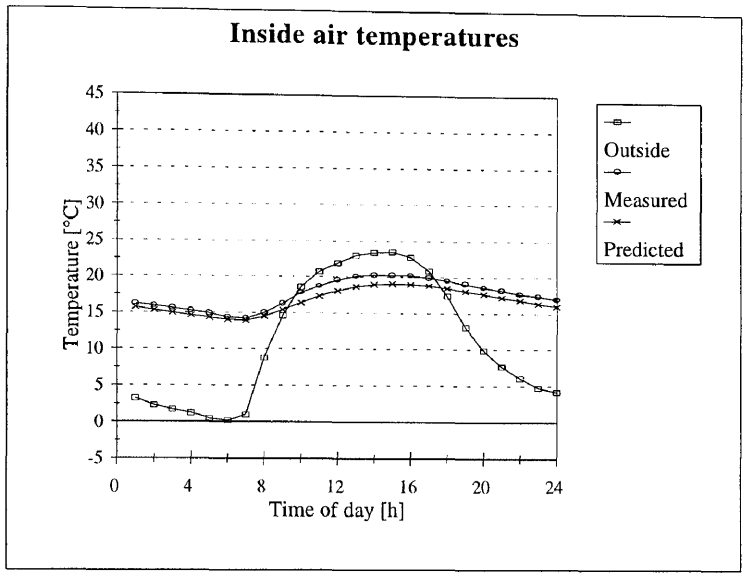

Hour	Measured	Predicted	Hour	Measured	Predicted
1	16.2	15.66	13	20.1	18.66
2	15.9	15.30	14	20.3	18.97
3	15.6	14.96	15	20.3	19.10
4	15.2	14.64	16	20.2	19.02
5	14.9	14.32	17	19.9	18.81
6	14.4	14.03	18	19.5	18.48
7	14.2	13.91	19	19.1	18.10
8	15.0	14.48	20	18.6	17.68
9	16.3	15.41	21	18.2	17.25
10	17.8	16.40	22	17.7	16.83
11	18.7	17.31	23	17.4	16.42
12	19.6	18.08	24	17.0	16.04

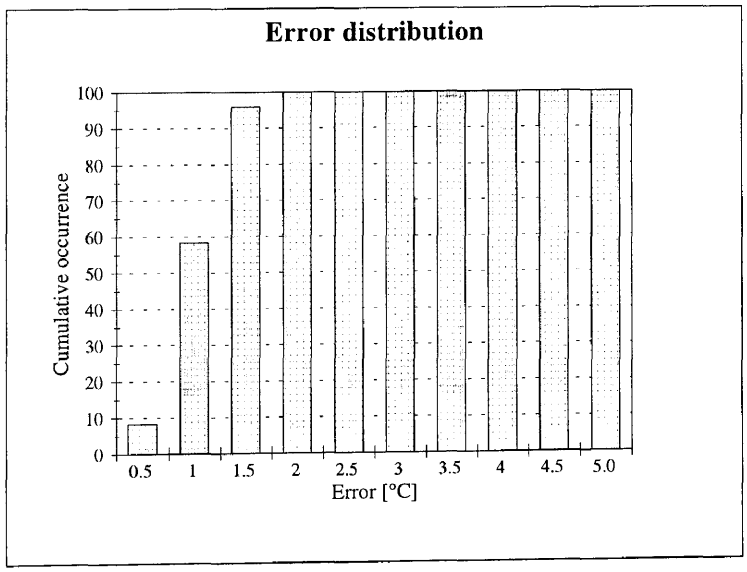

Study 28

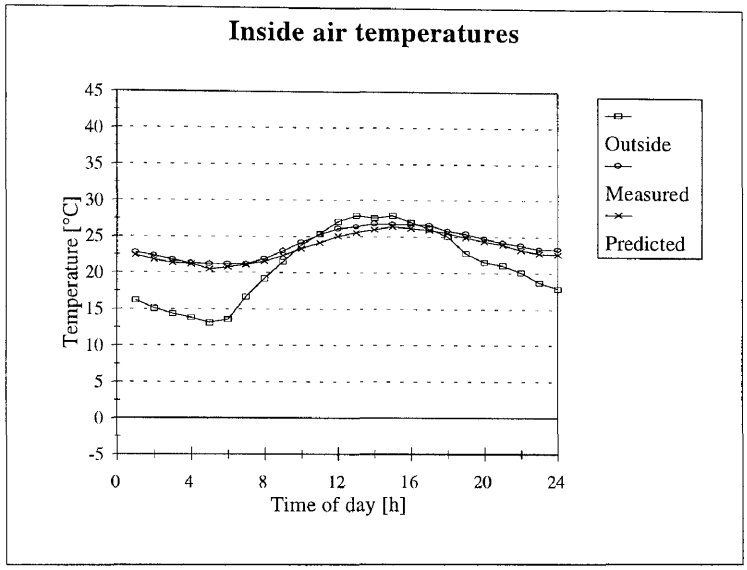

Hour	Measured	Predicted	Hour	Measured	Predicted
1	22.8	22.46	13	26.4	25.58
2	22.4	21.77	14	26.8	25.98
3	21.8	21.35	15	26.7	26.37
4	21.3	21.22	16	26.7	26.19
5	21.2	20.50	17	26.6	25.93
6	21.2	20.77	18	25.8	25.50
7	21.2	21.13	19	25.4	24.91
8	21.9	21.57	20	24.8	24.39
9	23.0	22.42	21	24.2	23.92
10	24.2	23.32	22	23.8	23.19
11	25.3	24.13	23	23.3	22.73
12	26.1	25.09	24	23.3	22.60

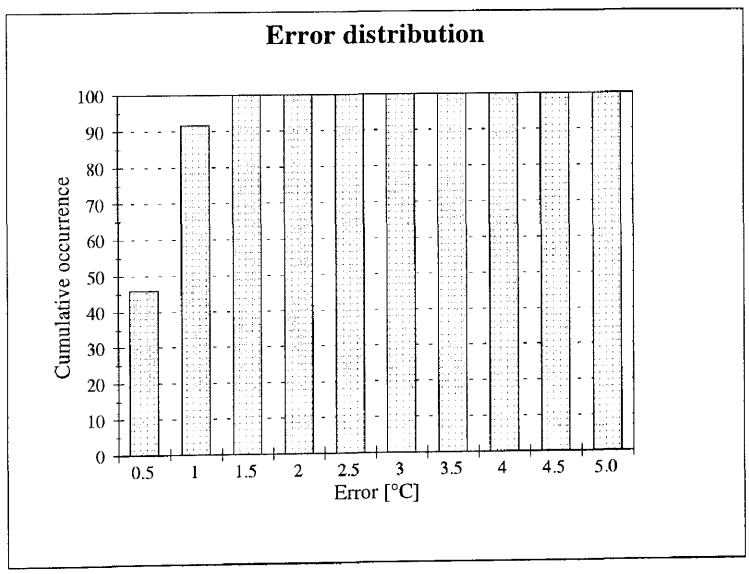

Study 29

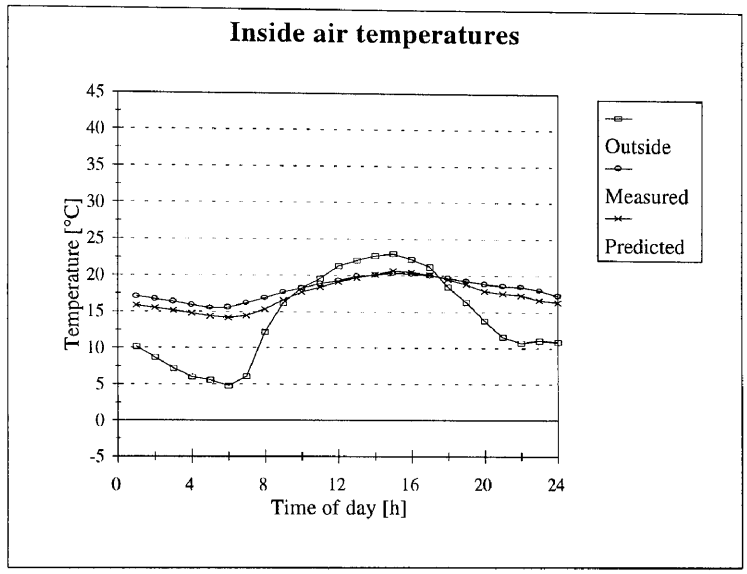

Hour	Measured	Predicted	Hour	Measured	Predicted
1	17.1	15.86	13	19.9	19.73
2	16.7	15.53	14	20.1	20.12
3	16.4	15.16	15	20.4	20.66
4	15.9	14.79	16	20.3	20.49
5	15.5	14.41	17	20.0	20.19
6	15.6	14.15	18	19.7	19.50
7	16.2	14.46	19	19.3	18.86
8	16.9	15.32	20	18.9	17.96
9	17.7	16.64	21	18.6	17.61
10	18.3	17.66	22	18.5	17.32
11	18.9	18.40	23	18.0	16.67
12	19.3	19.15	24	17.3	16.35

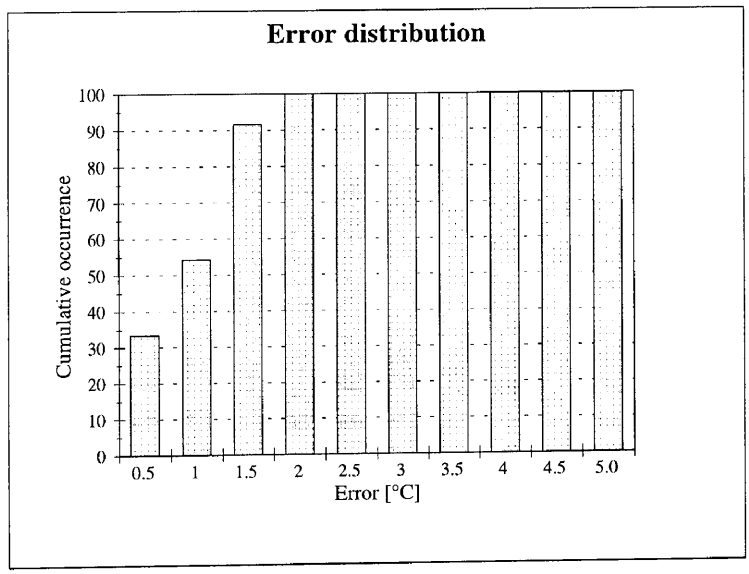

Study 30

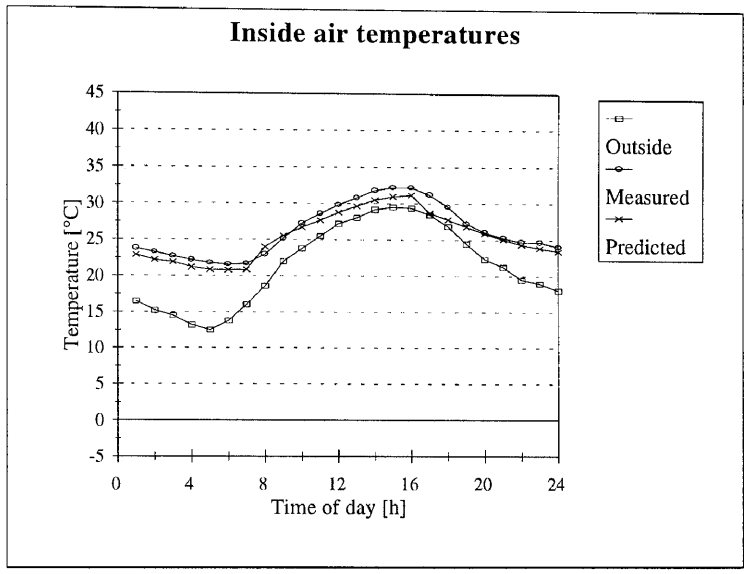

Hour	Measured	Predicted	Hour	Measured	Predicted
1	23.8	22.92	13	30.8	29.63
2	23.3	22.23	14	31.8	30.49
3	22.7	21.90	15	32.2	30.97
4	22.2	21.23	16	32.2	31.18
5	21.8	20.91	17	31.2	28.73
6	21.6	20.81	18	29.6	27.79
7	21.7	20.89	19	27.3	26.88
8	23.0	24.02	20	26.1	25.91
9	25.2	25.59	21	25.3	25.09
10	27.3	26.70	22	24.7	24.37
11	28.6	27.70	23	24.7	23.94
12	29.8	28.78	24	24.1	23.47

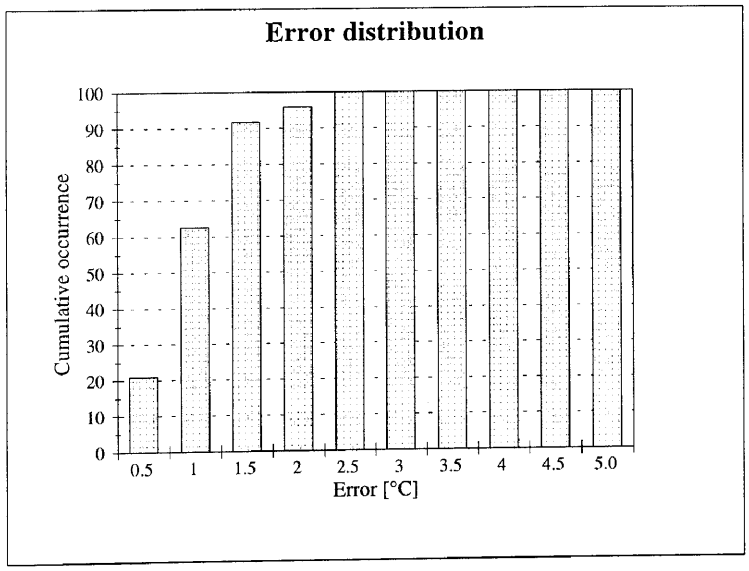

Study 31

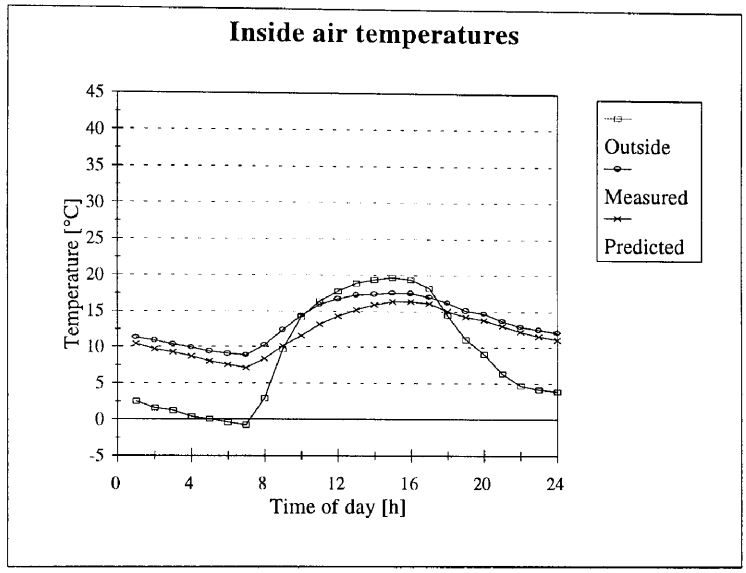

Hour	Measured	Predicted	Hour	Measured	Predicted
1	11.3	10.46	13	17.3	15.23
2	10.9	9.72	14	17.4	15.93
3	10.4	9.28	15	17.6	16.42
4	9.9	8.71	16	17.5	16.38
5	9.4	8.05	17	17.0	16.11
6	9.1	7.57	18	16.2	15.04
7	8.9	7.14	19	15.1	14.30
8	10.3	8.35	20	14.7	13.82
9	12.4	10.17	21	13.7	13.02
10	14.4	11.60	22	12.9	12.23
11	15.9	13.18	23	12.5	11.58
12	16.7	14.32	24	12.1	11.10

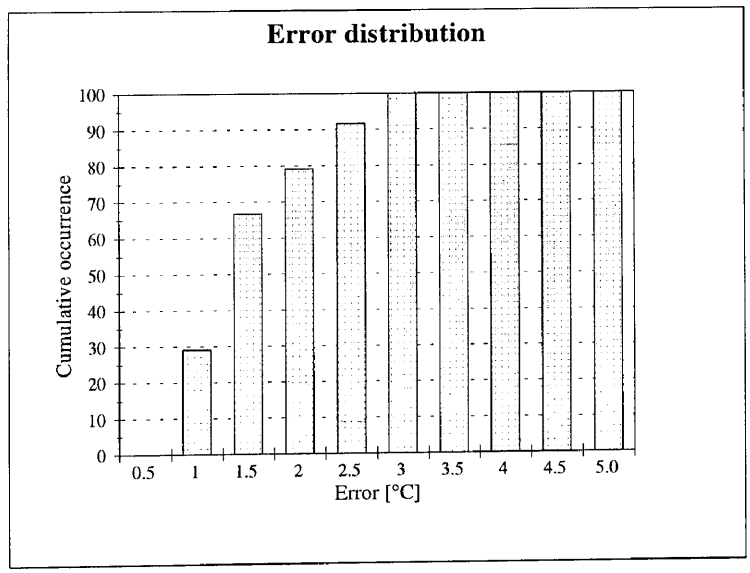

Study 32

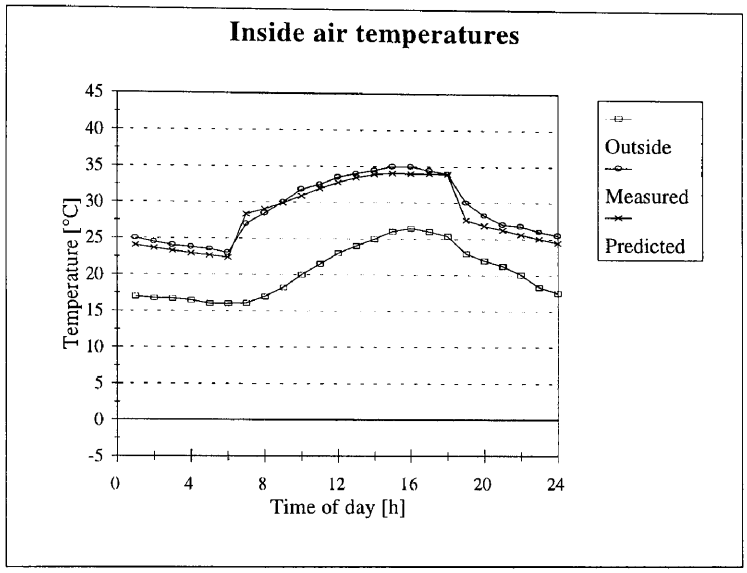

Hour	Measured	Predicted	Hour	Measured	Predicted
1	25.0	24.05	13	34.0	33.49
2	24.5	23.64	14	34.5	33.91
3	24.0	23.28	15	35.0	34.11
4	23.8	22.96	16	35.0	34.06
5	23.5	22.66	17	34.5	34.04
6	23.0	22.40	18	34.0	33.97
7	27.0	28.39	19	30.0	27.63
8	28.5	29.04	20	28.3	26.87
9	30.0	29.90	21	27.0	26.24
10	31.8	30.89	22	26.8	25.64
11	32.5	31.89	23	26.0	25.05
12	33.5	32.80	24	25.5	24.53

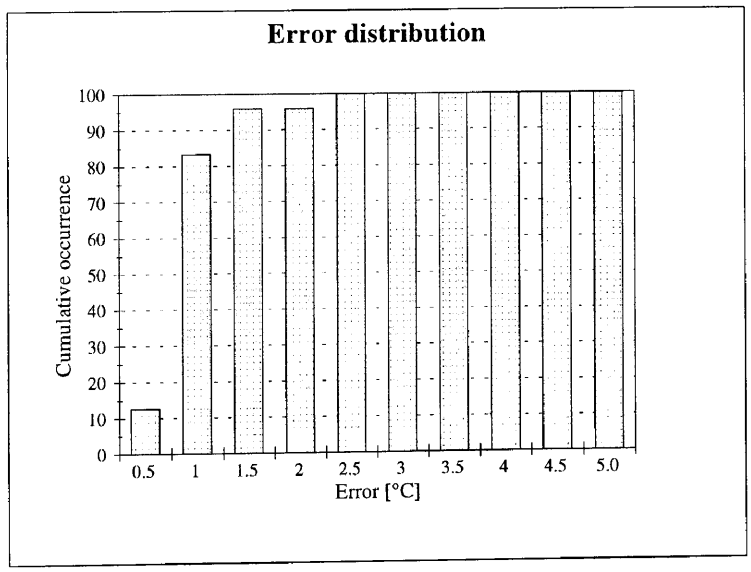

Study 33

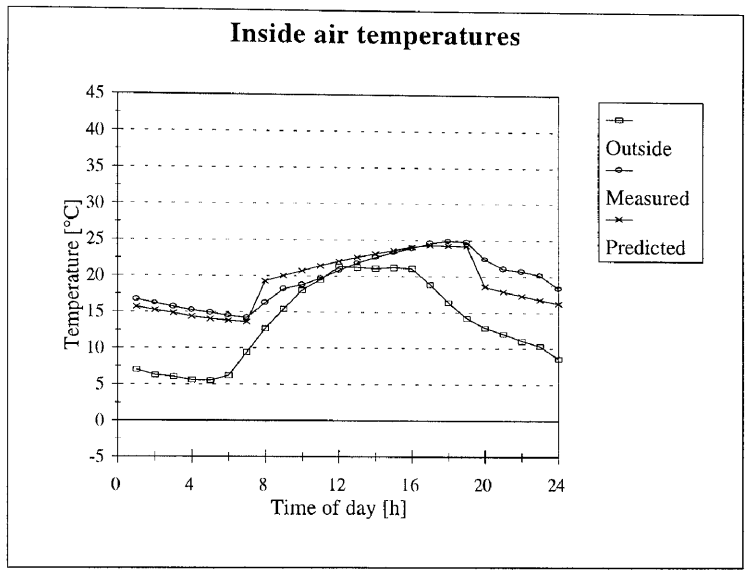

Hour	Measured	Predicted	Hour	Measured	Predicted
1	16.7	15.72	13	21.8	22.63
2	16.2	15.24	14	22.6	23.12
3	15.7	14.82	15	23.3	23.60
4	15.2	14.42	16	23.9	24.11
5	14.9	14.07	17	24.6	24.34
6	14.5	13.78	18	24.9	24.29
7	14.2	13.64	19	24.8	24.23
8	16.3	19.28	20	22.4	18.63
9	18.2	20.00	21	21.1	17.95
10	18.8	20.72	22	20.7	17.34
11	19.7	21.40	23	20.2	16.79
12	20.8	22.06	24	18.4	16.24

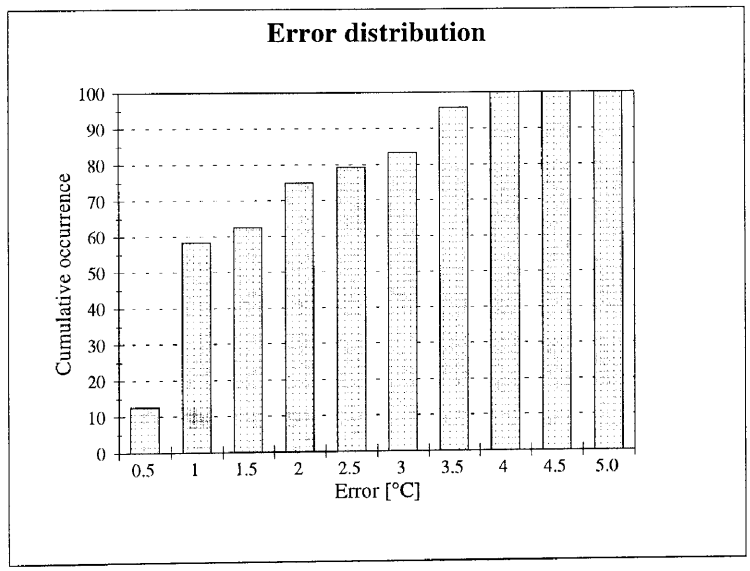

Study 34

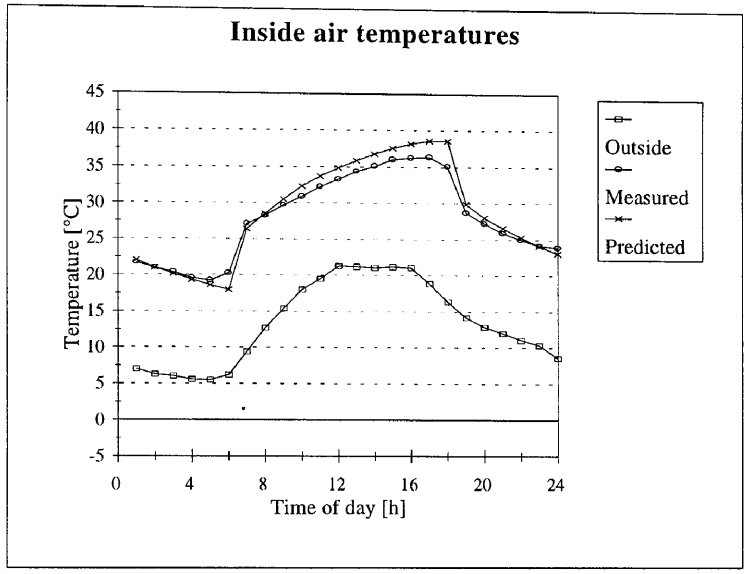

Hour	Measured	Predicted	Hour	Measured	Predicted
1	21.7	22.00	13	34.4	35.88
2	21.0	21.01	14	35.1	36.80
3	20.4	20.13	15	36.0	37.58
4	19.6	19.31	16	36.3	38.23
5	19.2	18.59	17	36.4	38.62
6	20.3	17.99	18	35.1	38.58
7	27.1	26.39	19	28.7	29.89
8	28.3	28.49	20	27.2	28.06
9	29.7	30.53	21	25.9	26.60
10	30.9	32.32	22	25.0	25.32
11	32.3	33.73	23	24.2	24.19
12	33.3	34.83	24	23.9	23.08

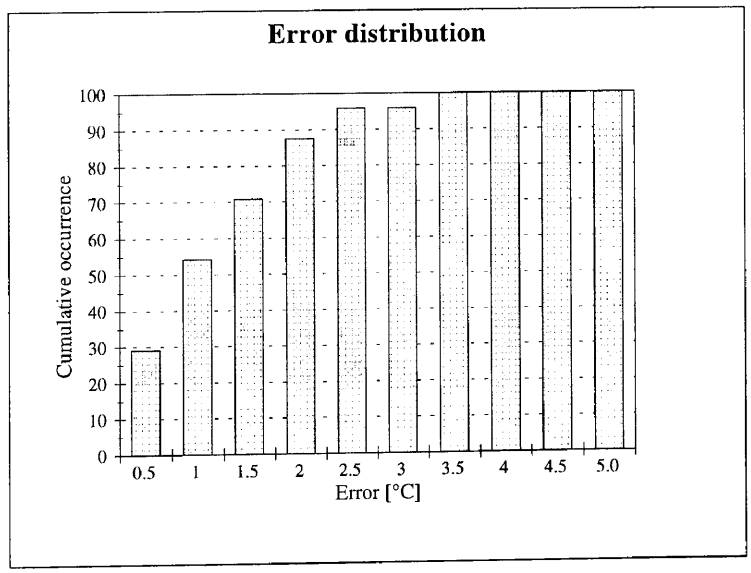

Study 35

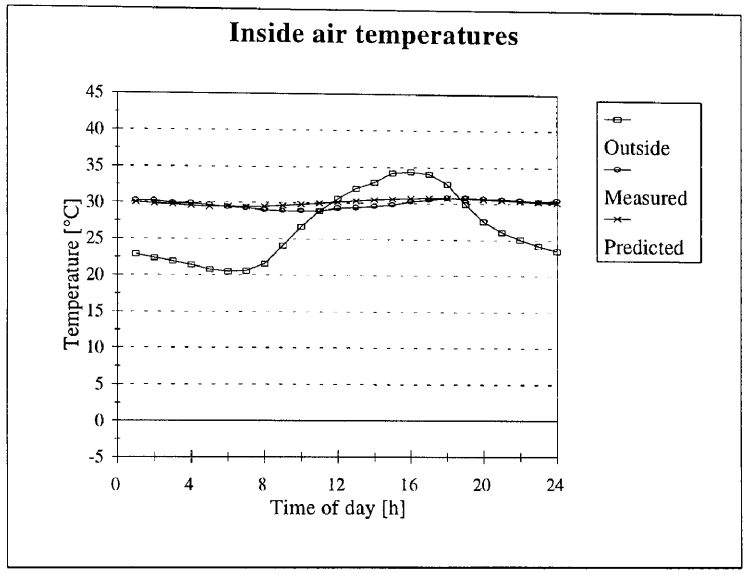

Hour	Measured	Predicted	Hour	Measured	Predicted
1	30.3	30.02	13	29.4	30.33
2	30.3	29.88	14	29.6	30.50
3	29.9	29.74	15	29.8	30.65
4	29.9	29.60	16	30.3	30.74
5	29.7	29.44	17	30.5	30.78
6	29.4	29.50	18	30.8	30.78
7	29.3	29.47	19	30.8	30.71
8	29.0	29.51	20	30.7	30.61
9	28.9	29.62	21	30.6	30.51
10	28.9	29.78	22	30.5	30.40
11	28.9	29.97	23	30.3	30.28
12	29.3	30.19	24	30.5	30.15

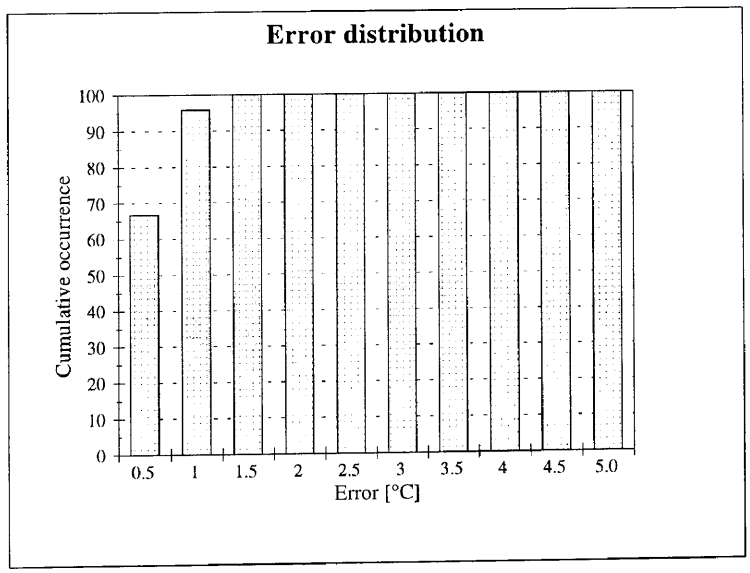

Study 36

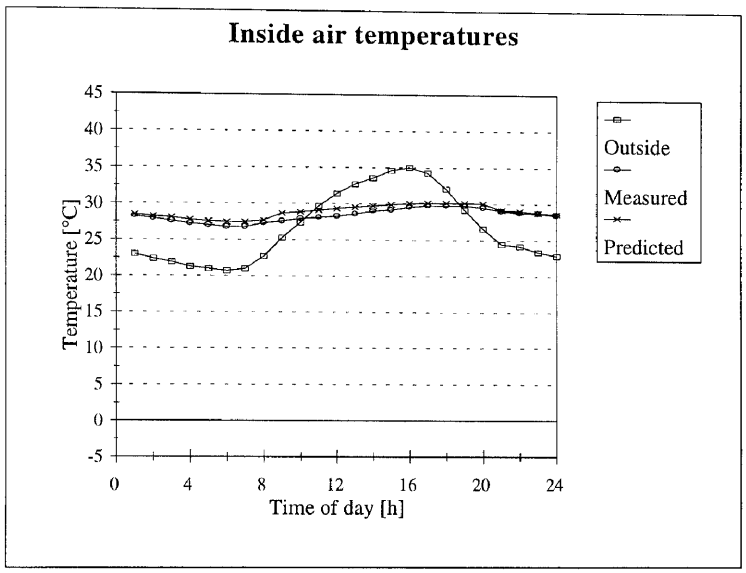

Hour	Measured	Predicted	Hour	Measured	Predicted
1	28.2	28.46	13	28.6	29.56
2	27.9	28.23	14	29.0	29.76
3	27.6	28.01	15	29.2	29.94
4	27.2	27.76	16	29.6	30.08
5	27.0	27.56	17	29.8	30.16
6	26.8	27.46	18	29.8	30.18
7	26.8	27.43	19	29.8	30.15
8	27.3	27.70	20	29.5	30.09
9	27.6	28.68	21	29.1	29.19
10	27.9	28.88	22	28.8	29.04
11	28.1	29.11	23	28.7	28.79
12	28.3	29.34	24	28.5	28.58

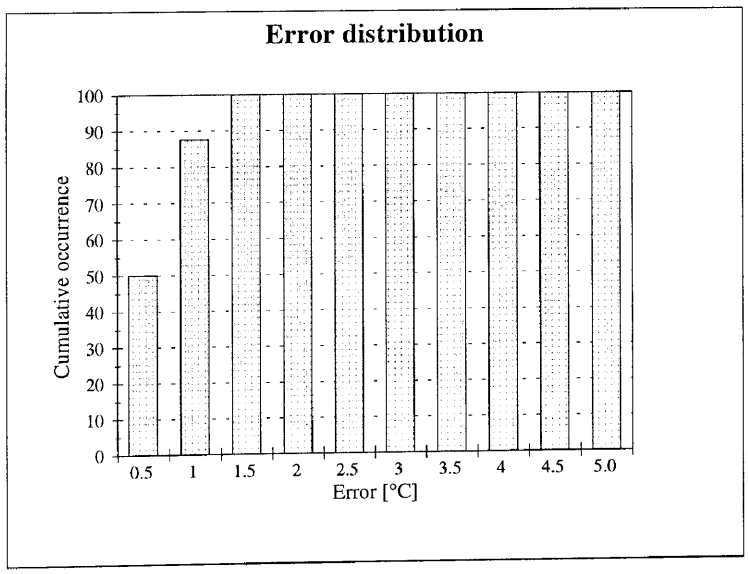

Study 37

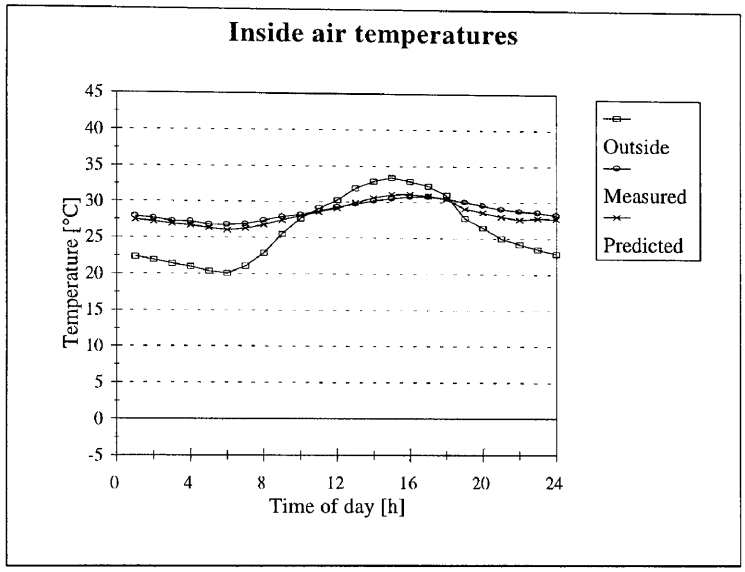

Hour	Measured	Predicted	Hour	Measured	Predicted
1	27.9	27.48	13	29.7	29.94
2	27.7	27.21	14	30.2	30.59
3	27.3	26.89	15	30.5	31.08
4	27.2	26.67	16	30.8	31.14
5	26.8	26.31	17	30.8	30.90
6	26.8	26.04	18	30.5	30.51
7	26.9	26.29	19	30.0	29.12
8	27.4	26.77	20	29.6	28.60
9	27.9	27.43	21	29.1	28.00
10	28.2	28.03	22	28.8	27.64
11	28.7	28.59	23	28.6	27.77
12	29.3	29.15	24	28.3	27.76

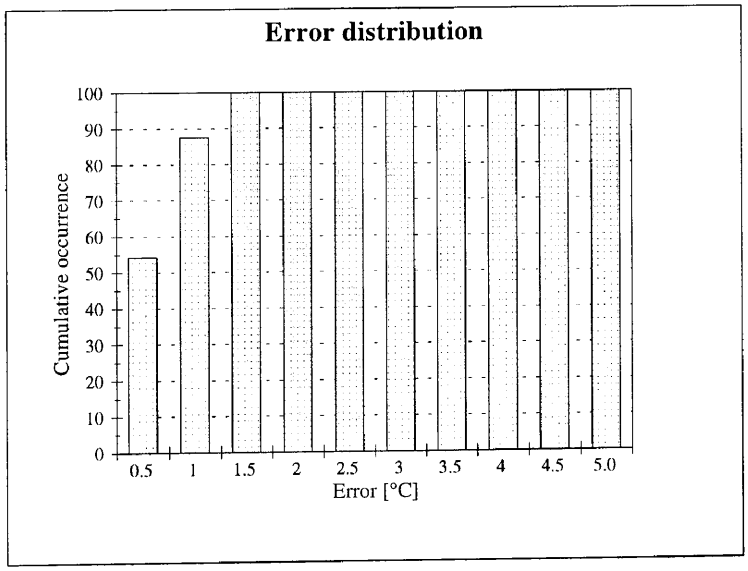

Study 38

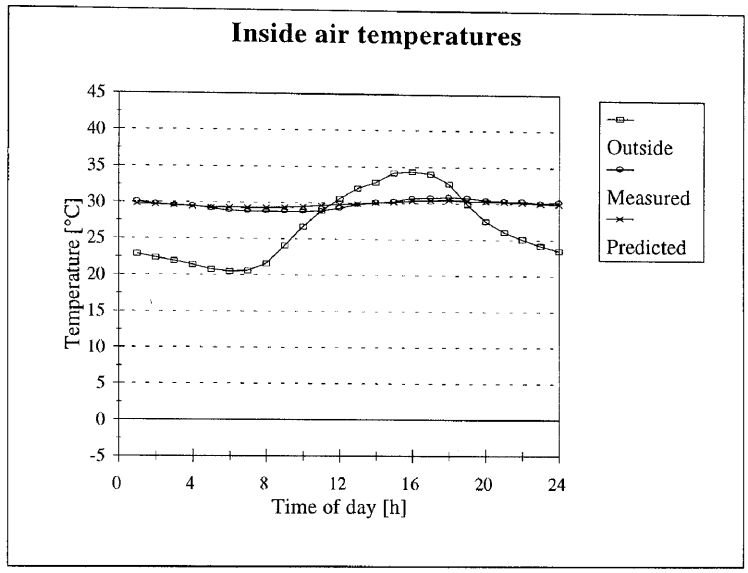

Hour	Measured	Predicted	Hour	Measured	Predicted
1	30.1	29.82	13	29.8	29.95
2	29.8	29.70	14	30.1	30.11
3	29.6	29.58	15	30.3	30.19
4	29.5	29.44	16	30.7	30.39
5	29.2	29.30	17	30.8	30.46
6	28.9	29.34	18	30.9	30.47
7	28.8	29.30	19	30.8	30.41
8	28.8	29.30	20	30.5	30.33
9	28.8	29.37	21	30.4	30.24
10	28.8	29.48	22	30.4	30.15
11	28.9	29.64	23	30.1	30.05
12	29.3	29.83	24	30.3	29.94

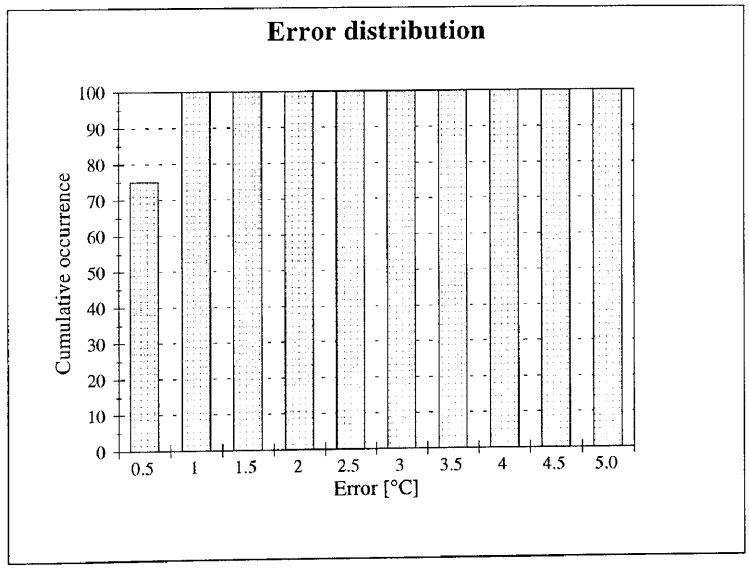

Study 39

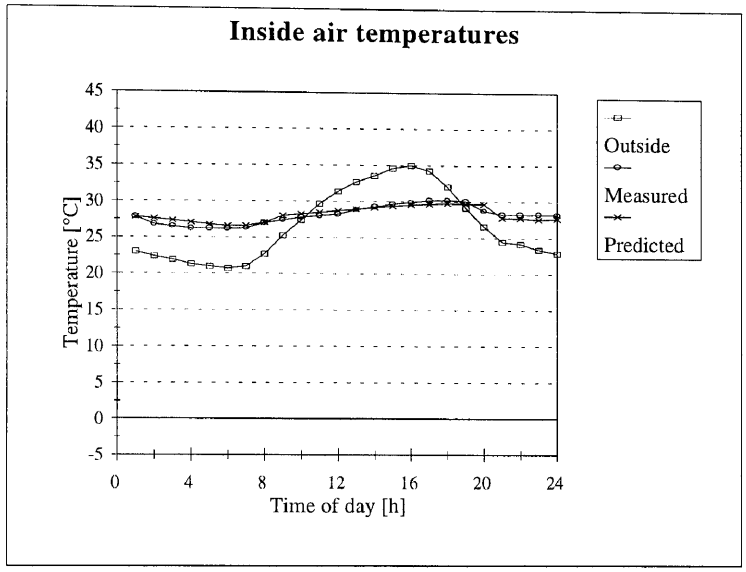

Hour	Measured	Predicted	Hour	Measured	Predicted
1	27.8	27.81	13	28.9	28.96
2	26.8	27.60	14	29.3	29.19
3	26.5	27.35	15	29.7	29.41
4	26.2	27.04	16	29.9	29.60
5	26.2	26.80	17	30.2	29.73
6	26.2	26.65	18	30.3	29.77
7	26.3	26.65	19	30.1	29.75
8	27.0	27.09	20	28.8	29.71
9	27.4	28.05	21	28.3	27.78
10	27.8	28.24	22	28.3	27.76
11	28.0	28.48	23	28.3	27.60
12	28.3	28.71	24	28.2	27.71

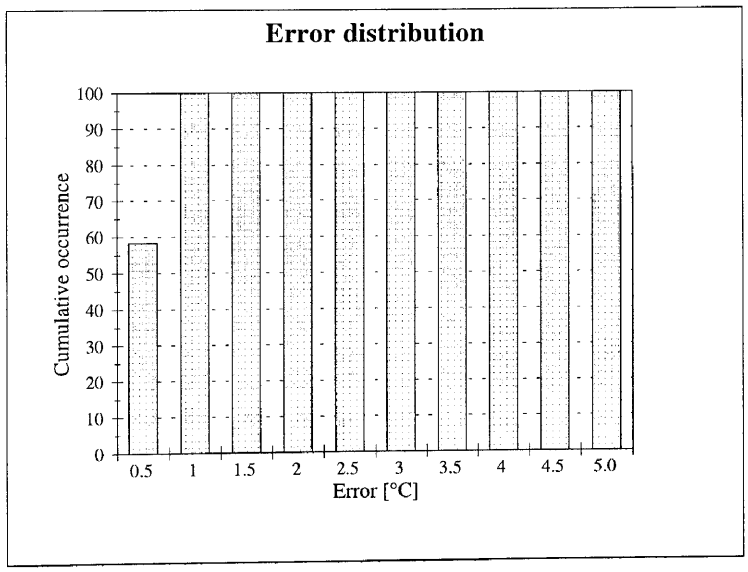

Study 40

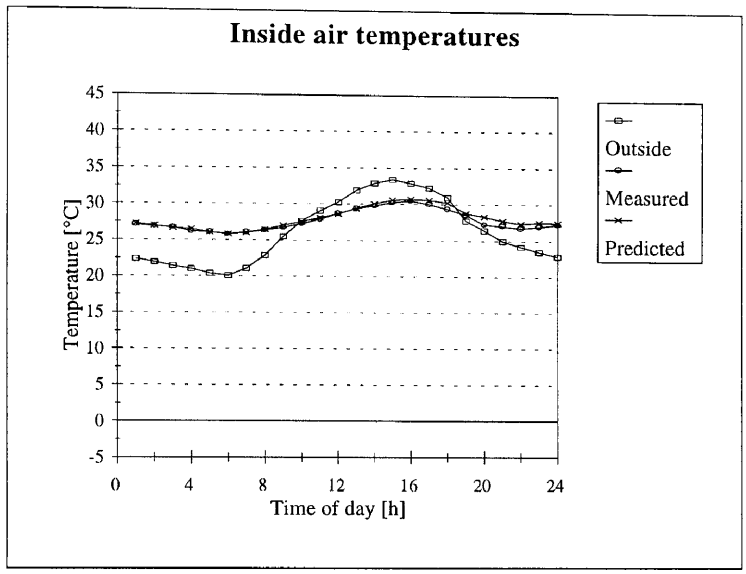

Hour	Measured	Predicted	Hour	Measured	Predicted
1	27.1	27.25	13	29.4	29.44
2	26.9	26.99	14	29.8	30.11
3	26.7	26.66	15	30.3	30.63
4	26.2	26.48	16	30.5	30.71
5	26.1	26.10	17	30.0	30.61
6	25.8	25.86	18	29.4	30.24
7	26.1	26.04	19	28.6	28.88
8	26.4	26.48	20	27.3	28.36
9	26.8	27.04	21	27.1	27.77
10	27.3	27.56	22	26.8	27.42
11	27.9	28.13	23	27.0	27.55
12	28.7	28.66	24	27.3	27.53

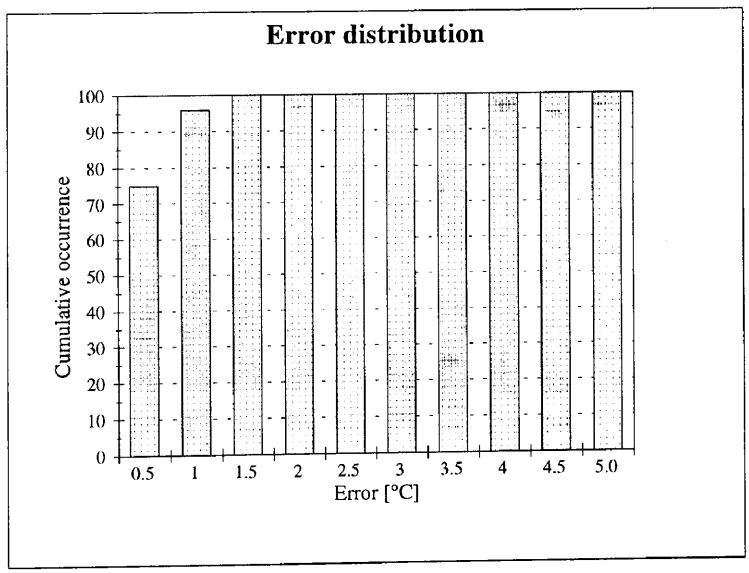

Study 41

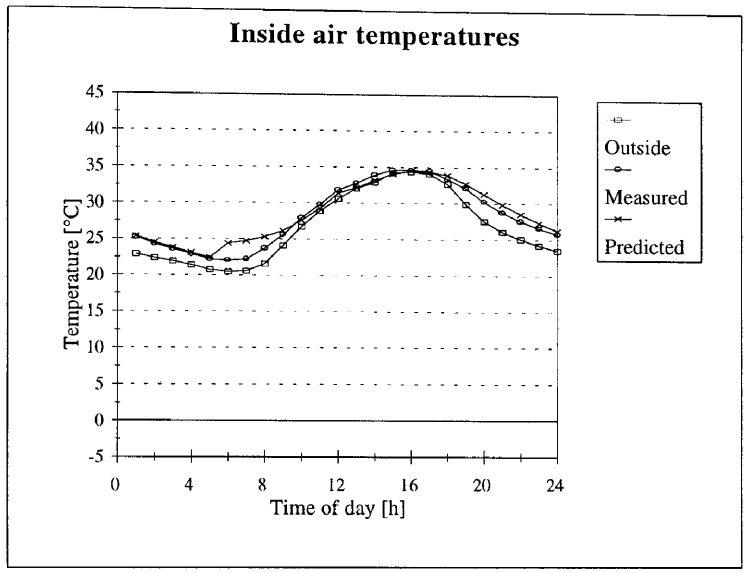

Hour	Measured	Predicted	Hour	Measured	Predicted
1	25.2	25.33	13	32.8	32.19
2	24.3	24.51	14	33.9	33.21
3	23.6	23.78	15	34.6	34.06
4	22.9	23.10	16	34.6	34.48
5	22.2	22.45	17	34.5	34.38
6	22.0	24.37	18	33.4	33.96
7	22.2	24.73	19	32.1	32.73
8	23.7	25.29	20	30.3	31.29
9	25.6	26.14	21	28.8	29.85
10	27.9	27.54	22	27.6	28.54
11	29.8	29.26	23	26.6	27.34
12	31.8	31.35	24	25.8	26.28

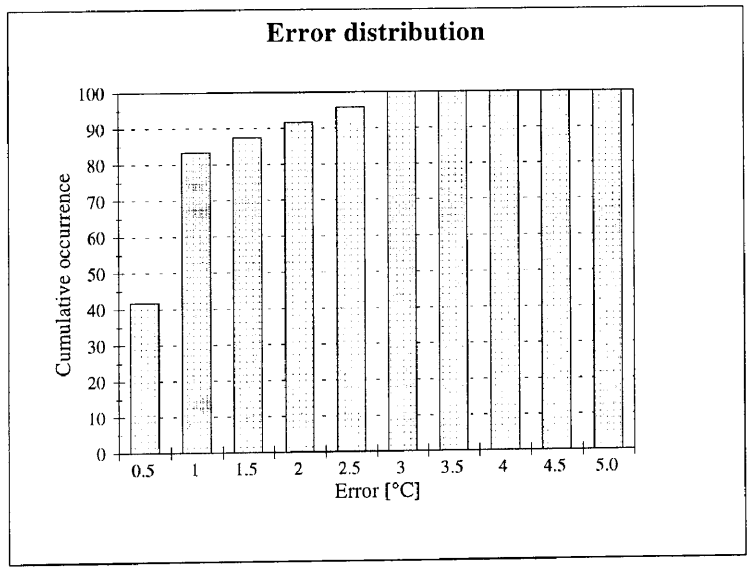

Study 42

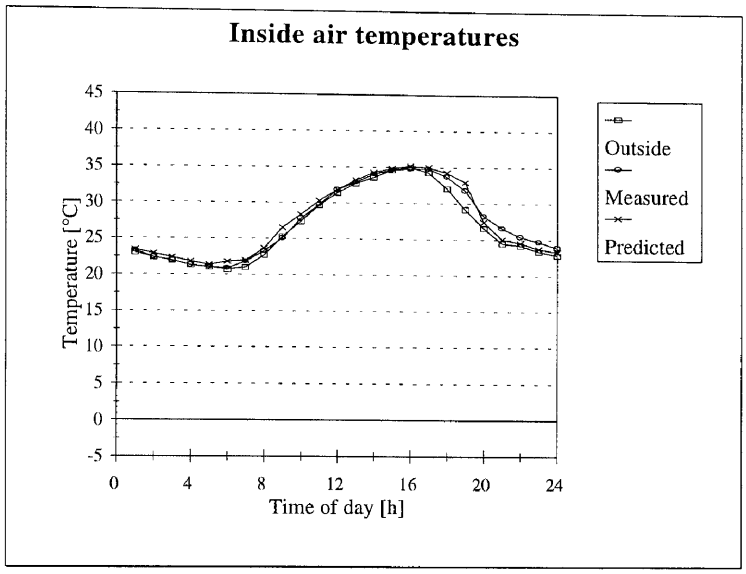

Hour	Measured	Predicted	Hour	Measured	Predicted
1	23.3	23.39	13	32.9	33.21
2	22.4	22.89	14	34.0	34.24
3	21.9	22.39	15	34.6	34.87
4	21.3	21.78	16	34.8	35.18
5	21.1	21.37	17	34.8	34.97
6	20.9	21.77	18	33.7	34.25
7	21.8	21.98	19	31.8	32.93
8	23.3	23.63	20	28.3	27.45
9	25.1	26.55	21	26.6	25.05
10	27.8	28.42	22	25.4	24.57
11	29.8	30.32	23	24.7	23.76
12	31.8	31.88	24	23.9	23.33

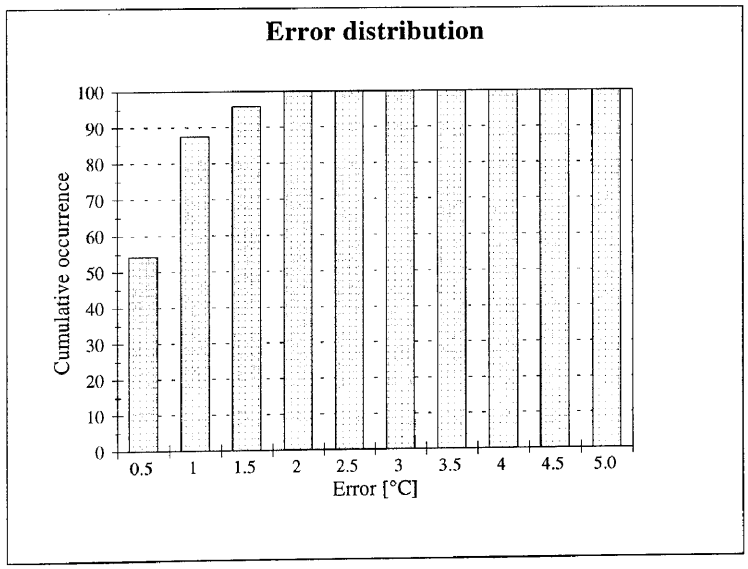

Study 43

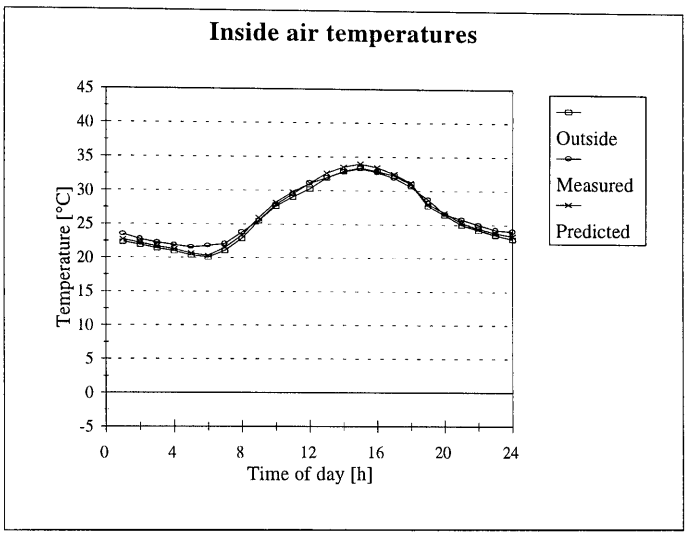

Hour	Measured	Predicted	Hour	Measured	Predicted
1	23.5	22.75	13	31.9	32.62
2	22.8	22.23	14	32.8	33.51
3	22.3	21.69	15	33.3	33.98
4	21.9	21.30	16	32.7	33.47
5	21.6	20.69	17	31.9	32.53
6	21.8	20.32	18	30.6	31.20
7	22.1	21.53	19	28.8	28.09
8	23.8	23.36	20	26.6	26.79
9	25.6	25.99	21	25.8	25.30
10	27.9	28.29	22	25.0	24.46
11	29.5	29.81	23	24.3	23.84
12	31.1	31.11	24	24.0	23.31

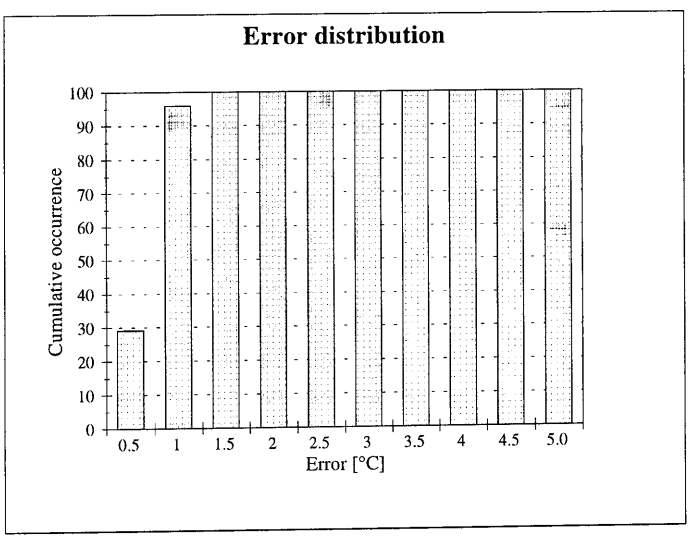

Study 44

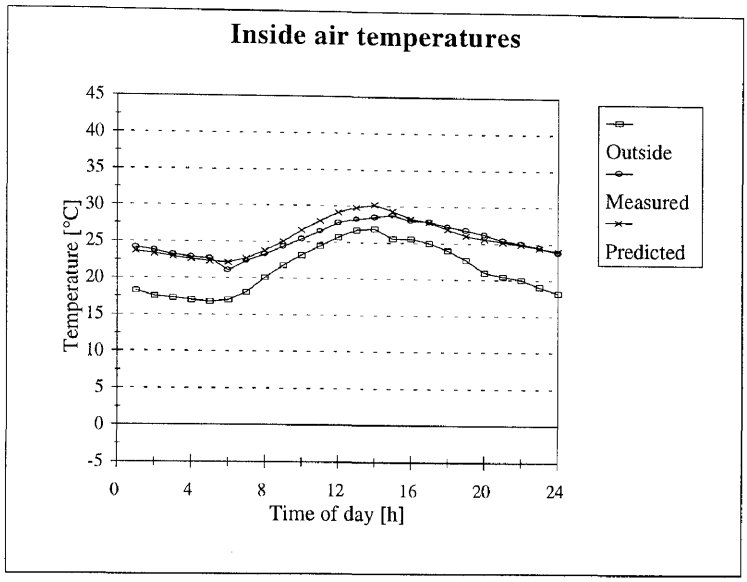

Hour	Measured	Predicted	Hour	Measured	Predicted
1	24.2	23.73	13	28.2	29.84
2	23.8	23.31	14	28.5	30.23
3	23.2	22.99	15	28.8	29.33
4	22.9	22.65	16	28.0	28.34
5	22.7	22.33	17	27.9	27.85
6	21.1	22.13	18	27.3	26.91
7	22.4	22.71	19	26.8	26.07
8	23.3	23.79	20	26.2	25.55
9	24.4	25.07	21	25.4	25.21
10	25.4	26.61	22	25.0	24.87
11	26.5	27.95	23	24.5	24.45
12	27.7	29.14	24	23.8	24.01

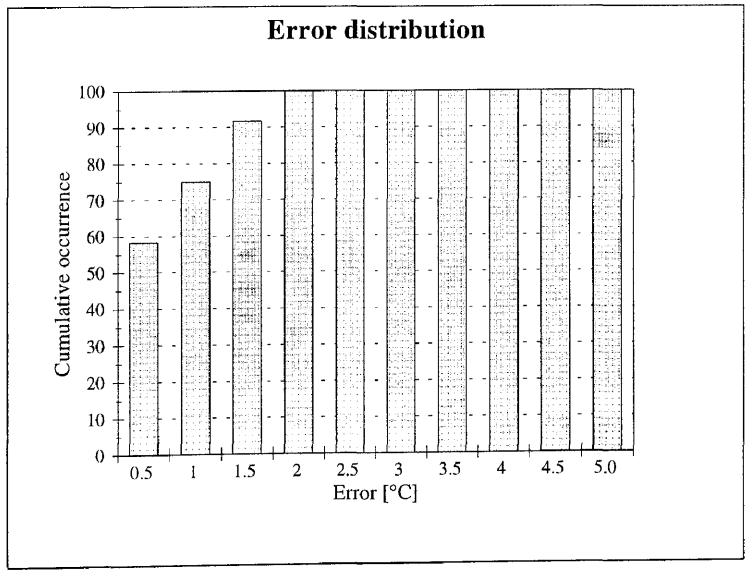

Study 45

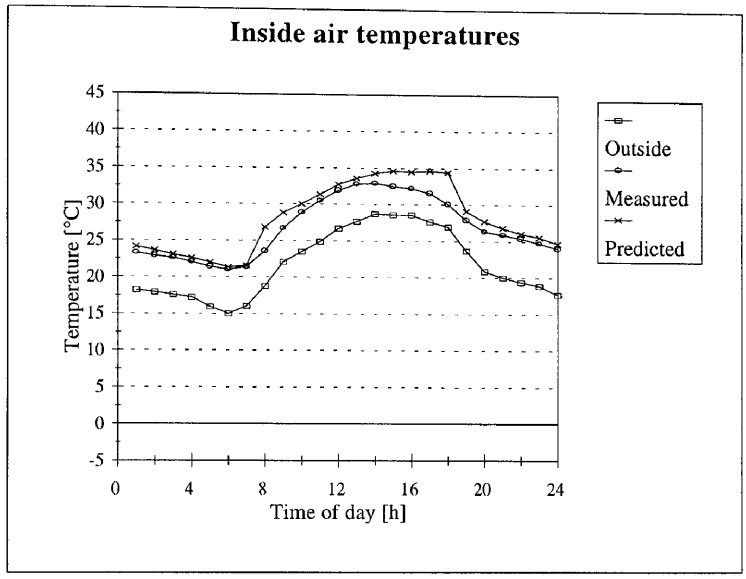

Hour	Measured	Predicted	Hour	Measured	Predicted
1	23.3	24.14	13	32.8	33.59
2	22.9	23.64	14	32.9	34.29
3	22.6	23.11	15	32.5	34.58
4	22.0	22.63	16	32.2	34.53
5	21.4	21.97	17	31.6	34.65
6	21.0	21.36	18	30.1	34.43
7	21.4	21.57	19	27.9	29.12
8	23.6	26.86	20	26.4	27.76
9	26.7	28.86	21	25.9	26.87
10	28.9	30.07	22	25.4	26.11
11	30.5	31.37	23	24.8	25.54
12	31.9	32.72	24	24.0	24.72

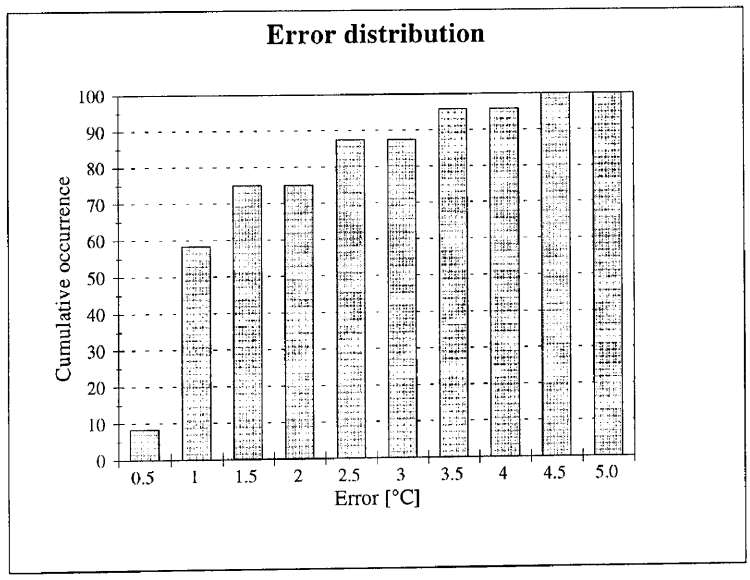

Study 46

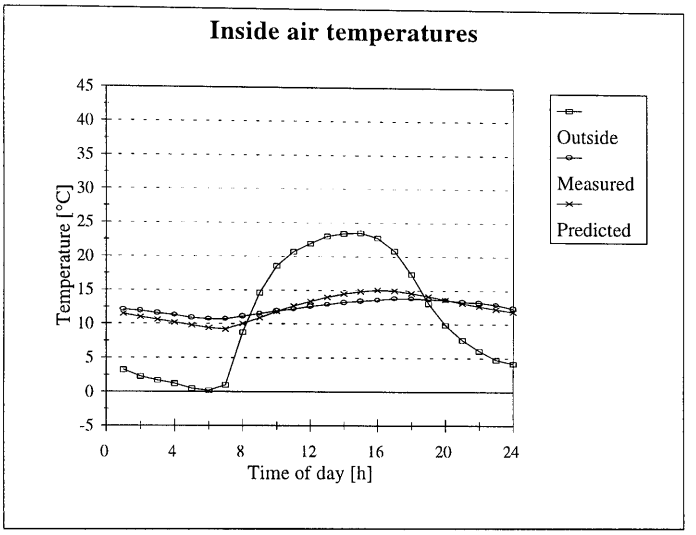

Hour	Measured	Predicted	Hour	Measured	Predicted
1	12.1	11.45	13	12.9	13.99
2	11.9	11.02	14	13.2	14.47
3	11.6	10.61	15	13.4	14.85
4	11.3	10.22	16	13.6	15.04
5	10.9	9.80	17	13.8	14.99
6	10.7	9.42	18	13.8	14.60
7	10.7	9.21	19	13.7	14.14
8	11.1	10.01	20	13.6	13.64
9	11.5	10.91	21	13.3	13.15
10	11.9	11.86	22	13.2	12.69
11	12.2	12.66	23	12.9	12.24
12	12.6	13.35	24	12.4	11.86

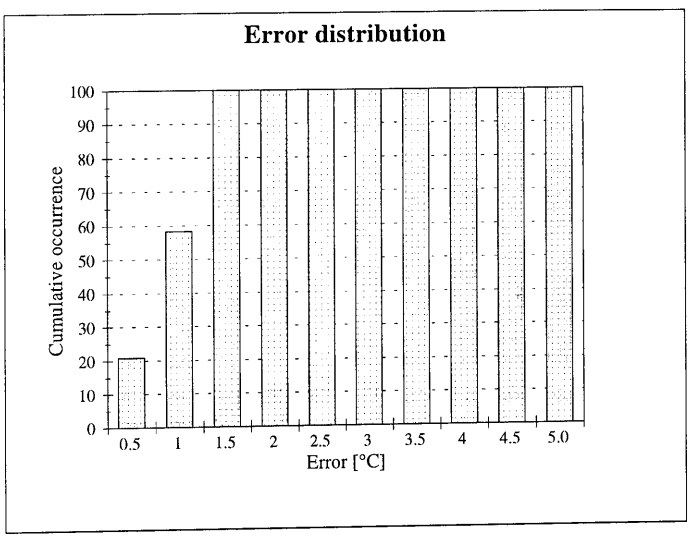

Study 47

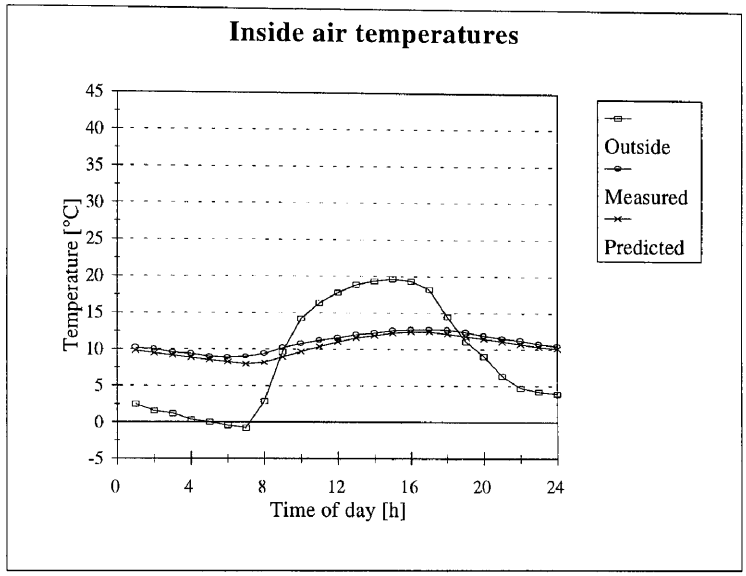

Hour	Measured	Predicted	Hour	Measured	Predicted
1	10.2	9.81	13	12.0	11.54
2	10.0	9.47	14	12.3	11.94
3	9.6	9.18	15	12.6	12.27
4	9.4	8.86	16	12.7	12.44
5	9.0	8.56	17	12.8	12.45
6	8.9	8.27	18	12.7	12.13
7	9.0	7.98	19	12.4	11.79
8	9.4	8.22	20	11.9	11.48
9	10.2	8.94	21	11.5	11.08
10	10.8	9.69	22	11.2	10.70
11	11.2	10.39	23	10.8	10.40
12	11.6	11.01	24	10.5	10.15

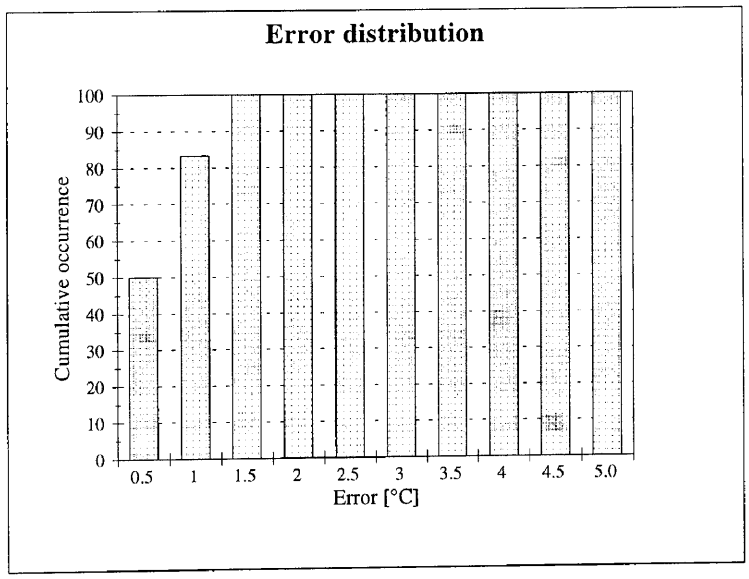

Study 48

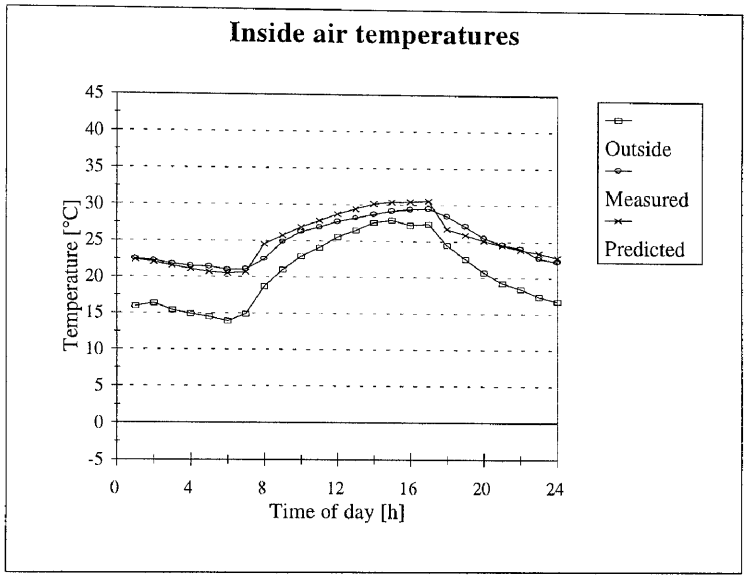

Hour	Measured	Predicted	Hour	Measured	Predicted
1	22.5	22.39	13	28.2	29.46
2	22.3	22.03	14	28.7	30.13
3	21.8	21.50	15	29.2	30.41
4	21.5	21.05	16	29.4	30.45
5	21.4	20.69	17	29.5	30.55
6	21.0	20.47	18	28.5	26.75
7	21.1	20.67	19	27.1	25.94
8	22.5	24.57	20	25.5	25.14
9	24.9	25.75	21	24.6	24.51
10	26.3	26.90	22	24.1	23.85
11	26.9	27.77	23	22.7	23.44
12	27.7	28.74	24	22.3	22.83

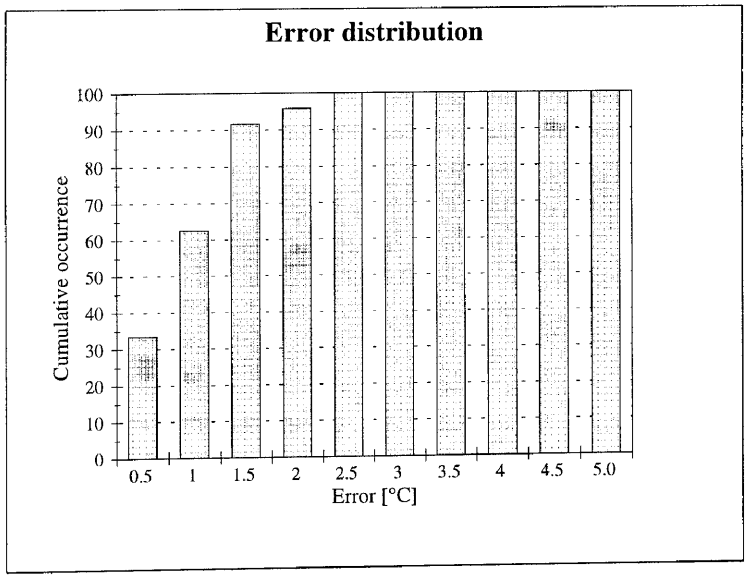

Study 49

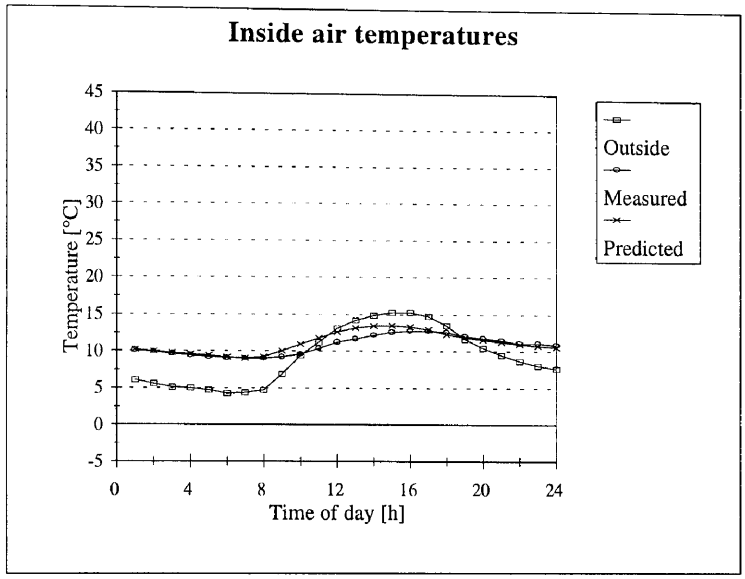

Hour	Measured	Predicted	Hour	Measured	Predicted
1	10.1	10.23	13	11.7	13.19
2	9.9	9.98	14	12.2	13.45
3	9.6	9.75	15	12.6	13.53
4	9.4	9.58	16	12.8	13.38
5	9.2	9.39	17	12.8	12.97
6	9.1	9.18	18	12.6	12.34
7	9.0	9.05	19	12.1	11.90
8	9.0	9.25	20	11.8	11.56
9	9.2	10.00	21	11.5	11.28
10	9.6	10.95	22	11.1	11.02
11	10.4	11.83	23	11.1	10.80
12	11.2	12.65	24	10.9	10.62

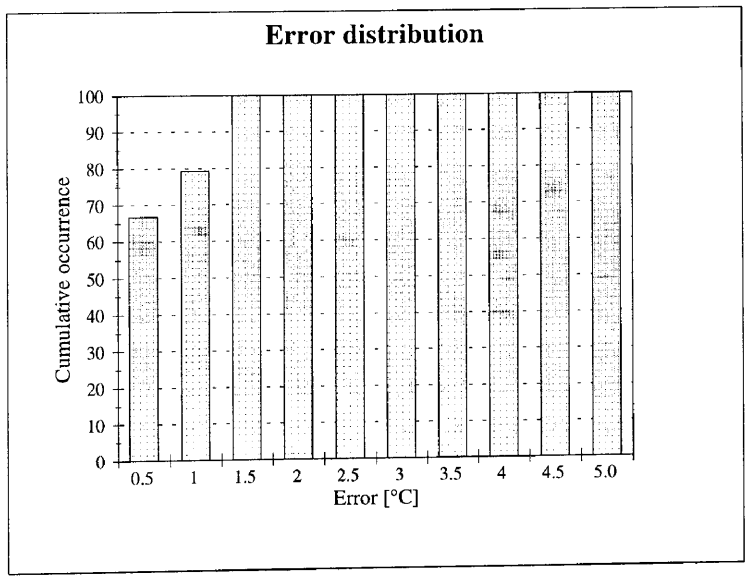

Study 50

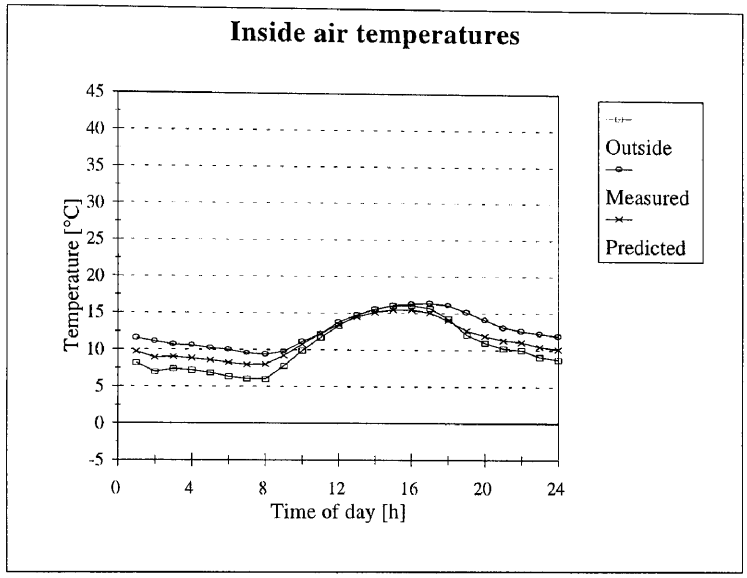

Hour	Measured	Predicted	Hour	Measured	Predicted
1	11.6	9.76	13	14.8	14.50
2	11.1	8.95	14	15.6	15.10
3	10.7	9.06	15	16.1	15.44
4	10.6	8.88	16	16.3	15.45
5	10.3	8.63	17	16.4	15.07
6	10.0	8.25	18	16.1	14.05
7	9.6	7.99	19	15.1	12.68
8	9.4	8.00	20	14.1	11.90
9	9.8	9.25	21	13.1	11.37
10	11.1	10.79	22	12.6	11.10
11	12.2	12.20	23	12.3	10.48
12	13.8	13.45	24	11.9	10.14

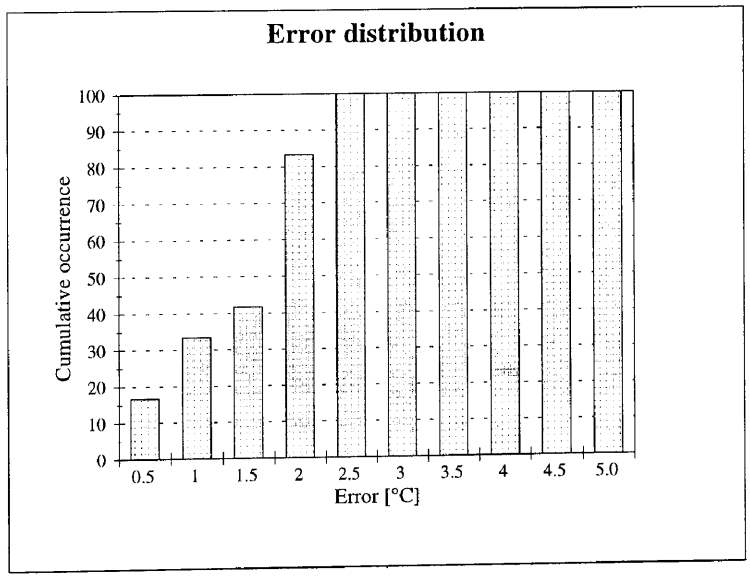

Study 51

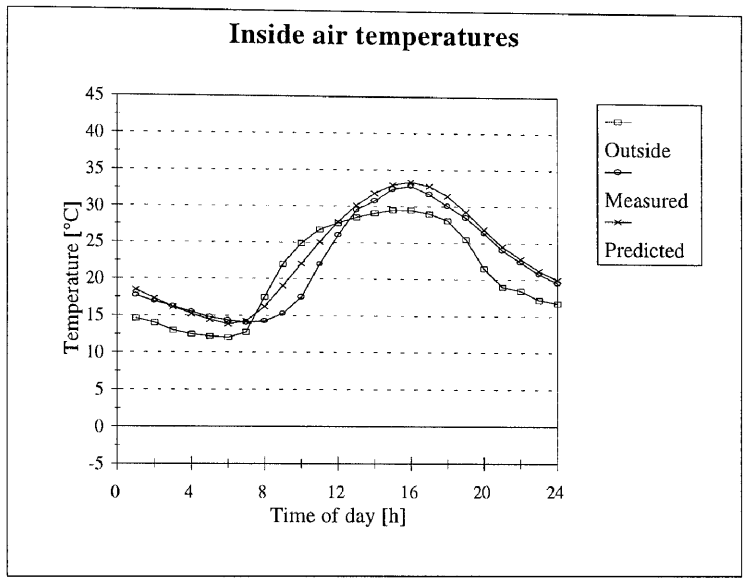

Hour	Measured	Predicted	Hour	Measured	Predicted
1	17.7	18.48	13	29.5	30.12
2	16.9	17.28	14	30.8	31.77
3	16.2	16.15	15	32.4	32.96
4	15.5	15.21	16	32.8	33.35
5	14.8	14.45	17	31.7	32.77
6	14.4	13.88	18	30.1	31.49
7	14.1	14.24	19	28.5	29.29
8	14.3	16.20	20	26.4	26.85
9	15.3	19.06	21	24.0	24.54
10	17.5	22.11	22	22.4	22.83
11	22.0	25.04	23	20.8	21.23
12	26.0	27.88	24	19.6	19.99

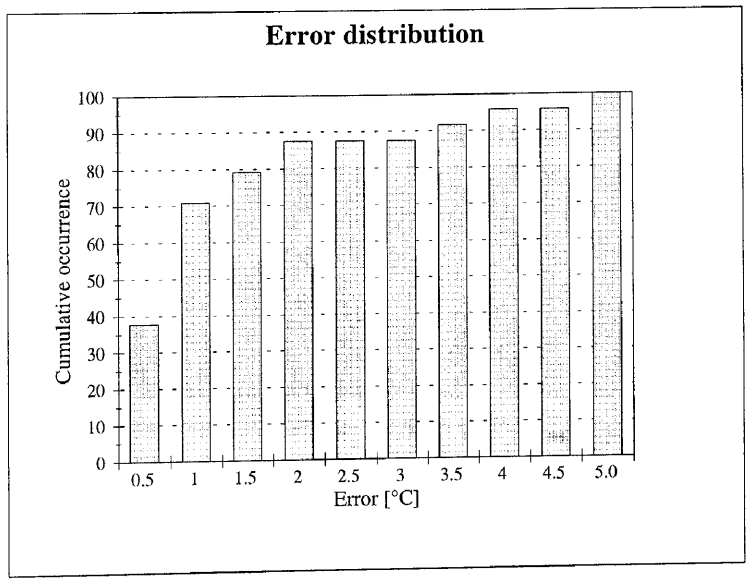

Study 52

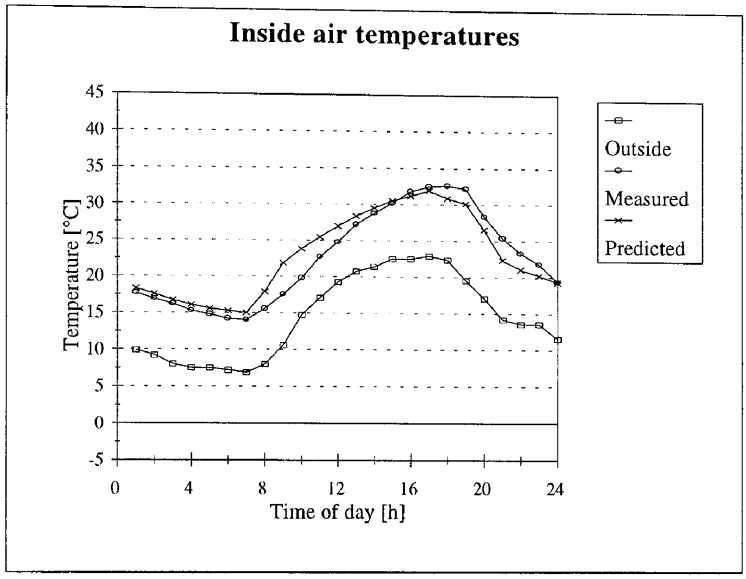

Hour	Measured	Predicted	Hour	Measured	Predicted
1	17.7	18.34	13	27.2	28.37
2	16.9	17.55	14	28.8	29.53
3	16.2	16.75	15	30.2	30.56
4	15.3	16.08	16	31.8	31.21
5	14.8	15.58	17	32.5	31.89
6	14.2	15.28	18	32.6	30.91
7	14.0	15.00	19	32.2	30.16
8	15.6	17.90	20	28.4	26.56
9	17.6	21.86	21	25.4	22.37
10	19.8	23.82	22	23.3	21.09
11	22.7	25.47	23	21.8	20.27
12	24.8	26.97	24	19.4	19.31

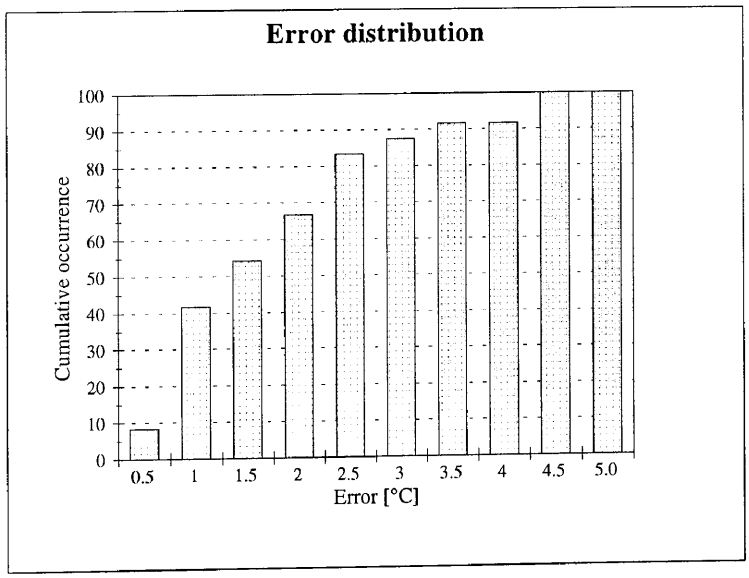

Study 53

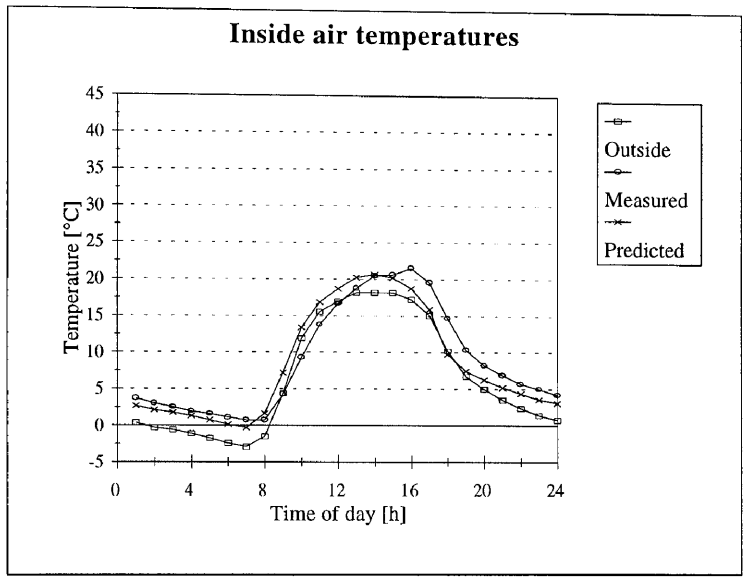

Hour	Measured	Predicted	Hour	Measured	Predicted
1	3.7	2.67	13	18.8	20.26
2	3.0	2.09	14	20.5	20.66
3	2.5	1.74	15	20.6	20.20
4	1.9	1.28	16	21.5	18.80
5	1.6	0.75	17	19.6	15.91
6	1.1	0.16	18	14.7	9.74
7	0.7	−0.31	19	10.4	7.43
8	0.7	1.62	20	8.3	6.25
9	4.3	7.21	21	6.9	5.20
10	9.3	13.40	22	5.7	4.38
11	13.8	16.91	23	5.0	3.61
12	16.7	18.74	24	4.2	3.08

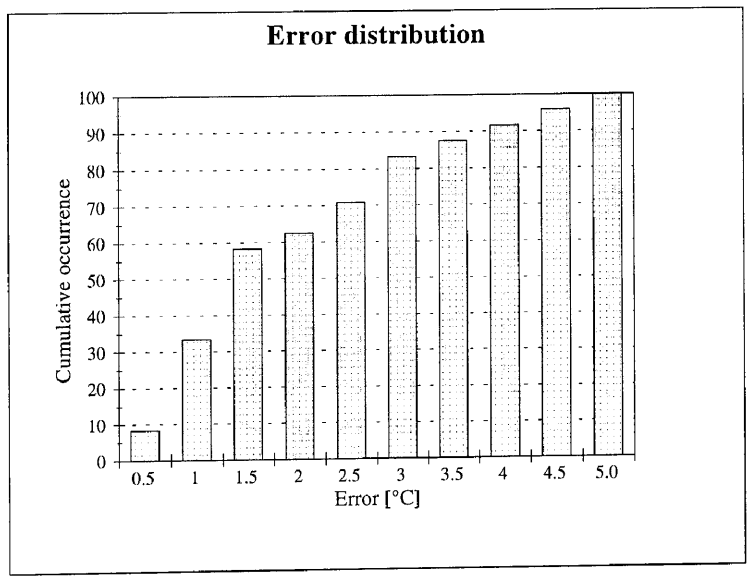

Study 54

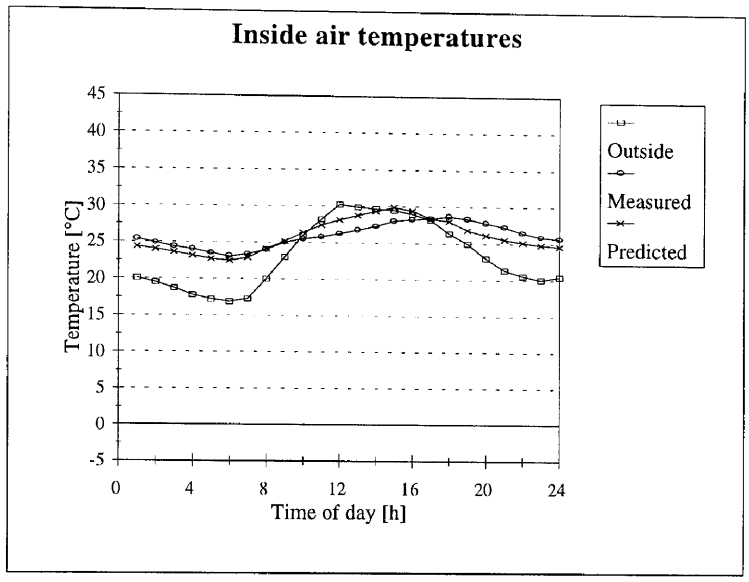

Hour	Measured	Predicted	Hour	Measured	Predicted
1	25.4	24.39	13	26.8	28.79
2	24.9	24.04	14	27.3	29.36
3	24.4	23.62	15	28.0	29.95
4	24.0	23.17	16	28.3	29.45
5	23.5	22.76	17	28.4	28.39
6	23.1	22.49	18	28.7	28.02
7	23.4	22.92	19	28.4	26.84
8	24.0	24.14	20	27.8	26.17
9	25.0	25.17	21	27.3	25.58
10	25.5	26.42	22	26.5	25.16
11	25.8	27.41	23	25.9	24.81
12	26.3	28.15	24	25.7	24.68

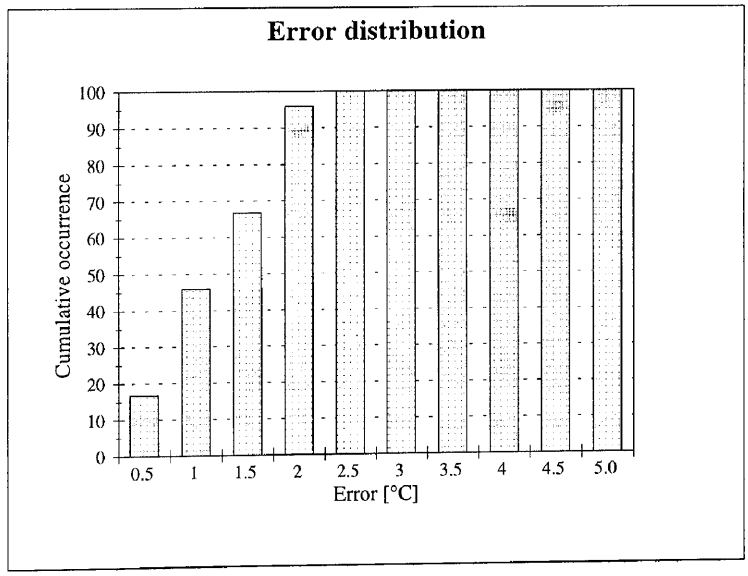

Study 55

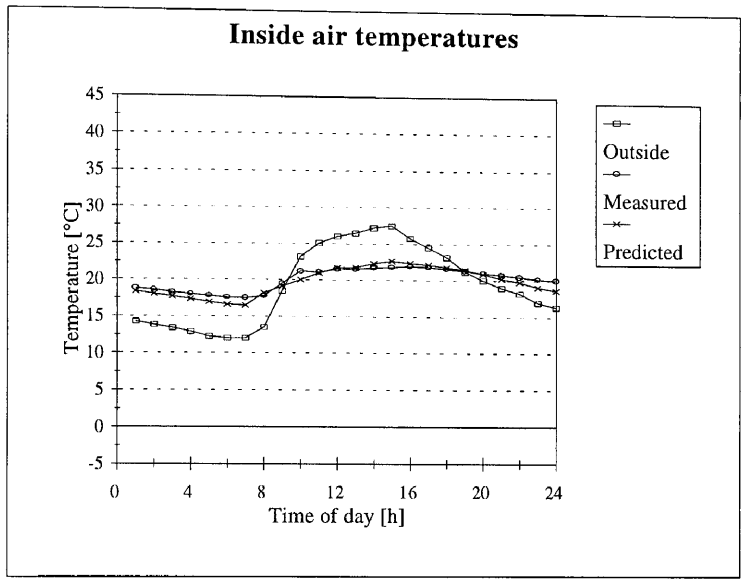

Hour	Measured	Predicted	Hour	Measured	Predicted
1	18.8	18.41	13	21.5	21.76
2	18.6	18.04	14	21.7	22.33
3	18.3	17.71	15	21.8	22.66
4	18.0	17.35	16	21.9	22.38
5	17.8	16.95	17	21.8	22.14
6	17.6	16.63	18	21.6	21.82
7	17.5	16.47	19	21.3	21.49
8	17.8	18.20	20	21.0	20.90
9	19.5	19.12	21	20.8	20.28
10	21.2	20.01	22	20.5	19.84
11	21.1	20.99	23	20.2	19.12
12	21.5	21.68	24	20.0	18.69

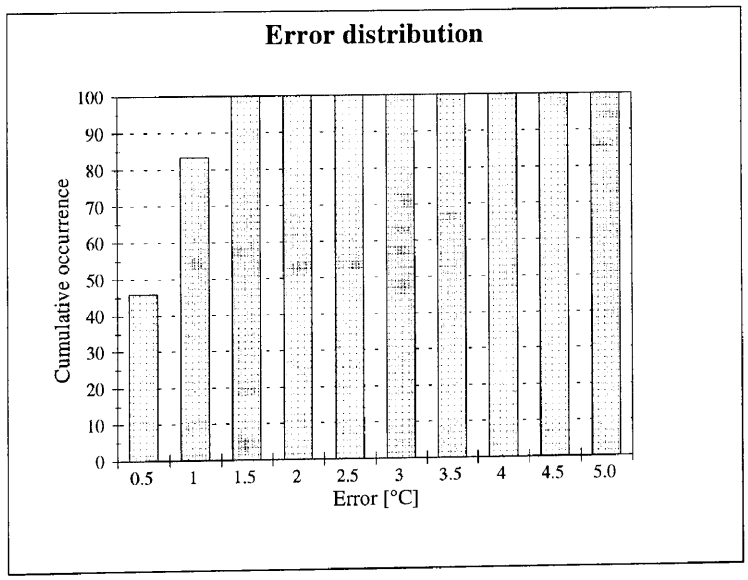

Study 56

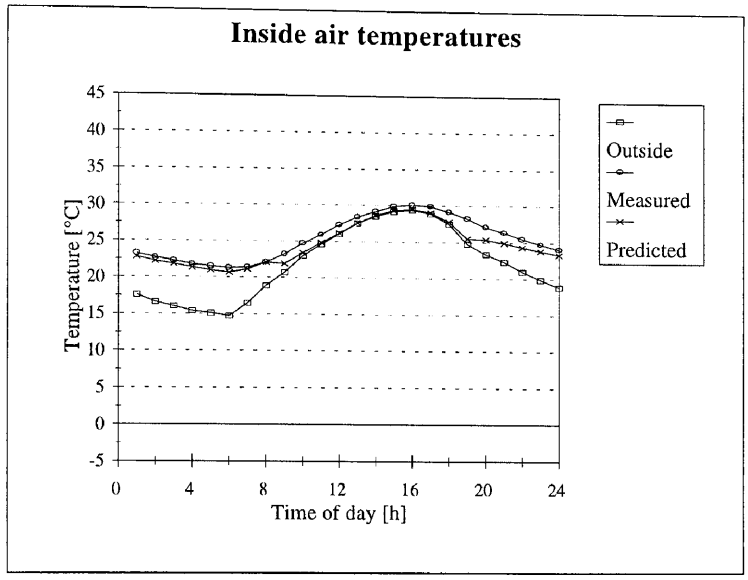

Hour	Measured	Predicted	Hour	Measured	Predicted
1	23.2	22.78	13	28.4	27.61
2	22.7	22.22	14	29.2	28.59
3	22.3	21.77	15	29.9	29.33
4	21.8	21.34	16	30.1	29.51
5	21.5	20.99	17	29.9	29.04
6	21.3	20.67	18	29.2	27.77
7	21.4	21.14	19	28.3	25.52
8	22.1	22.10	20	27.1	25.41
9	23.2	21.93	21	26.4	24.94
10	24.7	23.41	22	25.5	24.39
11	25.9	24.82	23	24.8	23.87
12	27.3	26.16	24	24.1	23.37

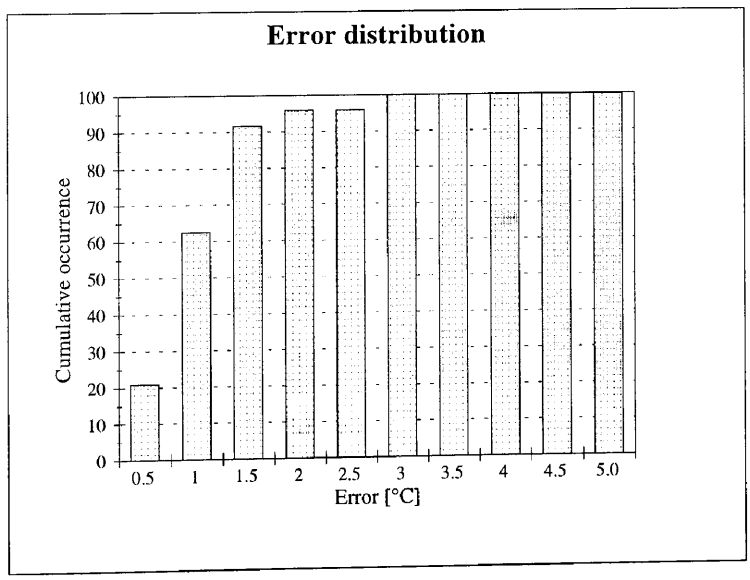

Study 57

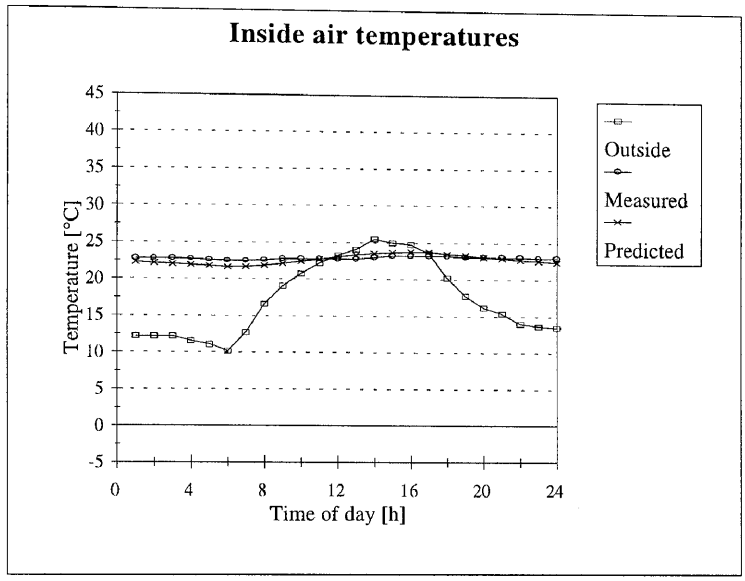

Hour	Measured	Predicted	Hour	Measured	Predicted
1	22.8	22.28	13	22.8	23.34
2	22.8	22.14	14	23.0	23.60
3	22.8	22.02	15	23.2	23.73
4	22.7	21.90	16	23.2	23.82
5	22.6	21.78	17	23.2	23.83
6	22.5	21.65	18	23.2	23.51
7	22.5	21.66	19	23.1	23.31
8	22.6	21.86	20	23.1	23.11
9	22.8	22.13	21	23.1	22.93
10	22.8	22.43	22	23.1	22.75
11	22.8	22.75	23	23.0	22.59
12	22.8	23.06	24	23.0	22.44

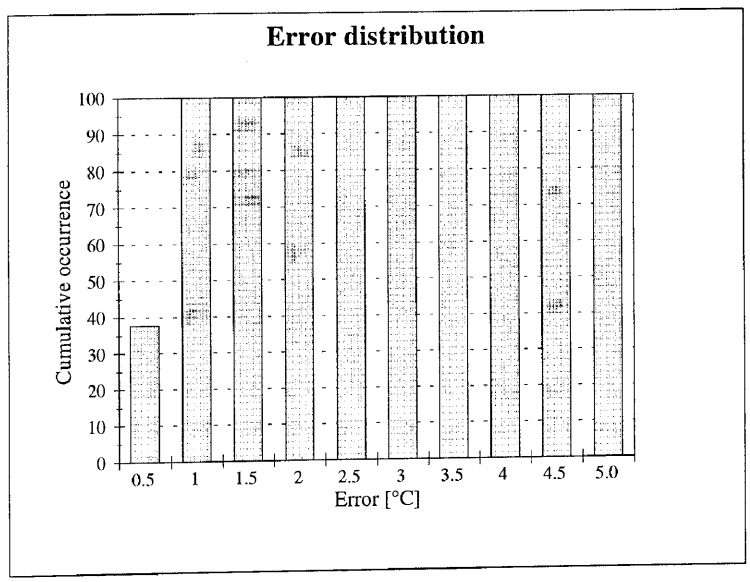

Study 58

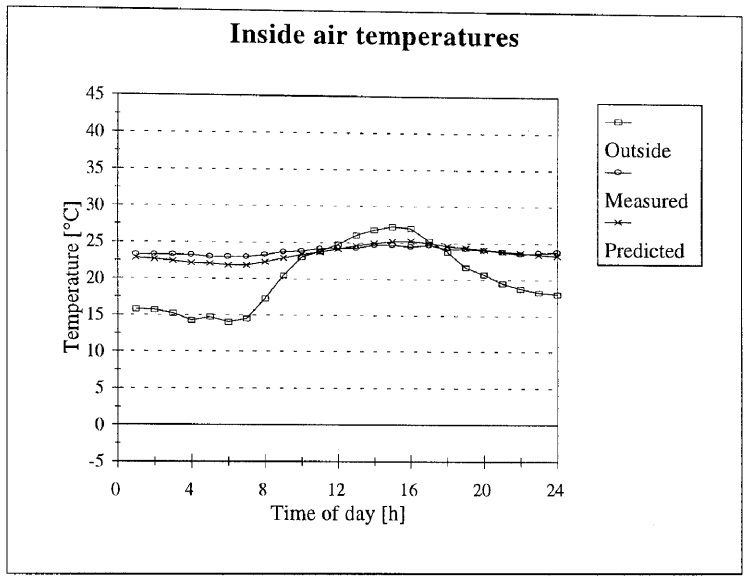

Hour	Measured	Predicted	Hour	Measured	Predicted
1	23.3	22.85	13	24.3	24.64
2	23.3	22.67	14	24.7	24.98
3	23.3	22.45	15	24.7	25.25
4	23.2	22.17	16	24.5	25.28
5	23.0	22.09	17	24.7	25.01
6	23.0	21.86	18	24.2	24.60
7	23.0	21.85	19	24.2	24.38
8	23.3	22.32	20	24.0	24.15
9	23.7	22.87	21	23.8	23.88
10	23.8	23.35	22	23.5	23.66
11	24.2	23.71	23	23.7	23.45
12	24.3	24.18	24	23.8	23.28

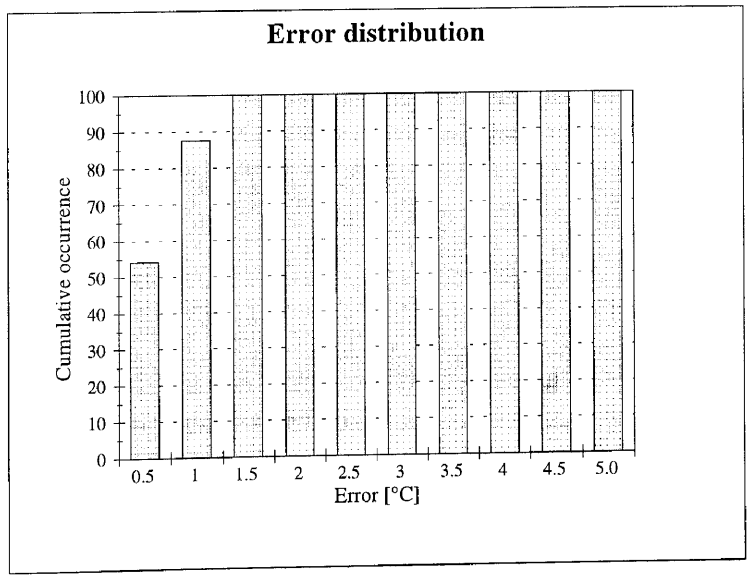

Study 59

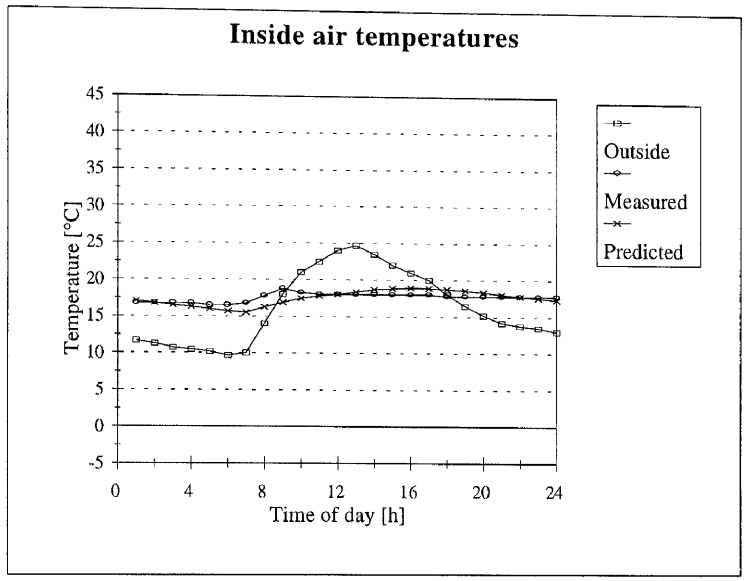

Hour	Measured	Predicted	Hour	Measured	Predicted
1	16.8	17.06	13	18.0	18.42
2	16.8	16.78	14	18.0	18.71
3	16.8	16.50	15	18.0	18.86
4	16.8	16.24	16	18.0	18.93
5	16.5	15.99	17	18.0	18.92
6	16.5	15.73	18	17.8	18.78
7	16.8	15.53	19	17.8	18.59
8	17.8	16.26	20	17.8	18.35
9	18.8	16.91	21	17.8	18.09
10	18.3	17.43	22	17.8	17.84
11	18.0	17.77	23	17.8	17.60
12	18.0	18.05	24	17.8	17.35

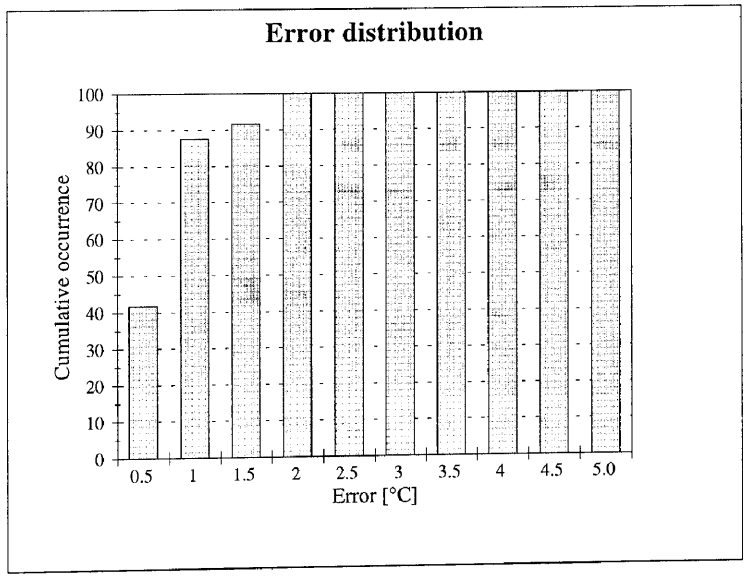

Study 60

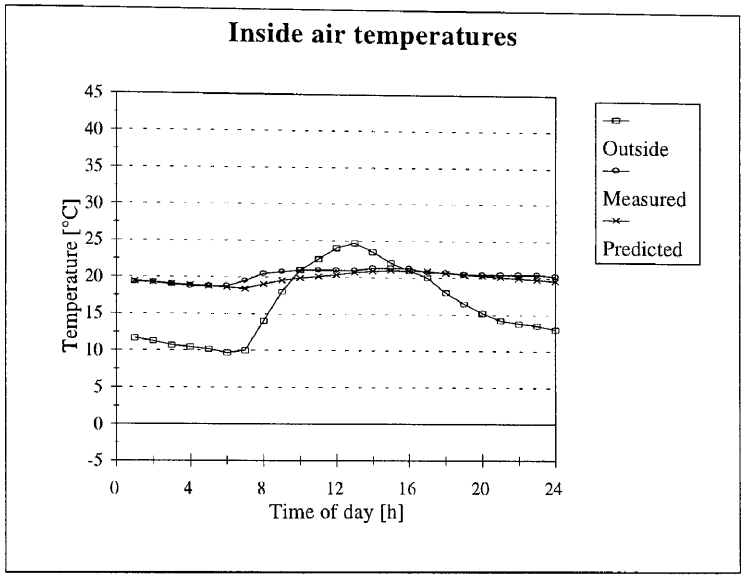

Hour	Measured	Predicted	Hour	Measured	Predicted
1	19.3	19.45	13	21.0	20.72
2	19.3	19.28	14	21.3	20.92
3	19.0	19.10	15	21.3	21.00
4	18.8	18.93	16	21.3	20.95
5	18.8	18.77	17	20.8	20.94
6	18.8	18.60	18	20.8	20.66
7	19.5	18.46	19	20.5	20.50
8	20.5	19.05	20	20.5	20.33
9	20.8	19.54	21	20.5	20.15
10	21.0	19.92	22	20.5	19.98
11	21.0	20.15	23	20.5	19.81
12	21.0	20.37	24	20.3	19.64

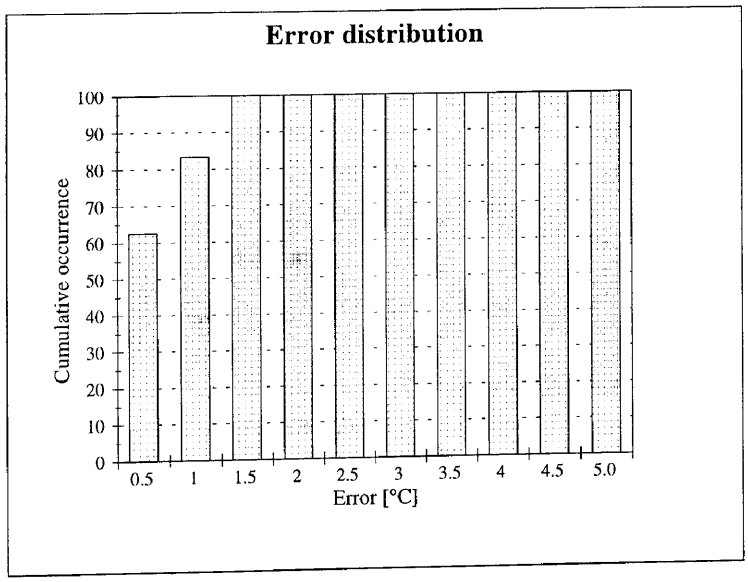

Study 61

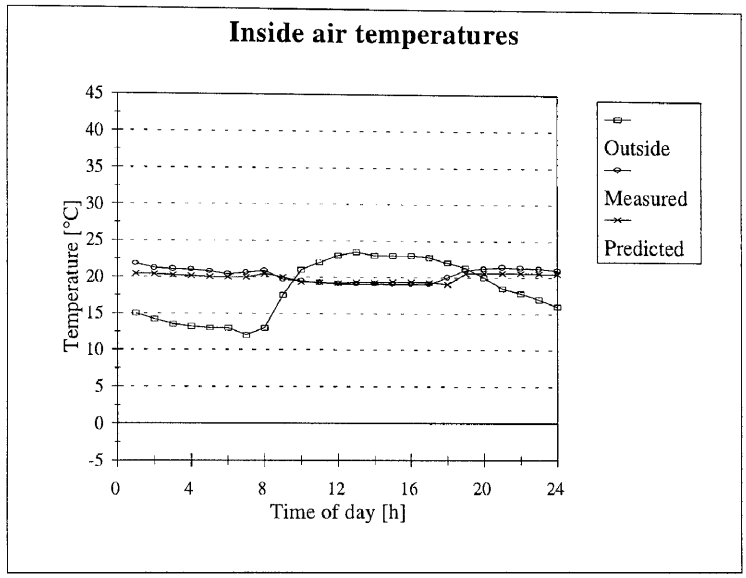

Hour	Measured	Predicted	Hour	Measured	Predicted
1	21.8	20.44	13	19.1	19.36
2	21.2	20.35	14	19.1	19.28
3	21.1	20.26	15	19.1	19.42
4	21.0	20.16	16	19.1	19.41
5	20.8	20.06	17	19.1	19.32
6	20.4	19.97	18	20.0	19.11
7	20.6	19.97	19	21.0	20.56
8	20.9	20.46	20	21.2	20.61
9	19.7	20.02	21	21.4	20.62
10	19.5	19.32	22	21.3	20.60
11	19.2	19.30	23	21.2	20.57
12	19.1	19.18	24	21.0	20.51

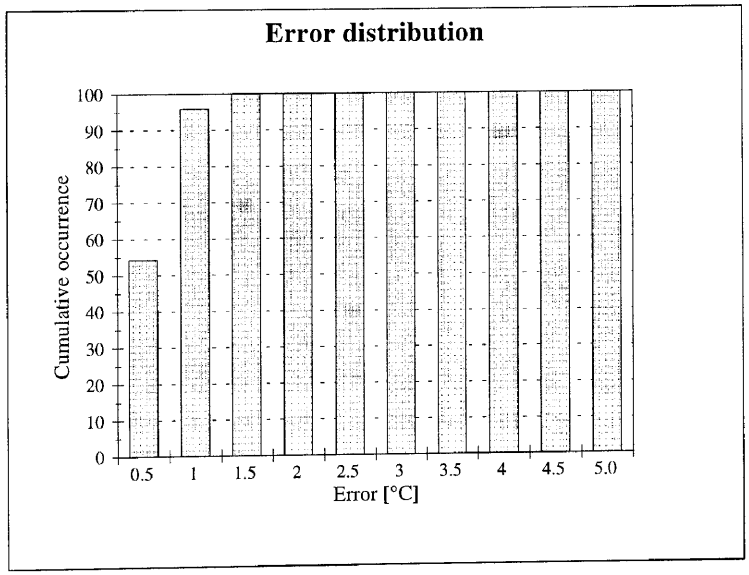

Study 62

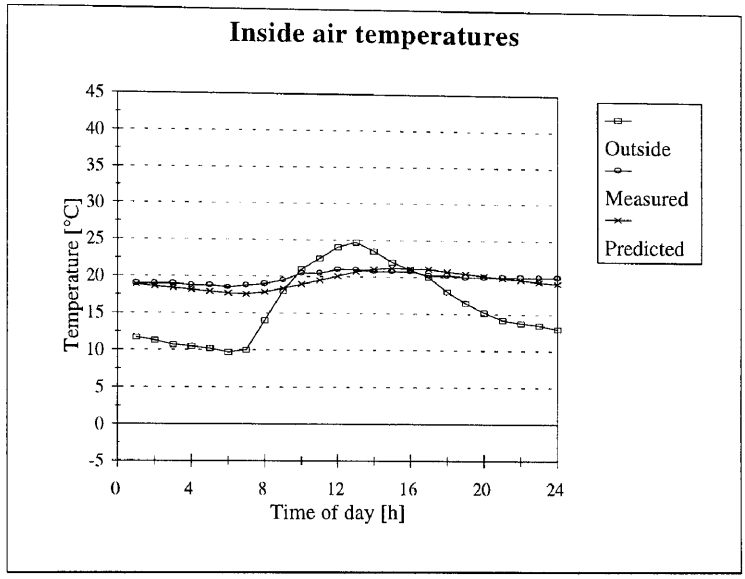

Hour	Measured	Predicted	Hour	Measured	Predicted
1	19.0	18.90	13	21.0	20.73
2	19.0	18.64	14	20.8	21.06
3	19.0	18.39	15	20.8	21.20
4	18.8	18.15	16	20.8	21.15
5	18.8	17.93	17	20.3	21.15
6	18.5	17.71	18	20.3	20.77
7	18.8	17.54	19	20.0	20.50
8	19.0	17.88	20	20.0	20.22
9	19.5	18.39	21	20.0	19.94
10	20.5	18.98	22	20.0	19.67
11	20.5	19.53	23	20.0	19.42
12	21.0	20.11	24	20.0	19.17

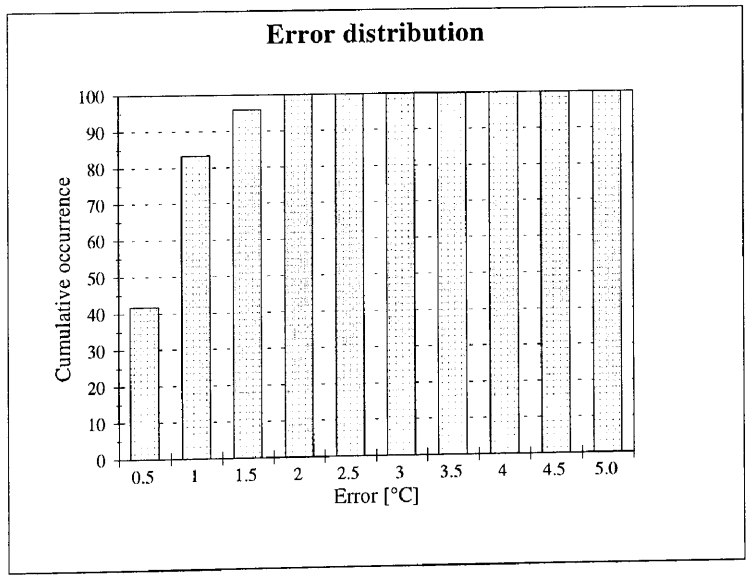

Study 63

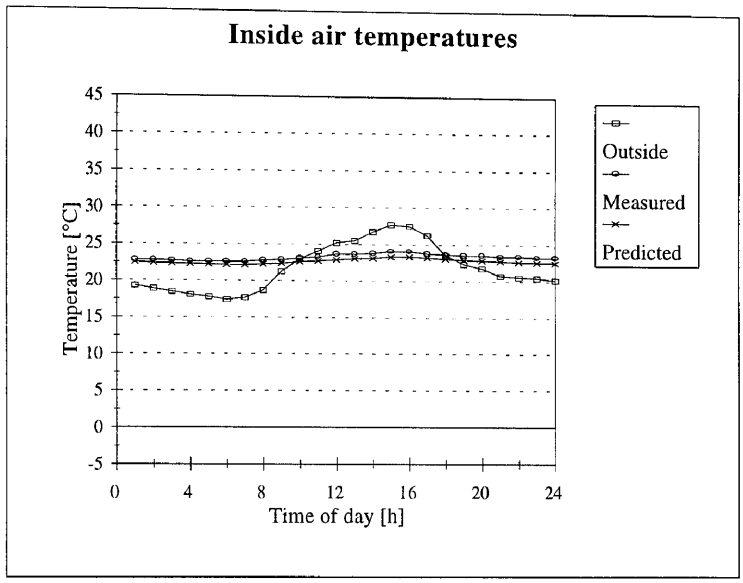

Hour	Measured	Predicted	Hour	Measured	Predicted
1	22.8	22.48	13	23.7	23.04
2	22.8	22.41	14	23.8	23.14
3	22.7	22.34	15	24.1	23.32
4	22.6	22.27	16	24.1	23.35
5	22.6	22.20	17	23.8	23.25
6	22.6	22.14	18	23.7	23.10
7	22.6	22.12	19	23.6	22.96
8	22.8	22.27	20	23.6	22.86
9	22.9	22.41	21	23.4	22.77
10	23.1	22.62	22	23.4	22.69
11	23.3	22.75	23	23.3	22.62
12	23.7	22.92	24	23.3	22.55

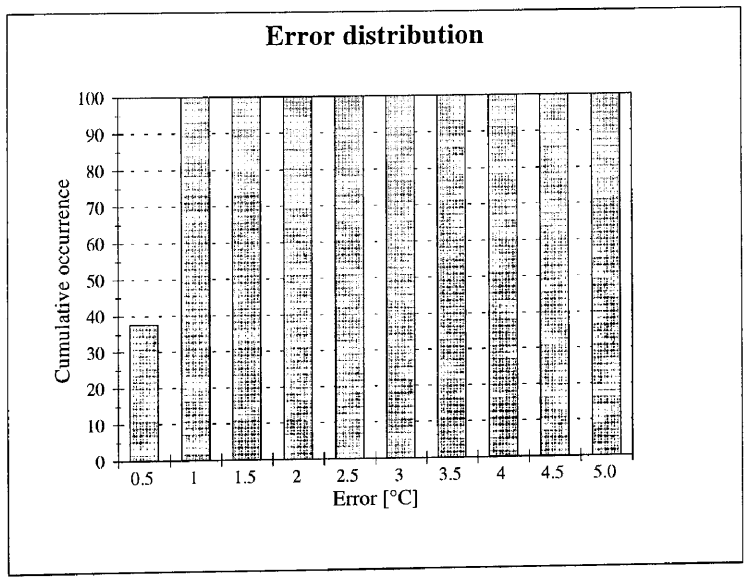

Study 64

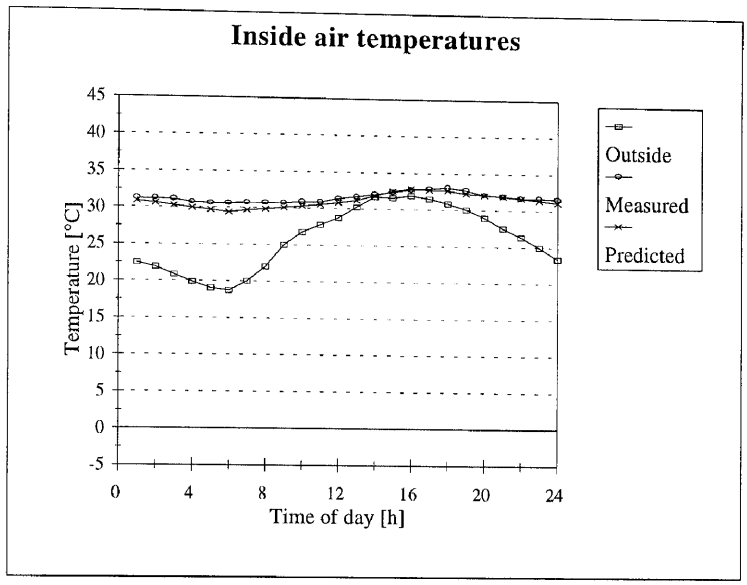

Hour	Measured	Predicted	Hour	Measured	Predicted
1	31.2	30.85	13	31.7	31.17
2	31.2	30.58	14	32.0	31.85
3	31.1	30.29	15	32.4	32.49
4	30.7	29.99	16	32.7	32.89
5	30.6	29.68	17	32.9	32.76
6	30.6	29.42	18	33.1	32.68
7	30.7	29.73	19	32.7	32.30
8	30.7	29.86	20	32.1	32.11
9	30.7	30.08	21	31.9	31.90
10	30.9	30.32	22	31.7	31.67
11	30.9	30.56	23	31.7	31.42
12	31.4	30.86	24	31.6	31.13

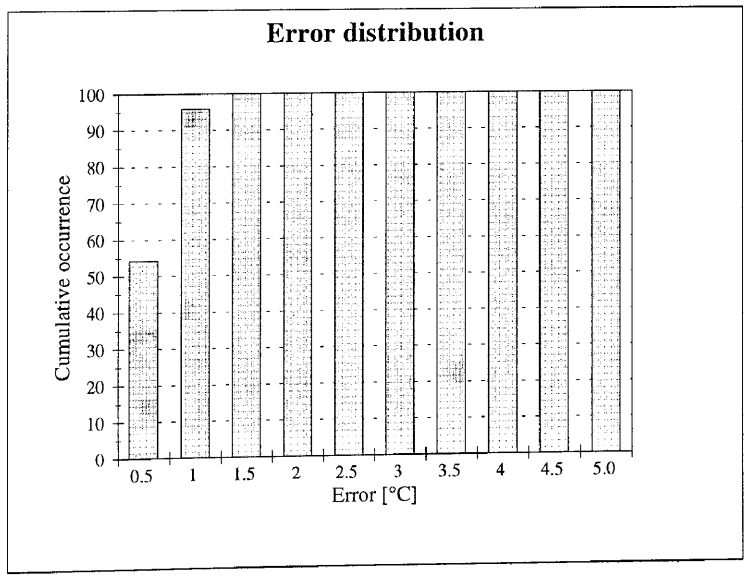

Study 65

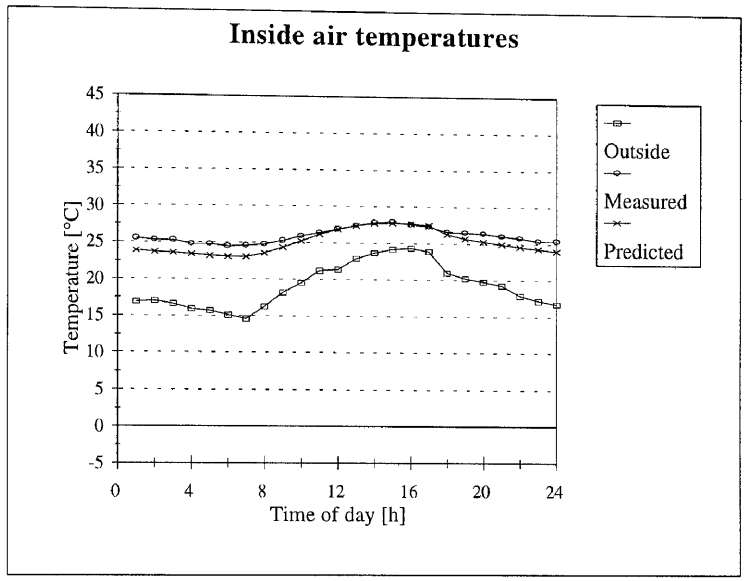

Hour	Measured	Predicted	Hour	Measured	Predicted
1	25.5	23.87	13	27.4	27.35
2	25.3	23.72	14	27.8	27.70
3	25.3	23.56	15	27.9	27.74
4	24.8	23.39	16	27.6	27.72
5	24.8	23.23	17	27.3	27.43
6	24.5	23.07	18	26.6	26.26
7	24.6	23.05	19	26.5	25.71
8	24.8	23.59	20	26.4	25.29
9	25.3	24.40	21	26.0	24.96
10	25.9	25.25	22	25.8	24.61
11	26.4	26.16	23	25.4	24.31
12	26.9	26.87	24	25.4	24.06

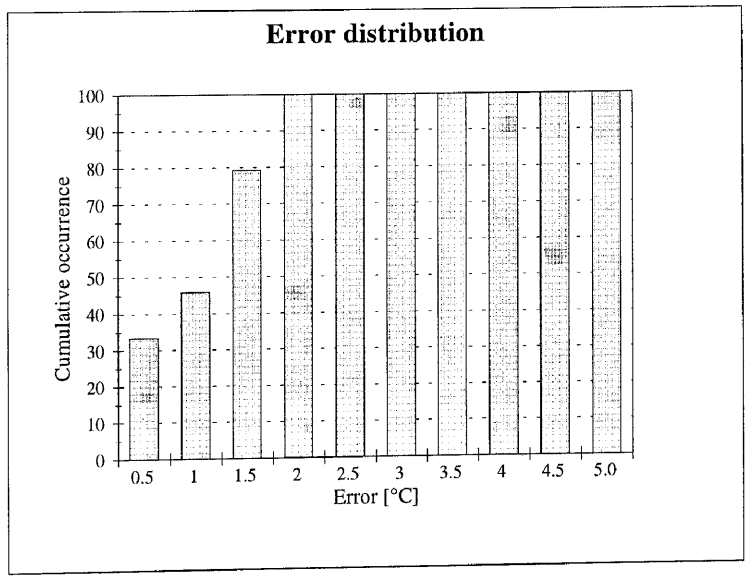

Study 66

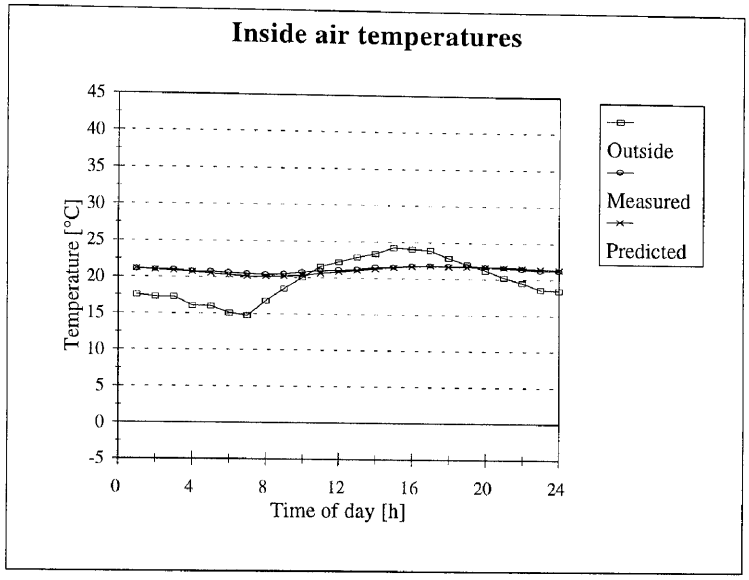

Hour	Measured	Predicted	Hour	Measured	Predicted
1	21.1	21.17	13	21.2	21.08
2	21.0	21.02	14	21.5	21.32
3	21.0	20.89	15	21.6	21.52
4	20.8	20.70	16	21.8	21.68
5	20.8	20.52	17	21.8	21.77
6	20.6	20.31	18	21.8	21.68
7	20.5	20.13	19	21.8	21.69
8	20.4	20.14	20	21.7	21.67
9	20.5	20.20	21	21.6	21.62
10	20.8	20.34	22	21.4	21.54
11	21.0	20.61	23	21.2	21.43
12	21.1	20.87	24	21.2	21.32

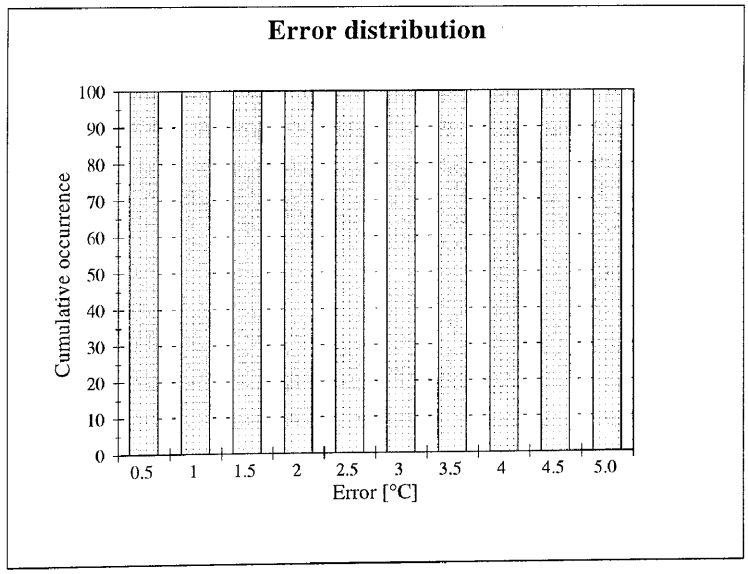

Study 67

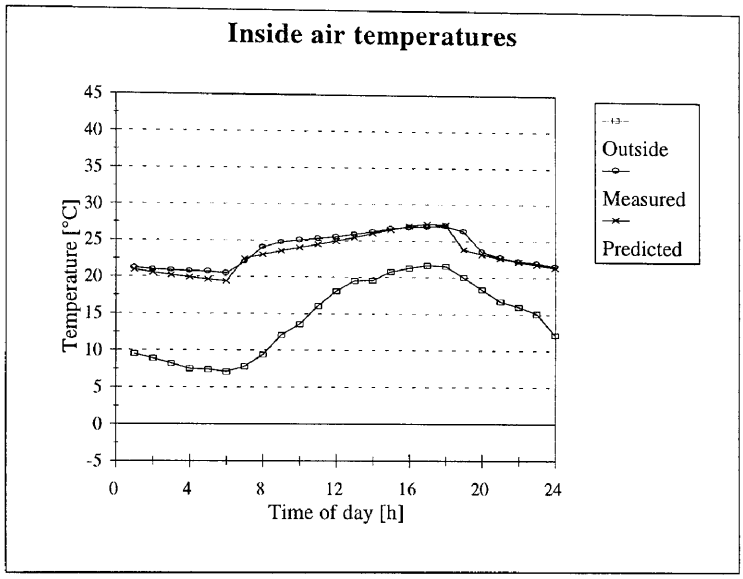

Hour	Measured	Predicted	Hour	Measured	Predicted
1	21.2	20.93	13	25.9	25.49
2	21.0	20.55	14	26.3	26.01
3	20.9	20.21	15	26.7	26.56
4	20.8	19.89	16	26.9	27.04
5	20.7	19.63	17	27.0	27.31
6	20.5	19.39	18	27.1	27.26
7	22.0	22.53	19	26.4	23.88
8	24.1	23.06	20	23.6	23.22
9	24.8	23.57	21	22.8	22.68
10	25.1	24.02	22	22.3	22.23
11	25.3	24.47	23	22.0	21.84
12	25.5	24.95	24	21.6	21.40

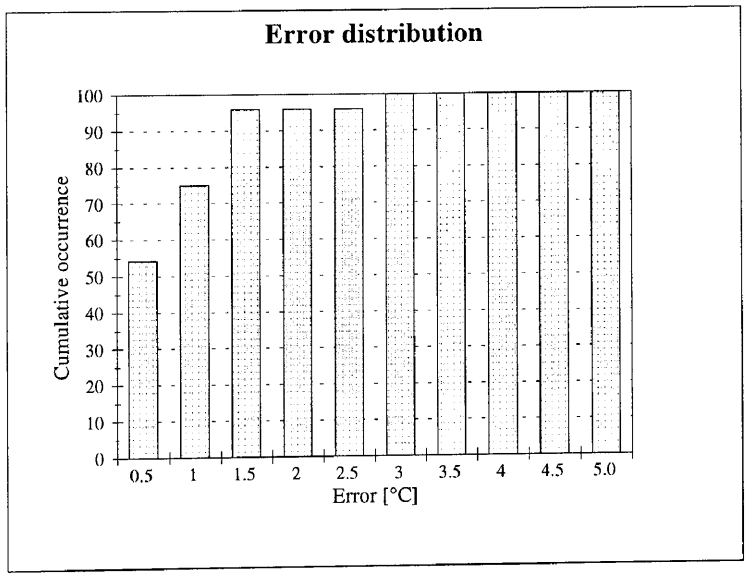

Study 68

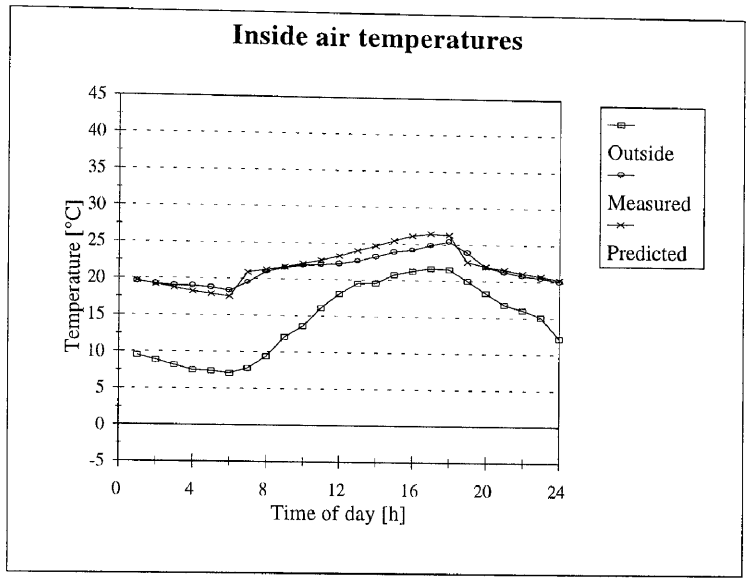

Hour	Measured	Predicted	Hour	Measured	Predicted
1	19.6	19.66	13	22.6	24.00
2	19.2	19.16	14	23.2	24.71
3	19.0	18.70	15	23.9	25.47
4	19.0	18.26	16	24.2	26.13
5	18.8	17.89	17	24.9	26.48
6	18.4	17.55	18	25.4	26.33
7	19.5	20.91	19	23.9	22.63
8	21.0	21.29	20	21.9	22.07
9	21.6	21.73	21	21.3	21.58
10	21.9	22.16	22	20.8	21.15
11	22.0	22.68	23	20.5	20.75
12	22.2	23.29	24	20.0	20.24

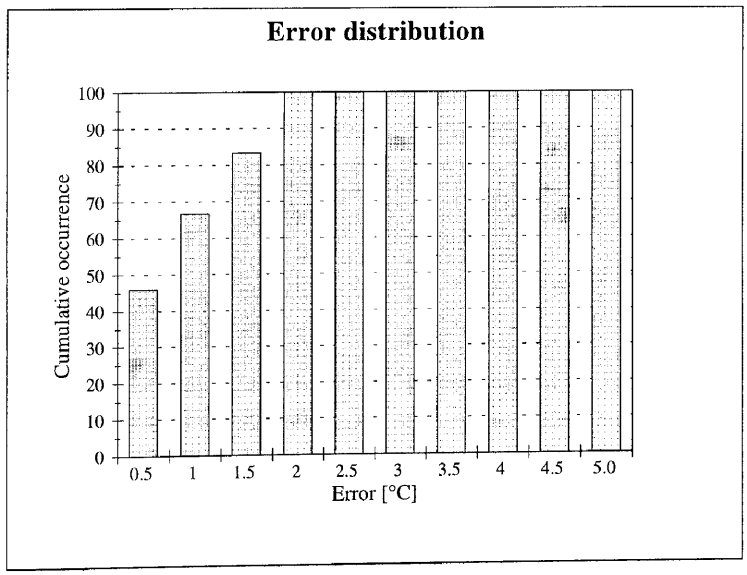

Study 69

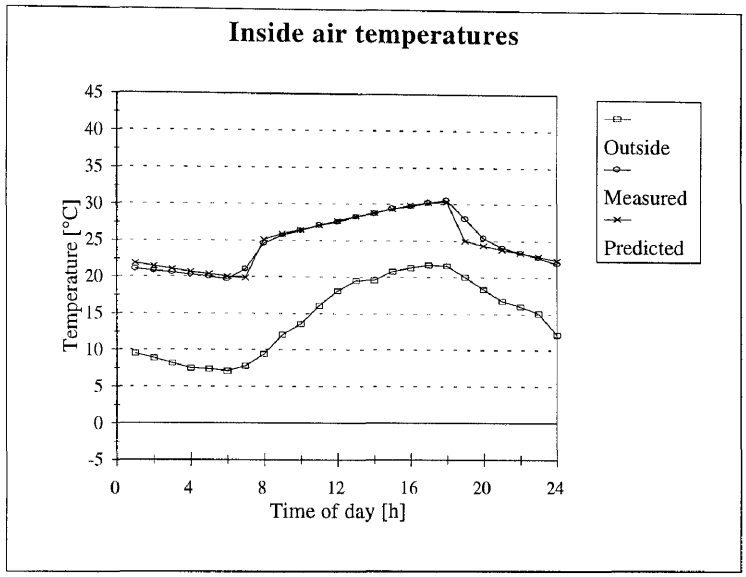

Hour	Measured	Predicted	Hour	Measured	Predicted
1	21.1	21.87	13	28.3	28.32
2	20.8	21.45	14	28.7	28.83
3	20.6	21.04	15	29.4	29.37
4	20.3	20.67	16	29.7	29.85
5	20.0	20.35	17	30.2	30.20
6	19.7	20.06	18	30.6	30.33
7	21.1	19.85	19	28.0	25.01
8	24.6	25.14	20	25.4	24.36
9	25.7	25.90	21	24.1	23.81
10	26.4	26.51	22	23.4	23.35
11	27.1	27.12	23	22.7	22.92
12	27.5	27.73	24	21.9	22.41

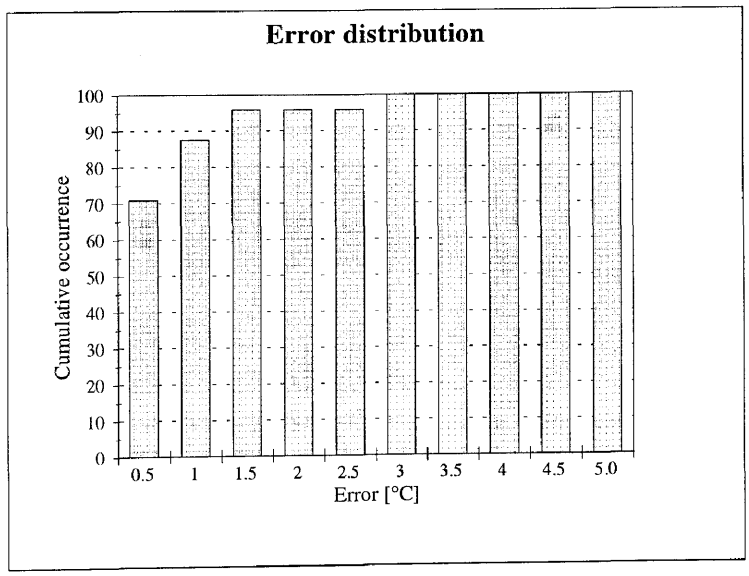

Study 70

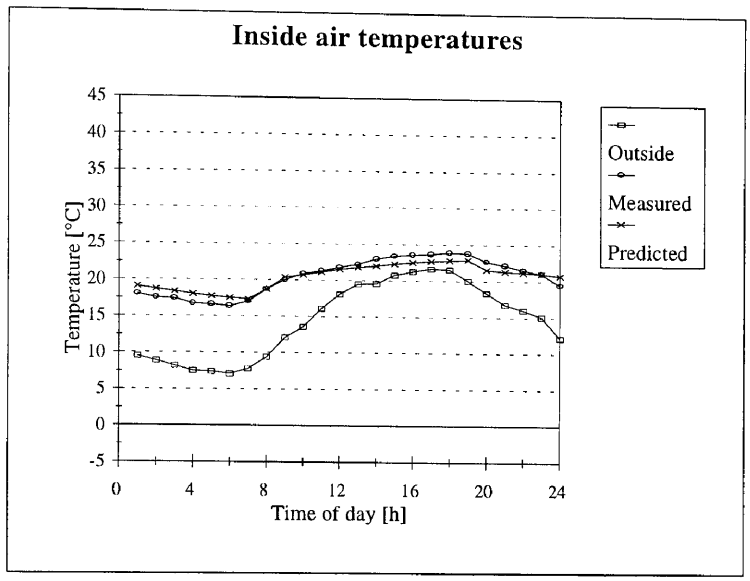

Hour	Measured	Predicted	Hour	Measured	Predicted
1	18.0	19.10	13	22.3	21.80
2	17.5	18.71	14	23.0	22.07
3	17.4	18.36	15	23.4	22.33
4	16.7	18.03	16	23.6	22.56
5	16.6	17.76	17	23.7	22.74
6	16.4	17.51	18	23.9	22.86
7	17.0	17.34	19	23.8	22.94
8	18.7	18.73	20	22.7	21.56
9	20.0	20.39	21	22.2	21.38
10	20.9	20.76	22	21.6	21.21
11	21.3	21.15	23	21.1	21.05
12	21.8	21.50	24	19.5	20.79

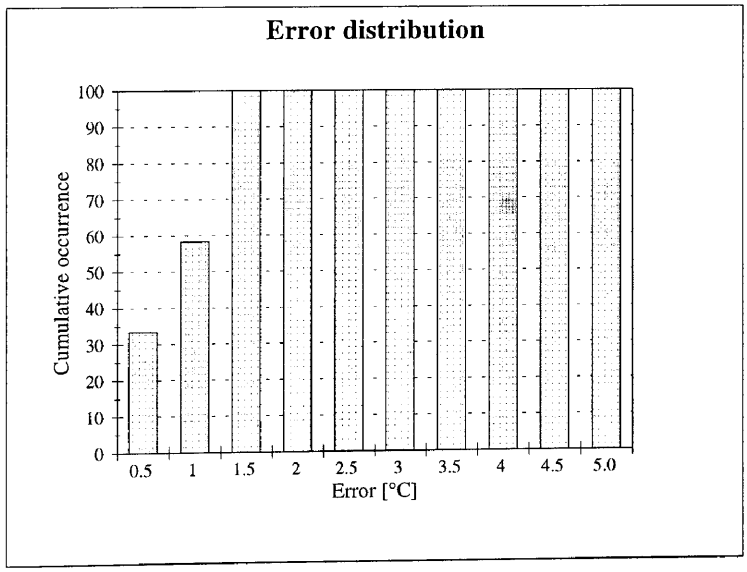

Study 71

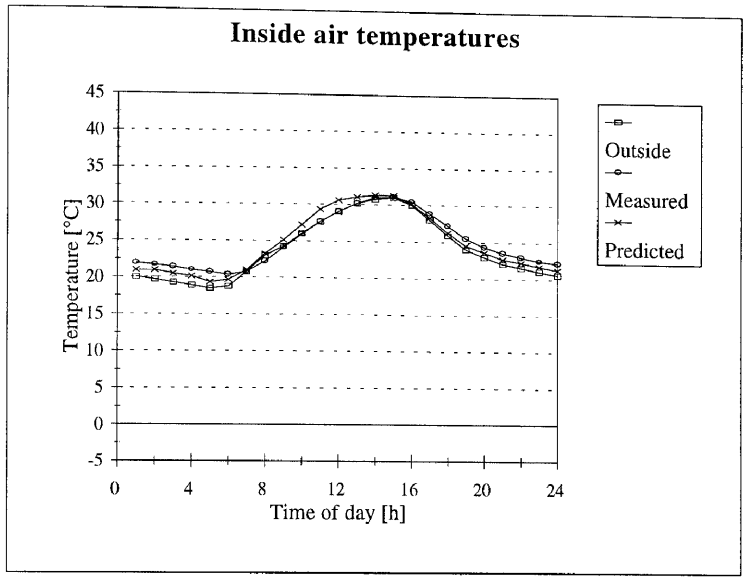

Hour	Measured	Predicted	Hour	Measured	Predicted
1	21.9	20.93	13	30.2	31.04
2	21.7	20.95	14	31.0	31.31
3	21.4	20.52	15	31.1	31.28
4	21.0	20.15	16	30.5	30.21
5	20.7	19.36	17	28.9	28.33
6	20.4	19.71	18	27.2	26.30
7	20.8	21.01	19	25.5	24.56
8	22.2	23.26	20	24.4	23.62
9	24.1	25.13	21	23.6	22.76
10	25.9	27.20	22	23.0	22.24
11	27.7	29.35	23	22.5	21.76
12	29.1	30.65	24	22.2	21.27

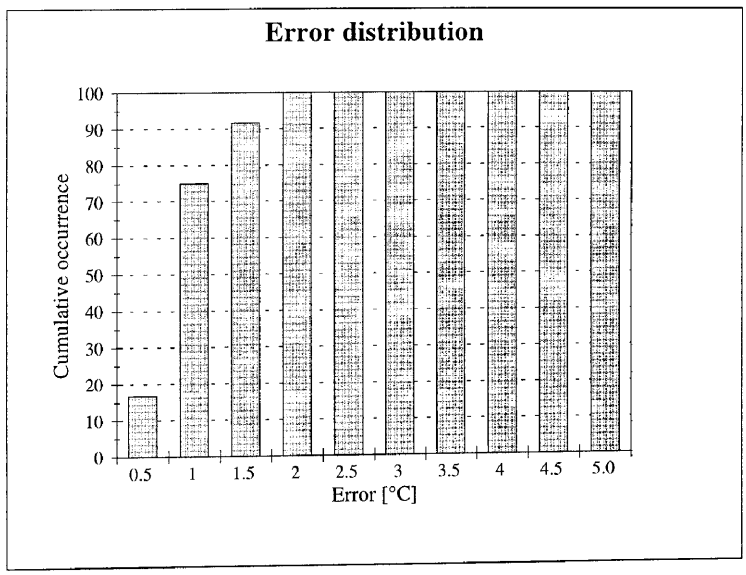

Study 72

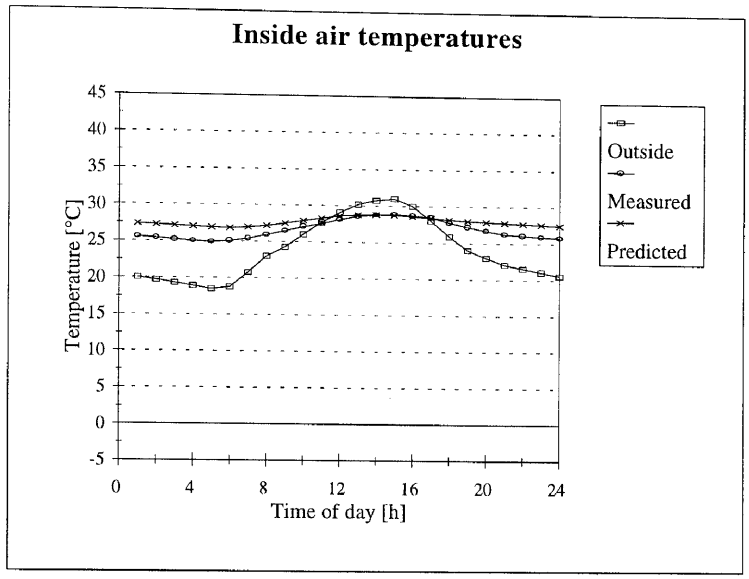

Hour	Measured	Predicted	Hour	Measured	Predicted
1	25.6	27.35	13	28.6	28.77
2	25.4	27.24	14	28.8	28.83
3	25.2	27.14	15	28.9	28.79
4	25.0	27.02	16	28.7	28.62
5	24.9	26.90	17	28.5	28.43
6	25.1	26.84	18	27.8	28.22
7	25.4	26.93	19	27.2	28.05
8	25.9	27.18	20	26.7	27.92
9	26.5	27.53	21	26.3	27.79
10	27.1	27.89	22	26.1	27.68
11	27.5	28.28	23	25.9	27.57
12	28.1	28.58	24	25.8	27.47

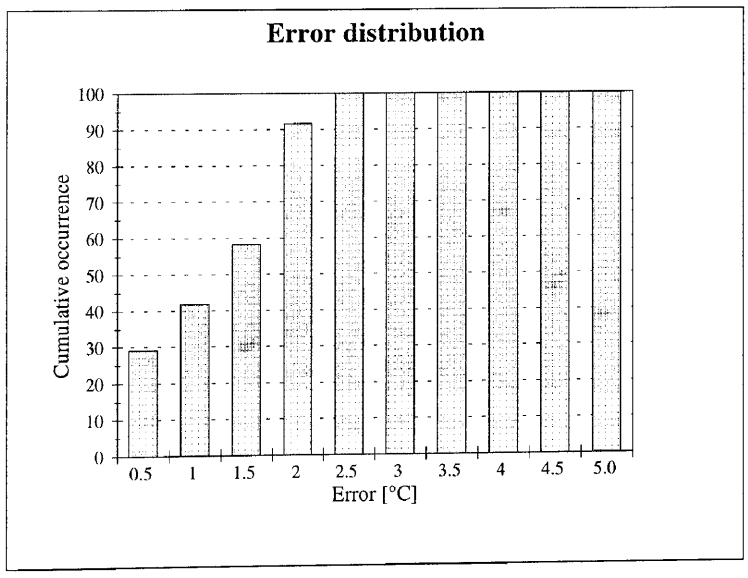

Study 73

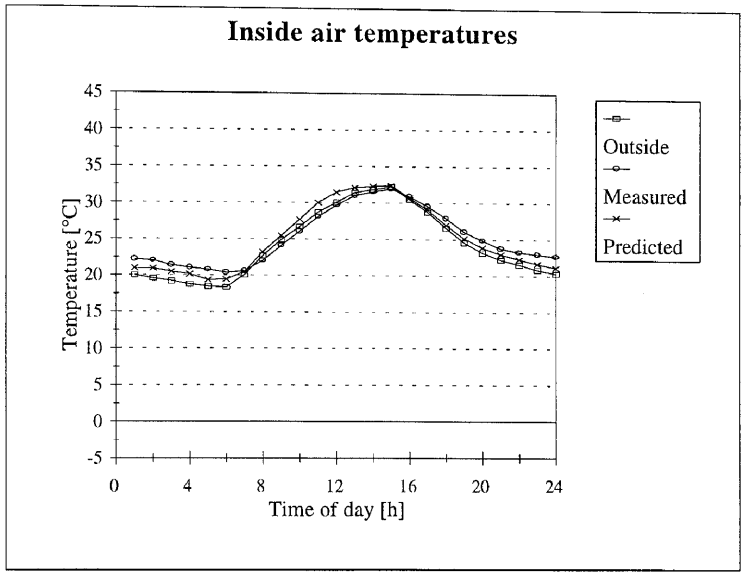

Hour	Measured	Predicted	Hour	Measured	Predicted
1	22.2	20.97	13	31.0	32.10
2	22.0	20.95	14	31.5	32.27
3	21.4	20.52	15	31.9	32.42
4	21.1	20.13	16	30.9	30.74
5	20.8	19.37	17	29.6	29.11
6	20.4	19.43	18	27.9	27.01
7	20.6	20.48	19	26.1	25.18
8	22.0	23.21	20	24.9	23.90
9	24.1	25.49	21	23.8	23.02
10	26.1	27.70	22	23.3	22.33
11	28.1	30.04	23	23.0	21.68
12	29.7	31.45	24	22.7	21.17

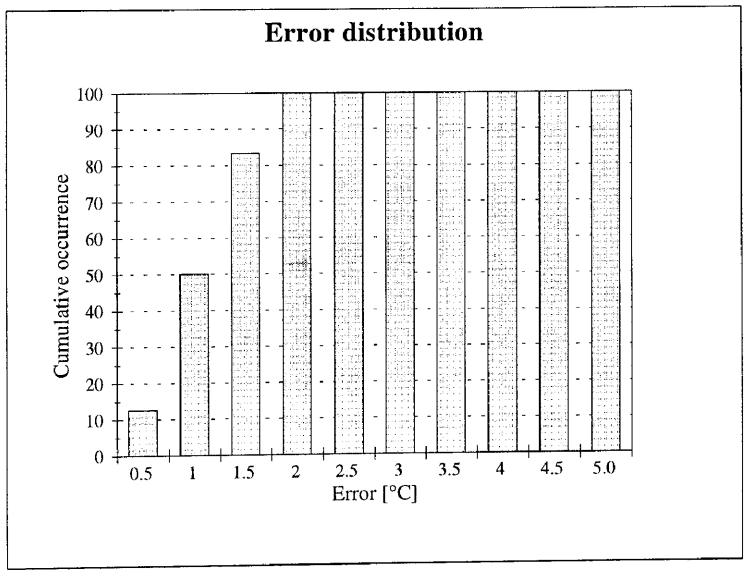

Study 74

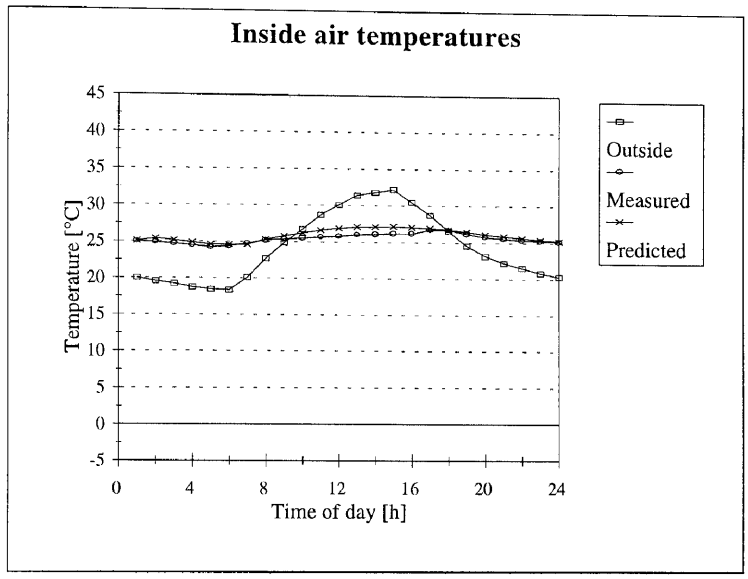

Hour	Measured	Predicted	Hour	Measured	Predicted
1	25.0	25.09	13	26.0	27.08
2	24.9	25.40	14	26.1	27.15
3	24.7	25.19	15	26.2	27.17
4	24.5	24.91	16	26.2	27.08
5	24.3	24.60	17	26.7	26.97
6	24.4	24.61	18	26.7	26.79
7	24.8	24.60	19	26.2	26.49
8	25.2	25.36	20	25.8	26.19
9	25.4	25.79	21	25.6	25.91
10	25.5	26.20	22	25.4	25.69
11	25.7	26.59	23	25.3	25.48
12	25.8	26.89	24	25.2	25.28

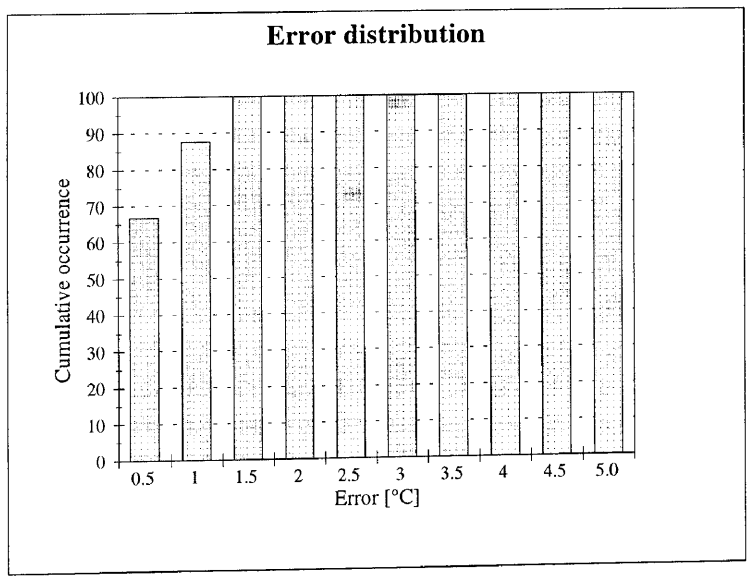

Study 75

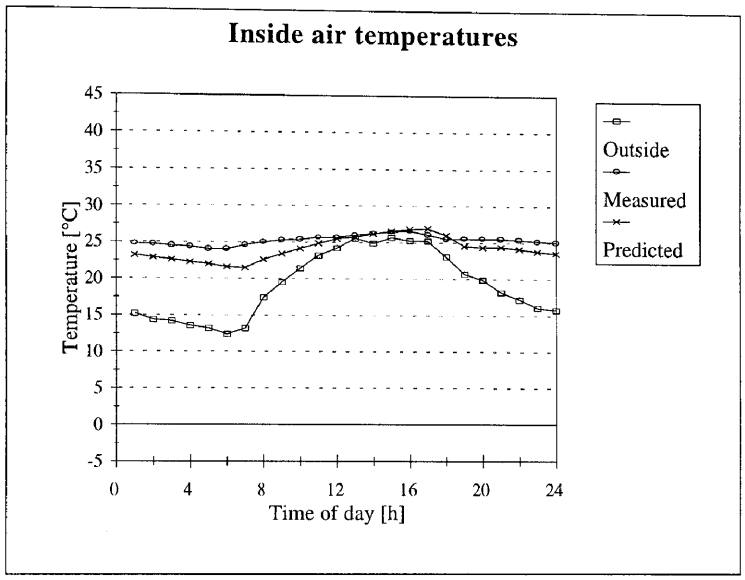

Hour	Measured	Predicted	Hour	Measured	Predicted
1	24.8	23.23	13	26.0	25.74
2	24.7	22.90	14	26.3	26.20
3	24.5	22.60	15	26.5	26.61
4	24.4	22.28	16	26.6	26.86
5	24.0	21.99	17	26.1	26.97
6	24.0	21.61	18	25.5	26.07
7	24.6	21.48	19	25.6	24.56
8	25.0	22.59	20	25.6	24.42
9	25.3	23.40	21	25.5	24.45
10	25.4	24.15	22	25.4	24.17
11	25.7	24.85	23	25.2	23.80
12	25.7	25.51	24	25.1	23.56

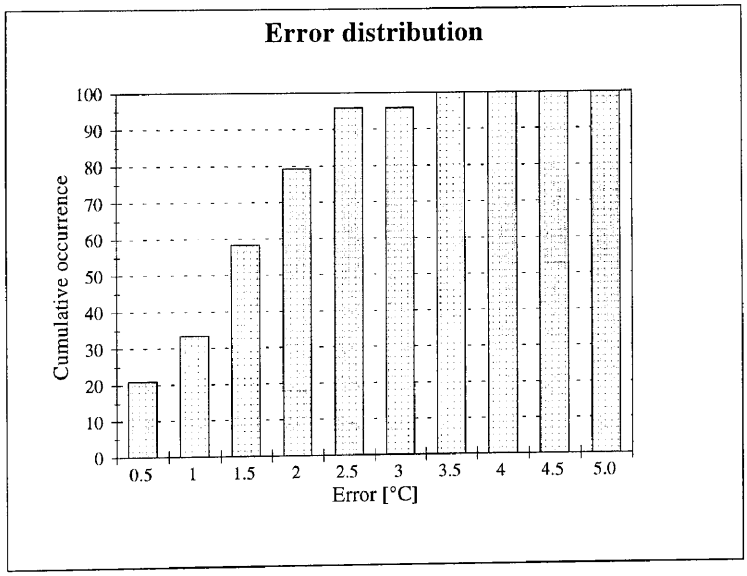

Study 76

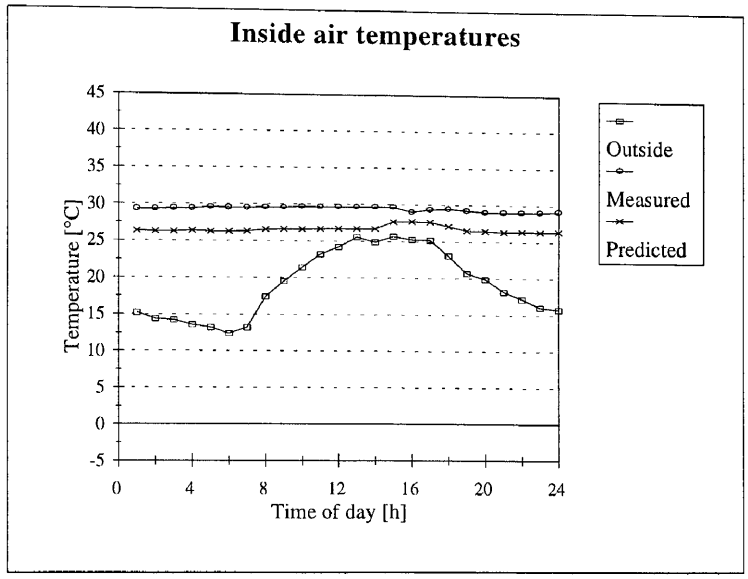

Hour	Measured	Predicted	Hour	Measured	Predicted
1	29.3	26.34	13	29.7	26.74
2	29.3	26.29	14	29.7	26.71
3	29.4	26.28	15	29.7	27.67
4	29.4	26.35	16	29.1	27.75
5	29.6	26.29	17	29.4	27.68
6	29.5	26.26	18	29.5	27.13
7	29.5	26.32	19	29.3	26.55
8	29.6	26.56	20	29.1	26.49
9	29.6	26.59	21	29.1	26.41
10	29.7	26.62	22	29.1	26.44
11	29.7	26.69	23	29.1	26.41
12	29.7	26.75	24	29.2	26.44

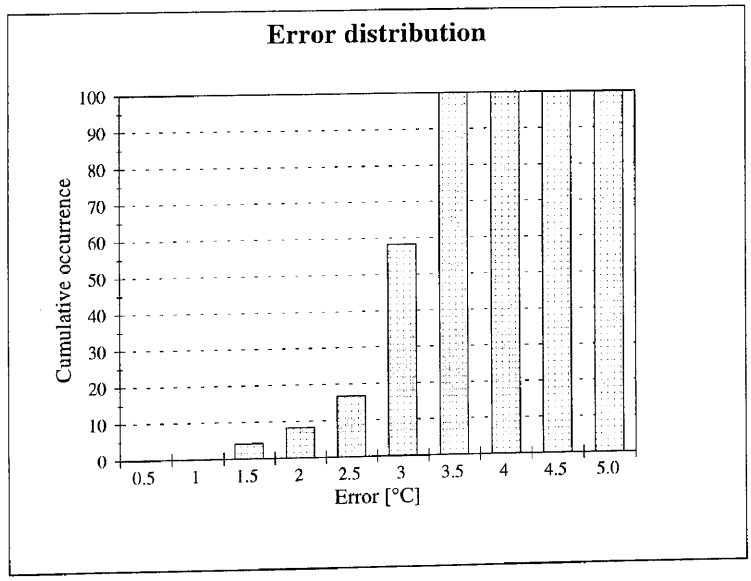

Study 77

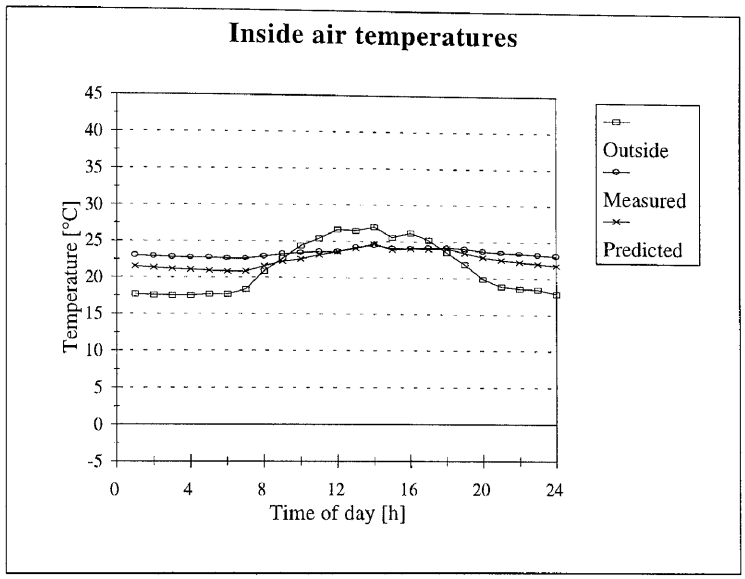

Hour	Measured	Predicted	Hour	Measured	Predicted
1	23.0	21.50	13	24.2	24.05
2	22.9	21.35	14	24.5	24.66
3	22.8	21.18	15	24.1	23.88
4	22.7	21.09	16	24.1	24.06
5	22.7	20.94	17	24.2	23.98
6	22.6	20.81	18	24.2	24.09
7	22.6	20.85	19	24.0	23.49
8	22.9	21.56	20	23.7	22.92
9	23.2	22.22	21	23.5	22.56
10	23.4	22.57	22	23.4	22.28
11	23.6	23.15	23	23.2	22.07
12	23.6	23.56	24	23.1	21.79

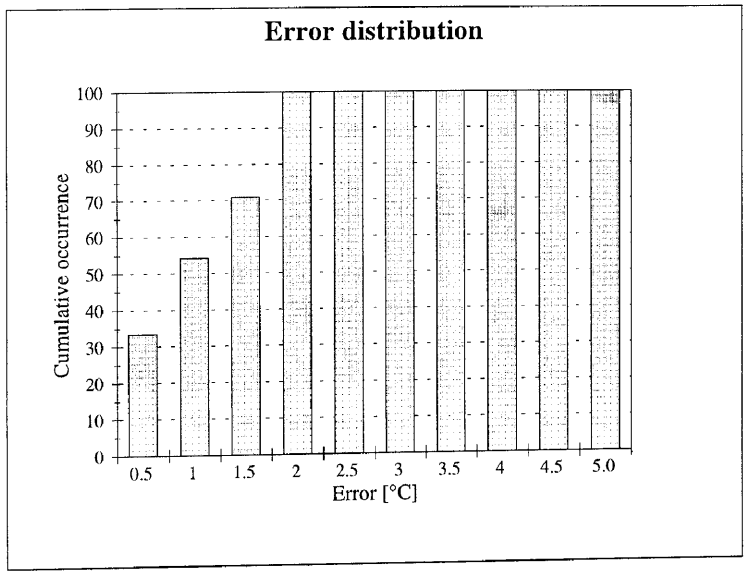

Study 78

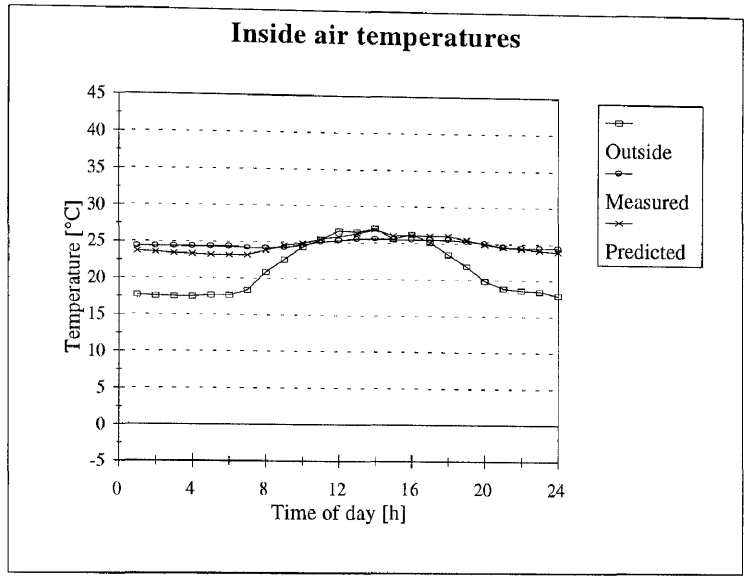

Hour	Measured	Predicted	Hour	Measured	Predicted
1	24.4	23.71	13	25.5	26.24
2	24.4	23.58	14	25.6	26.84
3	24.4	23.41	15	25.5	26.00
4	24.4	23.34	16	25.5	26.11
5	24.4	23.24	17	25.5	26.04
6	24.4	23.16	18	25.5	26.07
7	24.2	23.22	19	25.3	25.52
8	24.2	23.87	20	25.1	24.95
9	24.3	24.57	21	24.6	24.55
10	24.6	24.90	22	24.5	24.35
11	25.1	25.46	23	24.5	24.12
12	25.3	25.81	24	24.5	23.91

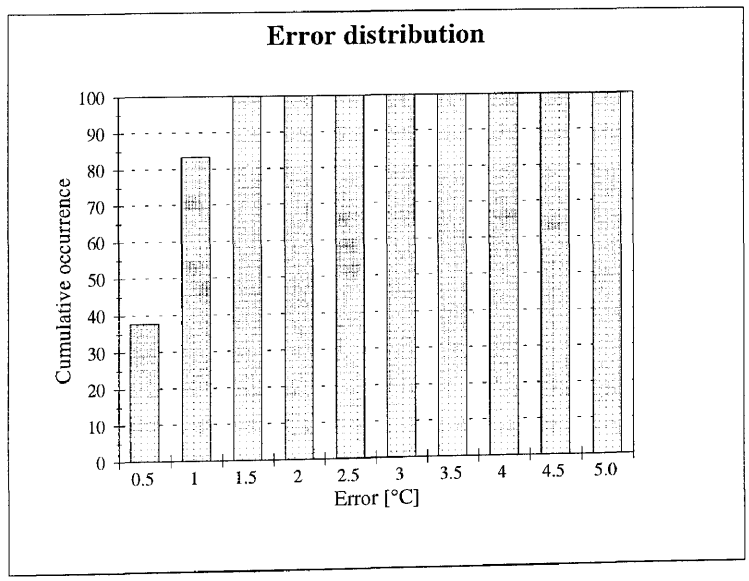

Study 79

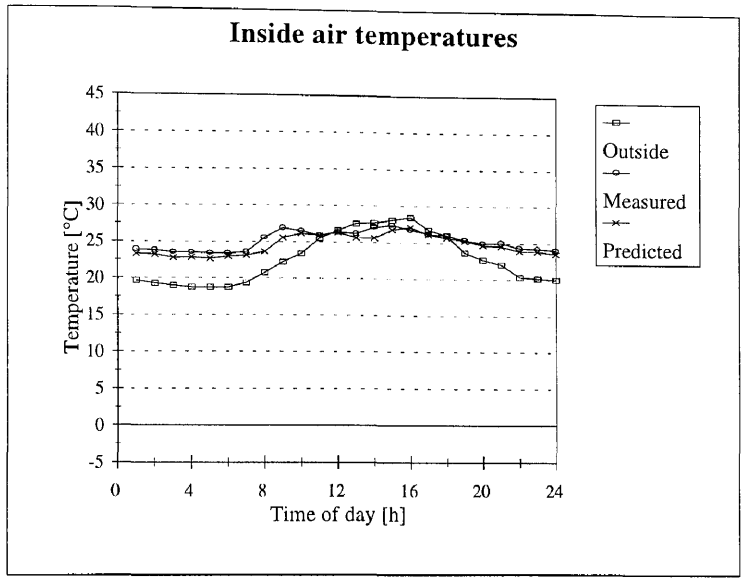

Hour	Measured	Predicted	Hour	Measured	Predicted
1	23.9	23.32	13	26.2	25.65
2	23.8	23.22	14	27.1	25.63
3	23.5	22.78	15	27.4	26.80
4	23.5	22.87	16	26.8	27.13
5	23.4	22.69	17	26.2	26.15
6	23.4	22.94	18	26.0	25.72
7	23.6	23.15	19	25.4	25.31
8	25.6	23.64	20	25.0	24.73
9	26.9	25.56	21	25.1	24.63
10	26.5	26.13	22	24.4	23.94
11	25.9	25.91	23	24.3	23.91
12	26.4	26.32	24	24.1	23.55

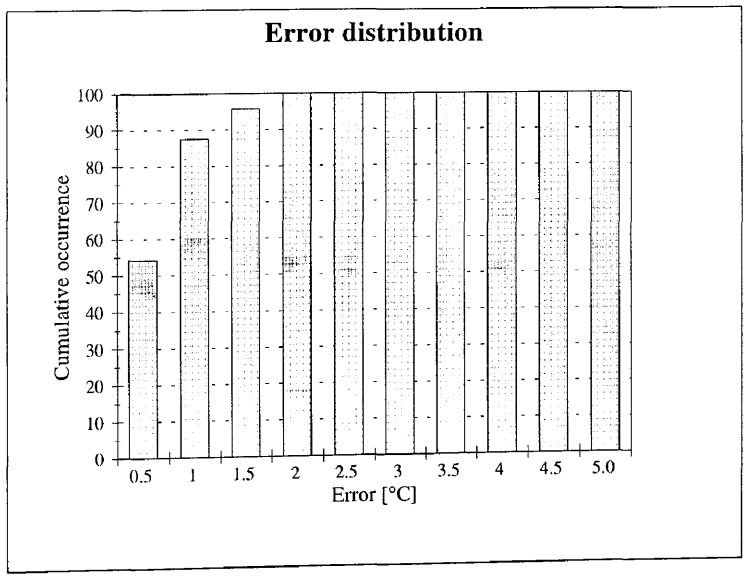

Study 80

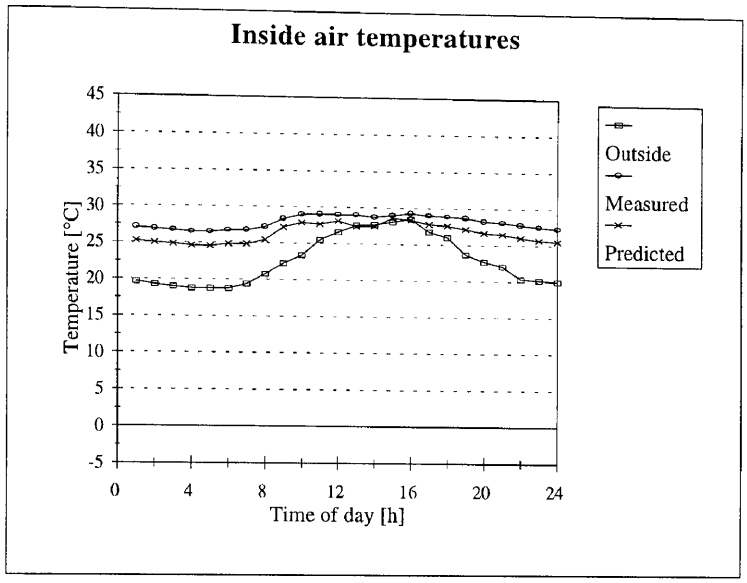

Hour	Measured	Predicted	Hour	Measured	Predicted
1	27.1	25.24	13	29.0	27.42
2	26.9	25.03	14	28.7	27.47
3	26.7	24.83	15	29.0	28.63
4	26.5	24.63	16	29.3	28.41
5	26.5	24.57	17	29.0	27.78
6	26.7	24.85	18	28.9	27.62
7	26.8	24.86	19	28.7	27.17
8	27.2	25.43	20	28.3	26.69
9	28.4	27.22	21	28.1	26.47
10	29.0	27.85	22	27.8	26.02
11	29.1	27.66	23	27.5	25.73
12	29.0	28.12	24	27.3	25.53

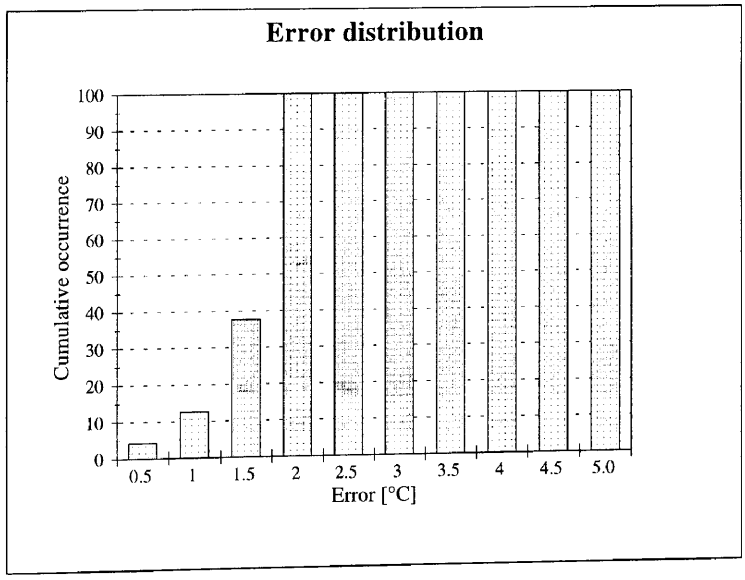

Study 81

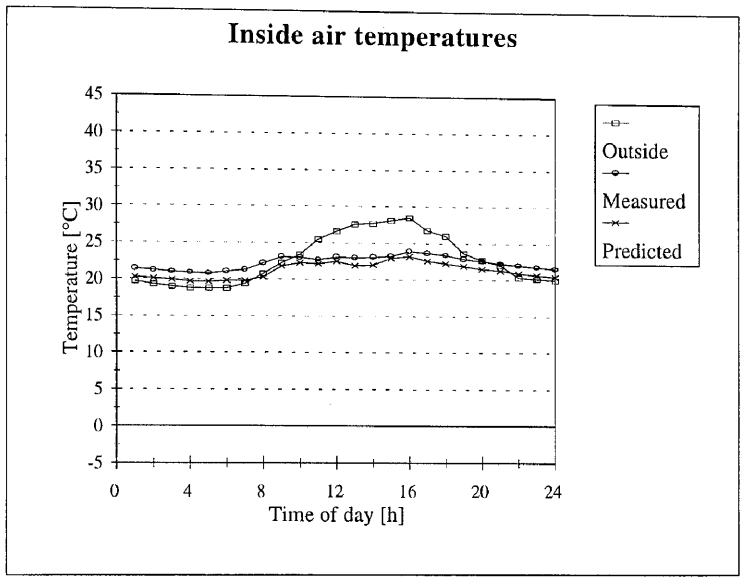

Hour	Measured	Predicted	Hour	Measured	Predicted
1	21.4	20.26	13	23.0	21.96
2	21.2	20.08	14	23.1	22.02
3	21.0	19.89	15	23.2	22.97
4	20.9	19.71	16	23.9	23.20
5	20.8	19.64	17	23.7	22.59
6	21.1	19.83	18	23.4	22.26
7	21.3	19.84	19	22.9	21.91
8	22.2	20.31	20	22.6	21.52
9	23.1	21.83	21	22.3	21.32
10	23.0	22.25	22	22.0	20.95
11	22.7	22.12	23	21.8	20.70
12	23.1	22.49	24	21.6	20.53

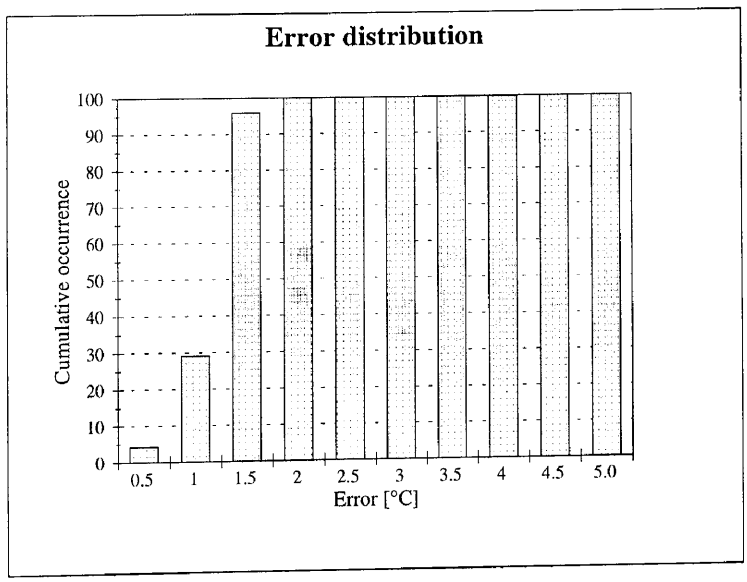

Study 82

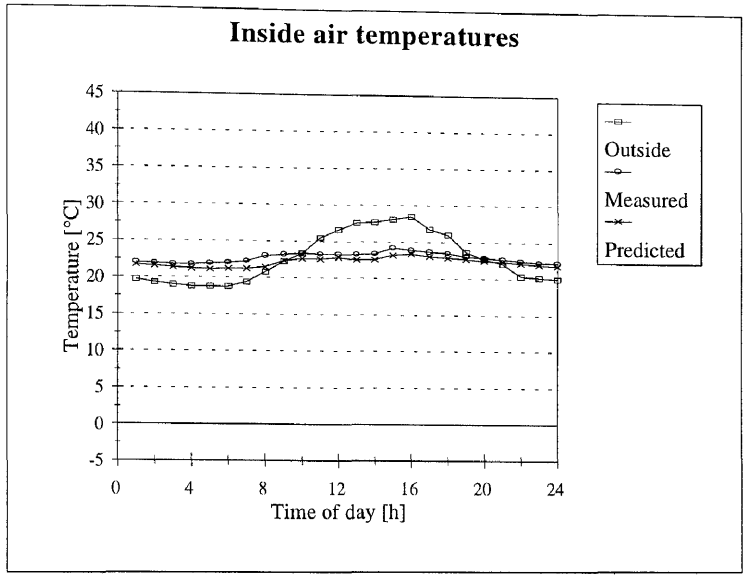

Hour	Measured	Predicted	Hour	Measured	Predicted
1	22.0	21.66	13	23.3	22.54
2	21.9	21.51	14	23.4	22.59
3	21.8	21.37	15	24.2	23.22
4	21.8	21.22	16	23.9	23.41
5	21.9	21.14	17	23.7	23.07
6	22.0	21.22	18	23.5	22.90
7	22.3	21.20	19	23.1	22.71
8	23.0	21.46	20	22.9	22.48
9	23.2	22.39	21	22.7	22.36
10	23.4	22.66	22	22.5	22.13
11	23.3	22.60	23	22.3	21.97
12	23.3	22.85	24	22.2	21.84

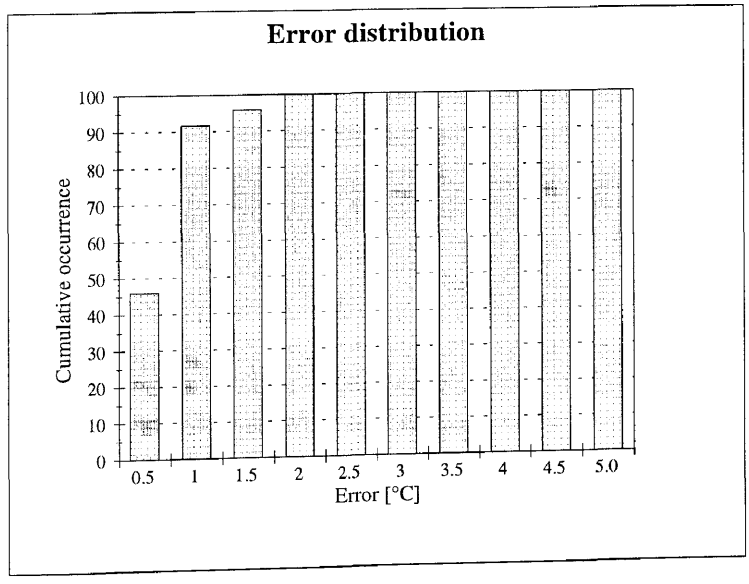

Study 83

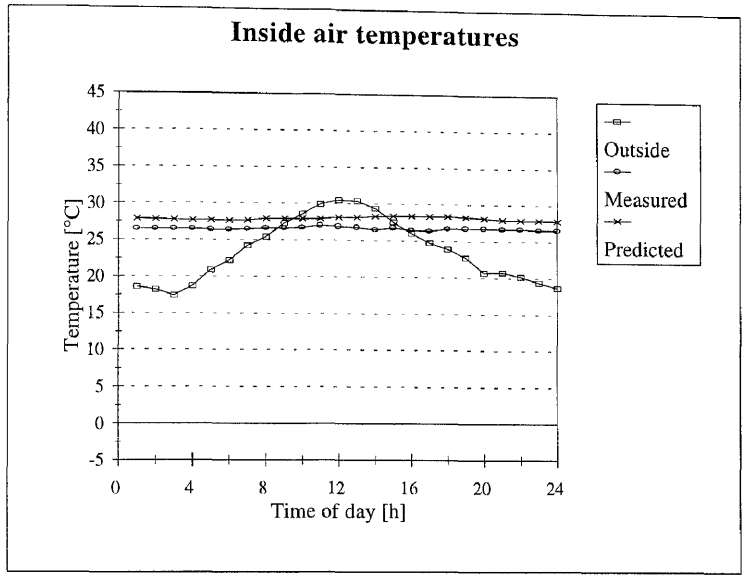

Hour	Measured	Predicted	Hour	Measured	Predicted
1	26.5	27.86	13	26.8	28.17
2	26.5	27.81	14	26.5	28.32
3	26.5	27.74	15	26.8	28.35
4	26.5	27.69	16	26.5	28.40
5	26.4	27.67	17	26.4	28.41
6	26.4	27.65	18	26.7	28.38
7	26.5	27.69	19	26.8	28.32
8	26.6	27.91	20	26.8	28.12
9	26.6	27.94	21	26.7	27.99
10	26.7	27.93	22	26.7	27.93
11	27.0	27.91	23	26.6	27.90
12	26.9	28.13	24	26.6	27.88

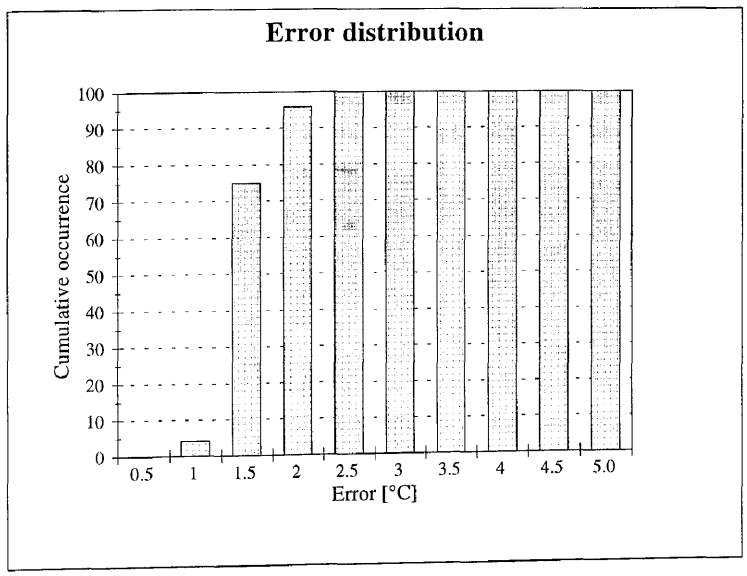

Study 84

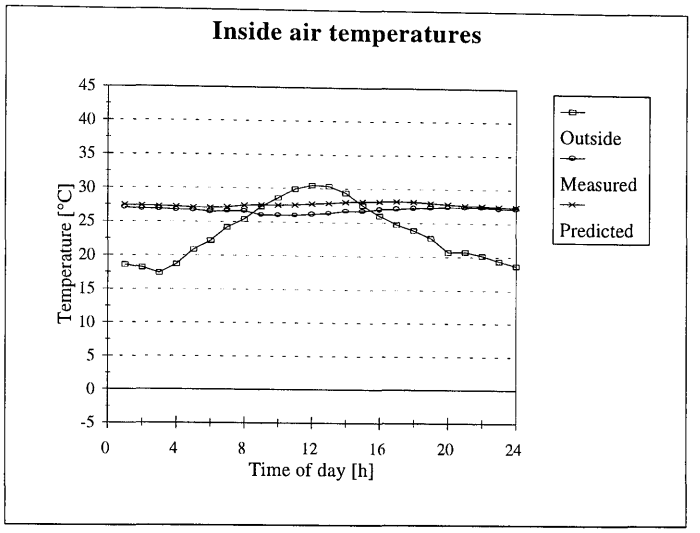

Hour	Measured	Predicted	Hour	Measured	Predicted
1	27.1	27.48	13	26.4	27.86
2	26.9	27.37	14	26.7	28.05
3	26.9	27.30	15	26.7	28.14
4	26.8	27.22	16	27.0	28.18
5	26.8	27.15	17	27.1	28.20
6	26.5	27.13	18	27.2	28.15
7	26.6	27.18	19	27.3	27.99
8	26.6	27.43	20	27.4	27.81
9	26.0	27.50	21	27.4	27.64
10	26.0	27.53	22	27.4	27.56
11	26.0	27.55	23	27.2	27.49
12	26.2	27.74	24	27.2	27.49

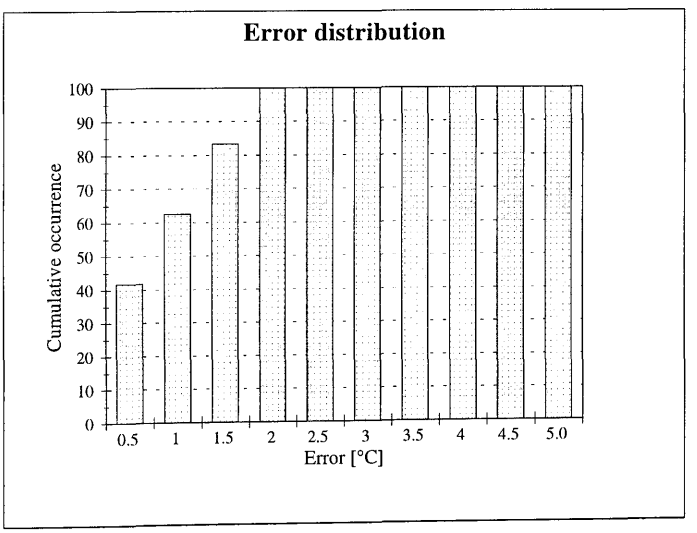

Study 85

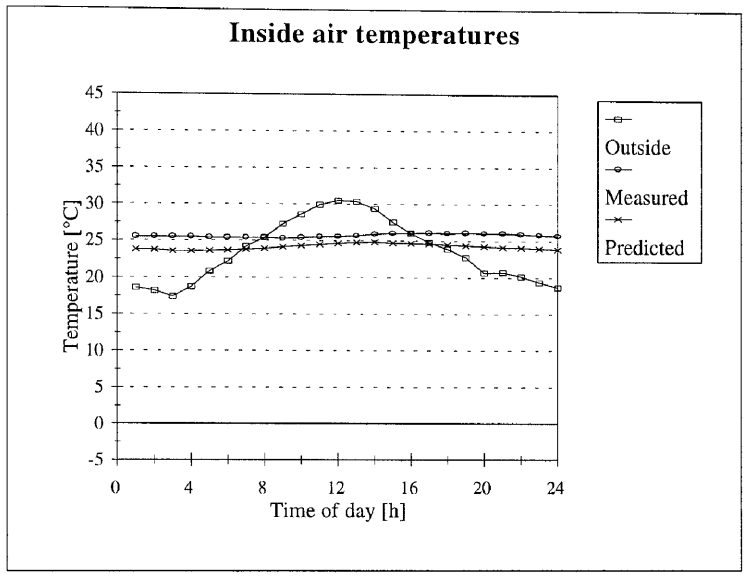

Hour	Measured	Predicted	Hour	Measured	Predicted
1	25.5	23.80	13	25.7	24.78
2	25.5	23.74	14	25.9	24.83
3	25.5	23.58	15	26.0	24.76
4	25.5	23.56	16	26.0	24.69
5	25.4	23.65	17	26.1	24.58
6	25.4	23.72	18	26.0	24.51
7	25.4	23.83	19	26.1	24.41
8	25.4	23.94	20	26.0	24.26
9	25.3	24.13	21	26.0	24.17
10	25.4	24.31	22	25.9	24.10
11	25.5	24.50	23	25.8	23.97
12	25.6	24.68	24	25.7	23.87

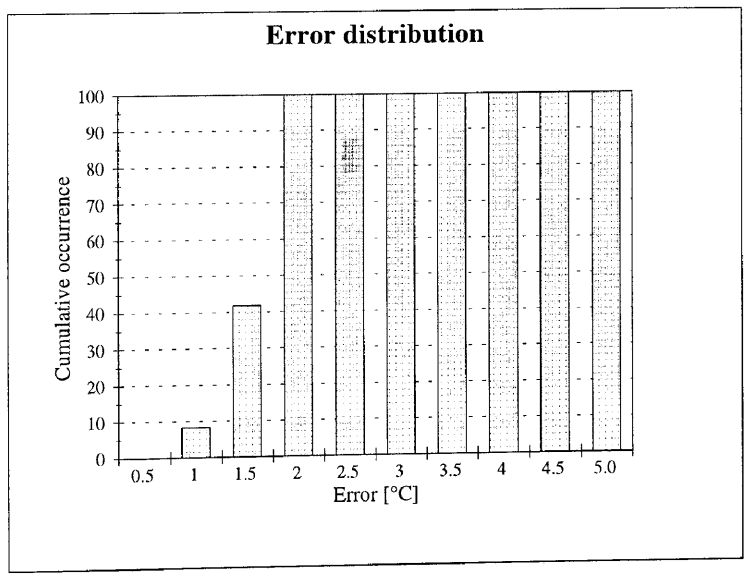

Study 86

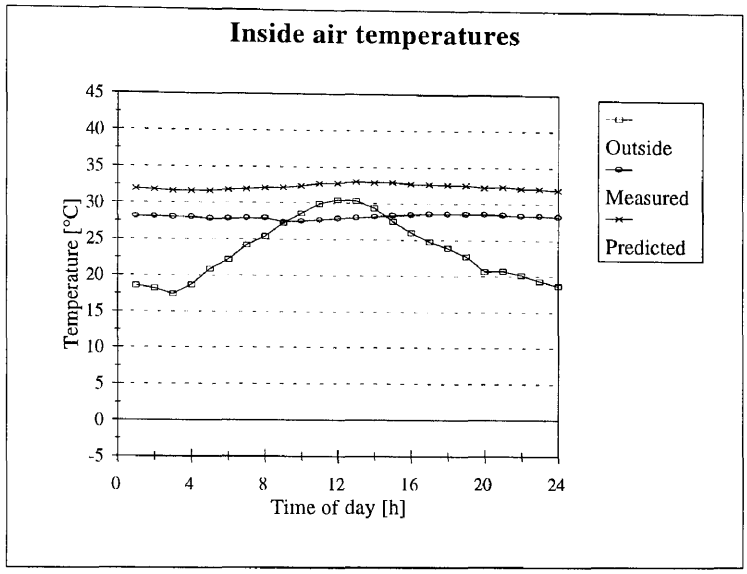

Hour	Measured	Predicted	Hour	Measured	Predicted
1	28.1	28.90	13	28.0	30.00
2	28.1	28.80	14	28.2	29.90
3	28.0	28.70	15	28.4	29.90
4	28.0	28.70	16	28.5	29.70
5	27.8	28.70	17	28.6	29.70
6	27.8	28.80	18	28.6	29.60
7	27.9	29.00	19	28.6	29.60
8	27.9	29.10	20	28.6	29.30
9	27.4	29.20	21	28.5	29.40
10	27.5	29.40	22	28.4	29.40
11	27.7	29.70	23	28.4	29.10
12	27.9	29.80	24	28.3	28.90

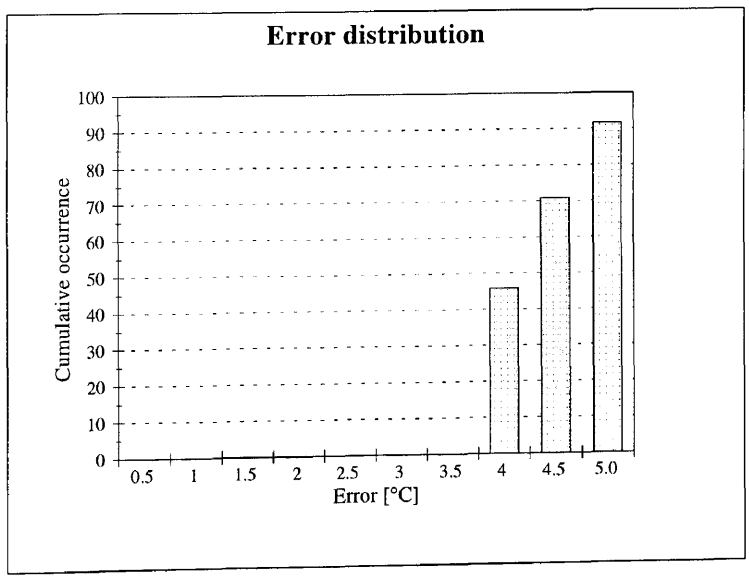

Study 87

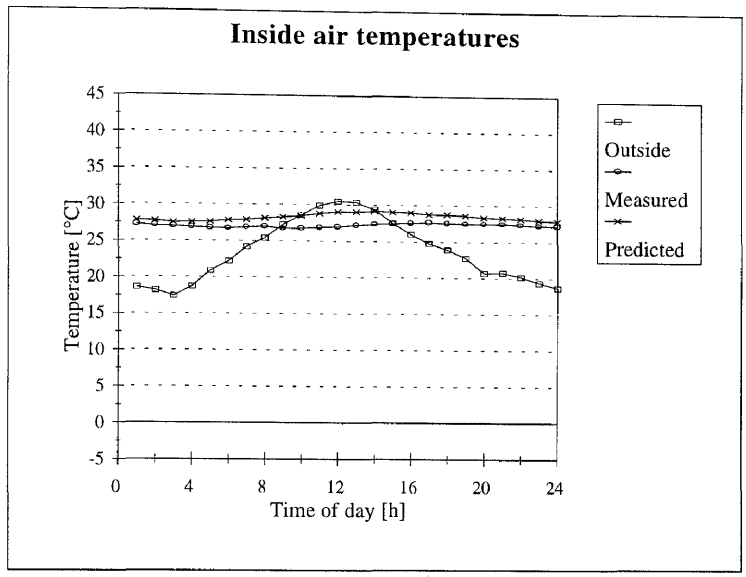

Hour	Measured	Predicted	Hour	Measured	Predicted
1	27.2	27.83	13	27.2	29.05
2	27.1	27.76	14	27.4	29.23
3	27.0	27.52	15	27.5	29.06
4	26.9	27.60	16	27.6	29.02
5	26.8	27.63	17	27.7	28.79
6	26.7	27.85	18	27.6	28.77
7	26.9	27.92	19	27.5	28.60
8	27.0	28.13	20	27.5	28.39
9	26.7	28.32	21	27.5	28.31
10	26.8	28.53	22	27.4	28.22
11	26.9	28.82	23	27.3	28.04
12	27.0	29.05	24	27.2	27.90

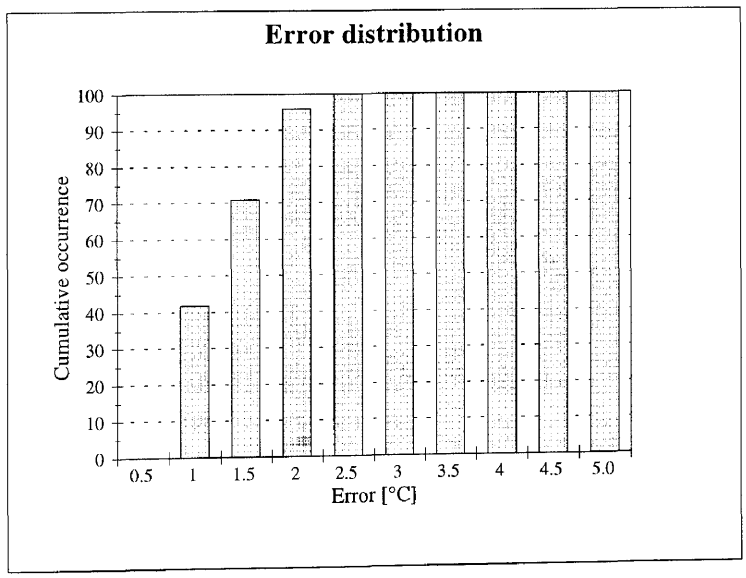

Study 88

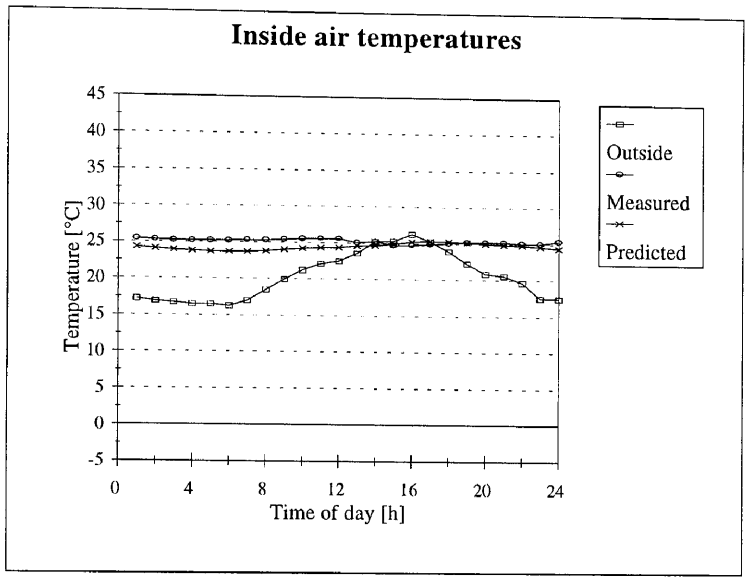

Hour	Measured	Predicted	Hour	Measured	Predicted
1	25.4	24.25	13	25.1	24.59
2	25.3	24.11	14	25.2	24.69
3	25.2	23.95	15	24.7	24.89
4	25.2	23.84	16	24.8	25.24
5	25.2	23.72	17	24.9	25.31
6	25.2	23.68	18	25.1	25.30
7	25.3	23.70	19	25.2	25.18
8	25.3	23.82	20	25.2	25.02
9	25.4	24.04	21	25.2	24.91
10	25.5	24.20	22	25.1	24.85
11	25.6	24.34	23	25.1	24.67
12	25.6	24.37	24	25.4	24.45

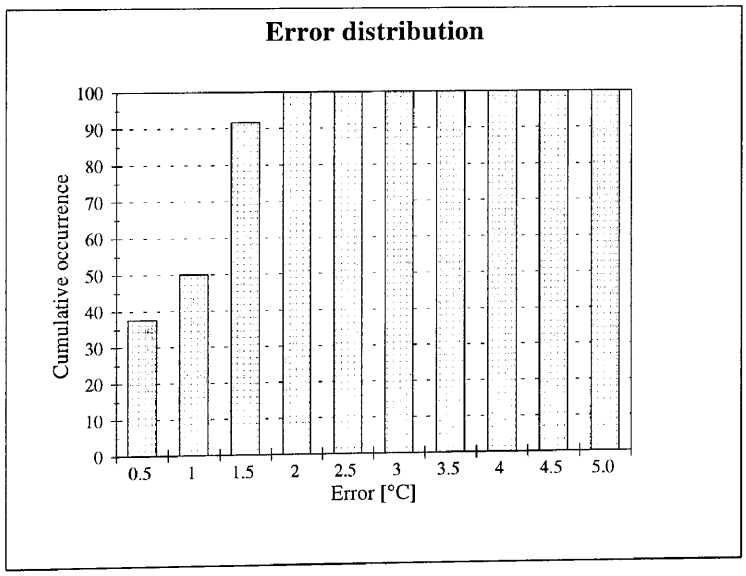

Study 89

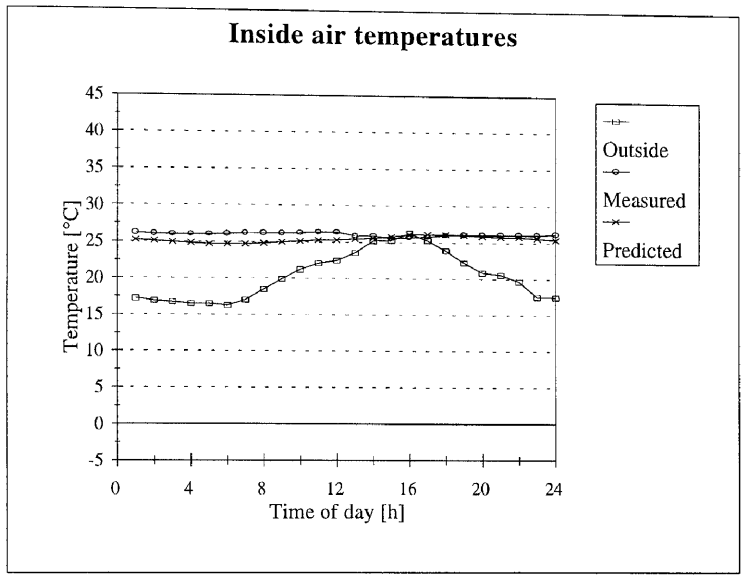

Hour	Measured	Predicted	Hour	Measured	Predicted
1	26.2	25.26	13	25.9	25.49
2	26.1	25.13	14	25.9	25.58
3	26.0	24.97	15	25.6	25.78
4	26.0	24.86	16	25.7	26.09
5	26.0	24.75	17	25.8	26.17
6	26.1	24.70	18	26.0	26.17
7	26.2	24.71	19	26.1	26.07
8	26.2	24.81	20	26.1	25.93
9	26.2	25.02	21	26.1	25.84
10	26.3	25.15	22	26.1	25.79
11	26.4	25.28	23	26.1	25.64
12	26.4	25.31	24	26.2	25.45

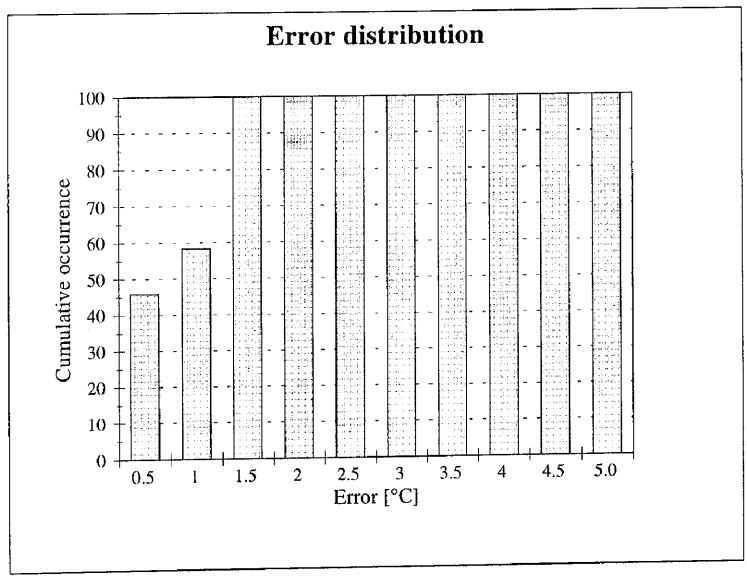

Study 90

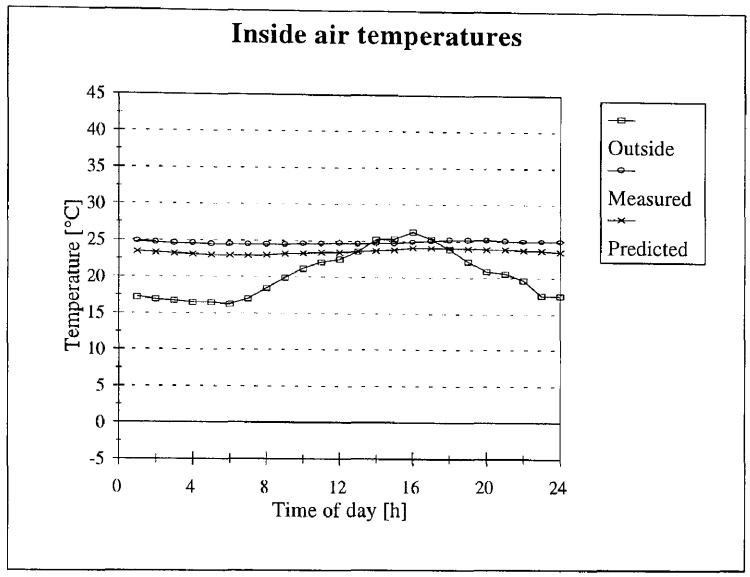

Hour	Measured	Predicted	Hour	Measured	Predicted
1	24.9	23.47	13	24.6	23.58
2	24.7	23.34	14	24.7	23.66
3	24.6	23.25	15	24.7	23.84
4	24.6	23.12	16	24.9	24.08
5	24.5	23.02	17	25.1	24.11
6	24.5	23.00	18	25.2	24.11
7	24.5	22.94	19	25.2	24.05
8	24.5	23.00	20	25.2	23.96
9	24.5	23.21	21	25.1	23.91
10	24.6	23.30	22	25.0	23.84
11	24.6	23.41	23	25.0	23.76
12	24.7	23.44	24	25.0	23.60

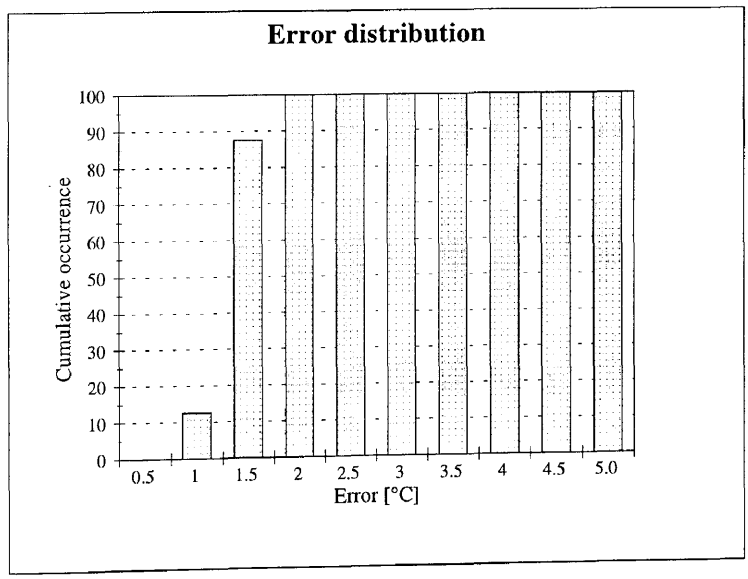

Study 91

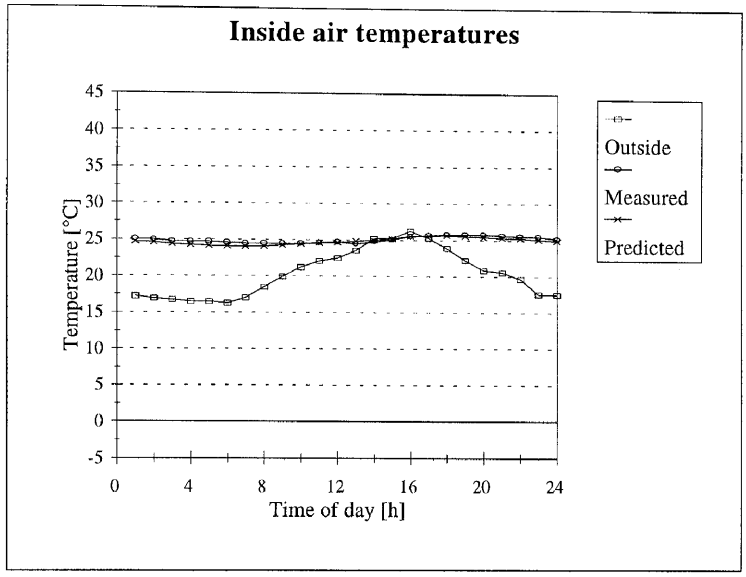

Hour	Measured	Predicted	Hour	Measured	Predicted
1	25.1	24.74	13	24.5	24.88
2	25.0	24.59	14	24.8	25.01
3	24.8	24.42	15	25.1	25.22
4	24.8	24.29	16	25.5	25.55
5	24.7	24.16	17	25.7	25.64
6	24.6	24.11	18	25.8	25.66
7	24.5	24.04	19	25.8	25.57
8	24.5	24.10	20	25.8	25.44
9	24.5	24.28	21	25.7	25.36
10	24.5	24.44	22	25.6	25.30
11	24.6	24.60	23	25.5	25.13
12	24.7	24.66	24	25.2	24.93

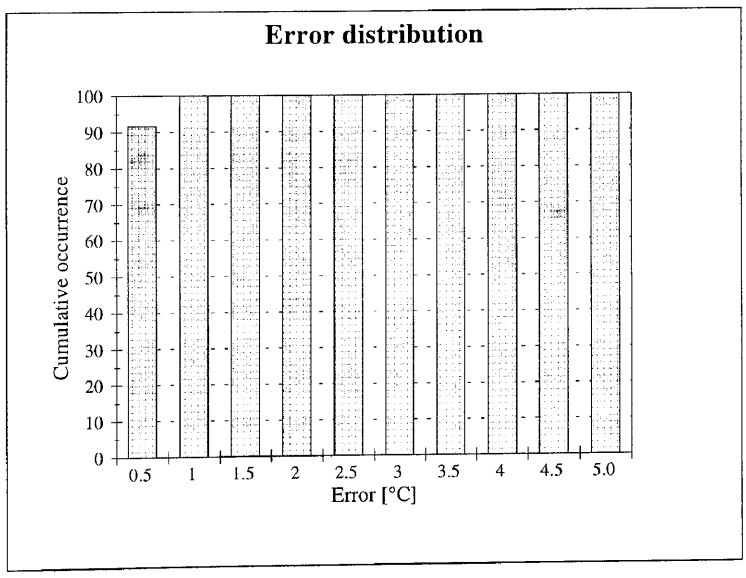

Study 92

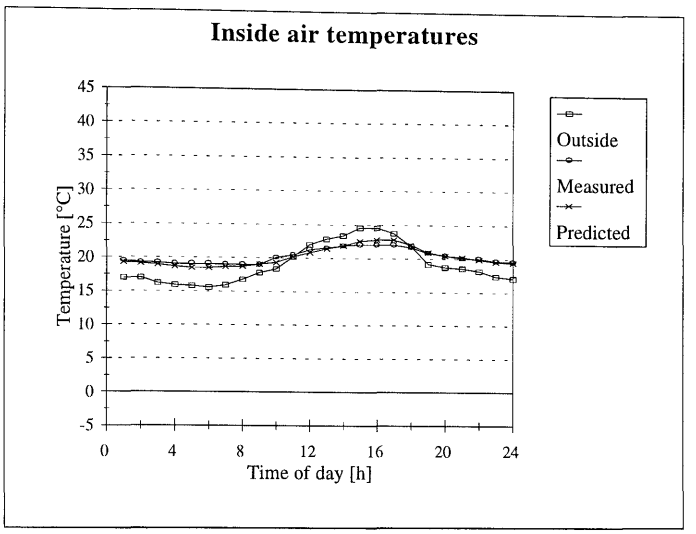

Hour	Measured	Predicted	Hour	Measured	Predicted
1	19.5	19.28	13	21.6	21.48
2	19.3	19.15	14	21.9	21.95
3	19.2	18.93	15	22.1	22.60
4	19.1	18.67	16	22.1	22.82
5	19.1	18.47	17	22.1	22.82
6	19.1	18.47	18	21.7	22.11
7	19.0	18.69	19	20.9	20.96
8	19.0	18.70	20	20.5	20.48
9	19.0	19.04	21	20.1	20.24
10	20.1	19.33	22	20.0	19.96
11	20.5	20.22	23	19.7	19.59
12	21.3	20.86	24	19.6	19.48

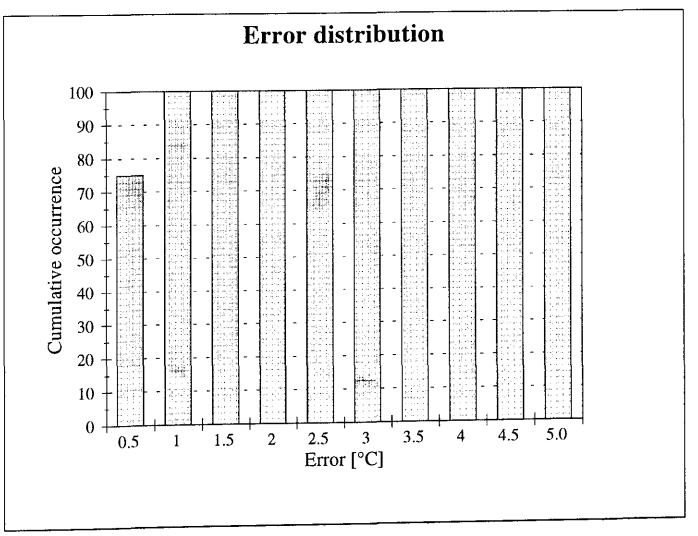

Study 93

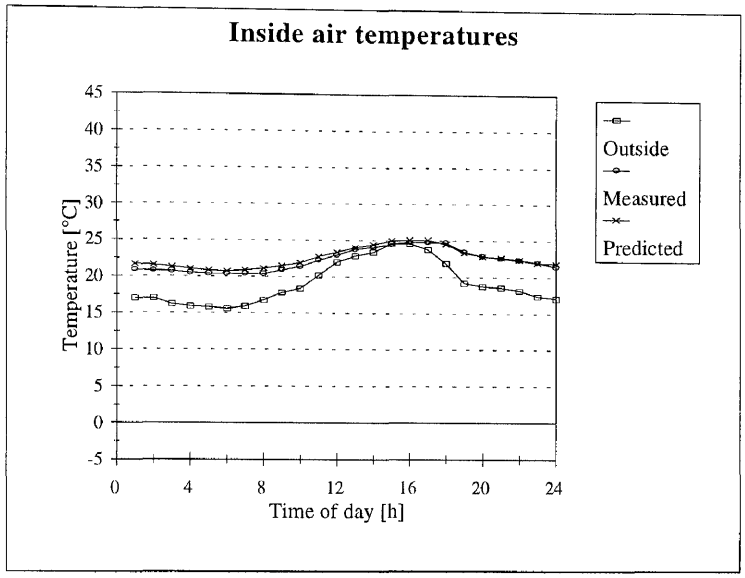

Hour	Measured	Predicted	Hour	Measured	Predicted
1	20.9	21.73	13	23.8	24.07
2	20.8	21.59	14	24.1	24.46
3	20.7	21.32	15	24.5	24.98
4	20.5	21.04	16	24.8	25.10
5	20.4	20.86	17	24.8	25.11
6	20.4	20.75	18	24.7	24.54
7	20.4	20.89	19	23.5	23.36
8	20.4	21.13	20	22.9	22.91
9	20.9	21.51	21	22.6	22.70
10	21.4	21.90	22	22.4	22.44
11	22.3	22.78	23	22.0	22.06
12	23.0	23.42	24	21.5	21.90

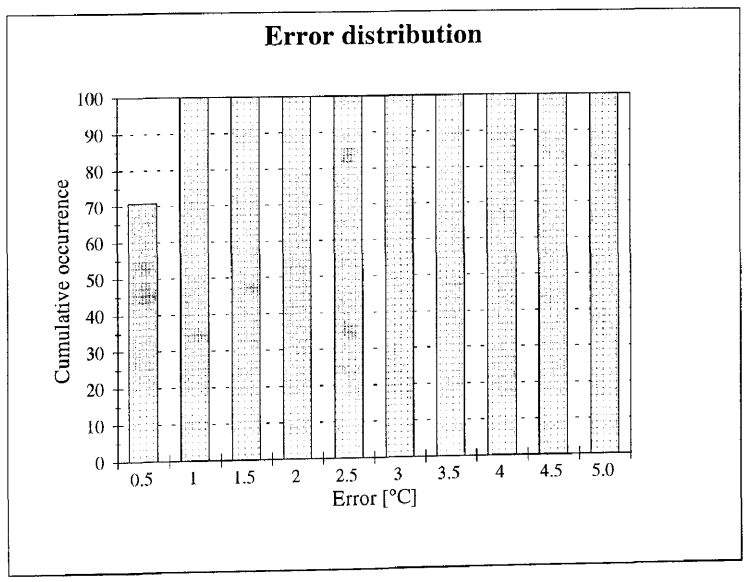

Study 94

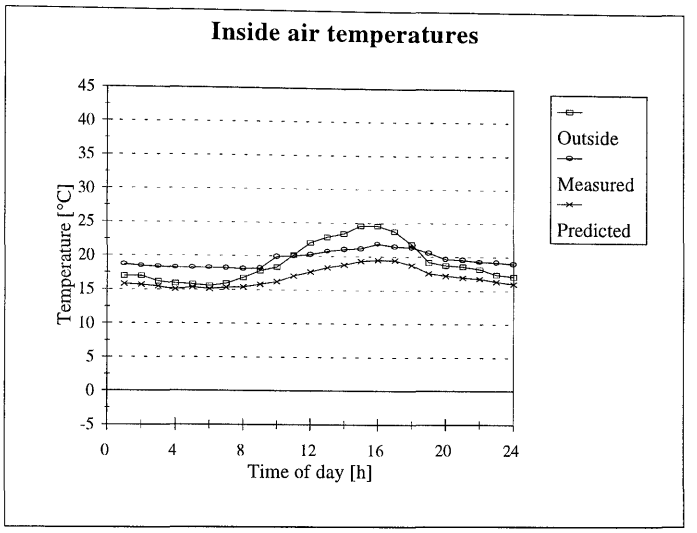

Hour	Measured	Predicted	Hour	Measured	Predicted
1	18.7	15.78	13	20.8	18.40
2	18.5	15.73	14	21.1	18.80
3	18.4	15.43	15	21.2	19.38
4	18.3	15.04	16	21.9	19.52
5	18.3	15.38	17	21.5	19.48
6	18.3	15.13	18	21.4	18.79
7	18.2	15.34	19	20.6	17.54
8	18.1	15.40	20	19.7	17.20
9	18.2	15.79	21	19.6	16.93
10	19.9	16.20	22	19.3	16.77
11	20.0	17.06	23	19.2	16.41
12	20.3	17.71	24	19.0	16.06

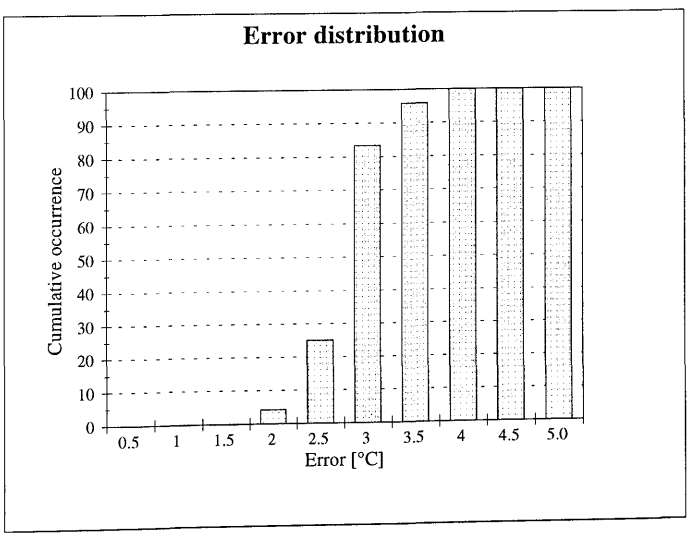

Study 95

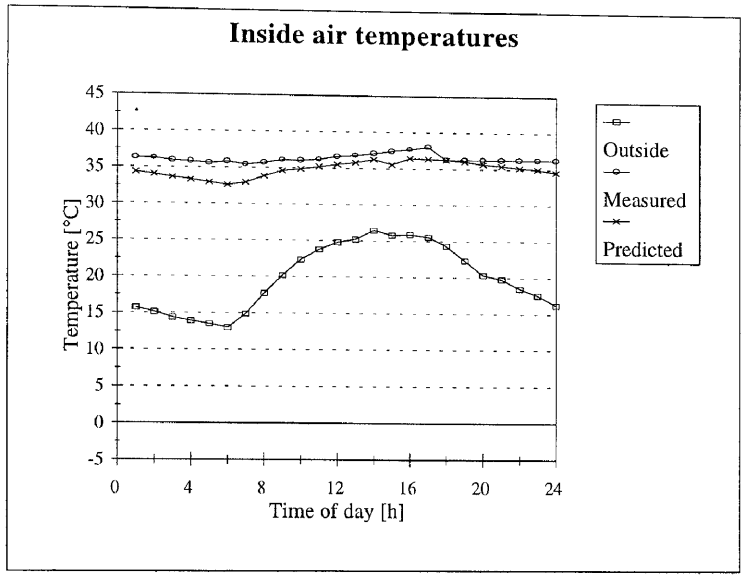

Hour	Measured	Predicted	Hour	Measured	Predicted
1	36.3	34.34	13	36.8	35.80
2	36.2	34.02	14	37.1	36.25
3	35.9	33.64	15	37.4	35.54
4	35.8	33.32	16	37.7	36.45
5	35.6	32.96	17	38.0	36.42
6	35.8	32.60	18	36.3	36.28
7	35.4	32.97	19	36.3	36.04
8	35.7	33.88	20	36.3	35.70
9	36.1	34.65	21	36.3	35.43
10	36.0	34.86	22	36.3	35.18
11	36.2	35.20	23	36.3	35.01
12	36.6	35.53	24	36.3	34.65

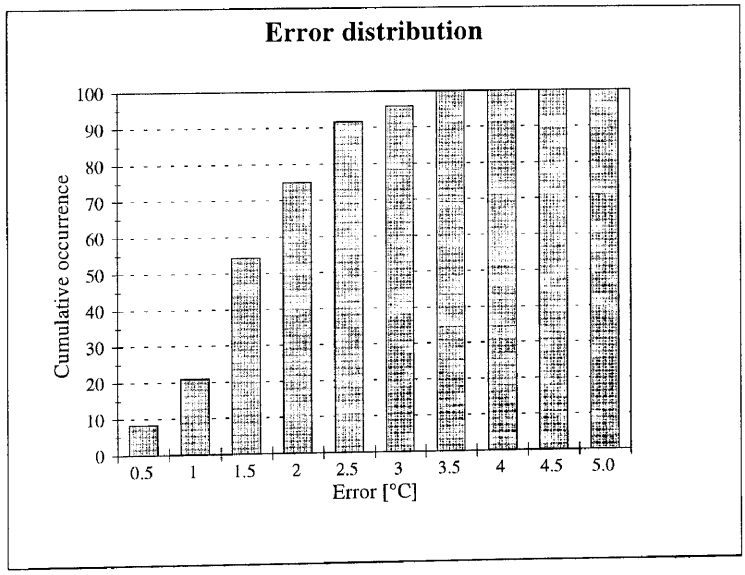

Study 96

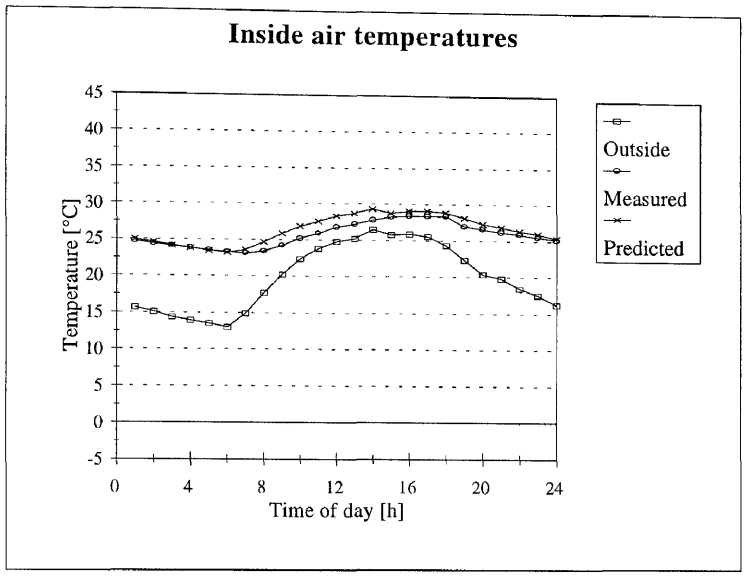

Hour	Measured	Predicted	Hour	Measured	Predicted
1	24.7	24.99	13	27.2	28.75
2	24.4	24.64	14	27.8	29.34
3	24.1	24.19	15	28.3	28.79
4	23.8	23.84	16	28.4	29.10
5	23.5	23.45	17	28.4	29.14
6	23.3	23.17	18	28.4	28.91
7	23.1	23.61	19	27.0	28.13
8	23.4	24.68	20	26.6	27.33
9	24.2	25.88	21	26.2	26.89
10	25.2	26.88	22	25.9	26.41
11	25.9	27.60	23	25.5	25.99
12	26.8	28.31	24	25.2	25.39

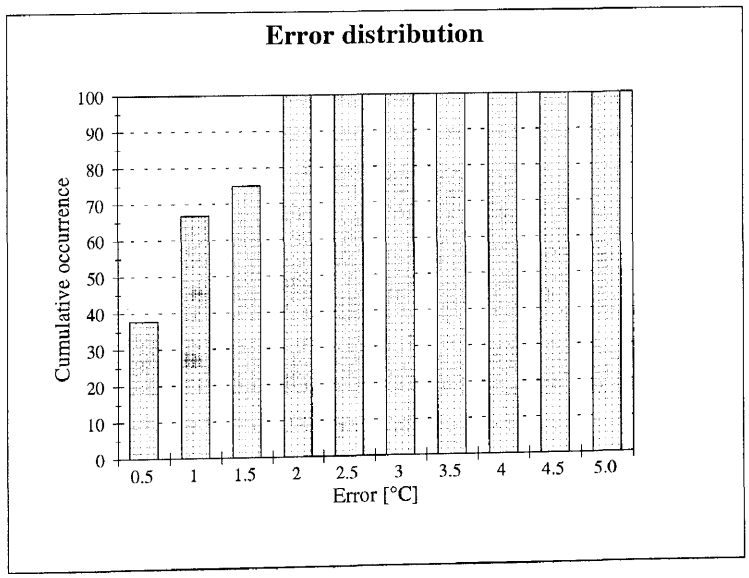

Study 97

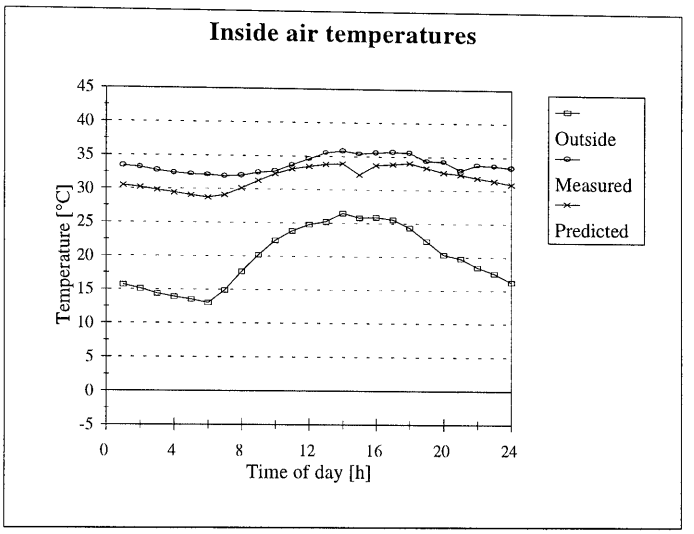

Hour	Measured	Predicted	Hour	Measured	Predicted
1	33.4	30.50	13	35.5	33.80
2	33.2	30.21	14	35.8	33.96
3	32.7	29.80	15	35.4	32.30
4	32.4	29.46	16	35.6	33.68
5	32.2	29.07	17	35.7	33.85
6	32.1	28.74	18	35.6	34.02
7	31.9	29.15	19	34.4	33.38
8	32.0	30.13	20	34.3	32.67
9	32.5	31.29	21	33.0	32.35
10	32.7	32.33	22	33.8	31.88
11	33.7	33.06	23	33.7	31.46
12	34.6	33.49	24	33.4	30.93

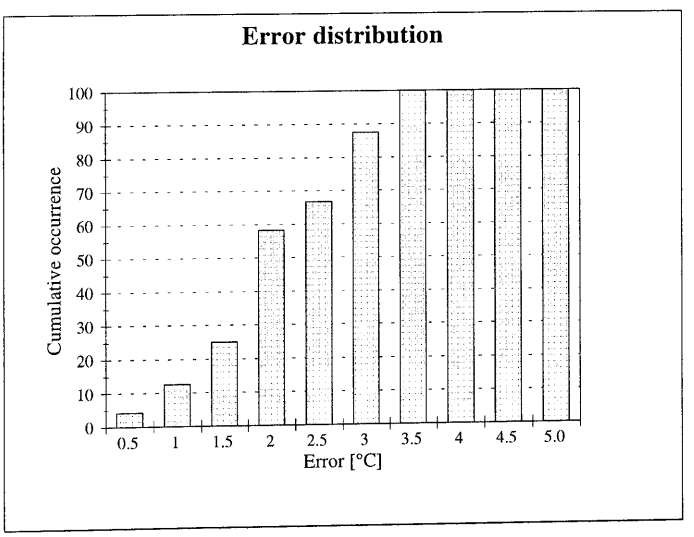

Study 98

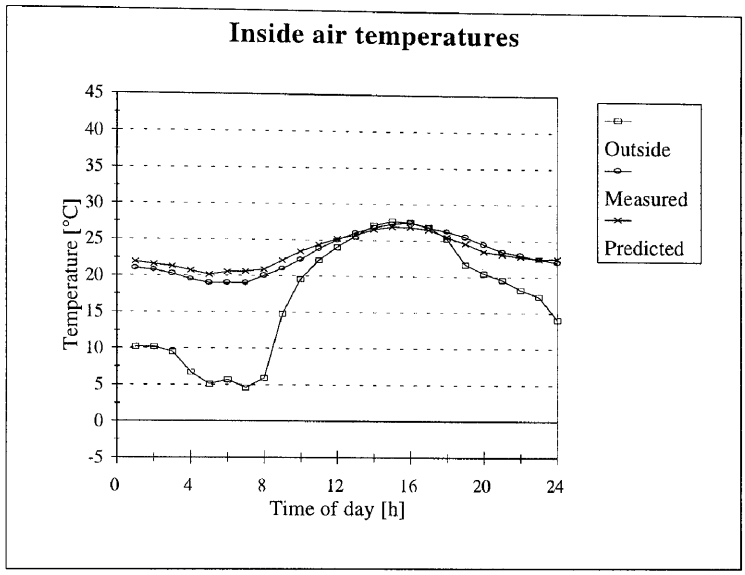

Hour	Measured	Predicted	Hour	Measured	Predicted
1	21.0	21.93	13	26.0	25.70
2	20.8	21.60	14	26.8	26.49
3	20.3	21.30	15	27.3	26.89
4	19.5	20.72	16	27.5	26.84
5	19.0	20.14	17	26.8	26.49
6	19.0	20.57	18	26.3	25.50
7	19.0	20.61	19	25.5	24.61
8	20.0	20.92	20	24.5	23.50
9	21.0	22.19	21	23.5	23.13
10	22.3	23.39	22	23.0	22.78
11	23.8	24.39	23	22.5	22.49
12	25.0	25.17	24	22.0	22.56

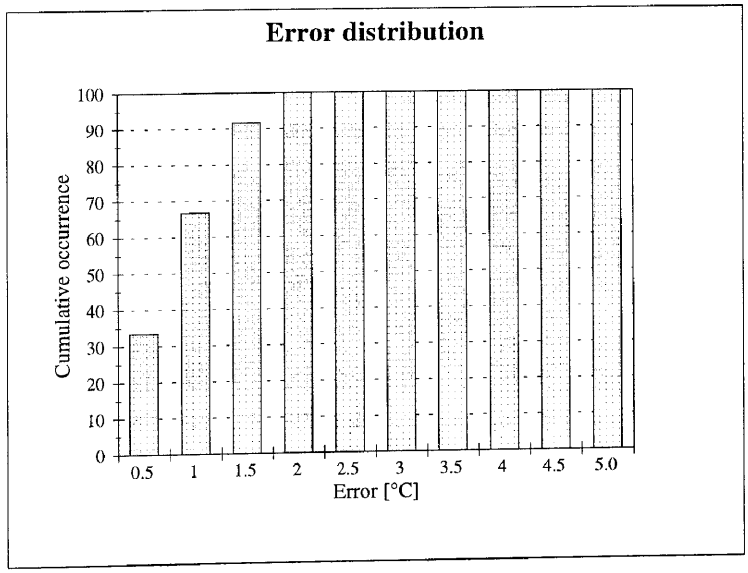

Study 99

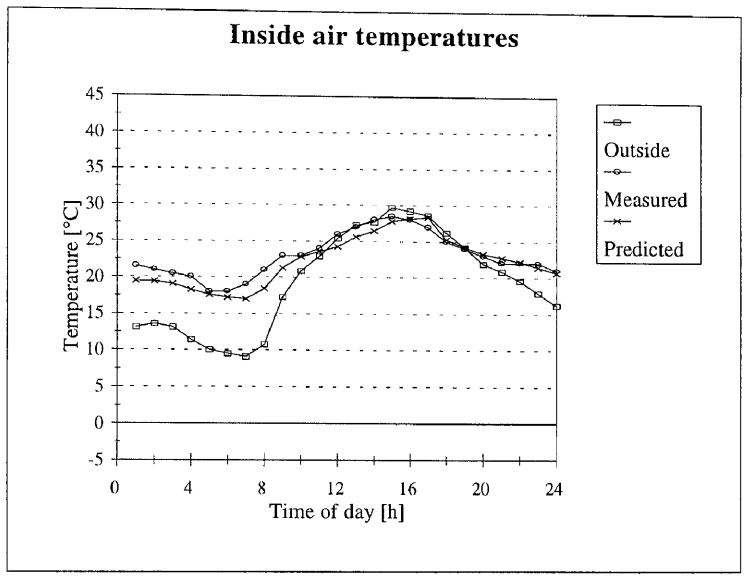

Hour	Measured	Predicted	Hour	Measured	Predicted
1	21.5	19.47	13	27.0	25.62
2	21.0	19.41	14	28.0	26.48
3	20.5	19.06	15	28.5	27.82
4	20.0	18.29	16	28.0	28.16
5	18.0	17.60	17	27.0	28.39
6	18.0	17.21	18	25.0	25.29
7	19.0	17.02	19	24.0	24.30
8	21.0	18.44	20	23.0	23.32
9	23.0	21.28	21	22.0	22.80
10	23.0	22.87	22	22.0	22.21
11	24.0	23.61	23	22.0	21.48
12	26.0	24.29	24	21.0	20.73

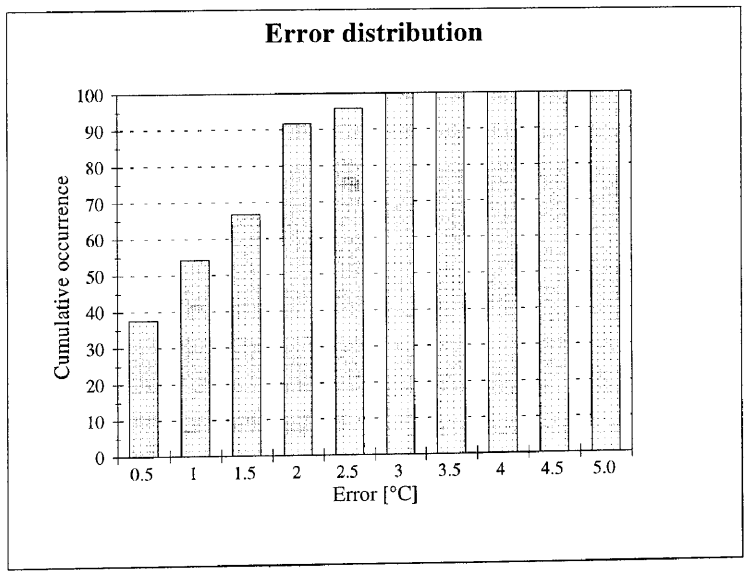

Study 100

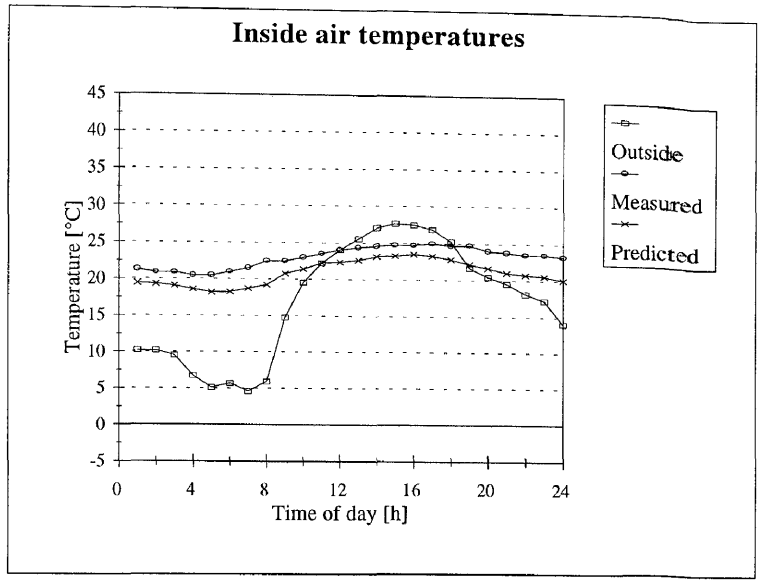

Hour	Measured	Predicted	Hour	Measured	Predicted
1	21.3	19.45	13	24.4	22.68
2	20.9	19.33	14	24.6	23.19
3	20.9	19.11	15	24.8	23.29
4	20.5	18.58	16	24.8	23.50
5	20.5	18.20	17	25.0	23.29
6	21.0	18.27	18	24.7	22.84
7	21.5	18.76	19	24.8	22.23
8	22.5	19.25	20	24.0	21.72
9	22.5	20.80	21	23.8	21.04
10	23.0	21.39	22	23.5	20.80
11	23.5	22.27	23	23.5	20.63
12	24.0	22.39	24	23.3	20.11

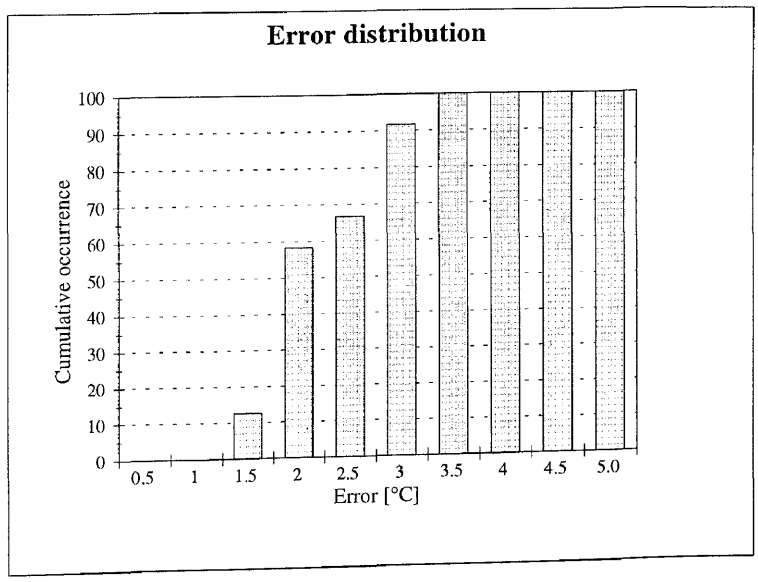

Study 101

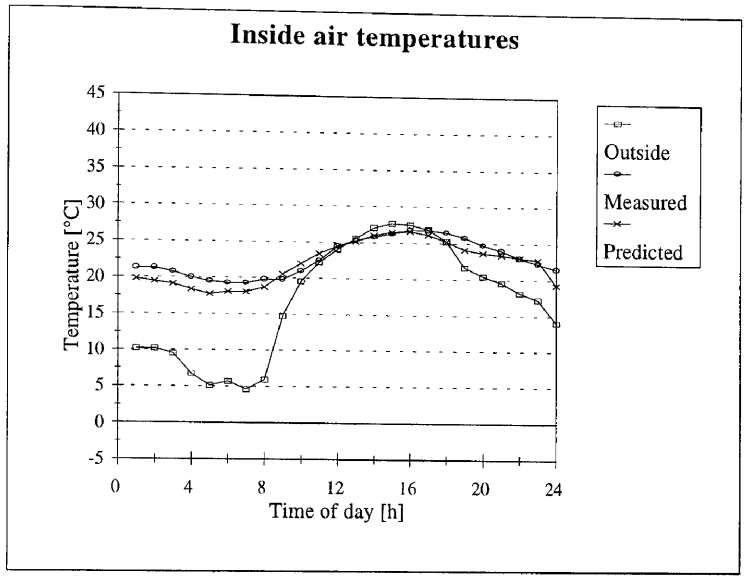

Hour	Measured	Predicted	Hour	Measured	Predicted
1	21.3	19.82	13	25.3	25.15
2	21.3	19.48	14	25.8	26.05
3	20.8	19.12	15	26.3	26.48
4	20.0	18.37	16	26.8	26.63
5	19.5	17.75	17	26.8	26.17
6	19.3	18.08	18	26.5	25.22
7	19.3	18.08	19	25.8	24.19
8	19.8	18.74	20	24.8	23.70
9	19.8	20.56	21	24.0	23.39
10	21.0	22.05	22	23.0	23.06
11	22.5	23.45	23	22.3	22.79
12	24.5	24.51	24	21.5	19.27

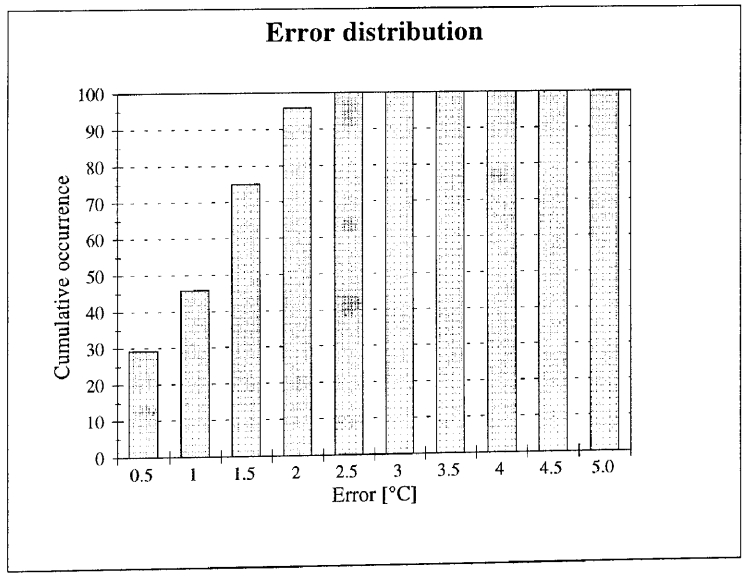

Study 102

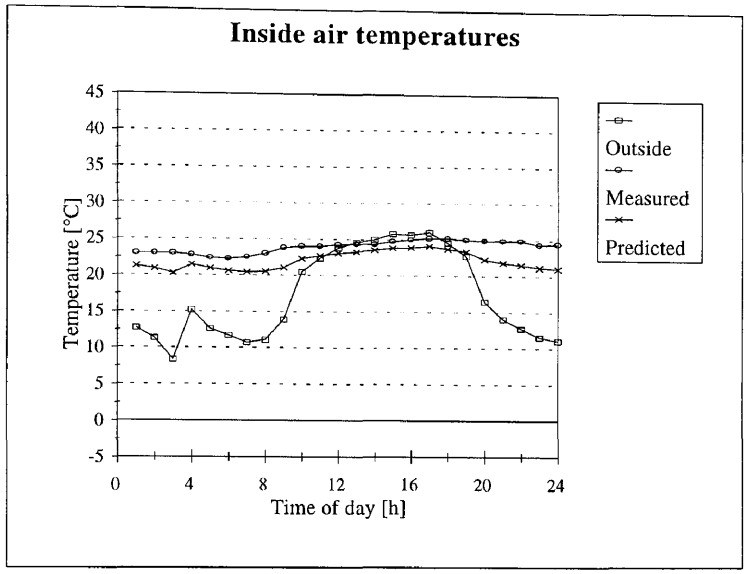

Hour	Measured	Predicted	Hour	Measured	Predicted
1	23.0	21.26	13	24.4	23.29
2	23.0	20.92	14	24.4	23.57
3	23.0	20.28	15	24.8	23.85
4	22.8	21.47	16	25.0	23.96
5	22.4	20.95	17	25.2	24.17
6	22.3	20.62	18	25.2	23.74
7	22.5	20.43	19	25.0	23.39
8	23.0	20.55	20	24.9	22.34
9	23.8	21.06	21	24.9	21.85
10	24.0	22.31	22	24.9	21.54
11	24.0	22.76	23	24.4	21.23
12	24.3	23.11	24	24.5	21.05

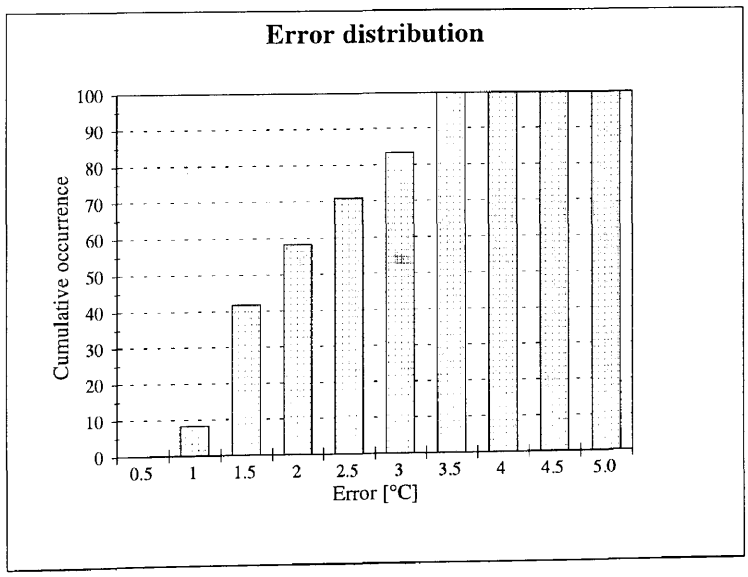

Study 103

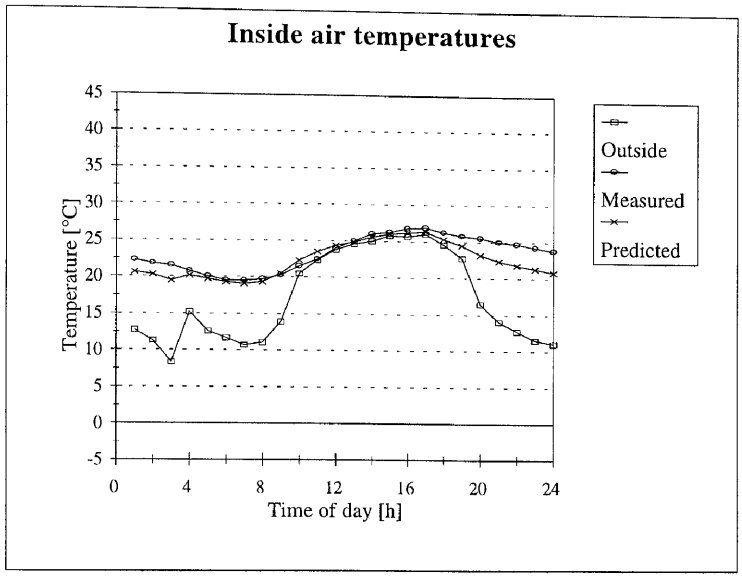

Hour	Measured	Predicted	Hour	Measured	Predicted
1	22.3	20.63	13	25.0	24.89
2	21.8	20.24	14	26.0	25.61
3	21.5	19.48	15	26.3	26.07
4	20.8	20.18	16	26.8	26.23
5	20.0	19.69	17	26.9	26.37
6	19.5	19.30	18	26.3	25.35
7	19.5	19.04	19	25.8	24.49
8	19.7	19.34	20	25.5	23.20
9	20.3	20.52	21	25.0	22.38
10	21.5	22.34	22	24.7	21.77
11	22.5	23.50	23	24.3	21.33
12	24.0	24.37	24	23.8	20.81

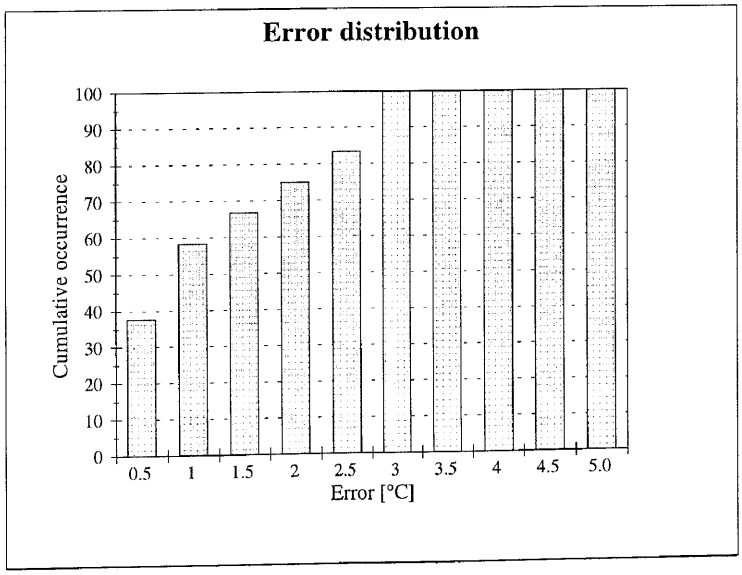

Appendix C

INPUT DATA FOR AGREMENT NORMS

C.1 CLIMATE DATA

Hot and cold day climate data for the following venues are provided in the climate database: Bisho, Bloemfontein, Cape Town, Durban, East London, George, Jan Smuts, Kimberley, Mmabatho, Phalaborwa, Pietersburg, Port Elizabeth, Pretoria, Secunda and Upington.

C.2 MATERIALS

The thermodynamic properties for a representative number of materials are provided in the materials data base.

C.3 DEFAULT VALUES

The following default values have been programmatically set:

Occupancy: The occupancy for a building is calculated on the basis of the floor area and is determined from:

$$Occupants = 0.111 \times floor\ area \tag{C.1}$$

It is assumed that all the occupants are in the building between 17h00 and 6h00. During the day time one third of the occupants are home.

Internal loads: Internal loads are generated from the occupancy data and from lights and cooking. The default values are:

$$Convective\ loads = 7 \times floor\ area\ [W] \tag{C.2}$$

$$Latent\ loads = 5.2 \times floor\ area\ [W]. \tag{C.3}$$

The energy used for heating is not included in these internal loads since the program calculates the required energy. This energy consumption forms part of the norms that are discussed in the next section.

C.4 INFILTRATION RATES

Infiltration rates are calculated from the relation suggested by ASHRAE [1], (see chapter 2) The natural ventilation rates are calculated as outlined in Richards [2].

Bibliography

[1] American Society for Heating Refrigeration and Air Conditioning Engineers, Inc. *ASHRAE Handbook*, 1992.

[2] P.G. Richards. *A Design Tool for the Thermal Performance of Buildings*. PhD thesis, Mechanical Engineering, University of Pretoria, 1992.

Appendix D

TYPICAL OUTPUT FOR AGREMENT NORMS

Agrement Report

Agrement uses a grading system to evaluate the thermal performance of a new building system. The thermal performance of the new system is rated relative to a number of standard buildings. This evaluation consists of the following two ratings:

1. The comfort temperature in summer, i.e. the maximum environmental temperature reached inside the dwelling.
2. The energy used to keep the building at 16 °C during the cold months for a given climate. The potential for condensation on any building surface is also given.

Comfort evaluation results for Venter's Home are as follows:

Pretoria	
Building description:	**Environmental temperature [°C]**
Brick house (30 m^2)	28.87
Brick house (100 m^2)	29.02
Brick house (53 m^2)	29.35
Brick house (77 m^2)	29.77
Venter's Home	37.15
Shack (41 m^2)	39.78

Energy evaluation results for Venter's Home are as follows:

Pretoria		
Building description	**Energy usage [kWh/m^2year]**	**Condensation**
Brick house (77 m^2)	2.79	No
Brick house (53 m^2)	5.05	No
Brick house (30 m^2)	7.01	Yes
Brick house (100 m^2)	7.58	No
Venter's Home	52.26	Yes
Shack (41 m^2)	202.56	Yes

Potential for condensation was found for the following surface(s) of the Venter's Home :

Surface:	**Condensation - Surface temperature [°C]**
Roof1	4.35
Back Wall	8.06
Front Wall	4.81
Side wall 1 South	1.92
Side wall 1 North	4.91
Side wall 2 South	2.07
Side wall 2 North	3.24

Appendix to Agrement Report: Building description summary

The Building zone: Main dwelling consists of the following elements:

Element: Floor	**Area [m^2]:** 35.00
Layers:	**Thickness [m]:**
Soil	0.075

Element: Back Wall	**Area [m^2]:** 8.82
Layers:	**Thickness [m]:**
Brickwork	0.110

Element: Front Wall	**Area [m^2]:** 7.22
Layers:	**Thickness [m]:**
Brickwork	0.110

Element: Front Door	**Area [m^2]:** 1.60
Layers:	**Thickness [m]:**
Wood Ply-	0.005
AIRSPACE	0.040
Wood Ply-	0.005

Element: Front Window	**Area [m^2]:** 1.00
Layers:	**Thickness [m]:**
Glass	0.006

Element: Back Window	**Area [m^2]:** 1.00
Layers:	**Thickness [m]:**
Glass	0.006

Element: Side wall 1 South	**Area [m^2]:** 11.78
Layers:	**Thickness [m]:**
Mild Steel	0.002
Expanded Polystyrene	0.013
Hardboard	0.004

Element: Side wall 1 North	**Area [m^2]:** 11.78
Layers:	**Thickness [m]:**
Mild Steel	0.002
Expanded Polystyrene	0.013
Hardboard	0.004

Element: Side wall 2 South	**Area [m^2]:** 11.78
Layers:	**Thickness [m]:**
Mild Steel	0.002
Expanded Polystyrene	0.013
Hardboard	0.004

Element: Side wall 2 North	**Area [m^2]:** 11.78
Layers:	**Thickness [m]:**
Mild Steel	0.002
Expanded Polystyrene	0.013
Hardboard	0.004

Element: Roof1	**Area [m^2]:** 11.78
Layers:	**Thickness [m]:**
Mild Steel	0.002
Expanded Polystyrene	0.013
Hardboard	0.004

Appendix E

INTEGRATED SIMULATIONS: Case Study 1

A building that has been retrofitted in order to achieve energy savings is investigated. Measurements of actual thermal performance are used to verify the simulation tool results. In this appendix, the details of the system parameters are presented. The results are shown and discussed in chapter 7.

E.1 INTRODUCTION

The building is a multi-storeyed combined laboratory and office building situated approximately 35 km west of Pretoria. The building was built in the seventies and supplied with a constant volume reheat HVAC system. The original system was designed as a constant volume system with the supply air temperature fixed for a given zone, irrespective of the load present inside the building or of the outside conditions.

During a retrofit study it was found that an enormous amount of energy is wasted on reheating the supply air at the reheat coils. A suggestion that the supply air temperature should be reset according to the outside air temperature was implemented. In this appendix, the detail of the building and system parameters are provided.

E.2 BUILDING DESCRIPTION

The building is a four-storeyed office and laboratory building. The total floor area is approximately 11 000 m^2. Sixty per cent of the building is used for laboratories, and forty per cent for offices. The building is divided into three phases, H-1, H-2, and H-5.

A large number of extraction hoods are installed in the laboratories. The extraction hoods are connected to three large extraction duct systems. H-2 has two extraction systems installed and there is one installed in H-5.

E.3 HVAC SYSTEM DESCRIPTION

The greatest part of the building is equipped with a once-through HVAC system. This is due to the fact that the substances used in the building are hazardous to human life.

A schematic of the building and its heating ventilation and air-conditioning system (HVAC system) is shown in figures E.1 to E.3. There are nine zones in all, each supplied by its own air-handling unit from the main plant room. The system was a constant volume constant temperature system with reheat.

There are three primary chiller units. At the time when the current measurements were taken, only two of the chillers were in operation. They are shown on the diagrams. All of them reject heat via cooling towers to the atmosphere.

The chillers supply nine air-handling units (AHUs) with chilled water. Most of the air-handling units are also equipped with a heating coil. Warm water is supplied from a heat exchanger where steam is used as a source of energy.

The supply air is transported to the various building zones via an air ducting system. Reheat coils at the entrance to each room or zone regulate the temperature in the room or zone. The warm water for these reheat coils comes from the same source as for the heating coils in a number of the AHUs.

A number of the AHUs are equipped with steam humidifiers. These are indicated in the schematic figures E.1 to E.3. The system components are listed in tables E.1 to E.3, for the sake of completeness.

Component	Make and Model	Status
Chiller	Carrier 30 HR 160A190	Non-operational
Cooling tower	Sulzer-Escher Wyss EWR 324-06020	Non-operational
Cooling coil	Searl Bush	Operational
Heating coils	Searl Bush	Operational
Supply air fans	Nikotra ADZ 500	Operational
Chilled water pump	KSB ETA 80-400	Operational
Condenser water pump	KSB ETA 125-315	Non-operational
Hot water pump	KSB ETA 80-400	Operational
Re-heaters	Dolphin Engineering NS/SP	Operational

Table E.1: Components for the HVAC system of building H-1.

Component	Make and Model	Status
Chiller	York HTD2C2-5BD	Operational
Cooling tower	B.A.C. VLT-125	Operational
Cooling coil	Searl Bush	Operational
Heating coils	Searl Bush	Operational
Supply air fans	Donkin BCC 48/1.0 (three of)	Operational
Chilled water pump	KSB ETA 125-400	Operational
Condenser water pump	KSB ETA 125-400	Operational
Hot water pump	KSB ETA 125-400	Operational
Re-heaters	Dolphin Engineering NS/SP	Operational

Table E.2: Components for the HVAC system of building H-2.

Component	Make and Model	Status
Chiller	York	Operational
Cooling tower	B.A.C. VLT-125 D	Operational
Cooling coil	Searl Bush	Operational
Heating coils	Searl Bush	Operational
Supply air fans	Donkin BCC 36/1.0 (two of) Donkin BCC 33/1.0	Operational
Chilled water pump	KSB ETA 125-400	Operational
Condenser water pump	KSB ETA 125-400	Operational
Hot water pump	KSB ETA 125-400	Operational
Re-heaters	Dolphin Engineering NS/SP	Operational

Table E.3: Components for the HVAC system of building H-5.

Although most of the information can be determined from the given specification in the tables, the procedure to determine them will be outlined in section E.4.

E.4 SYSTEM MODEL PARAMETER SUMMARY

There are various components that make up this HVAC system and the building. Each of these systems will be treated in a separate section. For each class of component, the parameters of one will be determined in some detail, and for the others, only the results will be given. It should be pointed out that the models will not be repeated here since they are available in reference [1].

E.4.1 Building zones

The building consists of a large number of laboratories and offices. Every office and laboratory cannot be simulated as a separate zone. This would make the simulation excessively complicated. The building was divided into zones by lumping all the areas that are serviced by the same air-handling unit together. At the time that the measurements were taken there were nine active AHUs, thus there were nine zones used in the simulation.

The zones are specified by specifying each building element. The roofs, floors and walls are specified by the areas, layers from which they are made, and whether they are internal, external, partitions or in ground contact (in the case of some of the floors). An internal wall (roof or floor) is one that has another zone on the other side. An outside wall (roof or floor) is exposed to the

outside environment. A partition is a building element (wall, roof or floor) that is inside a given zone.

For elements that are exposed to the outside environment, the emissivity and absorptivity need to be specified. For windows, the transmissivity is also required. The details of these zones can be found in the project file on the magnetic disc at the back of this document.

E.4.2 Chillers

Two chillers were operational at the time the studies were performed. The one is a centrifugal YORK chiller (HTD2C2-5BD). The other is a reciprocating CARRIER chiller (30 HR 160 A 190).

The modelling for the chiller is done using the following correlation expression for the capacity:

$$Q_e = a_0 + a_1 m_c + a_2 m_e + a_3 t_c + a_4 t_e \tag{E.1}$$

and the power consumed by:

$$Pwr = b_0 + b_1 m_c + b_2 m_e + b_3 t_c + b_4 t_e \tag{E.2}$$

where

a_i, b_i	Correlation coefficients
Q_e	Evaporator capacity, kW
Pwr	Power consumed by the compressor, kW
m_c	Mass flow rate of the water into the condenser, kg/s
m_e	Mass flow rate of the water into the evaporator, kg/s
t_c	The temperature of the water entering the condenser, °C
t_e	The temperature of the water entering the evaporator, °C.

The resultant coefficients were obtained by means of a least square fit on the manufacturer's data, and are given in tables E.4 and E.5.

YORK HTD2C2-5BD					
coefficient number	0	1	2	3	4
a	0.219	$4.9\ 10^{-4}$	20.917	-0.005	0.004
b	439.811	$-3.9\ 10^{-4}$	-5.867	0.003	6.857

Table E.4: Correlation coefficients for the York chiller model.

CARRIER 30 HR 160 A 190					
coefficient number	0	1	2	3	4
a	75.413	3.437	15.068	-1.189	2.826
b	39.347	7.917	-9.646	0.973	1.571

Table E.5: Correlation coefficients for the Carrier chiller model.

E.4.3 Cooling towers

Two cooling towers were operational at the time of measuring. They were B.A.C. VLT-125 D and Sulzer-Escher Wyss EWR 324-06020. The performance of a cooling tower is modelled using the overall thermal resistance:

$$AU = a_0 + a_1 m_l + a_2 t_{li} + a_3 m_l^2 + a_4 t_{li}^2 + a_5 m_l t_{li} \tag{E.3}$$

where

AU Overall thermal resistance, °C /W
a_i, Correlation coefficients
m_l Mass flow rate of the water into the tower, kg/s
t_{li} The temperature of the liquid entering the tower, °C.

The performance data for the cooling towers were not available from the suppliers. This is due to the fact that the equipment was no longer in production. Seeing that the cooling towers are not critical to the energy consumption of the building as a whole, the closest available towers were used. The correlation coefficients used for the cooling towers are shown in table E.6.

B.A.C. VLT-125 D						
coefficient number	0	1	2	3	4	5
a	1721.8	0.9836	-52.883	$-7.7\ 10^{-4}$	0.5565	$-6.9\ 10^{-3}$

Table E.6: Correlation coefficients for the B.A.C. cooling tower.

E.4.4 Pumps

The pumps that are used in this simulation are given in the tables E.1 through E.3. The pump performance is modelled using two coefficients. They are the flow coefficient defined as:

$$K_f = \frac{m_l}{\rho_l n D^3} \tag{E.4}$$

and the pressure head coefficient as:

$$K_h = \frac{dP_l}{\rho_l n^2 D^3}. \tag{E.5}$$

The relation between K_h and K_f is given by

$$K_h = a_0 + a_1 K_f + a_2 K_f^2 + \ldots + a_k K_f^k \tag{E.6}$$

and the relation between K_f and η is given by

$$\eta = b_0 + b_1 K_f + b_2 K_f^2 + \ldots + b_k K_f^k. \tag{E.7}$$

Here

K_f	Flow coefficient
K_h	Pressure head coefficient
η	Pump efficiency
a_i	Correlation coefficients for K_h versus K_f
b_i	Correlation coefficients for η versus K_f
D	Rotor diameter, m
dP_l	Static pressure rise, Pa
m_l	Mass flow rate through the pump, kg/s
n	Rotational speed of the pump, rpm
ρ	Density of the fluid, kg/m^3.

The coefficients used for pump KSB ETA 80-400 are given in table E.7, for pump KSB ETA 125-315 in table E.8, and for pump KSB ETA 125-400 in table E.9.

KSB ETA 80-400			
coefficient number	0	1	2
a	0.0015	1.8431	-5980.1
b	0.0866	3756.1	$-6.5\ 10^6$

Table E.7: Correlation coefficients for pump KSB ETA 80-400.

KSB ETA 125-315			
coefficient number	0	1	2
a	0.0012	0.2993	-490.797
b	0.2180	1395.7	$-8.2\ 10^5$

Table E.8: Correlation coefficients for pump KSB ETA 125-315.

KSB ETA 125-400			
coefficient number	0	1	2
a	0.0016	0.6849	-1111.7
b	0.1172	1778.9	$-1.3\ 10^6$

Table E.9: Correlation coefficients for pump KSB ETA 125-400.

E.4.5 Fans

The fans are modelled in a similar manner to the pumps, and the regressions, and head and pressure coefficients are defined as for the pumps. The subscript 'l' (for liquid) can be replaced by '*a*' (for air). Four distinct fan models were used in this building. These are Nikotra ADZ 500 (coefficients given in table E.10.), Donkin BCC 48/1.0, BCC 36/1.0, and BCC 33/1.0 (coefficients given in table E.11 to table E.13).

Nikotra ADZ 500						
coefficient number	0	1	2	3	4	5
a	0.0051	-0.2739	10.1945	-215.82	1697.63	-5038.04
b	0.1299	25.0555	-323.683	1015.07		

Table E.10: Correlation coefficients for fan Nikotra ADZ 500.

Donkin BCC 48/1.0			
coefficient number	0	1	2
a	$-8.0\ 10^{-4}$	0.4595	-25.1840
b	-1.9822	515.64	$-2.3\ 10^{-4}$

Table E.11: Correlation coefficients for fan Donkin BCC 48/1.0.

Donkin BCC 36/1.0			
coefficient number	0	1	2
a	0.0013	0.0725	-7.6054
b	-0.2498	206.11	-9.7029

Table E.12: Correlation coefficients for fan Donkin BCC 36/1.0.

Donkin BCC 33/1.0			
coefficient number	0	1	2
a	0.0010	0.1207	-9.6927
b	-0.2973	215.63	$-1.0\ 10^{4}$

Table E.13: Correlation coefficients for fan Donkin BCC 33/1.0.

E.4.6 Heating and cooling coils

The modelling of the coils is performed by specifying the heat transfer coefficient as a function of the face velocity of the incoming air. The heat transfer coefficient is given as

$$h_o = a_0 + a_1 V + a_2 V^2 + \cdots + a_n V^n \tag{E.8}$$

where

a_i Correlation coefficients
h_o Heat transfer coefficient, W/m^2 $^\circ$C
V Coil air face velocity, m/s.

As was the case with the cooling towers, the exact data for the cooling and heating coils were not available. The following data were used for the respective coils. The coefficients for the cooling, heating and reheating coils are given in tables E.14 to E.16.

Cooling coils				
coefficient number	0	1	2	Area ratio
a	18.2447	2.0115	0.02477	18.8

Table E.14: Correlation coefficients for cooling coils.

Heating coils				
coefficient number	0	1	2	Area ratio
a	18.6590	3.7534	-0.1714	13.8

Table E.15: Correlation coefficients for heating coils.

Re-heat coils				
coefficient number	0	1	2	Area ratio
a	18.7290	5.1079	-0.3912	11.3

Table E.16: Correlation coefficients for re-heat coils.

E.4.7 Control system

The parameters needed for the retrofit study are those of the heating and cooling coils. They can be seen in the following table:

	Throttling range		Controlled parameter		Outside air conditions		Reset setpoint	
	Low	High	Low	High	Low	High	Low	High
Cooling coils	16	14	1	0	24	14	15	20
Heating coils	13	11	0	1	24	14	10	15
Re-heating coils	19	22	1	0	-	-	-	-

Table E.17: Control parameters as implemented in the simulation tool.

The chilled water temperature was controlled at 8.5 °C and the condenser water at 30 °C.

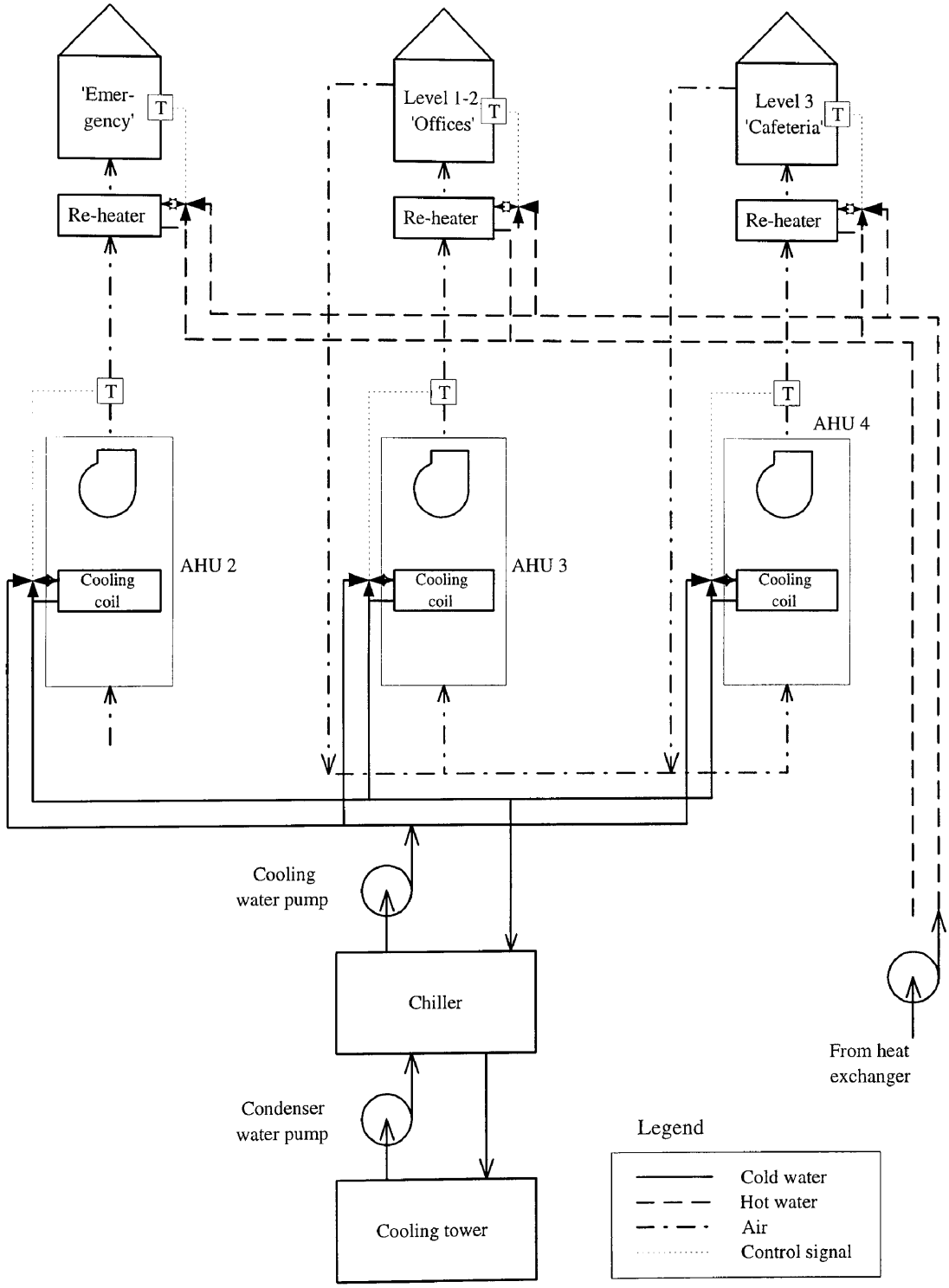

Figure E.1: Layout of the H-1 building HVAC system.

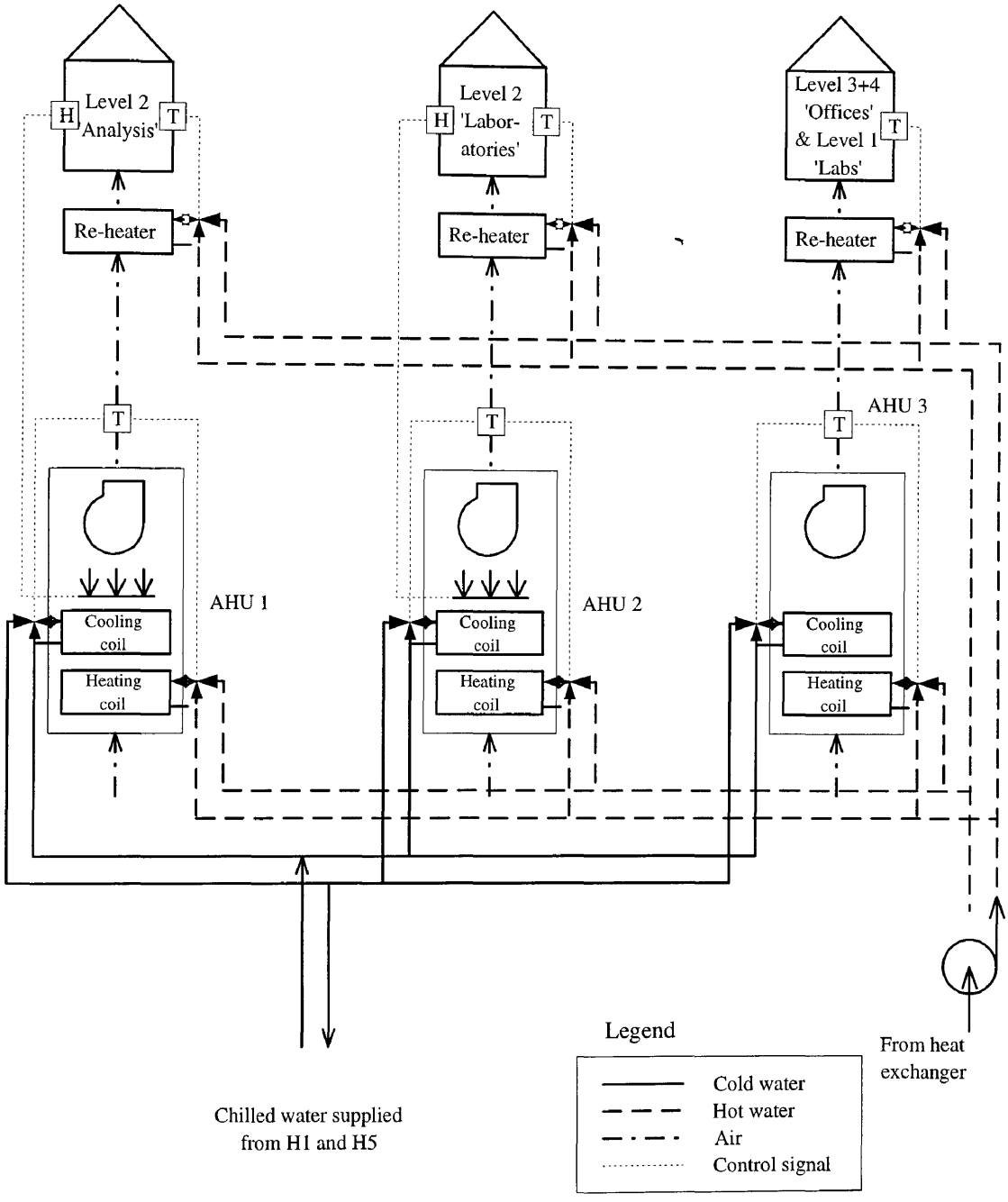

Figure E.2: Layout of the H-2 building HVAC system.

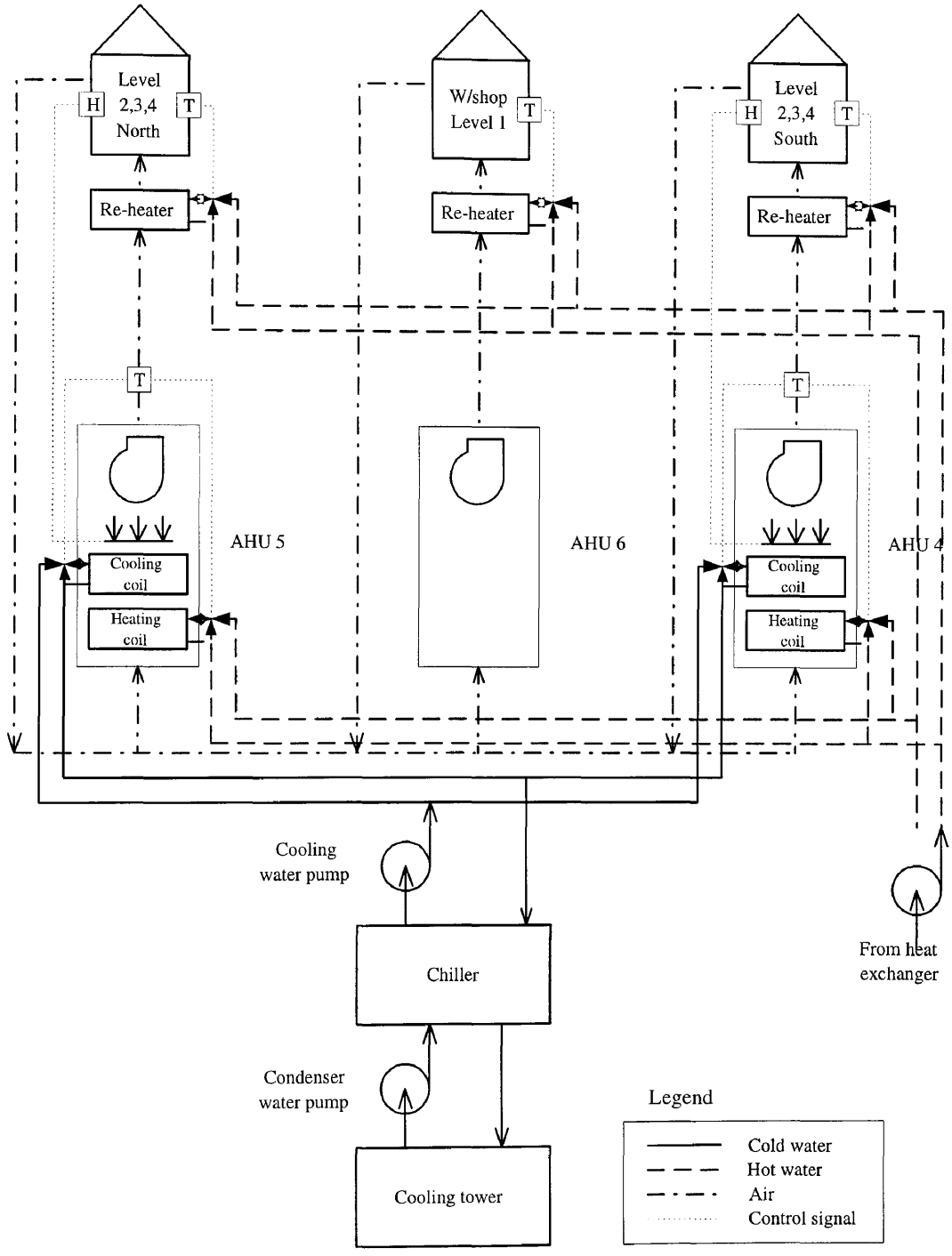

Figure E.3: Layout of the H-5 building HVAC system.

Bibliography

[1] P.G. Rousseau. *Integrated Building and HVAC Thermal Simulation*. PhD thesis, Mechanical Engineering, University of Pretoria, 1994.

Appendix F

INTEGRATED SIMULATIONS: Case Study 2

In this appendix, the details of the building and HVAC system for the second case study discussed in chapter 7 are described.

F.1 INTRODUCTION

The building is a double-storeyed house situated to the east of Pretoria. Four of the building zones are serviced by an air-conditioning unit. A schematic of the building and system is shown in figure F.1. Return air temperature is used as an indication of the effective average zone temperatures.

The model parameters are presented in section F.2.

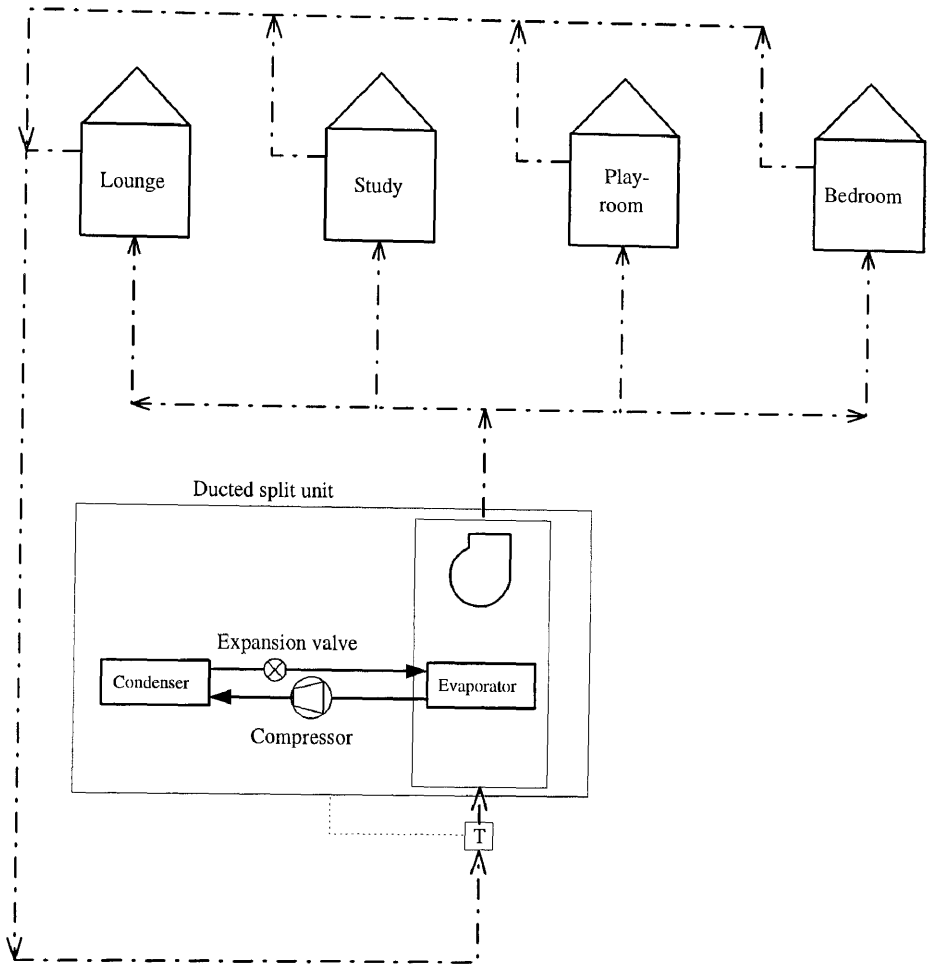

Figure F.1: Layout of the building and HVAC system.

F.2 SYSTEM MODEL PARAMETER SUMMARY

The building and HVAC system considered in this appendix are comparatively simple. The only regressions that are needed are those for the ducted split air-conditioning unit. Again, the model will not be repeated here since that it is available in reference [1].

F.2.1 Building zones

Only the four zones that are supplied by the air-conditioner are modelled in the simulation program.

The zones are specified by specifying each building element. The roofs, floors, and walls are specified by the areas, layers from which they are made, and whether they are internal, external, partitions or in ground contact (in the case of some of the floors). An internal wall (roof or floor) is one that has another zone on the other side. An outside wall (roof or floor) is exposed to the outside environment. A partition is a building element (wall, roof or floor) that is inside a given zone.

For elements that are exposed to the outside environment, the emissivity and absorptivity need to be specified. For windows, the transmissivity is also required. The details of these zones can be found in the project file on the magnetic disc at the back of this document.

F.2.2 Ducted split unit

A ducted split unit was used in the building. The modelling for the unit is done using the following correlation expression for the capacity:

$$Q_{et} = a_0 + a_1 m_e + a_2 t_{dbi} + a_3 t_{wbi} + a_4 t_{dbo} \tag{F.1}$$

for the latent load capacity:

$$Q_{el} = b_0 + b_1 m_e + b_2 t_{dbi} + b_3 t_{wbi} + b_4 t_{dbo} \tag{F.2}$$

and the power consumed by:

$$Pwr = c_0 + c_1 m_e + c_2 t_{dbi} + c_3 t_{wbi} + c_4 t_{dbo} \tag{F.3}$$

where

a_i, b_i	Correlation coefficients
Q_{et}	Evaporator total capacity, kW
Q_{el}	Evaporator latent capacity, kW
Pwr	Power consumed by the compressor, kW
m_e	Mass flow rate of the air into the evaporator, kg/s

t_{dbi} The dry-bulb temperature of the air entering the evaporator, °C

t_{wbi} The wet-bulb temperature of the air entering the evaporator, °C

t_{dbo} The dry-bulb temperature of the air entering the condenser (ambient air), °C.

Rheem ducted split unit					
coefficient number	0	1	2	3	4
a	5.801	4.931	$-7.7\ 10^{-7}$	-0.064	-0.090
b	2.319	6.493	0.379	-0.672	0.056
c	1.089	0.918	$-2.1\ 10^{-7}$	-0.059	0.090

Table F.1: Correlation coefficients for the Rheem ducted split unit.

F.2.3 Control system

On/off control is implemented in this system. The temperature at which the system is switched on is 19 °C, and it is switched off at 16.5 °C. The temperature in the return air duct is measured as an indication of the average zone temperatures in the four zones supplied by the air-conditioner.

Bibliography

[1] P.G. Rousseau. *Integrated Building and HVAC Thermal Simulation*. PhD thesis, Mechanical Engineering, University of Pretoria, 1994.

Appendix G

INTEGRATED SIMULATIONS: Case Study 3

The parameters used in the third case study described in chapter 7 are given in this appendix. The building is situated on the campus of the University of Pretoria.

G.1 INTRODUCTION

The building schematic is shown in figure G.1. The building is a two-storeyed building. One of the AHUs in the system supplies four building zones. These zones could be measured separately, therefore the zones will be modelled individually. The other two AHUs each supply to their own building zone.

Return air from the four zones is mixed, and the temperature and humidity are measured. The temperature is used as indication of the average of the zone temperatures. The other two AHUs' return air is measured and controlled directly. Dehumidification is performed by using the cooling coils. No humidification is attempted.

Heating is performed by using hot water supplied from an electric boiler. In this case study, the water temperature was measured, so the boiler was not modelled.

The system components are given in table G.1.

Component	Make and Model
Chiller	Trane LCG03A
Cooling coil	Trane
Heating coils	Trane
Supply air fans	Nikotra ADZ 180
Chilled water pump	KSB ETAX 40-250
Hot water pump	KSB ETA 40-160

Table G.1: Components for the HVAC system.

Although most of the information can be determined from the given specification in the tables, the procedure to determine them will be outlined in section G.2.

G.2 SYSTEM MODEL PARAMETER SUMMARY

There are various components that make up this HVAC system and the building. Each of these systems will be treated in a separate section. The complete models will not be repeated here since they are available in reference [1].

G.2.1 Building zones

The building consists of a number of studios and offices. The building was divided into zones by lumping all the areas that are serviced by the same air-handling unit together.

The zones are specified by specifying each building element. The roofs, floors, and walls are specified by the areas, layers from which they are made, and whether they are internal, external, partitions or in ground contact (in the case of some of the floors). An internal wall (roof or floor) is one that has another zone on the other side. An outside wall (roof or floor) is exposed to the outside environment. A partition is a building element (wall, roof or floor) that is inside a given zone.

For elements that are exposed to the outside environment, the emissivity and absorptivity need to be specified. For windows, the transmissivity is also required. The details of these zones can be found in the project file on the magnetic disc at the back of this document.

G.2.2 Air-cooled chiller

The chiller used is a Trane LCG03A that was modified to an air-cooled chiller. The modelling for the chiller is done using the following correlation expression for the capacity:

$$Q_e = a_0 + a_1 m_e + a_2 t_e + a_3 t_c \tag{G.1}$$

and the power consumed by:

$$Pwr = b_0 + b_1 m_e + b_2 t_e + b_3 t_c \tag{G.2}$$

where

a_i, b_i	Correlation coefficients
Q_e	Evaporator capacity, kW
Pwr	Power consumed by the compressor, kW
m_e	Mass flow rate of the water into the evaporator, kg/s
t_c	The temperature of the air entering the condenser, °C
t_e	The temperature of the water entering the evaporator, °C.

Trane LCG03A (modified)				
coefficient number	0	1	2	3
a	2.094	-1.432	2.347	-0.284
b	32.819	-7.623	0.538	0.008

Table G.2: Correlation coefficients for the Trane chiller model.

G.2.3 Pumps

The coefficients used for pump KSB ETAX 40-160 are given in table G.3 and for pump KSB ETA 40-250 in table G.4.

KSB ETAX 40-160			
coefficient number	0	1	2
a	0.0015	0.4214	-1041.4
b	0.0645	1724.7	$-1.33\ 10^6$

Table G.3: Correlation coefficients for pump KSB ETAX 40-160.

KSB ETA 40-250			
coefficient number	0	1	2
a	0.0015	2.0137	-9942.1
b	0.1106	3726.5	$-7.44\ 10^6$

Table G.4: Correlation coefficients for pump KSB ETA 40-250.

G.2.4 Fans

The coefficients used for fan Nikotra ADZ 180 are given in table G.5.

Nikotra ADZ 180				
coefficient number	0	1	2	3
a	0.0023	0.05593	-0.8597	2.3795
b	0.2044	15.4718	-130.437	-477.297

Table G.5: Correlation coefficients for fan Nikotra ADZ 180.

G.2.5 Cooling and heating coils

The coefficients for the cooling, heating and reheating coils are given in table G.6.

Cooling and heating coils				
coefficient number	0	1	2	Area ratio
a	28.5706	5.1147	-0.2492	11.3

Table G.6: Correlation coefficients for cooling and heating coils.

G.2.6 Control system

The controller parameters for the cooling and heating coils can be seen in the following table:

	Throttling range		Controlled parameter	
	Low	High	Low	High
Cooling coils (temp)	22	24	0	1
Cooling coils (humidity)	60	70	0	1
Heating coils	21.5	16	0	1

Table G.7: Control parameters for the cooling and heating coils as implemented in the simulation tool.

The parameters for the chiller control are shown in table G.8.

Loading		Unloading	
Temperature	Capacity	Temperature	Capacity
9.5	0.9	8.8	0
10	1.0	9.7	0.9

Table G.8: Control parameters for the chiller as implemented in the simulation tool.

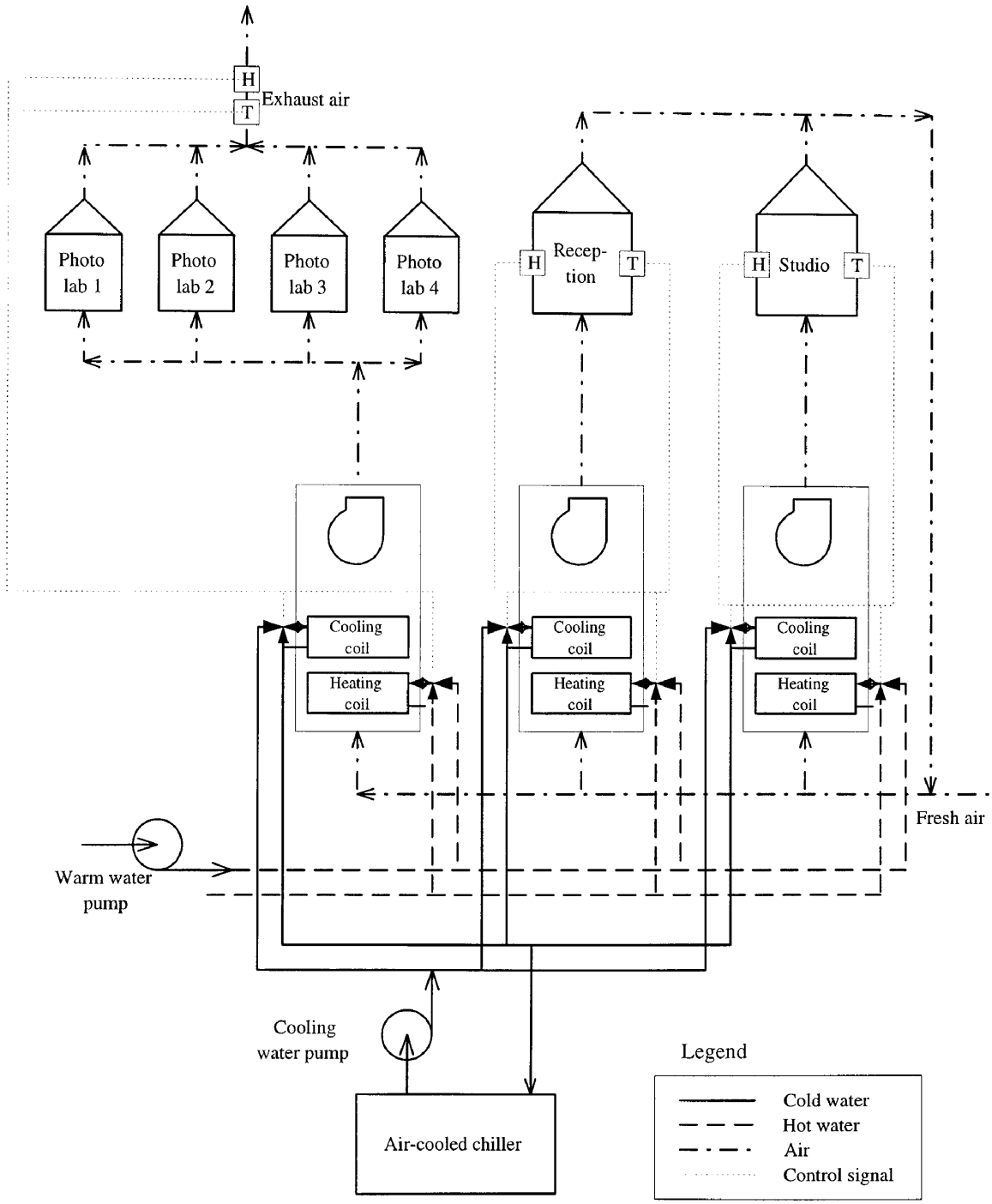

Figure G.1: Layout of the building HVAC system.

Bibliography

[1] P.G. Rousseau. *Integrated Building and HVAC Thermal Simulation*. PhD thesis, Mechanical Engineering, University of Pretoria, 1994.